University of Bath

PHD

An Improved Method for Simulation of Vehicle Vibration Using a Journey Database and Wavelet Analysis for the Pre-Distribution Testing of Packaging

Griffiths, Katharine

Award date:
2013

Awarding institution:
University of Bath

Link to publication

Alternative formats
If you require this document in an alternative format, please contact:
openaccess@bath.ac.uk

Copyright of this thesis rests with the author. Access is subject to the above licence, if given. If no licence is specified above, original content in this thesis is licensed under the terms of the Creative Commons Attribution-NonCommercial 4.0 International (CC BY-NC-ND 4.0) Licence (https://creativecommons.org/licenses/by-nc-nd/4.0/). Any third-party copyright material present remains the property of its respective owner(s) and is licensed under its existing terms.

Take down policy
If you consider content within Bath's Research Portal to be in breach of UK law, please contact: openaccess@bath.ac.uk with the details. Your claim will be investigated and, where appropriate, the item will be removed from public view as soon as possible.

Download date: 04. May. 2023

An Improved Method for Simulation of Vehicle Vibration Using a Journey Database and Wavelet Analysis for the Pre-Distribution Testing of Packaging

Volume 1 of 1

Katharine Rhiannon Griffiths

A thesis submitted for the degree of Doctor of Philosophy

University of Bath

Department of Mechanical Engineering

October 2012

COPYRIGHT

Attention is drawn to the fact that copyright of this thesis rests with the author. A copy of this thesis has been supplied on condition that anyone who consults it is understood to recognise that its copyright rests with the author and that they must not copy it or use material from it except as permitted by law or with the consent of the author.

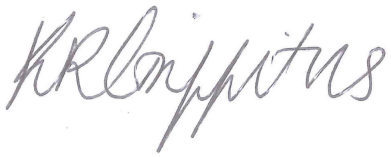

This thesis may be made available for consultation within the University Library and may be photocopied or lent to other libraries for the purposes of consultation.

ABSTRACT

Vehicle vibration is inherently random and non-stationary with a non-Gaussian distribution. In addition, variations in vehicle parameters, product payloads and distribution journeys mean that the characteristics of vibration are not identical for all distribution journeys. Because vehicle vibration and shock are key causes of damage during distribution, their simulation in pre-distribution testing is vital in order to ensure that adequate protection is provided for transported products.

The established method set out in the current testing standards utilises a global set of averaged accelerated power spectral density spectra to construct random vibration signals. These signals are stationary with Gaussian distributions and, therefore, do not fully represent actual vehicle vibration, only an average.

The aim of the investigation, reported on in this Thesis, was to create an improved test regime for simulating vehicle vibration for pre-distribution testing of packaging. This aim has been achieved through the construction of representative tests and the creation of realistic simulations with statistical significance.

A journey database has been created, in which historic road profile data along with a quarter vehicle model have been used to approximate a known vehicle's vibration on a specific distribution journey. Additionally, a wavelet decomposition method, in which wavelet analysis is used to decompose the approximate vehicle vibration in to a series of Gaussian approximations of varying amplitude and spectral content, has been developed. Along with theoretical work, case studies have been undertaken in order to validate the test regime.

ACKNOWLEDGEMENTS

First and foremost, I would like to acknowledge and give thanks to my academic and industrial supervisors. Firstly, Dr Ben Hicks and Prof Patrick Keogh, at the University Of Bath, for their guidance, advice, immense knowledge and enthusiasm, and secondly, Mr David Shires, at Smithers Pira, for sharing with me his extensive packaging testing expertise and supporting my research. The support of all three not only made this Thesis possible, but made my experience during it both enjoyable and memorable.

Thanks are also owed to Smithers Pira and the Engineering and Physical Sciences Research Council, who funded this research. I'd further like to thank Smithers Pira for providing me with access to their testing laboratory, and their laboratory technicians, who generously gave their time to assist me, and who always provided me a warm welcome.

I'd also like to acknowledge technicians Bernard Roe and Alan Jefferis, for their support and quick response with the MAST rig; researchers Mansur Darlington, Jason Matthews and Hamish McAlpine, for giving 'trucking' ago; and, researcher Michael Schlotter, for sharing with me his Matlab knowledge. Without the help of these few, this research would never have been finished.

I would also like to acknowledge the support and guidance given by my father, Dr Stephen Griffiths, whose expertise and advice on all things 'English', coupled with his patience, got me through the writing of this Thesis.

Finally, I would like to acknowledge and thank my Fiancé Sandy Hinxman, my parents and my sisters for their continued encouragement since I decided to carry out my PhD and their ongoing support, which enabled me to finish the Thesis.

CONTENTS

TABLE OF FIGURES

TABLE OF TABLES

1 INTRODUCTION

From 1980 to 2008 the value of goods globally distributed rose from $1.87 trillion to $17.63 trillion (Skills, 2008), with the value of exports from emerging economies such as India and China more than tripling between 2000 to 2008. Other regions such as Africa and South America also saw a dramatic increase in the value of their exports. This growth in distribution is illustrated in Figure 1 which shows the percentage increase in regional exports, ranging from 64% to 370+%.

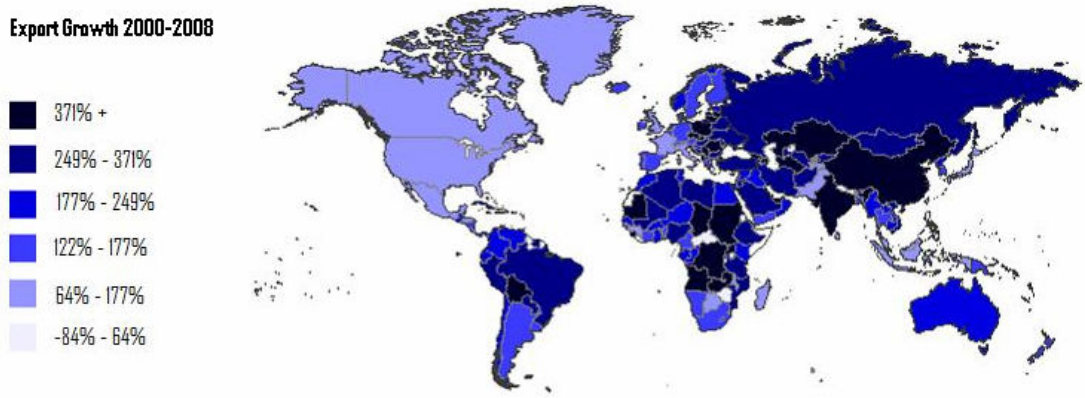

Figure 1: Map indicating the rate of growth of exports between 2000-2008 (Skills 2008)

This global increase has generated many logistical challenges due to the extended lengths and variations in distribution journeys (Robinson, 2006). These frequently cover several countries with changeable atmospheric conditions, varying quality transport routes and multiple modes of transport. The consequences are increases in distribution costs and the increased risk of damage and loss of goods during distribution.

Packaging, in its broadest sense, has been a key enabler in this growth of global distribution (Goodwin and Young, 2011). This includes distribution packaging such as shipping containers, stretch wrapping and pallet platforms, corrugated fibreboard boxes, shrink-film bundles, plastic totes, unit packaging and primary product packaging (Voortman, 2004). A primary advantage of distribution packaging is that it unitizes loads, helping to facilitate and ease distribution.

Furthermore, it provides products with essential protection from hazards in distribution, and it enables easy product identification. Whilst in many cases the primary packaging is concerned more with marketing the product, it can also offer invaluable protection from climatic and physical hazards, helping to prevent or postpone product deterioration. The use of incorrectly designed and/or inadequate packaging can result in substantial product damage and loss, and can increase the costs associated with distribution. Twede and Harte (2011) summarised the costs of inadequate packaging into five categories:

- *Transport* - added weight and space from excessive packaging increases fuel consumption and the number of or size of distribution vehicles required.
- *Storage* - oversized packaging requires more warehouse space.
- *Handling* - the cost of which depends on the unit load, the larger/heavier the unit load the higher the costs.
- *Inventory control* - is dependent on the ease of product identification.
- *Customer service* - relating to the quality of the product at its destination, its ease of opening and saleability, reduce quality can lead to reduced sales and/or lower product value.

While the risks associated with incorrect packaging have always been present, the growing diversity of distribution has meant that, for a company, the repercussions logistically, financially and with regard to their public reputation, are highly increased.

In addition to financial factors, environmental issues relating to over or under packaging are of increasing importance. Excessive packaging causes additional and unnecessary energy and material usage during the distribution cycle (INCPEN, 2008). However, insufficient packaging can lead to excessive product damage and waste (Olorunda and Tung, 1985). It has been recorded that approximately ten times more energy goes in to the production of a product than its packaging (Koojiman, 2000). Therefore, the negative environmental impact of product waste resulting from inadequate packaging is considerably higher than the impact of

slightly over-packaging a product to ensure its protection. Hence, when designing a packaging solution the life cycle of the product and packaging must be considered in order to reach an optimal balance. For example, a recent study into packaging of apples showed that each tonne of apples transported 'loose' in plastic reusable containers generated 67 kg more product waste than apples transported in non-biodegradable or biodegradable four packs. The energy used through the life cycle of apples distributed loose was 2818 MJ/tonne compared with 3104 MJ/tonne and 2419 MJ/tonne for non-biodegradable and biodegradable four-packs respectively (ERM, 2003).

According to the results of this study, the optimum packaging solution would not use the least packaging (loose option), but would be the four pack biodegradable option. This demonstrates the complexity of the packaged-product system and the importance of considering the entire life cycle of a product when designing a packaging solution.

Due to a lack of understanding of this complex balance, the food and drink sector has been heavily scrutinised because of apparent 'excessive' packaging (INCPEN, 2008). Unfortunately, a major focus is put upon luxury or gift items such as boxes of chocolates or Easter eggs where the primary packaging is as much a part of the purchase as the product itself. A consequence of the increased focus on removing or reducing packaging, is that very often the need for preserving and protecting goods, in order to reduce waste and maintain product quality for customer satisfaction and health and safety, is secondary or overlooked.

To meet the environmental challenges, many steps have already been taken in the optimisation of food and drinks packaging, such as reducing packaging weight, using recycled materials, using modified atmosphere packaging and improving seal integrity in order to increase the shelf life of products (WRAP, 2011). These include Kenco's 97% reduction in packaging, by using pouches to provide refills for their plastic jars (Kenco, 2012). Another example is the 75% reduction in the packaging for fresh chicken obtained by removing the base plastic tray (WRAP, 2010b).

Other changes made include modifications to the product itself. These include: the use of double strength cordial, to reduce the size of packaging by half (Tesco); and, using milk bags instead of bottles, reducing the packaging by 75% (Sainsburys). Notwithstanding such changes, there is still significant room for improvement (WRAP, 2011). Hence, in 2005 the government led Courtauld Commitment was established in the UK. For which the major UK supermarkets committed to reducing packaging waste across the grocery industry and delivering absolute reductions in packaging waste (WRAP, 2005). Phase two of the Commitment was established in 2010, whereby the major UK supermarkets agreed to reduce packaging by 10% within 3 years. Within the first year alone packaging was reduced by 5.1% (WRAP, 2010).

As a consequence of these financial and environment challenges and corresponding legislation, today's packaging must be designed to be 'just right', enabling product quality to be maintained in as economical and sustainable a manner as possible. A key stage in the packaging design process is simulated distribution testing (Hanlon et al, 1998). In order to optimise packaging – creating a 'just right' solution - the intended distribution cycle needs to be considered in full in order to evaluate the performance of a given packaging design.

1.1 Packaging and the Distribution Chain

The distribution cycle is a multi-staged process, which can be simplified to four stages: the suppliers; distributers; organisation (e.g. supermarket); and, the external customers (MacDonald, 1994). In reality the distribution cycle is far more complex, with each of the stages being represented by a number of sub-stages. Each can include multiple processes, packaging configurations, modes of transport and environmental conditions.

Packaged product damage can occur at each stage of distribution. The subsequent cost of this damage and the negative effect it may cause a company's reputation is a very real issue. A report for the food and beverage industry in USA stated that in 2005 the total cost of unsaleables equated to $2.05 billion US dollars, with 58% of

this being attributed to product damage during distribution. This equated to 1.05% and 1.17% of the value of gross sales for manufacturers and distributors, respectively (JIUSC, 2006).

There are a number of hazards that a packaged product may encounter during distribution that may lead to product damage, resulting in unsaleable goods. The packaged product's response to these hazards can vary during each stage in the distribution cycle. Paine and Paine (1992) summarised these hazards, which include:

- *Vehicle vibration and shock* - acting on the packaged product during transit which can lead to fatigue or stress damage.
- *Compressive loads* - over extended periods due to warehouse stacking and mechanical or manual handling errors, this can lead to impact damage.
- *Fluctuations in atmospheric conditions* - such as humidity, temperature and altitude, this can lead to loss of packaging integrity and accelerated product deterioration.
- *Interaction between packaged-products* - such as impact and scuffing.

It is self evident that the variety and intensity of these hazards depends on the distribution cycle, equipment used and the operators. It is also the case that each class of product, such as electronics, food and drink and hazardous waste, will require varying levels of protection depending upon the sensitivity to the conditions experienced during distribution. For these reasons the design of packaging for distribution is a complex task involving knowledge of the goods, the distribution cycle and the performance of the packaging material.

With such a high value of unsaleable goods in USA's food and beverage industry alone ($2.05 billion), the value of providing a product with a just right packaging solution, giving it adequate protection from the distribution environment, is apparent. By subjecting a packaging solution to accurate pre-distribution testing of the aforementioned hazards, this just right packaging solution, which optimises

material usage while providing adequate protection, can be created. This pre-distribution testing acts as a key aspect in the packaging design process.

1.2 Pre-Distribution Packaging Testing

Pre-distribution packaging testing, used to ensure that a proposed packaging solution is adequate, consists of a variety of atmospheric and dynamic tests, which simulate a range of anticipated hazards likely to be encountered (Hanlon et al, 1998). Several organisations provide standard test regimes for distribution packaging testing. These include but are not limited to: the International Safe Transit Association (ISTA, 2010); the American Society for Testing and Materials (ASTM, 2006); and, the International Standardisation Organisation (ISO, 2008); with the most commonly used being the ISTA and ASTM tests. Each provides details of how to perform physical and atmospheric tests, which have been constructed using averaged data collected in the field (Singh et al, 2007). Of particular importance is the mechanical/dynamic test used to simulate distribution vibration and shock. The severity of which has a significant influence on the volume and type of material used for protective packaging.

1.2.1 Vehicle vibration and Distribution Vibration Testing

The majority of mechanical damage in packaged products is attributed to vehicle vibration and shock. This damage arises as a consequence of either fatigue due to packaged-product resonance or the result of high level shock events (Garcia-Romeu-Martinez et al, 2008). Both forms of damage are possible due to the characteristically random non-stationary and non-Gaussian nature of vehicle vibration (Sek, 1996).

In addition to this, vehicle vibration is also uncertain due to its sensitivity to variations in vehicle parameters, such as: suspension type and stiffness; vehicle mass and payload; tyre stiffness; and, driver style. Changes in these parameters can affect the resonant frequencies, overall frequency content and severity of the vibration (Garcia-Romeu-Martinez et al, 2008, Singh et al, 2006). Furthermore,

variations in road construction and condition can lead to changes in a vehicle's input excitation and hence can influence the vehicle's response (Barchi et al, 2002). The complexity of vehicle vibration means that no two distribution journeys will produce exactly the same vibration profile. This has therefore made formulating a universal distribution test difficult.

Kipp (2008a) discussed the attempt made to overcome this issue, ultimately helping to build a test with statistical significance, meaning that the test can be said to be representative of the given journey. This is done by creating a vibration test simulation using the average of multiple journeys. This method underpins both the ISTA and ASTM standards (ISTA, 2010; ASTM, 2006).

1.2.2 Current Method of Vibration Testing

The current method of vibration testing, set out in both the ISTA and ASTM standards, formulates a random vibration simulation from a given Power Spectral Density (PSD) spectrum.

A PSD is calculated as the product of a signal's Fourier transform coefficients and its complex conjugate. Therefore while the coefficients of a signal's Fourier transform are complex, containing both the signal's magnitude and phase information, the PSD contains only real values. The PSD is therefore a representation of a signal's power (vibration energy) within different frequency bands.

To create a time domain simulation the given PSD must be inversed to find the Fourier coefficients. As the phase information was lost in the construction of the PSD, a random phase array must be applied to create complex Fourier coefficients. When doing this it is assumed that the phase array is random and uniformly distributed, ultimately resulting in a simulation signal with a normal distribution i.e. has a Gaussian distribution (Sek, 1996).

Each of the testing standards give a set of PSD spectra which are representative of a semi-trailer with an air ride suspension system, a semi-trailer with a leaf spring

suspension system and a pick-up and delivery vehicle on an 'average' distribution journey. In addition, the ASTM standards provide three intensity levels at which the test can be carried out, simulating gentle, moderated and harsh distribution environments.

Distribution journeys are typically long in duration, simulating the full length of a distribution journey in the laboratory is uneconomical and inefficient. Therefore the PSDs used to create simulations are accelerated, creating a simulation with increased amplitude and reduced duration that is equivalent to the actual distribution journey. This increase in amplitude of the PSD is inversely proportional to the decrease in test duration required (Shires, 2011). By creating an accelerated test the duration of simulations is greatly reduced and so too are the associated laboratory costs.

An example of the process is now given, whereby the PSD of the time domain vibration signal in Figure 2, where g = 9.81 m/s^2, is used to construct a simulation signal. The shock events within the vibration signal are clearly visible along with its varying intensity. These fluctuations in intensity make the vibration signal non-stationary.

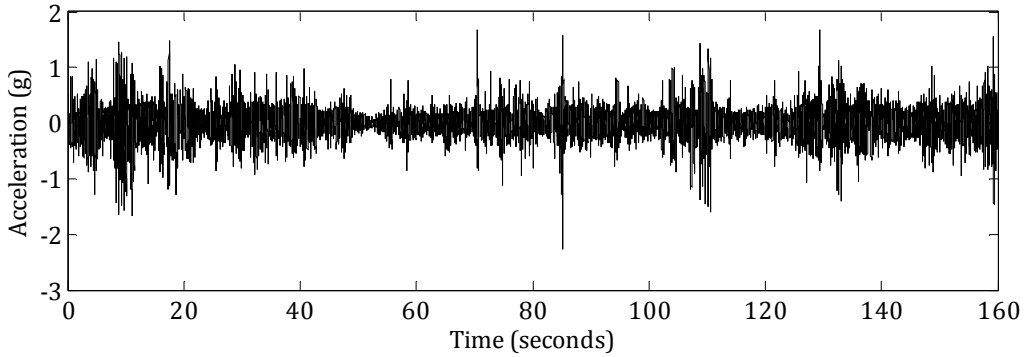

Figure 2: Example time domain vibration signal

The PSD corresponding to the signal in Figure 2 is presented in Figure 3. In addition to the actual signal's PSD, the accelerated version of the PSD is also given.

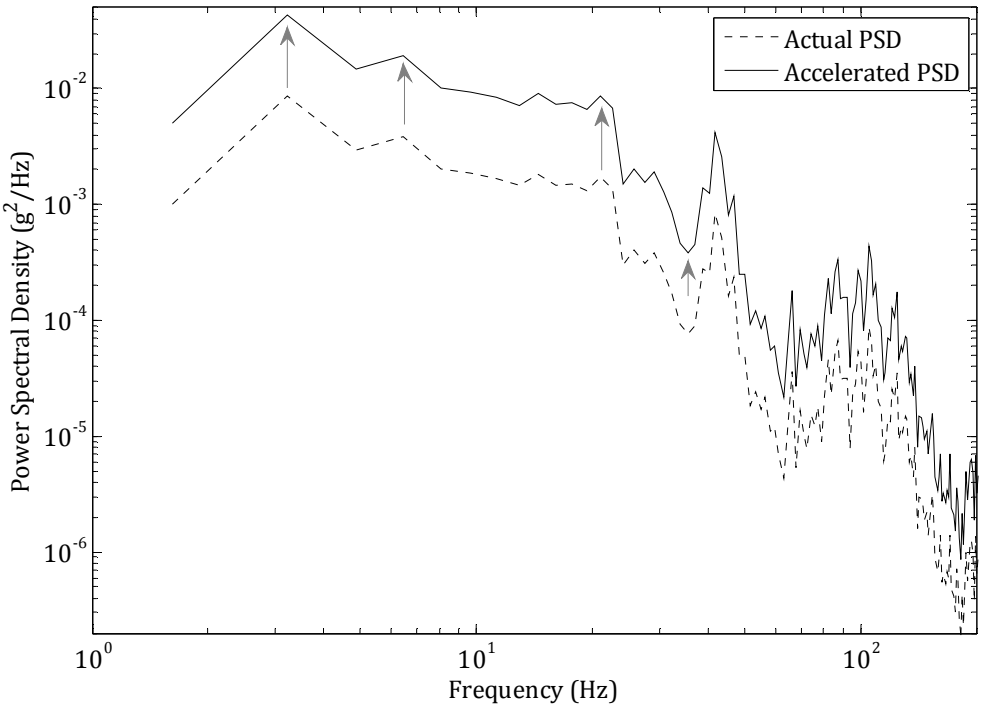

Figure 3: Actual PSD and accelerated PSD for the vibration signal in Figure 2

The simulation signal, constructed from the accelerated PSD, is given in Figure 4. It is clear that the duration of the simulation (30 seconds) is significantly less than the original signal's (160 seconds). The intensity of the simulation appears to be constant and doesn't fluctuate, unlike the original signal, where the acceleration fluctuated significantly with time.

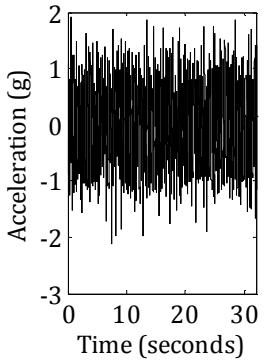

Figure 4: Accelerated random vibration simulation constructed from the accelerated PSD in Figure 3

Using this method to construct a vibration simulation, results in a simulation that has the same overall frequency content and acceleration energy as the original signal, but has a much shorter duration. Though, because the simulated signal is constructed from averaged data it is both stationary and has a Gaussian

distribution. The simulation can therefore be considered an accelerated Gaussian signal that is equivalent (in overall test intensity and power spectral density) to the original signal, but can't be considered an accurate representation of actual vehicle vibration.

The final stage of constructing the simulation is carried out using a vibration table. The user inputs the specified PSD and test duration into to the vibration table controller and the controller creates the simulation through the inverse process, and executes the simulation on the vibration table. Two examples of vibration tables are given in Figure 5, where (a) is a hydraulic multi axis simulation table (MAST rig) and (b) is a hydraulic single axis vertical vibration table.

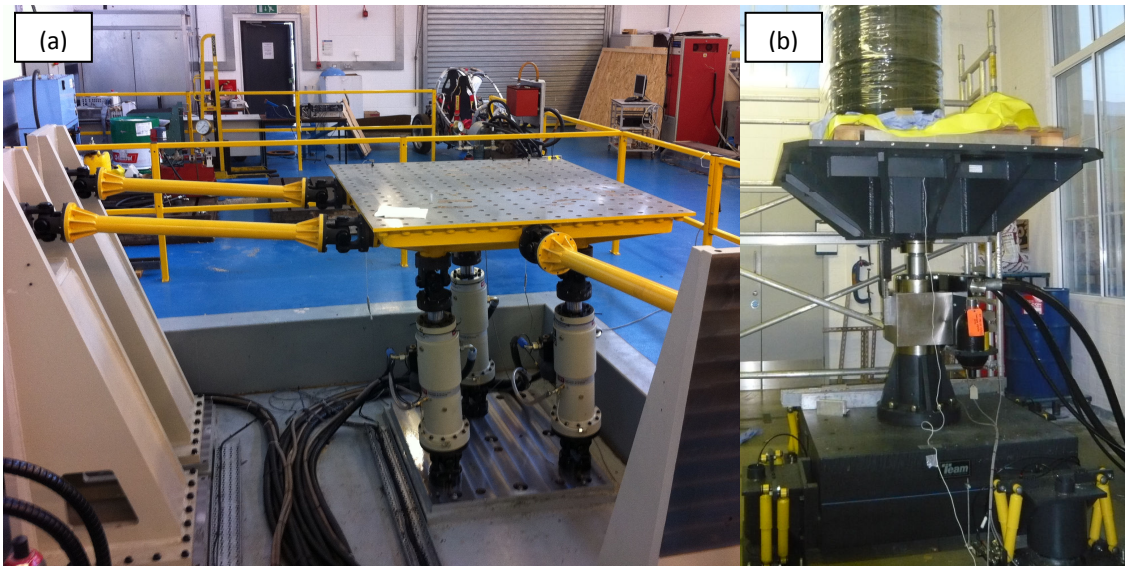

Figure 5: (a) MAST rig, (b) single axis vertical vibration table

As previously mentioned, the PSD is an average representation of the signal, and therefore when used to create a vibration signal, will construct an averaged signal, which is hence Gaussian. Therefore by using this method it is assumed that the original signal also has a Gaussian distribution. In reality vehicle vibration is highly non-Gaussian; this assumption is therefore incorrect and leads to errors in the accuracy of the simulation, with the more non-Gaussian the signals distribution the greater the error. Secondly, as the PSD is assumed to represent the entire journey, not an average, the vehicle vibration is considered to be stationary, e.g. the vibration intensity is constant. The resulting simulation is therefore stationary. In reality vehicle vibration is highly non-stationary. The consequence of these

assumptions and the resulting inability to recreate realistic vibration can lead to conservatism when considering packaging design.

The combination of increased global distribution and the ever-increasing awareness of the need for environmental, social and economic sustainability, requires packaging solutions to be designed 'just right'. A key part of this involves designing the packaging to meet the requirements of the specific product's distribution.

Unfortunately, as previously stated the current method of simulation makes incorrect assumptions regarding vehicle vibration. This has led to recent criticism regarding the appropriateness of the test method for simulation of vehicle vibration during distribution. Consequently, this has led to a reduced confidence in the test's ability to meet the needs of the packaging testing industry (Rouillard and Sek, 2000; Kipp, 2008a).

Aware of this issue, consultancies such as Smithers Pira, offer the ability to carry out vibration data acquisition on a specified distribution route. This enables vibration testing to be carried out using a more accurate representation of a given distribution journey and environment. However, formulating test simulations in this way is rare due to the associated time and cost inefficiencies. Additionally, whilst it allows a simulation to be formulated from representative vibration data, creating the simulation via the current method still produces an unrealistic simulation.

For these reasons, and in order to improve packaging design, Smithers Pira have identified a need for investigating new and improved methods for simulating vehicle vibration, and creating a representative test that does not require onerous data acquisition.

With a need for improved accuracy in testing, it is necessary to create a new and improved vibration testing regime, that more realistically simulates vehicle vibration in terms of the distribution environment, and provides a better representation of vehicle vibration. Importantly, for a new test regime to be

operable in all existing laboratories, the simulation method adopted must be compatible with all existing laboratory simulation table controllers. To achieve this, the method must incorporate the PSD approach for constructing random vibration simulations.

1.3 Creating an Improved Test Regime for Distribution Packaging Testing

As has been previously stated there is a need to research and create an improved vibration testing regime, that enables the creation of an accurate representation of the intended distribution environment, and therefore reduce the need for conservatism in packaging design. In meeting this need two challenges must be addressed. The first is to accurately represent the intended distribution environment, including the distribution journey and vehicle parameters. The second involves the creation of a simulation method that enables the realistic recreation of vehicle vibration and accounts for uncertainties.

Based on these challenges the aim of this thesis is to create an improved method for simulating vehicle vibration for the testing of distribution packaging, with a particular focus on building a representative test regime generated from an understanding of road conditions and vehicle dynamics.

In accordance with the aim, and previously stated challenges, two Research Questions are developed:

> **RQ1.** How can the effect of a vehicle's parameters and its journey conditions on the vehicle's vibration response be characterised?
>
> **RQ2** How can the simulation of vehicle vibration for packaging testing be improved so as to create a more representative test regime?

In order to explore the research questions seven objectives have been developed:

1. Evaluate current packaging vibration test methods through comparison with actual vehicle vibration in order to enable the identification of critical parameters.

2. Review improved methods that have been proposed for vibration simulation in order to establish their benefits and drawbacks.

3. Propose a more realistic test simulation which incorporates the key characteristics of vehicle vibration.

4. Establish the key journey and vehicle parameters that characterise vehicle vibration and propose a method to account for their influence on vehicle vibration.

5. Create a database of vehicle vibration data and propose a method by which this data can be used to approximate an alternative distribution journey.

6. Create an improved test regime with an integrated vehicle model which allows for the established variations in vehicle and journey parameters to be considered.

Table 1 defines which objectives satisfy the Research Questions. The Thesis chapters that relate to each objective are identified and the method by which each objective will be achieved is discussed.

Table 1: Research Questions, objectives and corresponding Thesis chapters

RESEARCH QUESTIONS	OBJECTIVES	METHODOLOGY	CH
How can the effect of a vehicle's parameters and its journey conditions on the vehicle's vibration response be characterised?	1. Evaluate current packaging vibration test methods through comparison with actual vehicle vibration in order to enable the identification of critical parameters.	Test simulation vibration will be compared with actual vehicle vibration, in order to establish similarities and disparities. The simulation method's underlying assumptions are then critiqued through a review of the theory upon which it is based.	**4**
	2. Review improved methods that have been proposed for vibration simulation in order to establish their benefits and drawbacks.	A critique of the various proposed improved simulation approaches is carried out. By carrying out a correlation study each simulation approaches ability to simulate actual vehicle vibration can be evaluated.	**4-6**
	3. Propose a more realistic test simulation which incorporates the key characteristics of vehicle vibration.	By considering the true nature of vehicle vibration alongside the advantages of proposed improved simulation approaches a new simulation method can be created. A correlation study then enables the evaluation of the methods ability to recreate vehicle vibration.	**7-8**
How can the simulation of vehicle vibration for packaging testing be improved so as to create a more representative test regime?	4. Establish the key journey and vehicle parameters that characterise vehicle vibration and propose a method to account for their influence on vehicle vibration.	A review of previous literature allows vehicle parameters and their effects on a vehicle's vibration response to be evaluated. Additionally, computational simulation of these parameters via a vehicle model is allows the effect small changes in these parameters have on the vehicle's response to be considered.	**3, 9**
	5. Create a database of vehicle vibration data and propose a method by which this data can be used to approximate an alternative distribution journey.	The effect variation in distribution journeys has on vehicle vibration response can be evaluated through previous literature. Based on this, a method of constructing a vibration test that is representative of a specific distribution environment can created and validated through a case study example.	**2, 3, 10**
	6. Create an improved test regime with an integrated vehicle model which allows for the established variations in vehicle and journey parameters to be considered.	By bringing together the improved simulation method with the method of creating a representative journey, an improved test regime can be constructed. By carrying out a final case study evaluating the use of the improved test regime its ability to simulate a specific distribution journey can be evaluated.	**11**

1.4 Research Methodology/Approach

The methodology adopted in this Thesis included an extensive critiquing of both: the established method of simulating vibration, set out in the current distribution packaging testing standards; and, proposed improved approaches; through empirical testing, establishing limitations and benefits of each method. This has then been used to set the requirements for a new approach. The new approach is then developed theoretically and verified through a case study.

In addition to this, an evaluation of distribution vehicle vibration, considering both the vehicle and the journey is carried out, identifying the critical parameters that shape the vehicle's response. Using this information an improved method for building representative simulations is developed. By combining this with the improved simulation method a new improved test regime is presented. A final case study is then used to validate this improved test regime.

1.5 Structure of the Thesis

In the first part of *Chapter 2* the area of packaging is examined, including its purpose, classification, the materials used in packaging and the theory behind the packaging design process. The second part then details the process of distribution and the distribution chain, highlighting potential hazards and indicating the need for appropriate packaging solutions. With the need for packaging testing emphasized, distribution packaging testing is then discussed. Included in this is an overview of the complete testing cycle within current testing standards.

Chapter 3 focuses on the particular hazard of vehicle vibration. The nature of vehicle vibration is described as well as its key characteristics. Following this, an in-depth review of how a vehicle's vibration response is defined by its parameters such as speed, suspension, and mass is conducted.

An in-depth critique of the current method for vibration testing of distribution packaging is provided in *Chapter 4*, followed by a review of proposed improved simulation methods, including advantages and disadvantages of each method. Alternatives are considered, including time-frequency analysis tools and multiple degrees of freedom testing.

In *Chapter 5* a case study, that uses the damage mechanism of scuffing to evaluate each simulation methods' ability to recreate vehicle vibration, is presented in order to establish the most appropriate strategy.

Chapter 6 contains a review of the use of multiple degrees of freedom (MDOF) simulation, previous studies are discussed and a case study evaluating the use of MDOF compared with single degree of freedom testing is presented.

The use of time-frequency analysis techniques in place of Fourier analysis is considered in *Chapter 7*. The advantages of each technique are then discussed.

Following the review of the current method and proposed improved simulation approaches, C*hapter 8* includes a new technique for vibration testing - Wavelet decomposition. Here a detailed description of the proposed improved simulation technique is given. An example application is then presented. A case study evaluating the appropriateness of the Wavelet decomposition method is then presented. Here a correlation study using the damage mechanism of scuffing is carried out and the results are compared with those presented in Chapter 5.

Chapter 9 considers the vehicle's parameters that affect the shape of its vibration response. The use of computational vehicle modelling to simulate a given distribution vehicle's vibration response from a road profile, is then presented, along with an inverse vehicle model for predicting road roughness from vehicle vibration. A sensitivity analysis on vehicle parameters is carried out and the limitations of using the model are then considered.

Chapter 10 considers Research Question 2 and deals with the variation in journey parameters. Following this, a method of decomposing a distribution journey and

constructing an equivalent simulation journey based on historical vibration data stored is presented, leading to the proposition of a journey database.

In Chapter 11 the journey database and the wavelet decomposition method are combined to create the improved test regime. A case study is then used to demonstrate the appropriateness of the test regime.

A discussion and conclusions are then presented in *Chapter 12* and areas of future work are highlighted.

2 DISTRIBUTION AND PACKAGING

Packaging is fundamental to distribution. It has been a key facilitator in the global distribution of goods. Through advances in packaging materials it has allowed for extended distribution times and successful distribution through varying climatic and physical conditions. The processes of packaging design are complex, so as to meet several main requirements relating to: ergonomics, logistics, sustainability, safety and marketing (Azzi et al, 2012). Furthermore, there are three different categories of packaging: primary; secondary; and, tertiary; each of which fulfils a different role in the distribution chain and can be manufactured from one of four main packaging materials: glass; metal; plastic; and, cardboard.

The logistical requirements of packaging are there to ensure that the needs of the complex process of distribution are met. This can consist of numerous stages and hazards, all of which must be considered alongside the properties of the product during the design process.

The requirements and common forms of packaging, the distribution cycle in the context of the food and drink sector and the possible hazards throughout distribution are discussed.

2.1 The Purpose of Packaging

Packaging design is a complex process that must account for the multiple needs of the product, distributor, retailer and customer. Azzi et al (2012) identified five main categories, the needs of which must be considered in order to create a successful packaging solution. These categories include: ergonomics, logistics, sustainability, safety and marketing. These overlap and are governed by various legislation and standards. Consequently, this means that all categories must be dealt with collectively during packaging design in order to achieve an appropriate design solution.

2.1.1 Ergonomics

IEA (2003) define ergonomics as: '*the scientific discipline concerned with the understanding of the interactions among humans and other elements of a system, and the profession that applies theory, principles, data, and methods to design in order to optimize human well-being and overall system performance*'.

In the distribution of goods there are many stages that include handling or lifting. As a consequence, for health and safety and an efficient distribution system, the ergonomics of the process must be considered. Aspects of packaging which affect ergonomics during distribution, include weight, dimensions and material (Azzi et al, 2012). International standards exists which impose limitations and guidelines regarding lifting and carrying, pushing and pulling and handling of low loads at high frequency. These include ISO 11228 parts 1-3 (ISO, 2009a; ISO, 2009b; ISO, 2009c).

The ergonomics of packaging also have to be considered in terms of the consumer. In the UK 67,000 people visit hospital for a packaging related injury each year (Winder et al, 2002). Many injuries occur whilst trying to open packaging. Much research into the 'openability' of packaging has been carried out (Yoxall et al, 2006; Voorbij and Steenbekkers 2002; Winder et al, 2002). Consideration for aspects such as 'openability', the ability to grip the packaging and the packaged product's weight and dimensions, must be considered to ensure an ergonomic packaging solution.

2.1.2 Logistics

Logistics apply to: '*...the process of planning, implementing, and controlling the efficient, effective flow and storage of goods, services and related information, from the point of origin to the point of consumption, for the purpose of conforming to customer requirements*' (CLM, 1998).

Logistics are concerned with the transportation, handling, storage and processing of products from the manufacturer to the point of sale. A product's packaging can

have a direct effect on logistical process efficiency and/or effectiveness. Therefore, consideration of packaged product shape and size must be made to ensure efficient use of distribution space.

Packaging must also meet the requirements of the distribution environment, ensuring it offers the product adequate protection from hazards during transportation and storage. Unitization is often used to help facilitate the logistical process, allowing multiple packaged products to be transported and stored at once so as to reduce handling (Rushton et al, 2010).

2.1.3 Sustainability

Sustainability involves: '*meeting the needs of the present without compromising the ability of future generations to meet their own needs*' (Brundtland, 1987)

Sustainability is often divided into three areas (Carter, 2008):

- *Environmental* - relating to material usage and waste.
- *Social* - how people interact with the packaging.
- *Economic* - the financial cost of packaging in terms of material, waste and the logistical process.

In short, for a packaging solution to be sustainable it must use minimal material that: is reusable or recyclable; meets the needs of the customer; and, helps distribution in order to minimise financial costs.

Environmental

Of the three areas, environmental sustainability is the most publicly discussed, with packaging being considered a major source of pollution in Europe (Bech-Larsen, 1996). UK market research found that 74% of people interviewed believed that companies should invest more in sustainable packaging (Mintel, 2012). This growing public awareness along with a need to reduce packaging waste and a

greater increase in knowledge on the subject of sustainability, has led to the introduction of directives and regulations including:

- *Packaging and Packaging Waste Directive 94/62/*EC (EPC, 1994)

Introduced by the European Commission in 1994, the directive endeavours to: keep packaging volume and weight to a minimum while maintaining levels of product safety, hygiene and acceptance; allow maximum possible reuse or recovery of packaging; and, minimise the amount of noxious or hazardous substances from packaging getting into emissions, ash or leachate from incineration or landfill.

- *Courtauld Commitment Phase1 and 2* (WRAP, 2005; WRAP, 2010)

The Courtauld Commitment was created to support the UK policy goal of a *'zero waste economy*' and to help towards the Climate Change Act objective to reduce greenhouse gas emissions by 34% by 2020 and 80% by 2050. The major UK supermarkets and some UK producers committed to Phase One of the agreement in 2005 with the aim of designing out packaging waste growth by 2008, deliver absolute reductions in packaging waste by 2010 and reducing food waste to 155,000 tonnes by March 2010.

As a result of these regulations there is a greater emphasis on packaging and waste reduction. Therefore when designing a packaging solution its lifecycle needs to be considered from manufacture to end use i.e. whether the packaging is reused, the material is recycled, or, if it becomes waste, whether it goes to compost, landfill or incineration. These options are now discussed.

- *Reuse or return* - in some cases the packaging used is in a condition where it can be reused e.g. carrier bags can be reused by the customer or home delivery plastic totes can be sent back for reuse. A specific example of reusable packaging is fibreboard trays used to deliver products by Riverford Organic (Riverford, 2012). One issue with this approach is that, the reuse of the carrier bags or the return of the fibreboard boxes is the customer's responsibility and therefore much of this packaging is wasted.

- *Recycle* – for items such as glass and aluminium, recycling is considered the best option. Recycling the material has major energy saving benefits when compared with the processing of virgin or new material. It was stated by DEFRA that in 2008 the UK recycled almost two-thirds of all packaging amounting to 6.6 million tonnes. Within the EU-15 the amount of packaging waste recycled increased from 46% to 62% between 1997 and 2008 (EUROSTAT, 2008).

- *Compost* – for materials that are biodegradable compost is the preferred option rather than sending the waste to landfill. This is also the preferred option for wasted food items such as fresh fruit and vegetables.

- *Landfill* – for the EU-15, between 1997 and 2008 the amount of packaging waste that was sent to landfill decreased significantly from 48% to 29% (EUROSTAT, 2008).

- *Incineration* – for energy recovery and generation has become slightly more popular for the European packaging waste industry. In 1997 only 7% of the EU-15 packaging waste was incinerated compared with 9% in 2011 (EUROSTAT, 2008).

Social

Social sustainability aims to '*promotion a democratic, socially inclusive, cohesive, healthy, safe and just society with respect for fundamental rights and cultural diversity that creates equal opportunities and combats discrimination in all its forms*', EUROPEN (2009).

Social sustainability relates to social well-being and the interaction of people with packaging. In terms of packaging this can cover a multitude of areas including:

- conditions for workers producing, handling and distributing packaging
- protecting public health through protection from hazardous products and product preservation

- preservation of the environment for people through reduced product waste and the use of environmentally friendly packaging.

Economical

A good packaging design not only means that a product is well protected, but additionally that it will facilitate efficient and economical distribution. Over packaging leads to greater material costs, distribution weight and space, which in turn leads to the use of more fuel and larger or additional vehicles. There are many costs associated with distribution (Coles and Kirwan, 2011):

- *Transport and storage* – the size and weight of packaged products ultimately affects the storage and transport requirements and hence the cost. Larger items require more space for storage and larger and/or a greater number of transport vehicles. Additionally, the heavier the load the greater is the fuel consumption of a vehicle.

- *Handling* – handling costs are dependent on the unit load - the greater and heavier the load the greater the cost.

- *Inventory control* – the packaged products need to be easily identifiable thereby reducing the length of time the inventory takes.

- *Customer service* – the better the packaging protects the product, the better its condition when it reaches the customer leading to a higher level of customer satisfaction, more repeat business and less returns.

- *Environmental impact* – the costs associated with the materials used with regards to manufacturing, preparation for reuse and disposal charges.

Each of these costs needs to be considered in order to create an economically sustainable packaging solution.

2.1.4 Safety

Product safety and protection in terms of chemical, mechanical and biological hazards and risks has, historically, been the key consideration in the packaging design process (Hellstrom and Saghir, 2007). The process of distribution can be long with multiple stages that can include a variety of transport modes, geographical locations and varying climatic and physical conditions. It is critical that packaging is designed to protect the product from hazards associated with these conditions.

The food and drink industry is an area in which the benefit of packaging is especially evident. Each year 40% of the UK's food comes from imports, the majority of which are fresh goods such as fruit, vegetables and meat (Office, 2008). The delicate nature of these products makes them prone to distribution damage, the likelihood of which is increased due to extended distribution journeys.

2.2 Marketing

For most products, primary packaging is an important marketing and promotional tool for the product and the brand. It has been referred to as '*the salesman on the shelf*' (Pilditch, 1972). Today, with so much choice, a brand must ensure prominence to the customer. In some cases the packaging is so critical that it becomes part of the product. For example, WPO (2008) states that 48% of the product cost for cola soft drink is in the packaging as it plays a key role in product and brand identification. Packaging design is also important to consumers. A survey revealed that 73% of those interviewed rely on packaging to help them select products (Wells et al, 2007).

Meyers and Lubliner (1998) suggest that in order for a packaging solution to be a successful marketing tool it must:

- make the product stand out among competitors

- identify the product and the brand
- make the product appealing
- communicate product attributes and information
- identify product specific factors such as varieties, flavours, sizes, etc
- enhance the product making it ergonomically appealing.

2.3 Categories of Packaging

In order to meet its numerous requirements, packaging is typically formed of several layers, each of which serves a specific purpose. The types of packaging can be divided into three categories: primary; secondary; or, tertiary. The latter two form the distribution packaging. Hellstrom and Saghir (2007) provide an illustrated explanation of distribution packaging and this is shown in Figure 6.

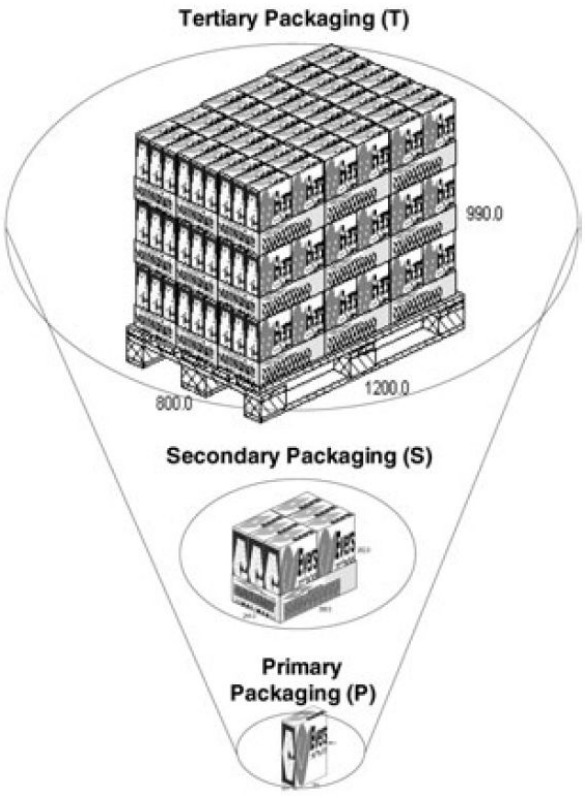

Figure 6: Example primary, secondary and tertiary packaging (Hellstrom and Saghir, 2007)

Here the primary packaging consists of a single container, which is then shrink-wrapped in a fibreboard tray of six to form the secondary packaging. This is then shrink-wrapped and palletised to form the tertiary packaging. The definition of each is now given.

2.3.1 Primary Packaging

Primary packaging is that which is in direct contact with the product (Hellstrom and Saghir, 2007). In Figure 7 examples of primary packaging and the materials used are given.

Figure 7: Examples of primary packaging

Primary packaging forms a barrier between the product and any hazards in the external environment (Levy, 1999). In the case of perishable goods, such as those

illustrated in Figure 7, this barrier is essential in preserving the product and preventing degradation. This helps maintain the product's integrity, quality and safety, resulting in minimal product loss during the distribution process which can take several weeks (Boonruang et al, 2012). Although the primary packaging requires certain protective capabilities, for most products it is a major marketing tool. Examples of primary packaging materials and their properties are given in Table 2. For each an example product is given, the packaging type and material are given along with its properties and reasons for use.

Table 2: Primary packaging examples

PRODUCT	PACKAGING	PROPERTIES
Wine bottle	Glass bottle	Chemically inert therefore it doesn't react with the product. Impermeable to gases, preventing oxidation. It is strong, durable and transparent allowing the product to be well protected and visible to the customer. Promotes an image of quality for the product which is pleasing to the customer.
Coca-cola© can	Aluminium	Light weight. Impermeable to moisture, gas and light, preventing damage and preserving the product. Allows for pressurisation, preventing the product from going flat. Highly recyclable.
Box of chocolates	Cardboard and plastic (inner tray)	Stiff, giving the packaging a rigid structure. Printable surface enabling colourful packaging. Low cost packaging solution. Versatile, therefore easy to form in to complex shapes and structures. The plastic inner tray adds to the rigidity of the package, it also prevents chocolates from damage by separating and protecting them.
Apple four pack	Plastic shrink-wrapped Carton board tray	Protects the product from pests and moisture. Provides regimented way of product stacking and storage which protects products from surrounding products, preventing inter product damage.
Packaged meat	Plastic film	Provides high shrinkage allowing it to collapse around product shape. Excellent protective barrier properties preventing oxygen and moisture damage. Extends product shelf life.

2.3.2 Distribution Packaging

Distribution packaging, sometimes referred to as logistic or transport packaging, is used to preserve and protect products in distribution. Included in this category are: shipping containers; interior protective packaging; and, any unitizing materials (Marsh, 1997).

a. Secondary Packaging

The secondary packaging is a protective packaging that encases and unitizes the primary packaged product. It helps to ease product handling, and maintain quality and integrity of the primary packaged product by protecting it from both the distribution environment and possible interactions with other products (Levy, 1999). The most common type of secondary packaging is the corrugated paper board boxing, its quality and grade is dependent on the protection required. Additional product protection is provided by: liners; flutes; and, cushioning materials. These not only add additional protection during distribution, but also give additional compressive strength, giving structural strength during stacking and unitization (Hanlon et al, 1998). An illustrated example of secondary packaging is given in Figure 8. The product being packaged is wine, the primary packaging is the glass bottle, and the secondary packaging consists of a corrugated paperboard box with internal flutes which prevent products from interacting with each other, and provide additional structural strength enabling the stacking of boxes.

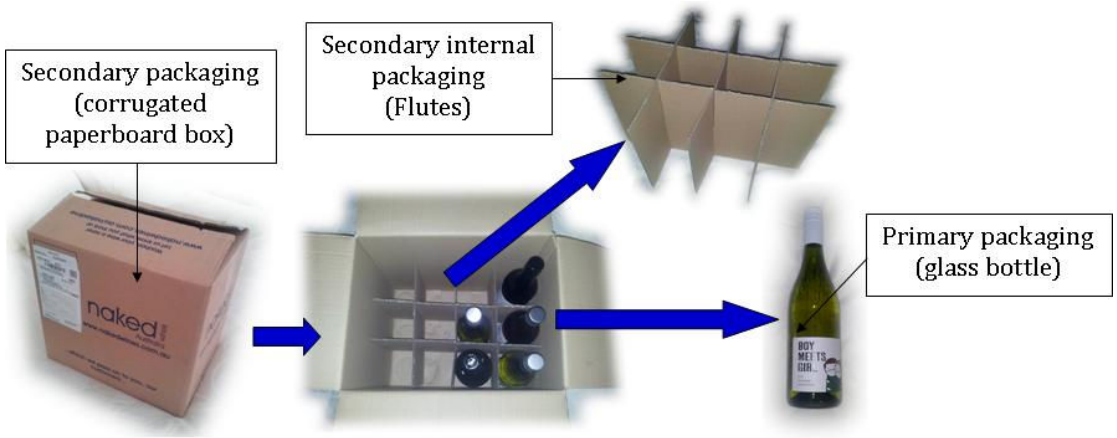

Figure 8: Example of secondary packaging for wine bottles

In some cases, the secondary packaging forms part of the retail packaging. An example of this is food items that are unitized in 'shelf ready' or 'display ready' packaging. Examples of which are given in Figure 9. In this case, whilst providing protection to the primary packaged product and facilitating distribution, the

secondary packaging must also be preserved so that it is presentable for in store display.

Figure 9: Examples of secondary packaging (a) Display ready packaging (b) Shelf ready packaging (http://www.packaging-int.com)

Further types of secondary packaging include: shrink-wrapped trays used to unitize packaged products and ease handling for the retailer; and, corrugated board boxes which hold several items but do not form part of the sales packaging, e.g. box used to hold six/twelve wine bottles.

b. Tertiary Packaging

Tertiary packaging eases product handling and transportation by unitizing secondary packaged products, protecting them from transport and handling hazards and adverse weather conditions (Ek et al, 2009). By the time the product reaches the point of sale the majority of tertiary packaging has been removed, consequently it tends not to form part of the sales or marketing strategy. In order to help distribution, tertiary packaging can contain information regarding the product, its point of origin or destination.

Typical forms of tertiary packaging include (Rushton et al, 2010):

- *Pallets* – where the packaged products are stored uniformly on top of the pallet and are shrink-wrapped to give structural stability. Pallets allow the

use of forklifts for mechanical handling without risking damage to the product.

- *Cage and box pallets* – made of steel or plastic with high mesh sides to contain the packaged products.
- *Roll-cages* - made from steel they consist of a mesh cage with shelves inside to stack packaged products. These are often used during retail distribution as they allow for mixed loads to be safely stored.

Figure 10: Examples of tertiary packaging

2.4 Packaging Materials and Their Uses

Material selection for packaging depends on the product need. This includes: protection; preservation; presentation and decoration; and, economics (Twede and Goddard, 1998). The percentage of packaging materials used by consumption for the world and the UK is given in Figure 4 (a) and (b), respectively.

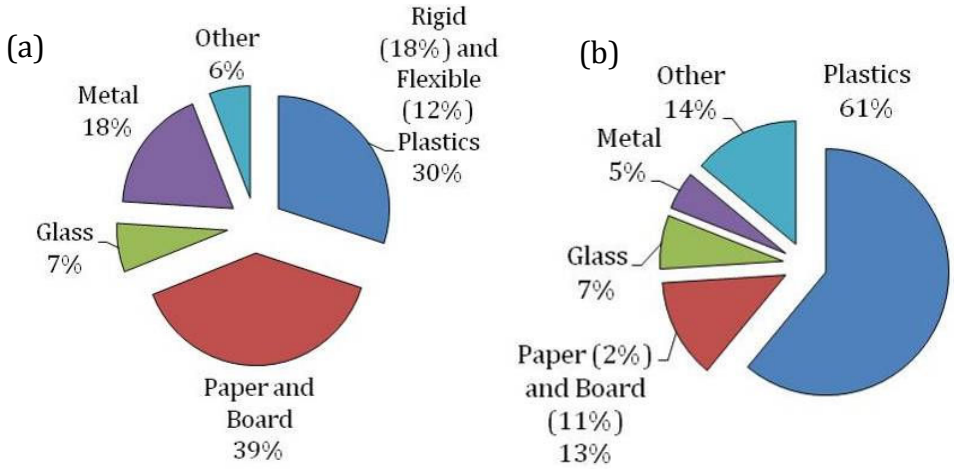

Figure 11:(a) World packaging consumption by material, 2003 (WPO, 2008) (b) UK Food primary packaging by material, 2011 (Mintel, 2012)

For distribution packaging paper and board, and plastics are most commonly used. These materials are now discussed with respect to their protective capabilities and typical use.

2.4.1 Paper and Board

Paper and board materials are the most commonly used in packaging holding 39% market share, with corrugated fibreboard box shipping containers forming 40% of this (Twede and Goddard, 1998). Their popularity is due to rigidity, stacking strength and ease of storage and distribution. Consequently they provide good product protection. There is also the added benefit of its recyclability, though strength degrades when recycled. There are several forms of paper packaging each designed to have specific properties such as high strength or oil/water resistance (Twede and Goddard, 1998).

Paperboard is less commonly used in primary food packaging, accounting for only 13%. Its poor barrier properties mean it is not suitable for use to protect perishable goods from deterioration over the, sometimes, long duration distribution cycles. It is more frequently used in dry food packaging prior to which it is often treated in some way to improve its properties i.e. waxed, coated or laminated (Marsh and Bugusu, 2007). Other forms of wood based packaging used

for distribution are pallets, which are typically combined with shrink-wrap plastic to restrain units (Hanlon et al, 1998).

Some examples of paper and board packaging are given in Figure 12, these include secondary packaging, primary packaging and protective cushioning/filling material.

Figure 12: Examples of paper and board packaging

2.4.2 Plastics

Plastics are the second most common materials used in the packaging sector, holding 30% market share, with 61% of the UK's food packaging being plastic. Hanlon et al (1998) states the reason for its popularity is: ease of shaping; low density; resistance to breakage; brilliant colours; and, transparency. In addition to this plastics are relatively low cost.

There are numerous types of plastic available, some widely used plastics are discussed in (Marsh and Bugusu, 2007), they include:

- ***Polyethylene terephtalate (PET)*** – popular for use in food packaging particularly carbonated beverage bottles. This is because it acts as a good barrier between the product and external gases and moisture, and it has good resistance to heat, oils, solvents and acids.

- ***Polyethylene (PE)*** – Polyethylene is the most widely used mass produced plastic. Piringer and Baner (2008) discuss the three common forms of PE: Low density PE (LDPE), linear LDPE (LLDPE) and high density PE (HDPE). All of which have good chemical stability, but their mechanical properties vary:

    - *LDPE* – is used for films or bags due to its soft and flexible nature. It also offers good transparency. It has a low softening and melting point which also makes it good for heat sealing.

    - *LLDPE* – is also used for films, but as it stiffer, tougher and has better barrier properties than LDPE, the film can be made much thinner and therefore less material is used. It also provides improved transparency to LDPE.

    - *HDPE* – is much stiffer, harder and stronger than LDPE but is much less translucent. It is therefore commonly used to for packaging such as milk bottles, bleach and detergent bottles, or, shampoo bottles. It is also used in plastic totes or crates for distribution packaging (Figure 13).

- ***Polypropylene (PP)*** **–** is typically used for margarine tubs and microwavable food trays and containers. It is a tough and flexible plastic which is reasonably translucent. Additionally, it provides a good moisture barrier, but poor oxygen barrier. It has a higher softening point than PE.

- ***Polystyrene (PS)*** **–** Hard, transparent, high brilliance, it has high resistance to many chemicals, and good thermal and moisture resistance. It has a high permeability to gases and is therefore typically used for short shelf life products such as yoghurt pots or egg cartons. Expanded PS (EPS) is used as a protective filler packaging on many products, such as electronic items, due to its cushioning properties, its dimensional stability and its mouldability, allowing it to be custom made to fit the product easily.

- ***Polyvinyl Chloride (PVC)*** **–** is heavy, stiff, ductile transparent and has medium strength. It has excellent resistance to chemicals and is typically used in medical and other non-food packaging, but is sometimes used in films and bottles for food. It is easy to thermoform and is therefore used for meat or pharmaceutical blister packaging.

Examples of types of plastic primary packaging were given previously in Figure 7. Additional examples of plastic distribution packaging are given in Figure 13.

Figure 13: Examples of plastic packaging

2.5 The Packaging Design Process

The design process for packaging is generally accepted to comprise of six steps (Marsh, 1997):

Step 1: Identification of product characteristics

The specification of the product needs to be defined such as its size, weight and fragility, in order to understand the protective requirements of the product.

Step 2: Identify marketing and distribution requirements

Details about the product distribution process including frequency, density, units per container, modes of transport, distribution channels and any specific handling or storage capabilities required of the packaging, are required.

Step 3: Identify environmental (dynamic and atmospheric) hazards

Evaluation of the distribution environment's atmospheric and dynamic conditions and hazards such as temperature and humidity fluctuations and extremes, transit vibration and shock, handling errors and warehousing and storage conditions.

Step 4: Consideration of packaging and packaging material

All packaging and unitization methods are considered allowing appropriate material selection.

Step 5: Packaging specification generated

The specification allows a suitable packaging solution to be designed that meets the needs of the product, including: the container; interior packaging and, unitization packaging.

Step 6: Performance testing of packaging solution

An iterative approach is taken to the packaging design process so that the packaging can be refined and retested until the appropriate level of protection is obtained. In some cases it can prove more cost effective to redesign the product rather than the packaging if the cost of damage to the product is

significant. Further to this, developing the product packing method to give maximum protection and stability is also an important part of improving the packaging design.

Throughout the design process all work should be documented. This includes a specification detailing the identified requirements of the product-package and all of the testing carried out.

The performance testing carried out in Step 6 is a vital part of the iterative design process. By testing packaging prior to distribution, it is possible to ensure the packaging provides suitable protection for the product, therefore minimising the risk of product loss or damage during distribution.

2.6 The Distribution Cycle

To fully understand the possible hazards a packaged product will face during distribution, the cycle of distribution needs to be evaluated from point of production to the end consumer.

The conditions for distribution will vary depending on product complexity, place of manufacture and end location. For the majority of products a general distribution cycle can be followed. Figure 14 illustrates this simplified distribution cycle as described by (Hellstrom and Saghir, 2007). This process takes the product from the manufacturer, to one or multiple distribution centres, where the unit packaging is broken down into the required orders, and then to the retail store and end consumer.

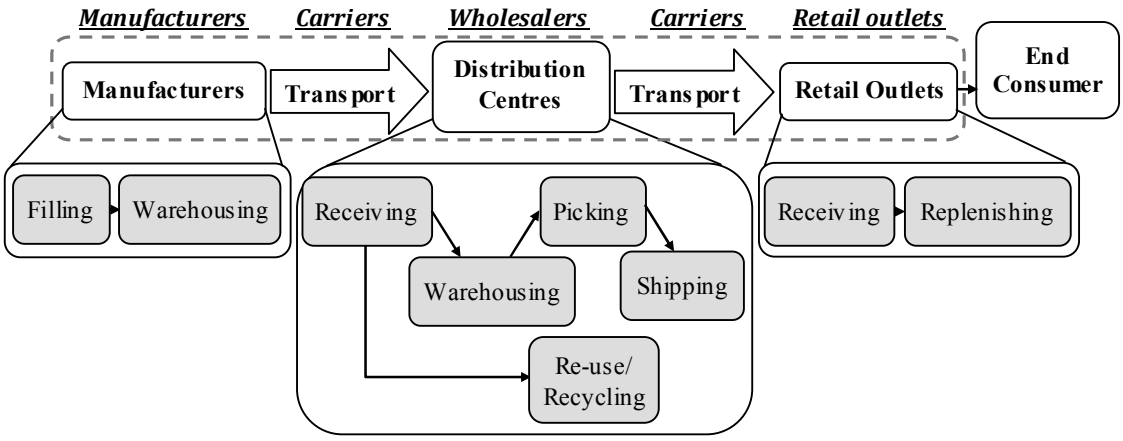

Figure 14: Example of a consumer goods distribution cycle (Hellstrom and Saghir, 2007)

Within Figure 14, the term 'manufacturers' represents the multi-facetted production process. In some cases, such as in the manufacture of processed foods, a number of products may be involved. These products will have been subjected to their own process of distribution. In order to simplify the scope of this research, which is concerned only with distribution and more specifically distribution packaging, the process of manufacture and the processes prior to manufacture are not considered.

Today, the fast moving consumer goods (FMCG) industry demands for readily accessible stock. Therefore primary consolidation centres (PCCs) are used to warehouse stock in order to ensure that, when needed, the stock at local (regional) distribution centres (RDCs) can be replenished. This reduces lead times and lowers distribution costs.

When products are received at the retail stores they are stripped of any additional packaging and are shelved ready for purchase. Once purchased, products are then transported to the consumer's home either by a method of delivery or by the consumer.

2.6.1 Food and Drink Distribution

The food and drink sector is one of the largest in the FMCG category. It covers a diverse range of product types with varied requirements, making it a complex and

time critical industry in terms of distribution. A typical supermarket distribution cycle has four key stages. These are:

Stage 1. ***Producer to the Primary consolidation Centre (PCC)***

Within the UK and Europe the majority of distribution is carried out in road vehicles. In cases where products are imported from greater distances e.g. Asia, Africa or America, several vehicles and types of transport including air and/or sea may form this distribution journey.

Stage 2. ***PCC to the Regional Distribution Centre (RDC)***

When stock is required it is transported to the RDC from the PCC using large road vehicles e.g. semi-trailers.

Stage 3. ***RDC to the retail store***

The RDC replenishes the retail store stock. Again this transport is carried out using road vehicles. These may be semi trailer vehicles for large stores where large amounts of multiple products are required or, smaller delivery vehicles for convenience or small size stores.

Stage4. ***Retail store to the customer's home***

Once purchased products are transported to the customer's home via: the customer using their own vehicle, on public transport or, on foot; or, home delivery where the retail store delivers the product in delivery vehicles.

Just under half (48%) of food miles occur during Stage 4. This highlights the significant distance products travel between the retail outlets and the customer's home (Steedman and Falk, 2009). The high proportion of food miles during this final stage, together with the significant reduction in protective packaging, renders products vulnerable to damage.

The remaining 52% of UK food vehicle miles are due to the transportation of food through Stages 1, 2 and 3. Of this, approximately 12% are due to transportation of

food overseas prior to reaching the UK, 35% are due to transportation of food within the UK and the remaining 5% of food vehicle miles are from the export of food from the UK to overseas (Smith et al, 2005). When considering distribution from the producer to the point of sale, 33% of the food vehicle miles, are overseas.

This overseas distribution accounts for 40% of the UK food supply, with 27% of the UK's food coming from EU countries and 13% from other non-EU countries, including, but not limited to: USA, Brazil, China, India and New Zealand (Barling et al, 2008). The distribution of the UK food supply source is indicated in Figure 15.

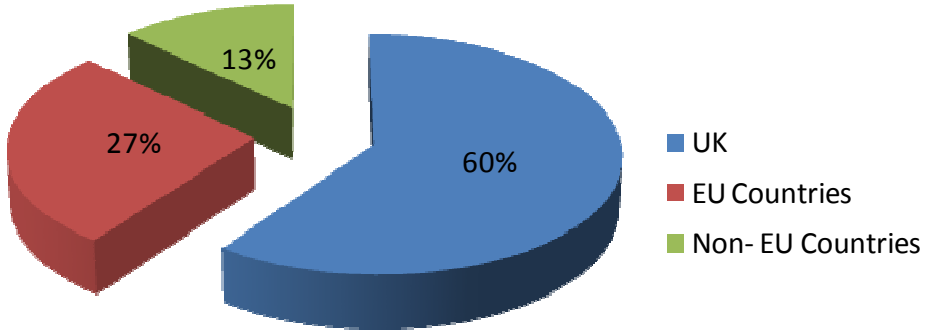

Figure 15: percentage of the UK's food supply by region

The majority of this distribution is carried out by road, with the proportion of distribution by rail, sea and air being insignificant by comparison. This is because transport by road is significantly cheaper then air and sea. Unfortunately, the conditions of road transport vary significantly between countries and therefore products travelling from different regions will experience different conditions during distribution.

With these numbers in mind it is clear that in many cases food will not only have travelled many miles in order to reach the end consumer. It will also have been subjected to varying transport modes and conditions relating to road types and quality, and temperature and humidity extremes and fluctuations. How these conditions vary between distribution journeys is now examined further.

2.6.2 Variation in Transport Conditions

Food distribution has been shown to be a global operation. It is therefore apparent that the distance products travel and the conditions of distribution to which they are subjected can vary significantly between products. Two key variants in distribution are the condition of distribution routes and vehicles. For example, Singh et al (2007) compare vehicle vibration on Indian roads to that presented in the current testing standards which are based on North American roads. The study showed that Indian roads produced more severe vibration than that simulated through the testing standards. The measurements carried out in India were mainly on paved roads classed as good. In reality, only 50% of Indian roads are paved, and reportedly only 20% of these are in good condition. In addition, it is reported that 30% of India's vehicle fleet is over 15 years old (ASIRT, 2004). Therefore, it is highly likely that the vehicle vibration resulting from a given distribution route and vehicle will be more intense than that recorded during this study. The variation in Indian roads to North American roads, on which the current testing standards are built, is further evident when it is considered that in 2007, 67.4% of North American roads were paved and 87% of roads were considered to be in a good to mediocre condition (AASHTO, 2009). Therefore, comparative to Indian roads, North American roads are in a much better condition and would therefore most likely provide less harsh distribution conditions.

Other factors which vary between countries are the day and night time temperatures and humidity fluctuations. Excessive temperature and humidity can lead to product damage and deterioration if not accounted for when designing the packaging or selecting the distribution vehicle (Paull, 1999).

The variation in conditions highlighted, illustrates the complexity of distribution and the numerous considerations that arise. It is therefore important that all aspects of distribution are considered when choosing or designing appropriate distribution packaging. This point is stressed by OECD (2002), which states that in order to create effective and efficient global distribution the diversity in social and geographical features between countries and their stages of economical

development, leading to widely divergent transport systems and operating structures, needs to be considered.

By considering such aspects of a product's distribution the requirement of its packaging can be defined. The typical protective requirements of packaging during the distribution cycle are now discussed.

2.7 The Requirement of Packaging in the Distribution Chain

Because of the variation in conditions of distribution between geographical locations, it is essential that to ensure the preservation of product quality during distribution, the intended distribution cycle and the hazards it may present, are understood, from the producer to the end consumer. By doing this the manufacturer, distributor and/or producer can package the product to meet the needs of distribution (Van Zeebroek et al, 2007). This is true for all products, whether they are being transported around the world or domestically.

Figure 16 shows the basic distribution cycle with the possible hazards faced at each stage. Three main areas of distribution are considered, namely: packing and unpacking; warehousing; and, transportation. The hazard groups identified for these areas are highlighted in red, with some of the possible hazards then labelled in green.

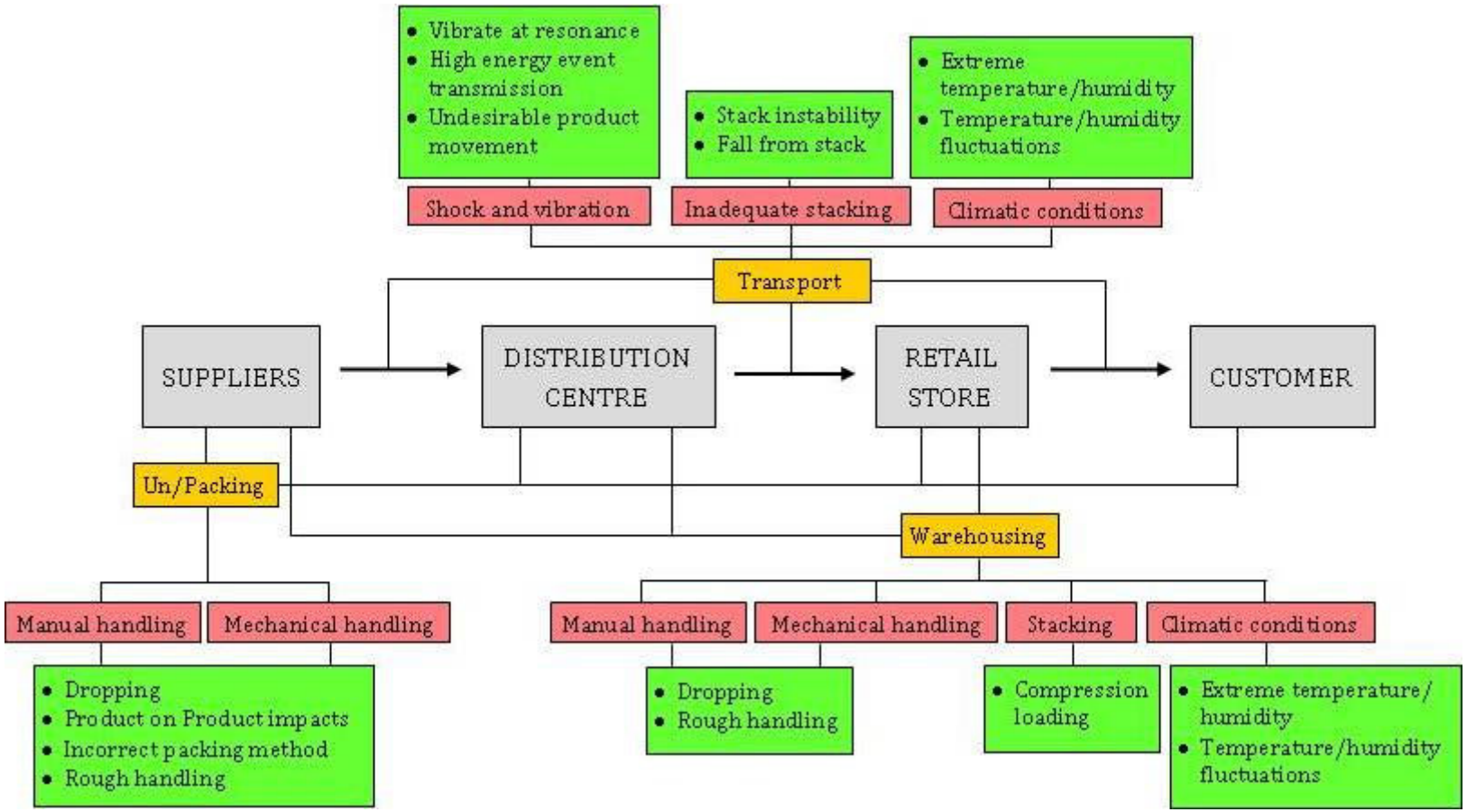

Figure 16: The distribution cycle and its possible hazards

The damage caused by hazards during any one or more of these three stages can manifest itself through product deterioration externally or internally. Some forms of damage are described in Table 3 and some examples of the forms of damage are illustrated in Figure 17.

Table 3: Examples of possible forms of product damage

CATEGORY	HAZARD	DAMAGE
Vibration and shock	Fatigue	Loss of structural integrity
	Impacts (product on product and product on vehicle)	Cosmetic and product damage such as: Bruising – reduce quality of fruit and vegetables, accelerate deterioration Rupturing – leading to product leakage Scuffing – ink transfer or damage to products packaging/product Gas build up – from constantly shaking product i.e. in a bottle of carbonated drink
	Resonance	Loosen components – excessive vibration could cause electrical wires to disconnect Extravagate product damage – excessive vibration could lead to fatigue damage in the product i.e. additional bruising
Mishandling	Dropping	Impact damage could lead to cosmetic damage of bruising, denting, rupturing of packaging which could itself cause product deterioration or leakages
	Forklift damage	Piercing of external packaging compromising packaging's integrity Piercing of products packaging leading to leakages Bruising of products through impact
Over stacking	Compression	Lead to cosmetic damage to packaging through compression which could also cause a loss of the packaging's structural integrity
Climatic fluctuations	Excessive temperatures	Overheating – cause product to melt or damage the chemical makeup of the product High temperatures – accelerate product deterioration Excessive cold – cause product to freeze and become brittle or change the chemical makeup of the product
	High or low humidity	High humidity- accelerate product deterioration Excessive moisture can affect the structural integrity of the packaging and additionally lead to cosmetic damage Low humidity – product may dry out damaging the product i.e. fresh flowers where dry conditions would cause the flowers to wilt.

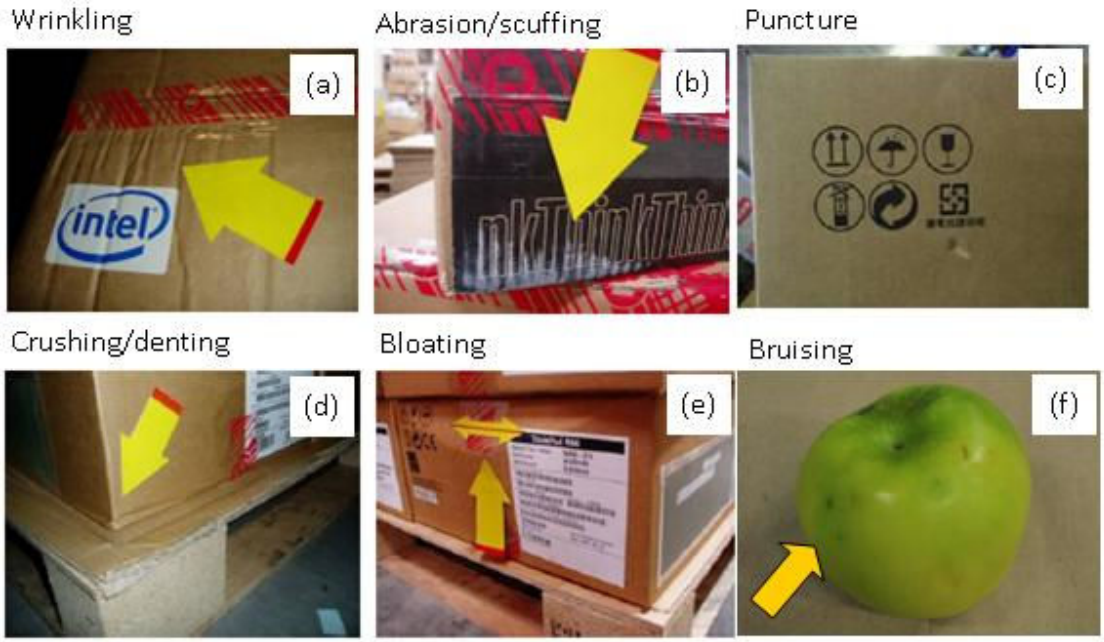

Figure 17: Examples of types of damage ((a) to (e) taken from (Bai, 2010))

The three main areas of distribution, along with the hazards present within each, are now discussed.

- ***Packing/unpacking***

Handling – Improper mechanical or manual handling can lead to product damage and increase its susceptibility to damage through the rest of the distribution cycle. For example, rough handling or dropping products can lead to impact damage.

Packing – Incorrect loading of products into packaging can leave it vulnerable to damage. Additionally, by packing products in mixed loads e.g. fragile items with heavy items, can further increases the risk of damage if items are not loaded in an appropriate manner or order.

- ***Warehousing***

Climatic conditions – Subjecting packaged products to harsh climatic conditions during warehousing can lead to product deterioration and damage, particularly with fresh produce. Further to this, leaving packaging

exposed to adverse weather conditions or high humidity levels can result in a loss of structural integrity and failure of the packaging.

Stacking – Excessive compressive force or incorrect stacking during warehousing can lead to product damage and compromise the structural strength and protective capabilities of packaging.

Handling – Mishandling during stacking can lead to severe product damage, particularly in cases where products are dropped from great heights. Mishandling when using forklifts can also lead to other damage such as piercing or denting.

- ***Transportation***

Vibration and shock – Vehicle vibration during transport, can lead to fatigue damage of the packaged product, particularly when it is subjected to lengthy distribution journeys or vibration at a resonant frequency. Furthermore, shock events caused by road defects or large displacements in the road surface can cause further product damage.

Inadequate stacking – Improper loading of items in the distribution vehicle can lead to excessive shaking, lateral movement or collapsing of stacked items.

Climatic conditions - Environmental factors such as temperature and humidity fluctuations can lead to product damage. Changes in temperature can affect the properties of materials and can cause damage to items which are temperature sensitive items, such as electronics. Increased levels of humidity can also lead to mould and bacterial growth. Moisture can also lead to degradation of fibreboard packaging such as corrugated boxes, which lose their structural integrity when wet.

It is important to consider the effects of minor damage that occurs during the distribution process as its cumulative effect may lead to significant damage. Because of this it is important that all events, including those of low and high amplitude, should be simulated together in a realistic manner. Testing standards exist for distribution packaging, which involve subjecting products to these hazards in order to ensure its protective capabilities.

It is evident that there are many hazards to consider during distribution. The distribution packaging, and in some cases primary packaging, must meet the protective requirements of the products. Testing standards provide performance tests with measured test levels to simulate these hazards to therefore ensure that a packaging solution provides adequate protection to the product.

2.8 The Testing Standards

Although packaging has many objectives, during distribution its main purpose is to protect and contain the product. To establish whether a packaging solution is fit for purpose tests which simulate distribution hazards are carried out. Over the years, a variety of testing standards have been created which specify test intensities and testing regimes including both climatic and physical tests.

2.8.1 Temperature and Humidity Testing

There are two forms of temperature and humidity testing, referred to as '*soak*' and '*cycle*' tests. Testing is carried out in an isolated test chamber where the temperature or humidity levels can be closely monitored and controlled.

'*Soak*' tests involve saturating the packaged-product at a particular temperature or level of humidity and maintaining it for a set period of time. The '*cycle*' tests expose the packaged product to repetitive temperature and humidity fluctuations. This is to simulate the climatic variations which products face during distribution. ASTM D1469-08 provides test levels that simulate the anticipated

rapid changes in conditions. The severity of the tests carried out depends on the level of assurance required. These tests evaluate the susceptibility of the packaged product to moisture or temperature damage, assessing cosmetic, structural and chemical damage.

Figure 18: Climatic chamber at Smithers Pira (2012)

These tests are carried out within either climatic chambers or cabinets, such as that shown in Figure 18. These climatic units are capable of cycling between temperatures as low as -80°C up to +150°C and relative humidity from 5 to 95%

2.8.2 Pressure Testing

Pressure/altitude testing is carried out on packages that are transported via methods that may result in a change in atmospheric pressure. The test schedule given in ASTM D1469-08 (Section I) covers low pressure (high altitude) environments, e.g. transportation via aeroplane. ISTA also caters for pressure testing on the '*soak*' and '*cycle*' methods to note the effects of constant low pressure and varying pressure that may occur when multiple methods of distribution are required.

2.8.3 Manual and Mechanical Handling Testing

Handling errors during distribution can cause substantial damage to a packaged product, ISTA (2006) states that single containers, small packages and any shipping containers that are manually handled up to a weight of 200 lb should be tested for manual handling hazards. This involves subjecting the packaged-

product to drop tests at specified heights using different orientations, assessing each face and edge for vulnerability to damage.

Mechanical handling tests are only carried out when mechanical handling is the only anticipated method of handling. These tests are intended for large and heavy shipping units, and unitized loads.

Both the mechanical and manual handling drop heights vary depending on the level of assurance required and the weight of the package, the heavier the package the lower the drop height. For example, in ISTA (2006) for packaging with a mass less than 9.1 kg drop heights range from 229-610 mm, whilst for packages with a mass between 45.4 kg and 90.7 kg, drop heights range from 104-254 mm.

Drop and impact tests are carried out on either free fall drop machines or mechanical impact machines, as required. Examples of both of these pieces of equipment are given in Figure 19.

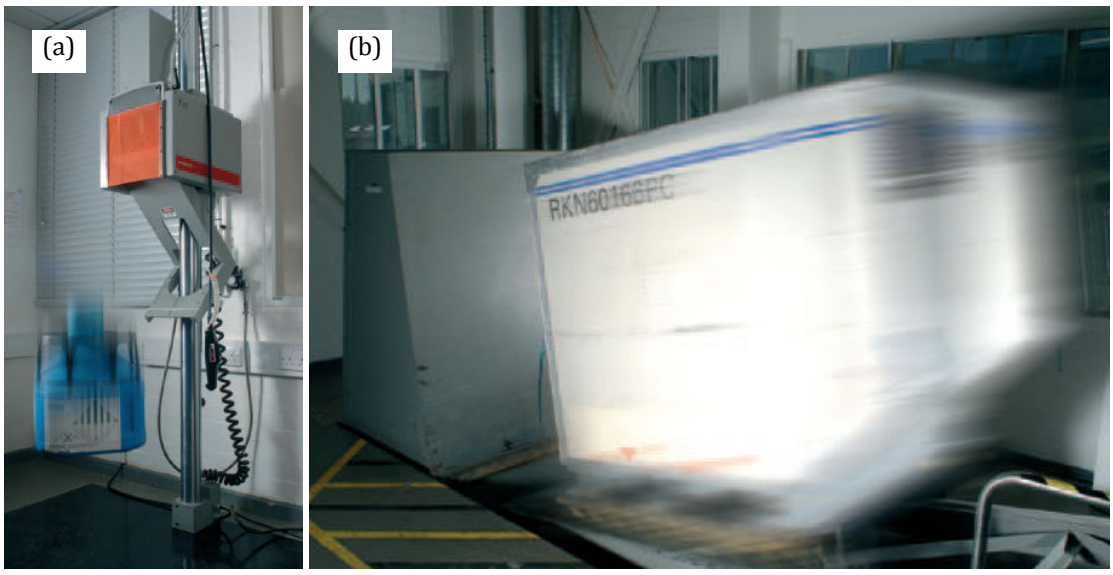

Figure 19: Free fall drop machine (a) and horizontal impact machine (b) at Smithers Pira (2012)

2.8.4 Compression Testing

During warehouse storage packaged products are subjected to compression loads. Both ASTM and ISTA have test schedules which simulate the loading a package may suffer during storage. Compression tests include both 'apply and release' and 'apply and hold' regimes. ISTA (2010) calculates the force applied during testing.

$$\text{Force (N)} = Wt * (S-1) * F * 9.8 * 1.4 \quad (1)$$

This is based on the weight (W_t) of the package, the total number of packaged products in the stack (S), 9.8 is representative of g and the duration for which the package is stacked, (compensation factor, F). For example, if the package is stacked for longer than 48 hours then F is equal to 3.

Figure 20: Compression testing machine at Smithers Pira (2012)

An example of a compression testing machine in given in Figure 20, where a guided steel plate is lowered on to the test specimen and applies the specified load.

2.8.5 Vibration Testing

There are two methods of vibration testing specified in the various standards. The simplest is sinusoidal testing, referred to as the 'resonance search and dwell' method in ASTM D-999 and ISO standards. Using a simple sine wave the frequency range of interest (from 3 to 100 Hz) is swept with constant amplitude typically 0.25g - 0.5g, where g is 9.81 m/s^2. During this the resonant frequencies of the packaged product are identified. The packaged product is then forced to

vibrate at, and around, each of its resonant frequencies for a time, typically 15 minutes (Goodwin and Young, 2011). This technique is useful when considering the response of the packaged product at resonance, but as a vibration test for simulating vehicle vibration it is an over test due to excessive and unrealistic vibration at the packaged product's resonant frequency.

Today it is more common to use an accelerated random vibration test, which creates a vibration signal based on an average power spectral density (PSD) spectrum measured from actual vehicle vibration. This test was designed to create a simulation that better represents the distribution environment. Test acceleration is carried out based on the theory of fatigue, with the increase in test amplitude being inversely proportional to the reduction in duration. The two most common tests include the ASTM and ISTA standards.

There are three types of vibration simulation tables used to carry out vibration testing. These include electro-hydraulic, which are the most commonly used with the ISTA and ASTM standards; electro-magnetic, which are capable of high frequency vibration (>2 kHz) but have a significantly reduced load capacity in comparison to the electro-hydraulic tables; and, mechanical, this is the most basic table and is only able to carry out cyclic vibration loading. Each of these tables is illustrated in Figure 21.

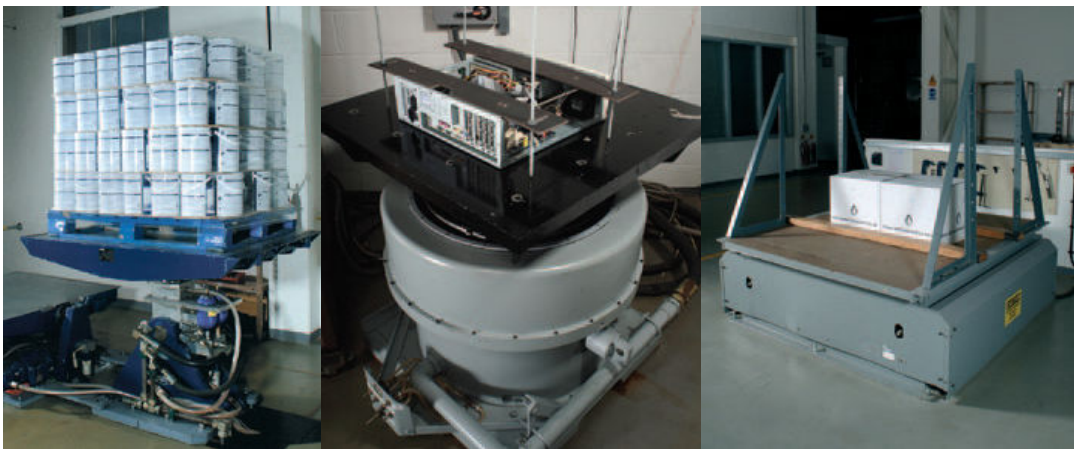

Figure 21: Electro-hydraulic table (a), electro-magnetic table (b) and mechanical table (c) from Smithers Pira (2012)

2.8.6 ASTM Testing Standards

The ASTM standard D4169 details the accelerated random vibration test method. It presents several simplified PSD spectra for truck, air and rail transport, which have been calculated using multiple field data and selecting appropriate break points. The PSD used during testing is dependent on the transport vehicle and the assurance level required, ranging from i to iii, maximum to minimum assurance. The PSD spectra provided in D4169 for trucks with leaf spring suspension is given in Appendix III, Figure 157. Following testing, acceptance of the package and product is dependent on the selected criteria: product undamaged (i); packaging intact (ii); or, both the packaging and product undamaged (iii).

The standards specify one spectral shape to be used for each type of vehicle e.g. all semi trailers with leaf spring suspension. However, they do propose that if adequate information about the shipping method and its environment is known, the test should be altered to suit that environment. ASTM D7386 for single parcel distribution provides a PSD for delivery vehicles.

Additional shock testing of the packaged product is also defined within D4169. This test applies a shock level vibration to the packaged product for a dwell time of 60, 40 or 30 minutes depending on the level of assurance. This dwell time is split between the three axes with 50% of the duration applied along the vertical, and the remaining 50% split between the lateral and longitudinal direction.

2.8.7 ISTA Testing Standards

The ISTA standards are built up in series test (ISTA, 2012):

Series 1. ***Integrity Tests*** –are used to evaluate the toughness and strength of the packaged product without simulating the distribution environment.

Series 2. ***Integrity Plus Tests*** – combine a mix of integrity tests with at least one general simulation.

Series 3. ***General Simulation Tests*** – simulate the distribution environment based on universal data. They contain standard sets of PSDs, drop heights and atmospheric conditions.

Series 4. ***Enhanced Simulation Tests*** – similar to Series 3, they simulate the distribution environment but additionally they include at least one element of focused simulation. This allows the user to integrate test levels based on a specific distribution environment.

The shape, weight and unitization of different packaged products can vary significantly and what might be a suitable test for one configuration may not suit all others. To simulate distribution realistically for different packaging types, each series contains a number of test standards to suit different configurations. A number of these packaging configurations and their available testing standards are given in Table 4.

Table 4: Package types and appropriate ISTA distribution tests (ISTA, 2012)

TEST	PACKAGE TYPE	DESCRIPTION
1A, 2A, 3A, 4AB	Weighing > 150 lb (70 kg)	A single uniform shaped shipment that is less than 150lb (68kg) i.e. corrugated board box. Typically transported in parcel carriers.
1B, 2B, 4AB	Weighing > 150 lb (70 kg)	A single uniform shaped a shipment that is greater than 150lb (68kg).
1E, 3E, 4AB	Unitized loads	A unit load of the same product i.e. palletised load. Typically transported in Semi Trailers.
2D, 3A, 4AB	Considered flat	Specifies specific tests and package faces to carry out tests.
2E, 3A, 4AB	Considered elongated	Specifies specific tests and package faces to carry out tests.
2F, 3B, 4AB	Less-Than-Truckload (LTL) shipments	Non-uniform shipments i.e. mixed load of packaged-products shipped together
7C	Reusable intermediate bulk containers	Plastic containers i.e. for transporting liquids
7A	Open reusable transport containers < 60 lb (27 kg) Unitized for shipment on a pallet	Wood/plastic crates or trays that are stacked and unitized
7B	Closed reusable transport containers for loads of 150lb (70kg) or less	Wood/plastic closed shipping containers
7D	Thermal controlled transport packaging for parcel delivery system shipment	For products which require specific atmospheric conditions i.e. refrigerated or insulated packaging.

Each test contains a random vibration test specification similar to ASTM standards. The random vibration testing in the ISTA standards specify one spectral shape to be used for each type of vehicle. The PSDs provided in the ISTA standards for leaf spring and air ride suspension semi-trailers and, over the road and pick-up and delivery vehicles are provided in Appendix III, Figure 158 and Figure 159, respectively. By comparison, the shape of the ISTA PSDs are more detailed than those provided in the ASTM standard, showing more specifically the definition between the three key resonant frequencies seen in vehicle vibration.

2.9 Concluding Remarks

It is evident that packaging plays a vital part in facilitating product distribution. The introduction of global distribution has only made its role more important. Already possessing a vital role, the requirements of packaging are further expanded through the need for: safety; sustainability; ergonomics; and, marketing. These requirements of packaging have been established throughout this Chapter and their fundamental inter-dependency, in order to create a successful packaging design, has been made apparent.

The importance of these requirements varies depending on the stage of distribution. During transportation the protective requirement relating to logistics and safety is critical. A particularly damaging hazard is that of vehicle vibration and shock during the stages of transportation.

The specific character of vehicle vibration can vary significantly depending on the type and quality of the roads and the country of travel. With 50% of the UKs food being imported from overseas it is important to consider the transport routes a packaged product will take in order to enable consideration of the modes and conditions of transport. Because of the potential hazards arising during transportation it can be argued that logistics and safety are most important at these stages. Without their consideration the successful distribution of the product would not be possible.

For the packaged product to meet its logistical requirements, it is essential that the packaging provides adequate protection from distribution hazards, whilst minimising weight and size and the material usage, thereby, enabling fast, efficient and economic distribution. This logistical role is important for primary packaging but is most important when considering the secondary and tertiary distribution packaging. To ensure that the logistical needs of the product are met, in particular the protective requirement, performance testing which simulates the distribution environment is used.

The tests provided in the distribution packaging testing standards, provide specific test conditions to use when evaluating the packaging. The vehicle vibration tests, which simulate the vibration occurring during transportation, are based on real data recorded on distribution journeys around North America. With the aforementioned increase in global distribution and the variation in vehicle vibration experienced within different regions due to: road type, road quality, and, the condition of distribution vehicle's used, the use of a single test (as provided by the current testing standards) to represent all distribution journeys, is inadequate. This is particularly true when considering the need for a just right packaging solution, in order to provide: economic, efficient and sustainable distribution, whilst ensuring product protection and quality is maintained.

In order to create a more representative vibration test regime, the characteristics and variations in vehicle vibration need to be assessed. Therefore, Chapter 3 examines vehicle vibration and the aspects of distribution that shape a vehicle's vibration response.

3 VEHICLE VIBRATION

Vehicle vibration arises from the interaction between the vehicle and the road surface. The severity of the vehicle's vibration is dependent on several factors relating to the system dynamics and the road surface roughness. The combination of these factors results in a vibration response that is random, non-stationary and non-Gaussian.

It is widely known that vehicle vibration and shock can cause significant product damage in packaged product distribution (Lu el al, 2008; Chonhenchob et al, 2008). A vehicle's vibration response can be greatly affected by small changes in vehicle parameters or the road input. This sensitivity is difficult to predict. To understand the sensitivity of a vehicle's response to changes in vehicle dynamics, such as: vehicle mass; suspension parameters; and, tyre stiffness, an understanding of these parameters is required.

A full description of the key characteristics of a vehicle's vibration response is given, followed by an examination of the vehicle dynamics that govern it. By examining these factors the requirements of the vibration testing of packaging through consideration of the distribution vehicle's dynamics is developed.

3.1 Terminology

Prior to discussing vehicle vibration, relevant definitions and theory covering vibration signals and statistical distributions are summarised.

3.1.1 Statistical Properties

The central statistical moments describe the distribution of the variable, *x*.

$$m^{th}, moment = (t_r) = \frac{1}{N}\sum_{i=1}^{N}\left(x_i - \overline{X}\right)^m \quad (2)$$

where:

$$\overline{X} = \frac{1}{N}\sum_{i=1}^{N} x_i \quad (3)$$

is the mean value.

1. Central Mean (μ)

The first order central statistical moment calculates the central mean of the data and by definition is equal to zero.

2. Variance $\left(\sigma^2\right)$

Variance is the second order moment, the square root of which gives the standard deviation, σ. The variance indicates the size of the spread of the distribution. If a distribution is *Normal* and consequently Gaussian, then 68.2% of the distribution will lie within $\pm 1\sigma$, 95.4% within $\pm 2\sigma$ and 99.7% within $\pm 3\sigma$ of the mean.

3. Skew (γ)

Skew is calculated with the third order moment. It is a measure of the symmetry of the signal where a negative value indicates the distribution is skewed towards the high values and a positive value indicate the distribution is skewed towards the lower values. For a *Normal* (Gaussian) distribution, γ is equal to zero.

4. Kurtosis (k)

The fourth order moment is kurtosis, which is a measure of the peakedness of a distribution. The greater the kurtosis the more spiked is the centre of the distribution. For a distribution centred on zero, this means that a greater portion of the distribution is focused around the lower values.

Dodge (2008) states that '*...the measures of kurtosis are a part of the measures of form and characterise an aspect of the form of a given distribution. More precisely, they characterise the degree of kurtosis of a distribution toward a normal distribution... To test the kurtosis of a curve we use the coefficient of kurtosis*'.

This coefficient of kurtosis is formed from the fourth statistical moment of a distribution. Typically, and within this Thesis, the standardised kurtosis is used to define the shape of a signals distribution independent of the unit of measurement. This is calculated by dividing Equation 2 by the standard deviation raised to the power four (σ^4):

$$k = \frac{\frac{1}{N}\sum_{i=1}^{N}\left(x_i - \overline{X}\right)^4}{\sigma^4} \tag{4}$$

A normal (Gaussian) distribution has a standardised kurtosis, $k = 3$.

3.1.2 Probability Density Function

The Probability Density Function (PDF), $P(x)$, is the derivative of the CDF, $F(x)$. It is used to calculate the probability that a random variable will take on a specific value or that it will fall within a particular range of values (Lutes and Sarkani, 2004):

$$P(x) = \frac{d}{dx}F(x) \tag{5}$$

Within vibration analysis the PDF is used to illustrate the spread and shape of a signal's distribution.

3.1.3 Cumulative Distribution Function

Lutes and Sarkani (2004), state that the cumulative distribution function (CDF) is probably the most general way to describe the probabilities associated with a

given random variable. The CDF, $F(x)$, is a measure of the probability that the variable x will take on a value equal to or less than X.

$$F(x) = \mathrm{P}(X \leq x) = \int_{-\infty}^{x} P(\xi) d\xi \tag{6}$$

3.1.4 Gaussian Distribution

A vibration signal is said to have a Gaussian or *Normal* distribution when its PDF follows a symmetric, bell shaped curve. The PDF of a vibration signal with a Gaussian distribution can be defined by:

$$P(x) = \frac{1}{\sigma\sqrt{2\pi}} e^{-\frac{1}{2}\left(\frac{x-\mu}{\sigma}\right)^2} \tag{7}$$

where μ is the mean value of the variable x and σ is its standard deviation.

3.1.5 Calculating the PDF

An example of a PDF is now given for a vehicle vibration signal (which is non-Gaussian) and a random vibration signal with a Gaussian distribution. Both of these vibration signals are illustrated in Figure 22.

The PDFs of both signals are then constructed by applying evenly spaced acceleration level bands (e.g. -5g to 5g with 0.05g increments) to the signal and finding the number of data points which fall within each band. By then comparing the number of data points in each acceleration band to the overall number of points the percentage distribution can be found. The PDFs for both signals are shown for comparison in Figure 23.

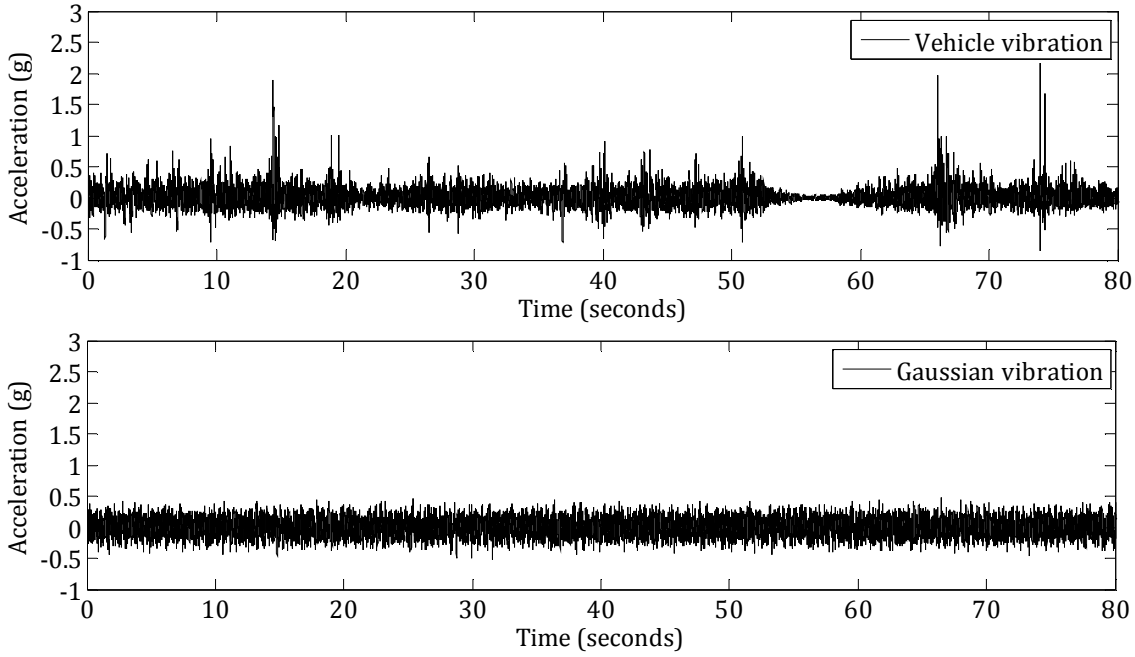

Figure 22: Example vehicle vibration and the equivalent Gaussian vibration

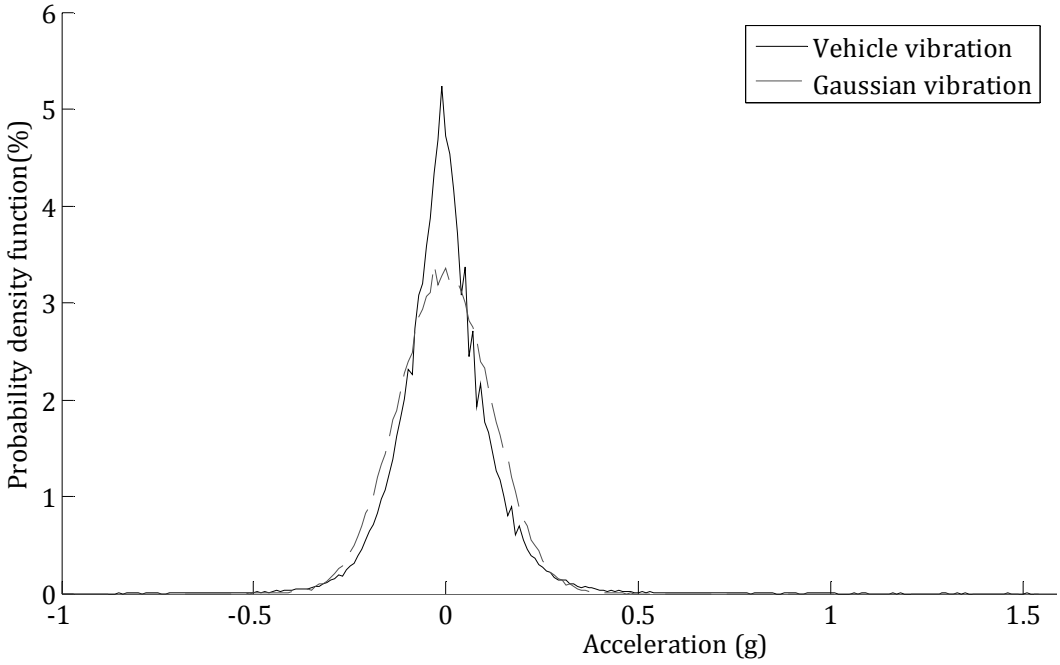

Figure 23: PDF of the vehicle and Gaussian vibration signals in Figure 22

The variation between the vehicle vibration and the Gaussian vibration can also be expressed through its kurtosis. For the vehicle vibration k = 10 this is significantly higher than the k = 3 for the Gaussian vibration. This variation between the two

PDFs is made apparent by the sharper peak and wider spread of acceleration levels in the vehicle vibration's PDF.

3.1.6 Ensemble Averages

An ensemble refers to a collection of samples $x_1(t)$, $x_2(t)$, $x_3(t)$, ... $x_n(t)$ which form a random process $x(t)$. The random process is formed from a number of samples, which separately can be considered as independent processes, therefore having their own statistical values (Newland, 1994).

3.1.7 Stationary Vibration

In the context of vibration the term 'stationary' refers to a signal's ensemble statistical properties being unchanged by any arbitrary shift along the time axis. This implies that for any sample of the signal the measured statistical properties will be unchanged.

When considering the definition of stationary in current research into vehicle vibration, a signal can be termed stationary the root-mean-square (RMS) of its acceleration remains constant. The stationarity of the vibration can therefore be evaluated be measuring the RMS acceleration for fixed length segments of the signal. If the RMS acceleration is constant the signal is said to be stationary, if the RMS acceleration varies then the signal is non-stationary (Rouillard and Sek, 2010).

Vehicle vibration is inherently non-stationary due to variations in vehicle speed and the road roughness (Rouillard and Sek, 2000). This non-stationarity is said to be exacerbated further, in the long term, because of variations in the vehicle's dynamics and payload (Rouillard and Sek, 2001).

In Figure 22, the vehicle vibration is an example of a non-stationary signal and the Gaussian signal is an example of a stationary signal. The stationarity of the two signals can be seen in Figure 10 where the distribution of the RMS acceleration of one second samples of both signals is given. For the vehicle vibration, the RMS

acceleration has a distribution spread over the acceleration range 0 – 0.25g, while the Gaussian signals RMS acceleration distribution is constant at 0.12g.

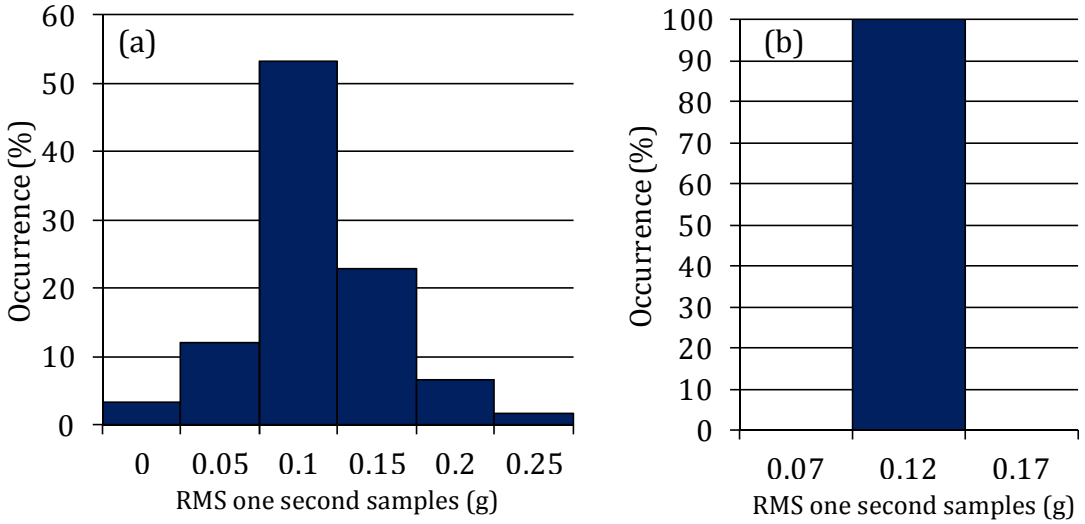

Figure 24: RMS acceleration distribution of one second segments (a) vehicle vibration (b) Gaussian vibration

3.1.8 Root-Mean-Square

The root-mean-square (RMS) refers to the square root of the mean of the squares of the values of the variable *x*:

$$RMS = \sqrt{\frac{\sum_{i=1}^{n} x_i^2}{n}} \tag{8}$$

The RMS can be used to identify the level of intensity of a vibration signal and as previously mentioned can be used to identify whether the signal is stationary.

3.1.9 The Fourier Transform

Fourier analysis says that a periodic function may be synthesized as the sum of its harmonic components (Newland, 1994). This therefore enables the frequency components within the periodic function to be identified. The continuous Fourier

transform, for the frequency ω_k, ($X(\omega_k)$), of a signal, $x(t)$, can be calculated using the Fourier integral (Wong, 2011):

$$X(\omega_k) = \int_{-\infty}^{\infty} x(t) e^{-i\omega_k t}\, dt \tag{9}$$

Vibration data acquisition is carried out by measuring acceleration, force or displacement at equally spaced time intervals over a finite period of time, resulting in a discrete time series. The frequency coefficients of a discrete time series can be calculated using the discretised version of the Fourier Transform (DFT). The DFT is expressed as (Wong, 2011):

$$X_k = \sum_{r=0}^{N-1} x_r e^{-i(2\pi kr/N)} \tag{10}$$

where X_k is the DFT of an input sequence x_r, of length N. r is the current sample being considered (0, 1, 2, ..., N-1) and k is the current frequency component being considered (0 1, 2, ..., N-1).

The Inverse DFT (IDFT) is given by:

$$x_r = \frac{1}{N} \sum_{r=0}^{N-1} X_k e^{i(2\pi kr/N)} \tag{11}$$

For a time domain signal, $x(t)$, with sample interval Δt, and finite duration $N\Delta t$, the DFT at frequency f_k Hz, can be found using the equation:

$$X(f_k) = \sum_{r=0}^{N-1} x(t_r) e^{-i2\pi f_k t_r} \tag{12}$$

where the DFT frequency, $f_k = k/N\Delta t$ Hz, and $t_r = r\Delta t$.

In frequency analysis the rate at which a signal is sampled sets a limit as to the maximum frequency that can be detected within that signal, this limitation is referred to as Shannon sampling theorem (Shiavi, 2007). This means that for a signal with a sampling frequency, $f_s = 1/\Delta t$ Hz, the highest frequency that can be detected within that signal is $f_n = f_s/2$ Hz, where f_n is often referred to as the

Nyquist frequency. When analysing a signal for frequencies greater than f_n, the frequency information becomes indistinguishable so that frequencies greater than f_n appear as false low frequencies, this is referred to as aliasing. An example of aliasing is given in Figure 25. The figure illustrates a sine wave with frequency, f = 8 Hz. This sine wave is then sampled with f_s = 10Hz, so that the maximum frequency that can be detected is f_n = 5 Hz, therefore aliasing will occur. Aliasing will cause the 8 Hz sine wave to be detected as a sine wave with frequency, ($f - f_s$), hence a sine wave with frequency, f = -2 Hz.

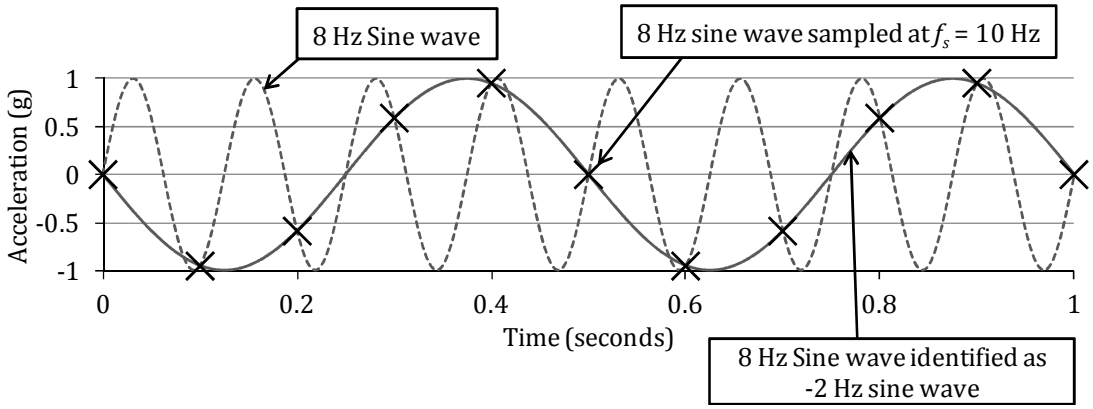

Figure 25: Example of signal aliasing

The Shannon sampling theorem gives the DFT the inherent property: $X(f_{N-k}) = X(f_k)$. The DFT therefore forms a two-sided spectrum, with positive and negative frequency values. For analysis purposes, typically, only the one sided spectrum is required. To create the one sided spectrum, the Fourier spectrum, $X(f)$, must be truncated after the $N/2$th value.

To speed up the calculation of the DFT the Fast Fourier Transform (FFT) computational algorithm is used. This efficiently calculates the DFT of a signal. While the DFT requires N^2 calculations, the FFT requires only $N\log_2 N$ calculations, which significantly reduces the processing time and computational power required to carry out the DFT (Newland, 1994).

3.1.10 Power Spectral Density

The power spectral density (PSD) spectrum '...shows how the different frequencies contribute to the variation in the signal.' (Shaivi, 2007). It does this by defining the power content within each frequency band (Δf) of the signal ($x(t)$) enabling key frequency components within a signal to be identified. Power is defined as the acceleration squared (g^2), where g = 9.81 m/s^2, so that the PSD is g^2/Hz.

Shiavi (2007) defines the equation for the PSD in two forms, firstly, as the Fourier transform of the autocorrelation function:

$$S(f) = \frac{1}{2\pi}\int R(\tau)e^{-i2\pi ft}d\tau \tag{13}$$

where the autocorrelation function is the cross-correlation of the signal, $x(t)$ with itself at time lag τ:

$$R(\tau) = \frac{1}{T}\int_0^T x(t)x(t+\tau)d\tau \tag{14}$$

Secondly, as a function of frequency:

$$S(f) = \frac{X(f)\bullet X^*(f)}{NT} \tag{15}$$

where, $T = 1/\Delta t$, is the sample period, is the sampling frequency, so that the frequency bandwidth, $\Delta f = 1/N\Delta t$ Hz. N is the number of data points within the signal being analysed (length of the DFT) and $X(f)$ is the Fourier spectrum of length N.

3.2 The Characteristics of Vehicle Vibration

Excitation of the vehicle as it traverses over a rough road surface results in vehicle vibration (Rouillard, 2007a; Rouillard and Sek, 2000). In addition to relatively consistent variations in the road surface roughness, large deviations due to

hazards such as potholes or speed bumps are also present. The occurrence and location of these are random in nature and are difficult to predict. Their presence can lead to discrete high energy events in the vehicle's response. The amplitude and shape of the vehicle's response is then further dependent on the vehicle's speed profile and parameters.

Although for different vehicles the amplitude and shape of the response will vary, several key characteristics will remain. Firstly, as previously stated, all vehicle vibration is random, non-stationary and of a non-Gaussian distribution. Secondly, all vehicle vibration embodies three key resonant frequencies 1 - 5 Hz suspension resonance, 10 - 15 Hz resonance of the unsprung mass or 'wheel hop' and 40 - 55 Hz structural resonance. The exact frequency of each depends on the vehicle's parameters (Singh et al, 2008; Rouillard and Sek, 2001).

A more in depth description of the key characteristics of vehicle vibration is now given.

3.3 The Non-Stationarity of Vehicle Vibration

Vehicle vibration is highly non-stationary due to constant fluctuations in vehicle speed and road roughness, and, in the long term, because of variations in a vehicle's dynamics and payload (Rouillard and Sek, 2000; Nei et al, 2008; Rouillard and Sek, 2001). These changes result in vibration with a continually varying RMS acceleration, as illustrated in Figure 24. The three main sources attributed to the non-stationarity of vehicle vibration are:

- *Fluctuations in road surface roughness* - road surface roughness is random and non-stationary (Bogsjo, 2006). This means that the severity of the input due to road roughness will vary with time, ultimately affecting the amplitude of the vehicle's vibration response (Rouillard and Sek, 2005).

- *Fluctuations in vehicle speed* - throughout a journey a vehicle's speed will experience large fluctuations due to changes in speed restrictions and

smaller fluctuations due to changing acceleration levels. When combined these result in a time variant vehicle response (Richards, 1990).

- *Frequency or spectral non-stationarity* - this third type of non-stationarity arises from structural excitation of the vehicle's modal frequencies. It is noted as being rare in road vehicles due to '*the relatively compliant suspension systems and slack-free coupling mechanisms*' (Rouillard and Sek, 2005).

3.4 Non-Gaussian Distribution of Vehicle Vibration

The statistical distribution of vehicle vibration acceleration levels has been shown on many occasions to be non-Gaussian (Otari et al, 2011; Garcia-Romeu-Martinez and Rouillard, 2011). A combination of consistent variations in the road surface roughness and large deviations due to road damage, traffic calming, kerbs, etc., results in a non-Gaussian road surface roughness, which ultimately results in a vehicle response that is also non-Gaussian in character (Bruscella et al, 1999; Bogjso et al, 2012)

When measuring the shape of the acceleration distribution for vehicle vibration, the value of kurtosis is often used for comparison with the Gaussian. Rouillard and Sek (2010) found that the kurtosis of vehicle vibration was much higher than the kurtosis value of 3 which represents a Gaussian distribution (Rouillard, 2007b). Their work showed the kurtosis varies between 5.5 and 14.7 for different vehicle types, as shown in Table 5.

The deviation in the vibration distribution from the Gaussian profile tends to manifests itself as a sharp peak at around zero and long tails. This is due to the presences of discrete high level shock events and low level vibration (Lu et al, 2008). An equivalent Gaussian signal (meaning a random vibration signal with a Gaussian distribution, with the same average RMS acceleration and frequency content as the original vibration signal) would consist of a higher level of constant vibration but would noticeably be missing the peak acceleration shock events.

Table 5: Overall kurtosis for various distribution vibration records (Rouillard and Sek, 2010)

ID	VEHICLE TYPE AND LOAD	ROUTE TYPE	KURTOSIS
MA	Utility vehicle (1 tonne capacity) Load<5% capacity	Suburban streets	**8.8**
MB	Prime mover + semi trailer (Air ride susp.) Load:90% capacity	Country roads	**9.7**
MC	Transport van (700 kg capacity) Load 60% capacity	Suburban streets	**7.3**
MD	Transport van (700 kg capacity) Load: 60% Capacity	Main suburban highway	**10.2**
ME	Transport van (700 kg capacity) Load: 60% Capacity	Motorway	**8.2**
MF	Prime mover + semi trailer (Leaf spring susp.) Load: <5% capacity	Country roads	**14.7**
MG	Tipper truck (16 tonne capacity, Air ride susp.) Load: 25% capacity	Country roads	**5.5**
MH	Small flat bed truck (1 tonne capacity, leaf spring susp.) Load: <5% capacity	Suburban streets	**8.4**
MK	Sedan car Load: 1 passenger	Suburban streets	**12.0**

This inherent non-Gaussian nature was also studied by Sek (1996), where the amplitudes of peak vehicle vibration acceleration levels were compared with the peak levels of the equivalent Gaussian signal. It was shown that for the vehicle vibration, 99.7% of acceleration levels fell within the limits +/- 1.25g, whilst for the equivalent Gaussian signal 99.7% of the data fell within the reduced limits of +/- 0.75g (where g = 9.81 m/s^2), hence highlighting further the fundamentally non-Gaussian nature of vehicle vibration.

It should be noted that within this Thesis vibration has been measured using acceleration using the unit g = 9.81 m/s^2.

3.5 Vehicle Vibration Frequency Response

The major frequencies contributing to the vibration of a vehicle generally fall below 100 Hz, with the most significant of these below 50 Hz. Frequencies above 50Hz tend to be insignificant in comparison (Vursavus and Ozguven, 2004; Peleg, 1985). A vehicle's vibration response is typically measured within the range of 1

Hz to 200 or 250 Hz (Chonhenchob et al, 2012; Singh et al, 2006; Lu et al, 2008). Within this range there are three key resonant frequencies:

1. ***Body resonance in the suspension system*** - this lies between 1 - 5 Hz, with air ride suspension systems typically in the range 1 - 1.5 Hz and leaf spring suspension systems 4 - 5 Hz (Garcia-Romeu-Martinez et al, 2008).

2. ***Resonance of the unsprung mass*** – i.e. the unsuspended part of the vehicle, is typically in the range 10 - 20 Hz (Singh et al, 2007). Vehicle dynamists refer to this resonance as 'wheel hop' which is typically around 12 Hz.

3. ***Resonance of the vehicle's structure*** - has been found to be up to 100 Hz (Suciu et al, 2012). More specifically, for semi trailer vehicles, this third frequency lies between 40 - 55 Hz (Singh et al, 2007).

Changes in vehicle parameters can lead to changes in the vehicle's resonant frequencies. For example, the lower the sprung mass of the vehicle the higher the first natural frequency. By reducing the suspension stiffness or tyre stiffness there will be a reduction in the corresponding natural frequency (Rajamani, 2012). A comparison of different vehicle types including: a passenger car (2 tonnes); pickup truck (2.7 tonnes); two small delivery vans (3.9 tonnes); and, a freightliner (7.3 tonnes); illustrated the variation in vehicle frequency response. The results of the study are shown in Figure 26.

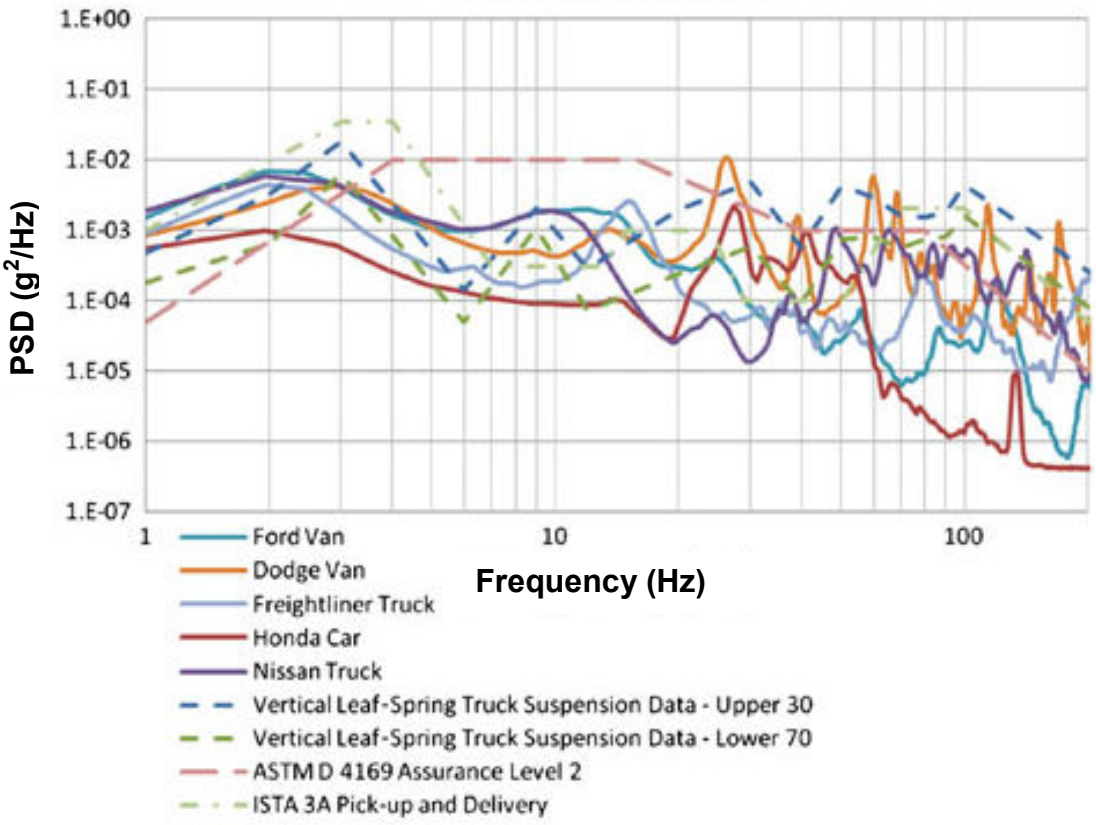

Figure 26: Comparison of PSD's for the vertical vibration response of different vehicle types (Chonhenchob et al, 2012)

In Figure 26 the freightliner's suspension resonant frequency is in the region of 3 - 4 Hz, whilst the suspension resonant frequency of the other smaller vehicles is around 2 Hz. What is also apparent is the overall variation in the energy content, with the Honda car having significantly lower energy content than the larger vehicles.

3.6 Vehicle Vibration's Multiple Degrees of Freedom (MDOF)

A vehicle's response is defined by the road input and its parameters. The irregular and asymmetric nature of these produces a six degree of freedom response at any point on the vehicle floor. This includes three linear: vertical; longitudinal; and, lateral; and, three rotational: pitch; roll; and, yaw. These are illustrated in Figure 27. Typically, the vertical vibration of the vehicle contains the most energy and therefore has the most significant damage potential, this has been corroborated in

a number of studies (Singh et al, 2006; Singh et al, 1992; Singh et al, 2008; Chonhenchob et al, 2012). Hence, historically, vibration testing of packaging has been carried out using a single degree of freedom (SDOF) test that represents the vertical motion of the vehicle floor. A further reason for this is the limitation of many vibration tables and controllers, which are restricted to single or a partial set of DOFs. However, multi axes rigs exist and it is thus possible to simulate the full motion of the vehicle floor, at a point.

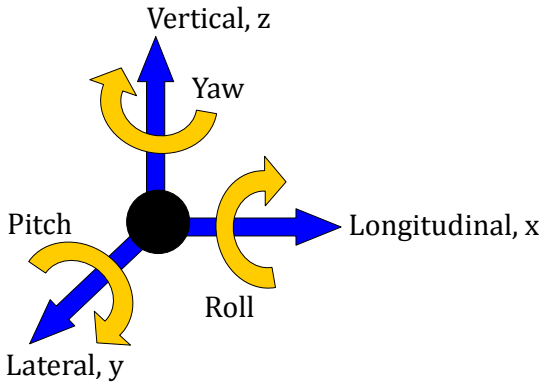

Figure 27: Translational and rotational axis of MDOF response of vehicle floor

In contrast, Bernad et al (2010) argue that there may be a need for MDOF testing. Bernard et al used operational modal analysis to compare the bending moments of a stack with the vertical resonances. The study concluded that, as packaging is primarily designed for compression strength, the effects of the lateral and longitudinal vibration on the stack may consequently be significant, and lead to either sliding and/or stack failure.

Singh et al (1992) considered the three translational degrees of freedom. When comparing the energy of the vibration of each of the three axes it was clear that below 20 Hz the vertical component was significantly greater than the longitudinal or lateral. However, above 20 Hz, the energies along each of the axes were similar. It was also noted that the more heavily laden a truck, the greater the amplitude of the lateral and longitudinal vibration.

Singh et al (2008) also measured the RMS acceleration values of each of the translational axis during a Less-Than-Truckload (LTL) shipment, these were

0.338g, 0.095g and 0.088g for the vertical, lateral and longitudinal axes, respectively. This variation in intensity for each translational axis is agreed with by Bernad et al (2011), where the RMS acceleration values were found to be 0.091g, 0.056g and 0.039g, respectively.

Contrary to the results shown in these studies, which use vibration measured on North American roads, results from a study measuring vibration on Indian roads showed that the lateral and longitudinal vibration was of greater significance. Here the average RMS acceleration values were 0.138g and 0.063g for the lateral and longitudinal vibration, respectively, and 0.151g for the vertical axis (Singh et al, 2007).

In a similar manner to the linear axes, Bernad et al (2011) also investigated the rotational axes of vibration. The results showed that the pitch and roll components of the measured vibration were much greater than the yaw component, with RMS acceleration values of 0.94, 0.81 and 0.525 rad/s^2, respectively. The pitching motion had a spectral peak at around 2 Hz and both pitch and roll showed a notable response at approximately 7 Hz. The roll motion showed a high frequency content above 20 Hz with its peak value at around 36 Hz.

Whilst a vehicle's vertical vibration may be greater in magnitude than its lateral and longitudinal vibrations, previous studies have shown that the amplitude of the latter two can become more significant depending on geographical location. Although in comparison, vibration in the other axes may appear insignificant, their combined affect at resonant frequencies could impact on product damage. It is therefore necessary to evaluate the contribution to damage of the other axes.

3.7 The Factors That Influence Vehicle Vibration

Vehicle vibration results from the complex interaction between the road surface and the vehicle. Vursavus and Ozguven (2004) determined that the road roughness; distance travelled; vehicle speed; product packaging; and, vehicle

characteristics, including the suspension and number of axles; influences the vibration measured response of the vehicle.

The input excitation of the road profile is shaped by constant surface roughness interjected with large displacement events, such as road damage or features e.g. potholes and speed bumps. Variables relating to the vehicle and driver then determine the shape and amplitude of the vehicle's excitation, leading to a vehicle response characterised by the vehicle's dynamics. The varying input and dynamics throughout the vehicle mean that, when measured at two separate locations in the vehicle, the measured response will be different. In addition to this, variations in the method used to measure vibration, including sampling parameters, will also influence the recorded response.

Figure 28 summarises the aforementioned: inputs; vehicle and driver variables; and, measurement parameters; which determine the vehicle's response that is subsequently used for analysis.

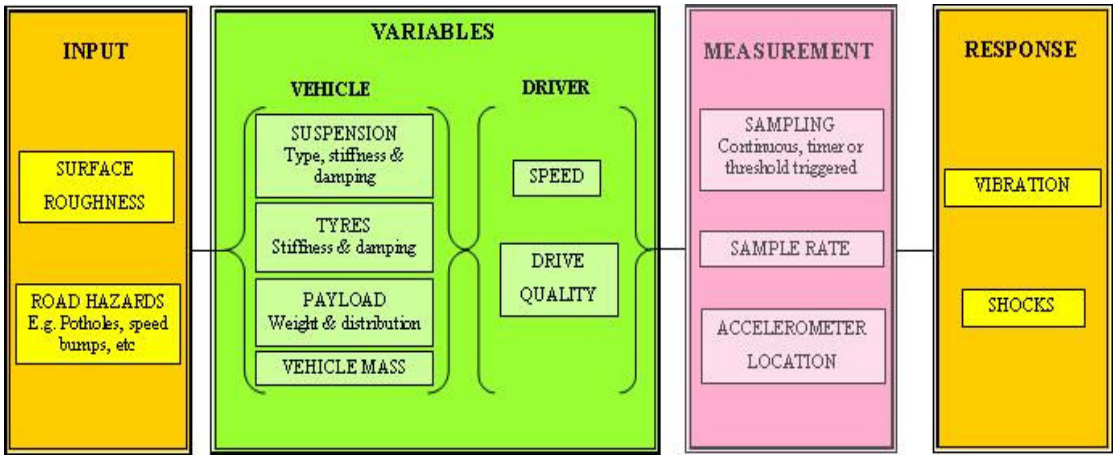

Figure 28: Inputs, variables, measurements and responses of vehicle vibration

3.8 Inputs

When considering its effect on road vehicles, road surface roughness is a measure of its longitudinal profile (Gillespie, 1985). It is well known that the profile of a road's surface varies across the width and length of the road. This variation in the

road profile is further increased by the presence of localized road damage or hazards in the form of large deviations in the road surface. These are typically random and rarely cover the width of the road. A combination of the surface roughness, road damage and hazards are what shape the initial excitation of the vehicle. Therefore from the outset, the vehicle's response is random, unpredictable.

3.8.1 Surface Roughness

It is universally accepted that the overall condition of roads varies significantly between countries. A review of the percentage of paved roads – roads which have been covered with a layer of material e.g. concrete, asphalt, bitumen, etc - highlighted the lack of infrastructure in some of the world's developing countries, such as Bolivia and Kenya where only 7.9% and 14.3% of the roads are paved, respectively (FAO, 2004). Evaluating a country's road quality by the percentage of paved roads is not a perfect indication of road quality due to anomalies, for example Australia. Here the percentage of paved roads is relatively low due to the size of the country and population distribution. Therefore, the percentage of paved roads can act as a good indicator of the general conditions of distribution and highlight the extremes of countries with a severe lack of infrastructure and that therefore are more likely to provide harsh distribution conditions.

In section 2.6.2 the variation in road conditions in India was compared with that of North America. Singh et al (2007) showed that in comparison with the PSD given in the current ISTA standards, the amplitude of the PSD recorded on Indian roads was 10 - 70 times higher in the frequency range of 1 – 5 Hz. This increased intensity at the low frequency range will lead to much larger vertical displacement of the vehicle, than that produced from the standards PSDs. This highlights the variation in road roughness between countries, with Indian roads having many more or larger road defects.

The roughness of roads in India was calculated by Ramji et al (2004) using the spatial PSD, measuring the roads vertical displacement (m) in relation to the road

length (m). An equation to approximate the spatial displacement PSD of the road surface is given as:

$$S(\omega) = C\omega^{-N} \tag{16}$$

where:

$S(\omega)$ = power spectral density

C = constant, the value of which depends on the road type

ω = spatial frequency (cycles/m)

N = constant varying between 1.9 and 2.1

The constant *C* found for each road type is given in Table 6, with the greater the value of *C,* the greater the roughness of the road surface. The results indicate large variations in the roughness of the road surfaces for different road types. The results of this study are consistent with a study by Zhou et al (2007) who considered the variation in vibration whilst travelling on different road types in China. The study showed a significant variation in the energy content of vibration over highways, arterial, secondary, tertiary and laterite (defined by Zhou et al as 'rutted, pothole-filled lanes on hardened clay, commonly used in Chinese villages roads'). The energy of vibration in the low frequency range (1 – 5 Hz) on tertiary and laterite roads was approximately twice that on highways. This indicates that the road surface on highways is much smoother than that of tertiary and laterite roads.

Table 6: value of constant C_{sp}, for varying road types (Ramji et al, 2004)

DESCRIPTION OF ROAD SURFACE	C_{SP}
Newly Laid surface road	0.3×10^{-06}
Smooth road	2.4×10^{-06}
Rough road (Highway with gravel)	4.4×10^{-06}
Smooth Highway road	0.5×10^{-06}
PCC (Portland Cement Concrete) road	0.6×10^{-06}

Cebon (1999) discusses the variation in road roughness, and presents suggested spectral limits for road roughness classifications. These are illustrated in Appendix

IV, Figure 134. By superimposing a road's surface profile displacement PSD onto the limits the roughness of the profile can be evaluated.

3.8.2 Road Hazards

The road construction also has a bearing on the vehicle's response, in terms of: paving material; man-made hazards such as traffic calming measures (speed bumps); kerbs or raised metal joints; and, road damage such as potholes. These can cause potentially damaging high amplitude shock events, depending upon the speed at which they are approached. Figure 29 shows the effect hazards have on a vehicle's response: (a) shows the response of a home delivery vehicle travelling at 15 mph over a speed bump when a peak acceleration of 2g was recorded and (b) shows the same vehicle's response when it mounted a kerb at 15 mph when a peak acceleration of 0.85g was recorded. Figure 30 shows the related hazards. The presence of hazards can greatly affect the overall response of the vehicle. It is therefore evident that when creating a simulation test the condition of roads throughout the distribution route needs to be taken into consideration.

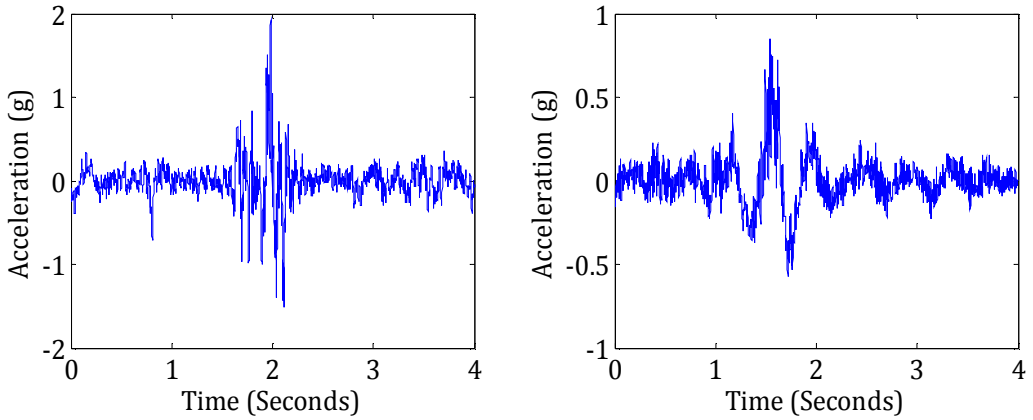

Figure 29: Vehicle vibration response to (a) Speed bump (b) Pavement kerb

Figure 30: (a) Speed bump (b) Pavement kerb

Variation in road roughness also arises from the use of different construction materials. This variation can be seen in one study where the PSDs determined from travel on concrete Spanish roads produced much higher spectral peaks and therefore a higher intensity vibration than the PSDs from travel on asphalt French roads (Barchi et al, 2002). The difference between the two spectra was evident with the first spectral peak at around 9 Hz varying from approximately 0.008 $(m/s^2)^2/Hz$ on Spanish roads to 0.003 $(m/s^2)^2/Hz$ on French roads. This difference can also be seen at the second spectral peak at around 20 Hz where the Spanish road's peak is approximately 0.15 $(m/s^2)^2/Hz$, and, the peak for French roads is 0.11 $(m/s^2)^2/Hz$. This shows overall, that the Spanish concrete roads produced a more severe journey.

Furthermore, another study compared a vehicle's response on roads constructed, respectively, of laterite (defined in the study as loose gravel on hardened clay, commonly used in farm regions), concrete (highway) and asphalt (highway). The results showed a significant difference in the amount of damage occurring to the test product. For a 2 tonne truck travelling at 40 km/hr, the average product damage on Laterite roads was 10%, on concrete 4.7% and on asphalt 2.0% (Jarimopas et al, 2005). This demonstrates that the road profile of laterite roads is much harsher than that of concrete or asphalt.

These studies highlight the fact that road surface roughness is not just characterised by road condition, but rather, a number of factors pertaining to the road's construction, material and also additional hazards that can result in large displacements of the road surface. Therefore, when estimating the intensity and

characteristics of vehicle vibration for a given distribution journey, the country of distribution and the road types travelled on should be considered.

3.9 Variables

Whilst the intensity of the initial input to the vehicle is determined by the roads travelled, the magnitude and shape of the vehicle's response to that input is characterised by the vehicle's parameters such as the suspension system, tyre dynamics and vehicle payload. The variations in vehicle parameters and their effect on a vehicle's response are now summarised.

3.9.1 Suspension

The suspension system is critical in protecting the vehicle from excessive shock and vibration loading, which can cause damage and/or fatigue (Garret et al, 2001). The vehicle's suspension system has a significant effect on the vehicle's handling and ride comfort. Because of this, many distribution vehicle manufacturers build a vehicle to suit the customer's requirements. This means that suspension characteristics can vary not only between vehicle types, but between similar vehicles depending on their intended load. Any variation in suspension characteristics will ultimately be seen in the vehicle's vibration response. There are three main categories of suspension system: passive, semi-active and active, these have each been described by Jalili (2002) as:

- ***Passive***

  Passive suspension systems consist of a stiffness member (spring) of stiffness K_S and a fixed rate damper, which dissipates vibration energy, with damping rate C_S. The performance of the passive system varies with frequency, with the system having a limited frequency range. It therefore has an inherent compromise on frequency isolation. Because of its fixed rate, the passive suspension system's performance is limited particularly when considering

broadband frequency range applications. Figure 31(a), illustrates a passive suspension system within a quarter vehicle model.

- ***Active***

By including an additional feedback controlled actuator, an active suspension system with adaptable to different driving conditions is created. By measuring the acceleration of the vehicle's mass and the unsprung mass, the actuator force can be controlled so as to minimise the force transferred to the vehicle floor.

The computation requirements and the additional components of an active suspension result in an expensive and complex system with high energy consumption. Figure 31(c), illustrates a passive suspension system within a quarter vehicle model.

- ***Semi-active***

A Semi-active system bridges the gap between the capabilities, and the limitations of the passive and the active suspension systems. Like the passive system, it comprises of a damper and spring element but, in addition, it allows for variation in its optimal frequency range, although by comparison to the active system this is relatively limited.

Air ride suspension is a semi active system, whereby the stiffness member consists of an air spring or hydro pneumatic system. Figure 31(b), illustrates a passive suspension system within a quarter vehicle model.

In Figure 31, M_V is a quarter of the vehicle mass, M_T is a quarter of the unsprung mass, K_T is the tyre stiffness, and, x_0, x_1 and x_2 are the vertical displacements of the: road, unsprung mass and vehicle, respectively.

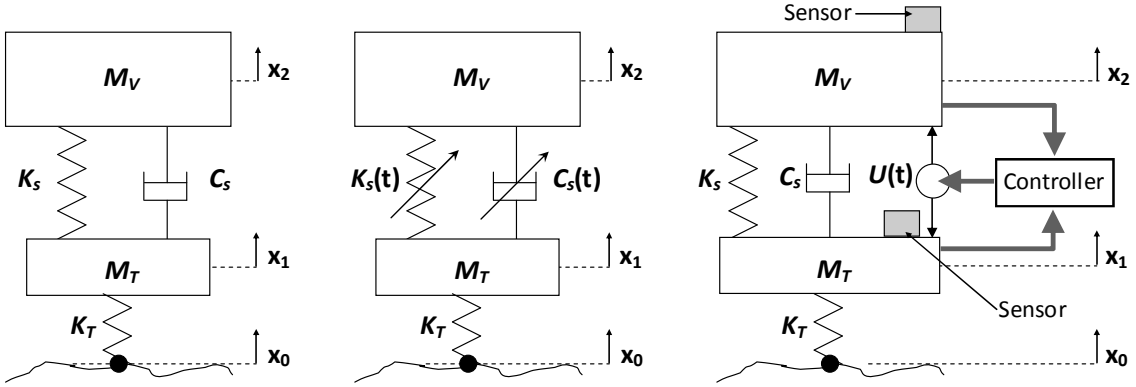

Figure 31: Quarter vehicle model with (a) passive (b) semi-active, and (c) active suspension

The two most common forms of distribution vehicle suspension system, which are both simulated in the current ASTM and ISTA standards are the passive spring leaf or semi-active air ride suspension.

3.9.2 Spring-Leaf and Air Ride Suspension

The stiffness of the leaf spring suspension system remains fixed for all load configurations. Therefore, when designing the suspension system, both the vehicle mass and its mass when fully laden need to be considered. This limitation means that the performance of a suspension system that is designed to attain and meet the requirements of a suitable ride height (distance of the vehicle floor from the road) for a fully laden vehicle will be greatly diminished. This will lead to a poor ride quality when the vehicle is part loaded or empty. Additionally, constant stiffness coupled with varied payload will cause variation in the vehicle's resonant frequency. As a way of improving ride quality in distribution vehicles, manufacturers tend to design the suspension system to meet the requirements of the load it is intended to carry. This means that suspension systems and their characteristics not only vary between vehicle manufacturers and models, but also between the individual vehicles themselves.

Damping within the spring leaf system is provided via either the spring friction (typically flat leaf springs, with high Coulomb friction) or, through shock absorbers with either fixed or variable damping depending on the system type

(Gillespie, 1985). An example of a leaf spring suspension system is given in Figure 32(b).

Semi-active air ride (air sprung) suspension is the main alternative to the passive leaf spring system. It consists of a pressurized elastomeric bag, which lifts the sprung mass of the vehicle. When the vehicle load varies, the pressure in the air springs also varies so that the correct ride height of the vehicle is maintained. Because the air spring's stiffness varies proportionally to the vehicle mass, its resonant frequency remains constant at all loads. Hydraulic shock absorbers are used to provide the necessary damping as the air spring's friction is too low to satisfy the damping requirement (Gillespie, 1985). An example of a leaf spring suspension system is given in Figure 32(a).

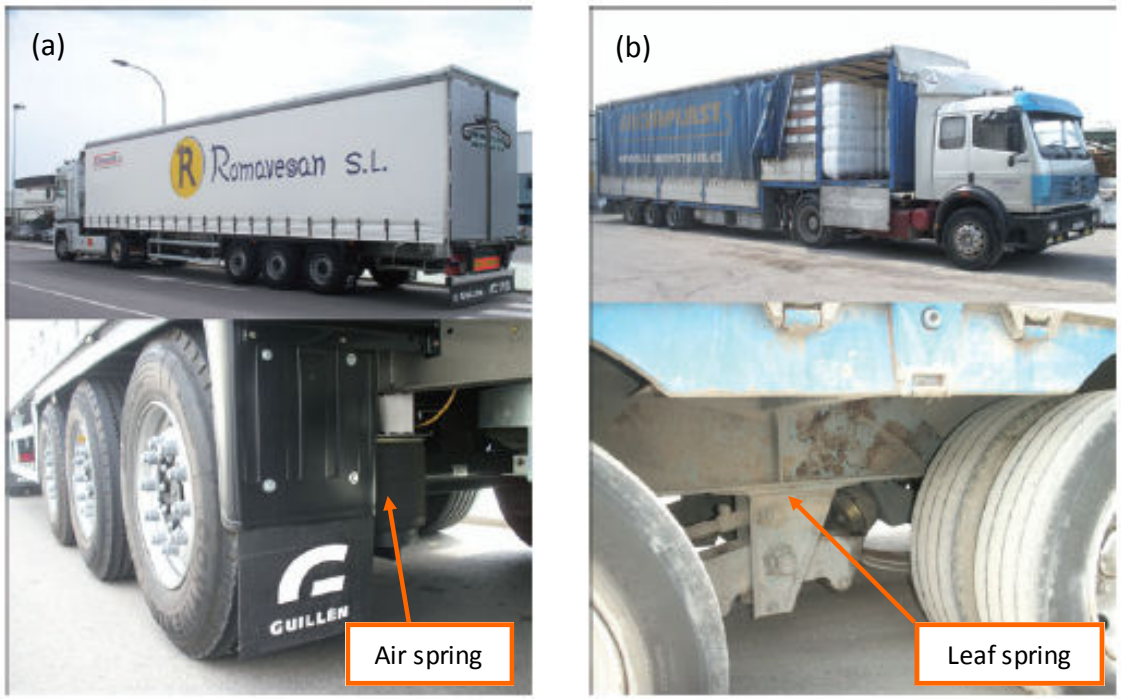

Figure 32: Examples of air ride (a) and leaf spring (b) suspension systems take from (Garcia-Romeu-Martinez et al, 2008)

The variation in 'ride quality' between the two suspension systems can be seen by comparison of the PSD spectra provided in the current testing standards (Appendix III: Figure 157, Figure 158 and Figure 159). The first spectral peak of the air ride semi-trailer PSD is 0.009 g^2/Hz, and it is 0.018 g^2/Hz, for the steel

spring semi-trailer, showing a significant increase in the force transmission between the road and the vehicle. A comparative study of air ride and leaf spring suspension systems showed variation in the first vehicle resonant frequency and the overall vibration intensity. The first natural frequency of a vehicle with air ride suspension was found in the range 1 – 3 Hz and in the range 3 – 5 Hz for a leaf spring suspension. The PSDs relating to the air ride and the leaf spring suspension are shown in Figure 33 and Figure 34, respectively (Singh et al, 2006).

The increased intensity and overall spectral content of the leaf spring system in comparison with the air ride is also apparent in Figure 33 and Figure 34, highlighting the benefit of the semi-active suspension provided by the air ride system. Another study comparing the two systems is in agreement with Singh et al, finding the RMS acceleration level of air ride vehicles to be less than half that of leaf-spring vehicles (Garcia-Romeu-Martinez et al, 2008).

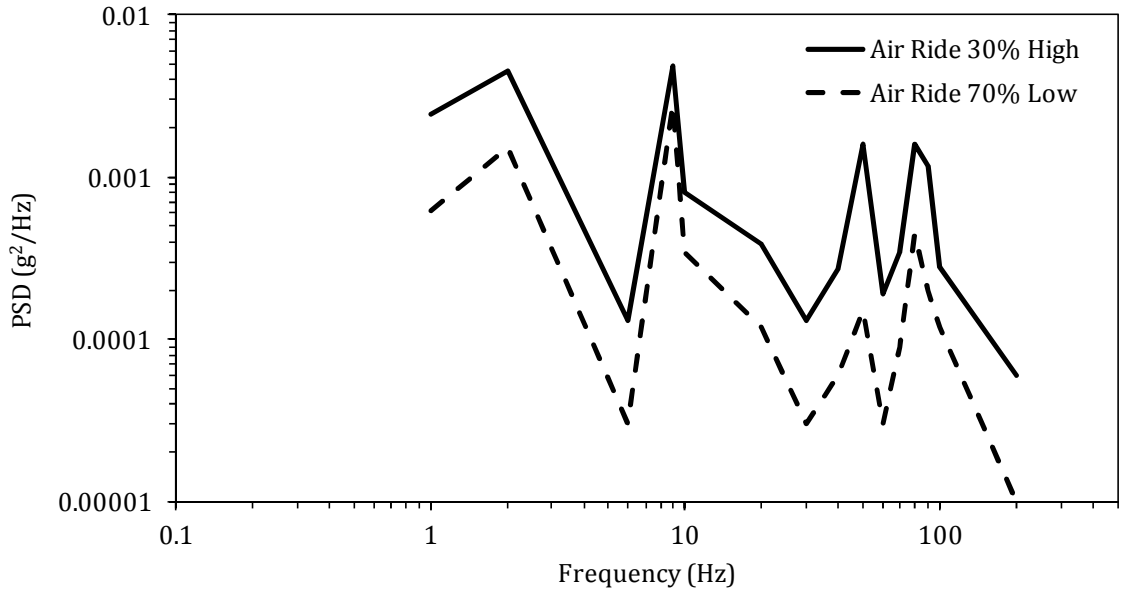

Figure 33: Average PSD for Air ride suspension vehicles showing the low 70% vibration and the high 30% vibration (Singh et al, 2006)

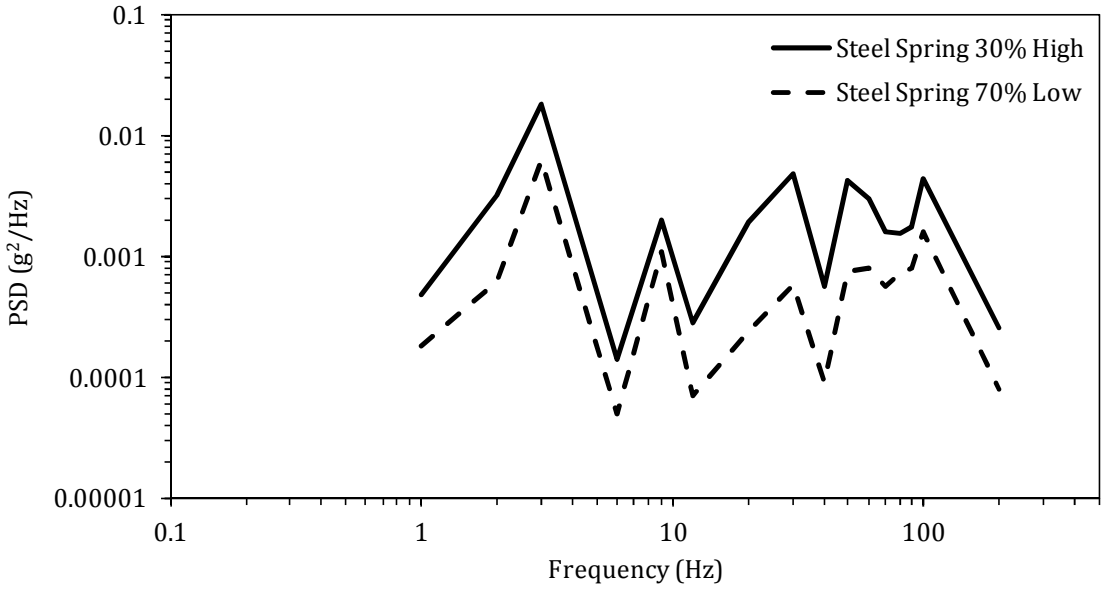

Figure 34: Average PSD for leaf spring suspension vehicles showing the low 70% vibration and the high 30% vibration (Singh et al, 2006)

3.9.3 Tyres

If imbalanced, tyre mass can cause undesirable vehicle vibration. These vibrations are most apparent when travelling over 40 - 45 mph (Yokohoma, 2003). Tyre misalignment can also cause a journey to be less smooth, leading to additional or amplified vibrations.

Tyre stiffness can be affected by over or under inflation. The increases in stiffness caused by over inflation results in a much harsher vibration response when traversing over the road surface, particularly over large displacements as the tyres are not able to isolate the effect of these as effectively. Over inflation of tyres reduces traction which leads to reduced handling capabilities, and more severe vibration response along all axes relative to the road. Cebon (1999) gives values of tyre stiffness for different tyre constructions and pressures. The load, stiffness and damping characteristics for different heavy vehicle tyre types, is given in Appendix IV, Table 40.

The size of tyres can affect the ride quality. The smaller the diameter of the tyre, the deeper the tyre will move into depressions and the quicker it will move over obstructions in the road, leading to a rougher ride.

3.9.4 Payload

During a distribution journey, a vehicle's payload can vary from being fully laden to partially laden. This is particularly true in the case of home delivery or delivery from a distribution centre to multiple stores. It is therefore important to consider the effect that this change in payload has on the vehicle's vibration response. Table 7 shows how increasing the payload decreases the average RMS value of the vehicle's vibration acceleration. This is expressed through the average RMS acceleration level (Garcia-Romeu-Martinez et al, 2008). For the vehicle with an air ride suspension, the added payload had the greatest effect between 0 - 40 km/hr where the RMS acceleration decreased by 32%. For the vehicle with a spring-leaf suspension, the added payload had the greatest effect between 40 - 70 km/hr where a decrease of 26% was experienced.

Table 7: Results from a study carried out by (Garcia-Romeu-Martinez et al, 2008) on vibration levels in Spain

VEHICLE	PAYLOAD	RESULTING VIBRATION RMS ACCELERATION (g) FOR EACH SPEED RANGE		
		0-40 km/hr	40-70 km/hr	70-110 km/hr
Air Ride (2 tonne)	0 Tonnes	0.068	0.087	0.093
Air Ride (2 tonne)	21 Tonnes	0.046	0.076	0.094
Spring-leaf (3 tonne)	0 Tonnes	0.212	0.238	0.254
Spring-leaf (3 tonne)	3 Tonnes	0.172	0.177	0.200

3.9.5 Vehicle Mass

Distribution vehicles range in size from a small family car to a large semi trailer. The size of the intended distribution vehicle and its kerb weight will denote certain other vehicle parameters, such as tyre pressure and suspension characteristics. The effect of vehicle size and mass on its frequency response has been discussed in

section 3.5, where the variations between a standard car and small and medium delivery vehicles, was evident. It has also been highlighted in the previous section that a vehicle's load level (payload) affects its vibration response.

3.9.6 Vehicle Speed

It has been observed in many studies that a vehicle's speed greatly affects its vibration response the higher the speed the greater the intensity of vibration (Singh et al, 2008; Garcia-Romeu-Martinez et al, 2008; Rouillard 2008). This is evident in Table 7, where the RMS acceleration was calculated for vehicles travelling at different speeds (Garcia-Romeu-Martinez et al, 2008). The same pattern can be seen in Figure 35, where the RMS acceleration measured in 5 second samples of a distribution journey and plotted against the vehicle's speed (Sek, 1996). There is a strong correlation between vehicle speed and RMS acceleration, with the RMS acceleration increasing proportionally with speed up to 20 mph and between 40 to 60 mph. Between 20 to 40 mph, the RMS acceleration remains approximately constant.

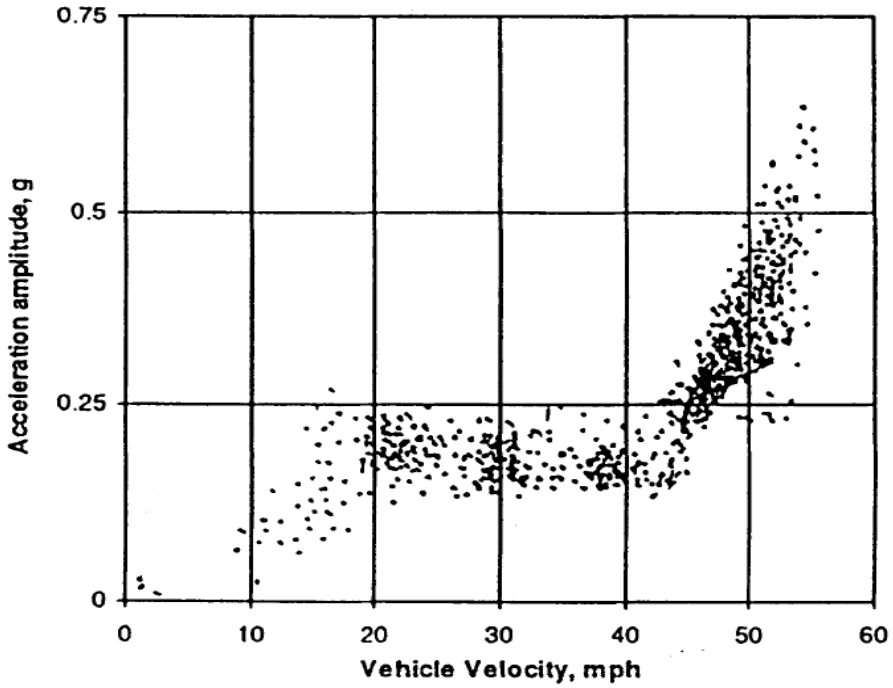

Figure 35: Variation of vibration severities with vehicle velocity, RMS acceleration (g) averaged over 5 second intervals (Sek, 1996)

A study by Lu et al (2010) also concluded that there was a positive correlation between the RMS acceleration and vehicle speed, with the proportional increase in the RMS acceleration being greater at lower speeds than higher speeds.

3.9.7 Drive Quality

Drive quality relates to the way in which the vehicle is driven. Poor drive quality is the result of poor handling and driver errors such as hard braking, high speed cornering and travelling over road hazards (e.g. speed bumps or potholes) at speed. These can cause substantial shocks to the vehicle, amplify the effects of adverse road conditions, and, can cause unnecessarily high rotational and linear movement leading to excessive multi axis vibration of the vehicle. Human factors and their effect on the vehicle response are extremely hard to determine, but consideration of the variation in the quality of driving should be considered when simulating a distribution journey. For instance, long duration distribution journeys can cause driver fatigue. Studies have shown that driver fatigue results in slower reaction times and low concentration. Driver fatigue can manifest itself through poor driving or road traffic accidents (Hartley and Arnold, 1994; Philip et al, 1999).

3.10 Measurement

The previous sections have discussed the factors that affect and characterise the vehicle's response. In all of the experiments the response is measured using accelerometers and data acquisition units. The measured response can be greatly affected by: the type of sampling, whether continuous or timed or level triggered; the rate at which data is sampled; and, the location in which the vibration is measured.

3.10.1 Continuous vs. Sampled Data Acquisition

The most accurate way to capture a vehicle's vibration response during a distribution route is to acquire data continuously. By doing this, every event within the distribution journey will be captured and can be analysed.

It has already been noted that vehicle vibration is highly unpredictable and if a journey is repeated using a single distribution vehicle it will not be replicated exactly, although the overall data averaged PSD is likely to be consistent. Since distribution journeys are long in duration, the large quantity of data required to accurately evaluate a single distribution route becomes apparent. For example, a 10 hour distribution journey with a sample frequency of 500 Hz, recording two channels namely, the vertical vibration and the sample time, would require 360 Mb of memory. If the GPS location and speed data are recorded every 5 seconds then an additional 1.5 Mb is required. However, many data acquisition units used within the distribution field are limited to a memory capacity which is much lower than that required for this amount of data - for example, the Lansmont© Saver 9x30 has a memory capacity of 128 Mb. Because of this limitation, data acquisition is typically carried out using some form of data sampling, either, time triggered sampling or trigger level sampling:

Time triggered sampling – where data are sampled at specified intervals for a set period of time. There is no specified sample interval or size, both of which have varied significantly across studies (Jarimopas et al, 2005), probably due to data limitations and the length of the journey studied.

Trigger level sampling – data are monitored continuously and once a threshold acceleration level is reached a sample of a set period is recorded. The choice of acceleration threshold trigger also varies across studies depending on the type and condition of the roads being monitored (Chonhenchob et al, 2012; Garcia-Romeu-Martinez et al, 2008). The implication of using threshold trigger level sampling is the possibility that the data will be biased towards higher acceleration levels, and therefore the data appears more severe than might actually be the case (Kipp, 2008a).

In some cases a combination of the two sampling techniques is used, but this can also result in the data being biased towards the extreme vibration levels. It is therefore wise to analyse the time and level triggered samples independently of each other, using the level triggered samples to evaluate the extreme data and treating the time sampled data as a means of evaluation (Rouillard and Lamb, 2008).

When using sampling, it is important that the sample rate, the sample size and/or the trigger level are selected to suit the distribution environment being measured. If the period between samples is too great, a poor representation of the environment will be obtained. Parts (a) and (b) of Figure 36 illustrate the results of time triggered sampling. Both have a sampling period of 60 seconds with different sample sizes of 10 seconds and 2 seconds respectively. In both cases shock events present in the full journey are missed out when sampling is used, this is particularly true when using the 2 second sample size.

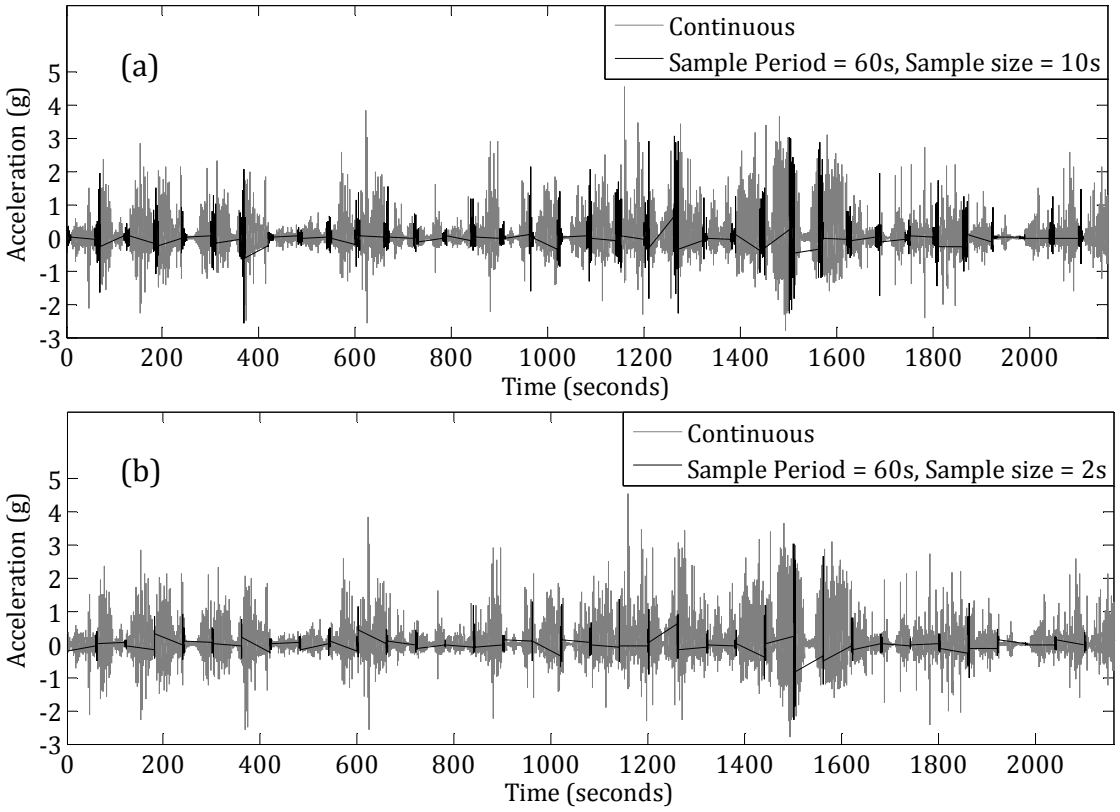

Figure 36: Example of time sampled data, 60s sample period (a) 10 second (b) 2 second sample size

This omission of critical vibration information is further evident in the RMS acceleration distribution shown in Figure 37, where the shape of the RMS acceleration distribution for the smaller sample size of 2 seconds does not show good correlation with the RMS acceleration distribution of the continually sampled data. This highlights the point that, by sampling at this rate, information in the actual signal will be lost.

This shows that the higher sample size of 10 seconds gives a more accurate representation of the full vibration signal, while a sample size of two seconds produces a distribution that is focused around 0.1g with a much narrower spread of data.

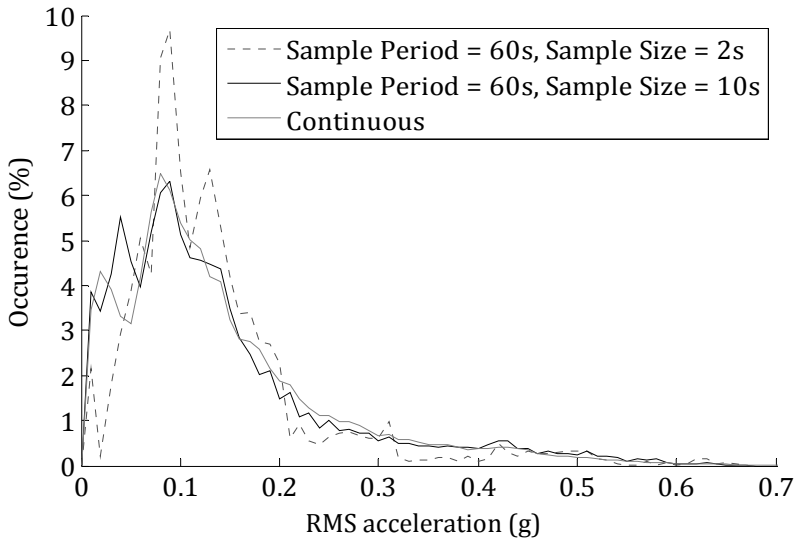

Figure 37: RMS acceleration distribution of 1 second samples

The PSDs of the continually sampled signal and both alternative sample rates are shown in Figure 38. Unlike the RMS acceleration distribution, neither PSD produced using the two sample sizes follows the full vibration signal's PSD exactly. In this case the sample size of 2 seconds produces an underestimate of the signal, while the sample size of 10 seconds, at points, overestimates the full signal's PSD.

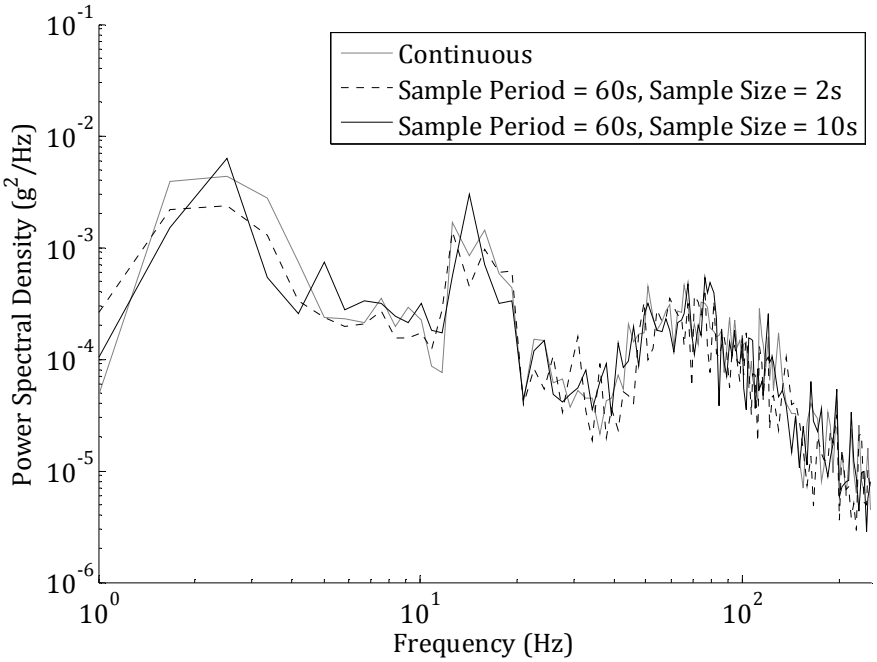

Figure 38: Average PSD's for full signal and sampled signals

It is therefore apparent that continuous data sampling is the only sampling method that will capture all events. Therefore, in order to create as accurate as possible a representation of distribution vibration continuous sampling should be used. In situations where this is not possible, Rouillard and Lamb (2008) state that in order to produce an accurate statistical representation of a distribution journey, at least 1/8th of the journey data should be recorded at evenly spaced intervals, for example, 2 seconds of data every 16 seconds.

3.10.2 Sample Rate and Frequency Range

The rate at which vibration data is sampled directly affects the frequency range over which the signal can be analysed with the frequency being inversely proportional to the sampling rate. In addition to this, when selecting a suitable sampling rate, the issue of aliasing, where the signal being analysed becomes distorted and false frequencies are detected, needs to be considered. Aliasing occurs when frequency range exceeds the sample frequency. To eliminate aliasing, the frequency range should be less than half the sampling frequency, this is often referred to as the Nyquist or folding frequency (Smith, 1989).

The vibration range of interest for vehicle vibration is between 1 and 200 Hz, therefore a sampling frequency of at least 400 Hz is required. This is consistent with previous studies which have used a sampling frequency of 500Hz (Chonhenchob et al, 2012), 651 Hz (Singh et al, 2007) and 1000 Hz (Garcia-Romeu-Martinez et al, 2008).

3.10.3 Location of Accelerometers in the Vehicle

It is known that vertical vehicle vibration is most severe at the rear of the vehicle on the kerb side (left hand side in the UK) (Zhou et al, 2007; Barchi et al, 2002; Singh et al, 2007). This is consistent with overseas studies such as a study on Indian roads which concluded that *'....preliminary data collected showed that the rear and kerb side location produced the highest levels of vertical vibration on most highways that are generally two-lane, and have poor shoulders causing vehicles to go over severe road imperfections*' (Singh et al, 2007).

The intensity of the vertical vibration can vary significantly depending on the location in the vehicle. One study showed vibration at the rear of the vehicle was 14 times greater than at the front (Barchi et al, 2002). This difference is confirmed by (Zhou et al, 2007) where the average RMS accelerations were found to be 1.91 m/s^2 and 1.62 m/s^2 at the rear and front of the vehicle, respectively. It is therefore important that when recording vehicle vibration, the location of the accelerometer is considered. If the position of the load is known, then the vibration at that point should be measured or the worst case should be considered. Other studies have measured the vibration at several points and presented it as an average (Bernad et al, 2011) but whilst this allows all points in the vehicle to be considered, it may still form an under test if loads are distributed unevenly across the vehicle floor.

In general, accelerometers are located in either two (front and rear) positions or, three (front, middle and rear) positions. An exception to this was a study carried out in Spain which measured the vibrations at the central span of the rear axle (Garcia-Romeu-Martinez et al, 2008). Other setups have the accelerometers set at 100 mm from the right hand wall (Barchi et al, 2002; Berardinelli et al, 2004) and

200 mm from the right hand wall (Vursavus and Ozguven, 2004) - these tests were carried out in Italy, Spain, France and Turkey where vehicles are driven on the right hand-side of the road.

3.10.4 Measurement Equipment

In recent years, a large proportion of studies of vehicle vibration for the purpose of distribution packaging testing have used a Lansmont© Saver data acquisition unit (Singh et al, 2008; Singh et al, 2007; Singh et al, 2006; Chonhenchob et al, 2012). This unit benefits from: being compact, with all equipment contained within the unit; allowing fast transfer of data for analysis; and, being simple to use, with easy selection of sampling and trigger levels. Since, as previously mentioned, the unit has limited capacity memory (128 Mb), there must be compromise between sampling rate, sample size and duration of recording, in order to ensure a full distribution journey is recorded. Furthermore, as the unit contains a single tri-axial accelerometer, vibration can only be measured at one location in the vehicle. This is not an issue when a single axis of vibration at a set point is required, but when the vehicle's multi-axial motion is to be studied, then several units are required.

It follows that in order to create as accurate a representation of the distribution journey as possible, the data acquisition equipment must fulfil the following criteria:

- ***Move-ability of accelerometers*** – allows for data collection at any location on the vehicle floor.
- ***Tri-axial and multiple single axis data recording*** – allows the vertical vibration of the vehicle to be recorded in several positions at once and must be flexible in allowing for tri axial data recording when required.
- ***High memory capacity*** –allows for continuous data collection on potentially long duration distribution journeys, without the requirement for data download during the journey.
- ***High speed data acquisition*** – allows for multiple channels of data to be recorded together without affecting the acquisition rate.

- ***Non intrusive*** – being small and compact and not hinder loading and unloading of the distribution vehicle.

3.11 Simulating Vibration in Laboratory Environment

Within the laboratory environment, vehicle vibration is simulated using either a single axis, tri-axial or multi axes vibration table. The table controllers have the capability of creating random vibration from a given PSD and more recently developed controllers have the capability to carry out time replication of the vehicle vibration. But, in many cases time history replication is usually an additional software packaging and therefore not all new controllers have this. Older controllers will not have the facility to carry out time replication, while older test rigs may not have the capability.

One issue with current vibration controllers is that when reproducing time history vibration they are limited to frequencies below 50 Hz (Kipp, 2001). In section 3.5, it was stated that, for vehicle vibration, the frequency range of interest is from 1 Hz to 200 Hz. Therefore when using time replication the frequencies above 50 Hz are not represented in the simulation. Additionally, the vibration rigs are also limited by the maximum stroke. On many vibration table, including those at Smithers Pira and University of Bath, the maximum stroke is +- 75mm.

This means that when creating a new simulation method, these limitations must be taken into account, so that the simulation method is created is usable on all existing controllers. The simplest way to ensure the method is suitable is to:

1. Create a simulation method that incorporates random vibration simulated from given PSDs.

2. Simulates vibration along only one axis at any one time.

3.12 Concluding Remarks

It is evident that the intensity and characteristics of vehicle vibration is influenced by a number of journey and vehicle parameters. Furthermore, changes in these parameters can have a significant effect on the vehicle's response. When these factors are considered, alongside the sensitivity of the vehicle's dynamics, the resulting vehicle vibration can be said to be highly varied and unpredictable. Accounting for all of the various parameters is therefore important when considering the simulation of a distribution cycle where numerous vehicle types and geographic locations can be involved. One example is supermarket distribution, where distribution vehicles can range from large heavy semi-trailers to smaller delivery vans travelling between continents, countries or regions, depending on the product. It is therefore apparent that in order to accurately simulate vehicle vibration to test for the potential for product damage, the experience of the packaged-product throughout each stage of the intended distribution should be considered and accounted for. This includes road, vehicle and driver characteristics.

This variation in vehicle vibration between vehicles types and distribution journeys emphasizes the need for accurate data acquisition that reflects the intended distribution. In order to recreate a journey as accurately and as confidently as possible, continuous data acquisition should be used. If sampling is used then careful consideration must be given to the sample interval and size.

Furthermore, it is clear that inadequate data acquisition or misplaced measurement equipment can severely manipulate the measured vibration amplitude and characteristics. It is therefore essential that when measuring vehicle vibration the position of the packaged product and its loading are considered ensuring as representative a measurement as possible.

Vibration in the vertical axis is the most dominant and therefore considered to have the most damage potential. It is therefore often the case that only the vertical vibration is considered. In reality any point on the vehicle floor is subjected to six

degrees of freedom in its movement. Previous work has shown vibration along the other two linear axes – lateral and longitudinal; and, the rotational axes - pitch, roll and yaw; to be less significant than the vertical. However, when considering the loading arrangement of packaged products their effects can be more significant and therefore the effect of the MDOF vibration on product damage should be examined.

With an understanding of vehicle vibration, the established method set out in the existing testing standards for simulating vehicle vibration for the purpose of packaging testing, along with other suggested approaches, can now be evaluated.

4 A REVIEW OF SIMULATION METHODS

Kipp (2008b) posed the question: '*How can we create meaningful random vibration profiles for laboratory testing, while at the same time accounting for, and simulating the effects of: varying amplitudes, different characteristics, and infrequently-occurring large-amplitude motions?*'.

This question has become more pertinent for two reasons in particular:

- increased pressure on packaging engineers to create optimal packaging solutions that are sustainable - economically, environmentally and socially
- the evolving capabilities of computers and laboratory equipment which make the use of more complex simulation methods possible, which has enabled more in depth research into the behaviour and nature of vehicle vibration.

More recent research has led to dissatisfaction with the established method which is currently used to simulate vehicle vibration for packaging testing. This in turn has resulted in the creation of a number of alternative simulation methods that are seen to improve on the shortcomings of the established method.

An in depth review of both the established method, which underpins the ISTA and ASTM standards, and, several alternative methods, proposed in the literature, has been undertaken in order to establish their relative capabilities together with their limitations.

4.1 A Critique of the Established Method

Post 1980's, accelerated random vibration testing, utilising Gaussian signals produced from PSDs (Accelerated Gaussian Equivalent Method), has been the norm in distribution packaging testing and underpins both the ISTA and ASTM

vibration testing standards. The established method of building a simulation using this method can be summarised as follows:

Step 1: Data from multiple distribution journeys is collected.

Step 2: The FFT is then used to convert the signals from the time to the frequency domain. The DFT which underpins the FFT is given in Equation 12 and is stated here for completeness.

$$X(f_k) = \sum_{r=1}^{N} x(t_r) e^{-i2\pi f_k t_r}$$

The length of the DFT (the number of data points over which it is calculated) denotes its frequency resolution so that the larger the DFT (N) the higher the resolution, where the frequency resolution $\Delta f = 1/(Ndt)$.

Step 3: The PSD is then calculated using Equation 15, which is the calculation of the product of the DFT spectrum, $X(f)$, with its conjugate ($X^*(f)$) divided the length of $X(f)$, (N), multiplied by the sample interval (Δt).

$$S(f) = \frac{\Delta t}{N} X(f) \bullet X^*(f)$$

Step 4: The PSD spectra from multiple signals can then be averaged together, the equation for which is given in (Garcia-Romeu-Martinez et al, 2008).

$$PSD = \frac{1}{n} \cdot \sum_{i=1}^{n} S_i(f) \tag{17}$$

where n is the number of spectra being averaged so that $i = 1,2,3,...,n$.

Step 5: In order to reduce long test durations, tests are time compressed (test accelerated). Test acceleration is carried out based on the representation of accumulated damage, where damage can be measured as the stress levels and the number of cycles leading to some critical level at which the product fails. The stress level compared with the number of cycles to

failure (*S* - *N*) curve is used in most fatigue theory concepts. For most specimens of a single material and configuration a large part of the *S* - *N* curve can be approximated by the Basquin expression (Basquin, 1910):

$$m = N_f S_r{}^K \tag{18}$$

where N_f is the fatigue life at stress level S_r, K is the slope factor of the curve and m is the material constant, which is dependent on the material being tested.

Using the Basquin expression in Equation 18, a relationship between test duration and intensity (RMS acceleration) is constructed. This equation can then be used to accelerate the test (Shires, 2011). The increase in test intensity is inversely proportional to the reduction in test duration following the power law. This is specified in the military standards (MOD, 1999).

$$\frac{T_{Actual}}{T_{Accelerate\ d}} = \left(\frac{RMS_{\ Accelerate\ d}}{RMS_{\ Actual}} \right)^K \tag{19}$$

A widely adopted approach, and what it is assumed is used in the existing test standards, is to set K at 2 and the time compression by five (Kipp, 2000).

Unfortunately, there is currently no accurate way to measure the amount of accumulated damage or the rate at which it grows. Additionally, different materials have different fatigue rates, with the fatigue rates of samples of the same material varying due to differences in construction and quality. Because packaging is typically constructed of several materials each with a different fatigue life, the process of calculating fatigue rate is further complicated. These limitations mean that by using fatigue theory to accelerate the test it is necessary to assume that for each product, each packaging system is identically constructed and that the packaging system acts as a single material.

Step 6: A vibration signal can now be created using the accelerated average PSD. This is done by firstly rearranging Equation 15 to find the magnitude of the Fourier spectrum using the accelerated PSD.

$$X(f) = \sqrt{S(f)Ndt}$$

Because when calculating the PSD the Fourier spectrum's phase information is lost, a random phase array must be applied to form the real and imaginary parts of the spectrum. Following this Equation 11 for the inverse DFT can be applied and a signal, of length *N* can be calculated. The processes in step 6 are then repeated until a signal of the required length (duration) is produced.

Rouillard (2007) states that the PSD '*...does not contain information on time-variant parameters such as possible variations in amplitude or frequency or the time at which these variations occur. Furthermore, the temporal averaging process inherent to the PSD cannot separate the effects of transients within the signal*'. Therefore when using this technique to construct a time domain signal, the signal will always be stationary signal with a normal (Gaussian) distribution.

Figure 39 gives an example of how the established method is used and illustrates how the vehicle vibration (original signal) (a) varies from the simulated signal (equivalent Gaussian signal) (c). The reduced spread of acceleration levels is evident in the equivalent Gaussian signal with the defined shock events that were present in the original signal now not present. Additionally, the PSD presented in the testing standards (Figure 157 and Figure 158) is much simpler than the PSD shown in Figure 39. This is due to the use of spectral smoothing reducing the number of breakpoints used to define the spectral shape. This simplifies the shape of the PSD, making it easier to compile spectra and reducing the computational time required to run a simulation.

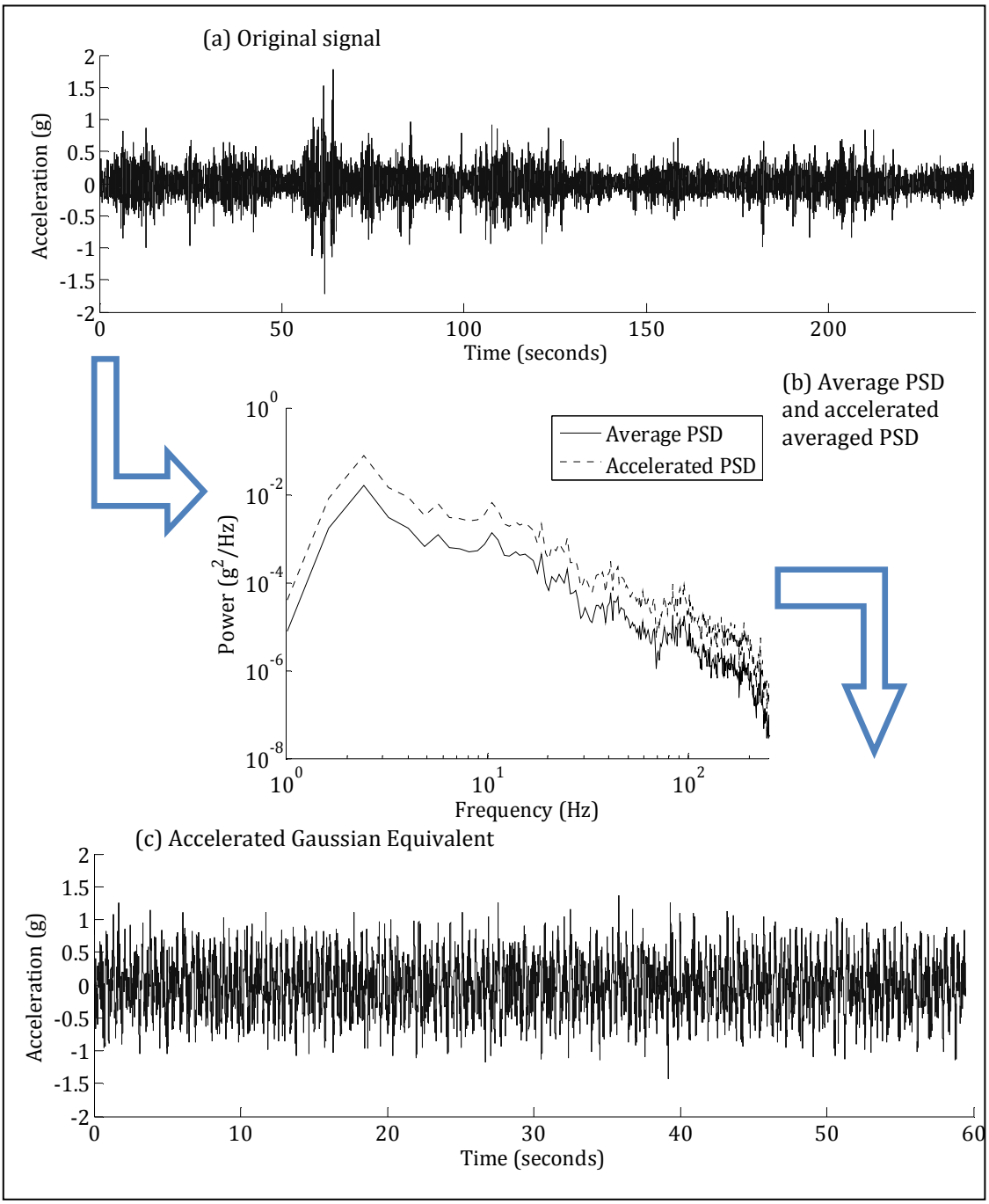

Figure 39: Example use of the accelerated Gaussian equivalent method

As previously discussed in section 3.7, accounting for the variations in distribution journeys is increasingly important. As a consequence of this, ISTA introduced test 4AB. When enough information about the intended distribution is available, this test allows the user to construct their own vibration PSD from historical data, so that a more relevant vibration test to be produced (ISTA, 2010). It is important to note that in order to create an accurate test with confidence, a large amount of

journey vibration data is required. Therefore, data collection on the intended distribution journey would need to be repeated several times to gain this confidence. The more times the journey was repeated, the higher the statistical significance of the resulting simulation.

4.1.1 Benefits of the Established Method

In section 3.7 the idea that no two distribution journeys will produce the same vibration is presented. A key benefit of the established method is that it lends itself easily to averaging. By creating a PSD from the vibration measured over several journeys, an averaged PSD with statistical significance and hence confidence can be produced (Kipp, 2001).

It would often be uneconomic and impractical to simulate the full duration of a distribution journey when testing packaging. By using test acceleration, the established method allows for a significant reduction of the test duration and the associated costs.

Furthermore, the simple nature of the method makes it straightforward to implement with the majority of laboratory controllers having the capabilities to execute the method.

The established method has been in use for many years and although it is limited in its ability to simulate shock induced damage or the complex variations in modern distribution, these points are generally well known and can be compensated for through conservative or over compensatory packaging design.

4.1.2 Limitations of the Established Method

Although there are benefits to the established method, it is subject to several limitations relating to the method and its application in the testing standards.

A key limitation is the nature of the simulation the method produces. The non-stationary and non-Gaussian nature of vehicle vibration has been discussed in

section 3.2. By simulating this vibration as stationary with a Gaussian distribution the high level acceleration events, which give vehicle vibration its non-Gaussian distribution, are absent. This means that the overall spread of acceleration levels changes, with actual vehicle vibration tending to have a distribution with longer tails and a sharper peak, while the simulated signal follows a bell shaped *Normal* distribution.

Additionally, a constant RMS acceleration level is used throughout the test. For actual vibration the RMS acceleration level will constantly fluctuate. Ultimately, this means that key characteristics of vehicle vibration are not simulated in the established method and hence the simulation produced is not an accurate representation of vehicle vibration. Simulating vibration in this way may manipulate fatigue damage or result in threshold level damage caused by high level acceleration events being neglected. While this limitation is known and can therefore be compensated for, the method cannot be used to optimise a packaging solution.

Furthermore, the fatigue theory used to accelerate the tests is not designed for the complex material construction of packaging and therefore may not be directly applicable to its application. This could lead to inaccurate simulation of product damage.

Whilst there are limitations regarding the method, the way in which it is applied in the testing standards is also limited. The standards use universal PSDs to simulate all semi-trailers with leaf spring suspension, or, all semi-trailers with air ride suspension, therefore not accounting for the variations in vehicle dynamics apparent between vehicles and payloads. Furthermore, using a single test to represent all distribution journeys may lead to cases of both over and under testing.

4.2 Improved Methods of Simulation

Many simulation methods have been proposed and developed to improve on the limitations of the established method. These can be grouped under six headings: time replication; two way split spectra; three way split spectra; shock on random; kurtosis control; and, RMS modulation.

4.2.1 Time Replication

Used in the automotive transport sector, to test for noise, durability, vibration and harshness, time replication testing requires the laboratory reproduction of a continuous time domain vehicle vibration for a given distribution journey. This allows for the complete recreation of the journey, which is therefore not '*statistically compromised*' (Bernad et al, 2011).

Whilst this may be beneficial for automotive testing, past studies into distribution vibration have shown that vibration intensities and characteristics vary between journeys due to changes in vehicle parameters and road conditions (Garcia-Romeu-Martinez et al, 2008). Therefore, using the time replication of a single journey would not sufficiently represent all journeys. A comparison of two journeys carried out on the same distribution route in the same vehicle is given in Figure 40 and Figure 41. Whilst the overall RMS acceleration for each journey was relatively similar at 0.197 and 0.207, respectively, the kurtosis of the signals varies dramatically, from 18 to 50 due to the presence of extremely high level shock events recorded on the second journey.

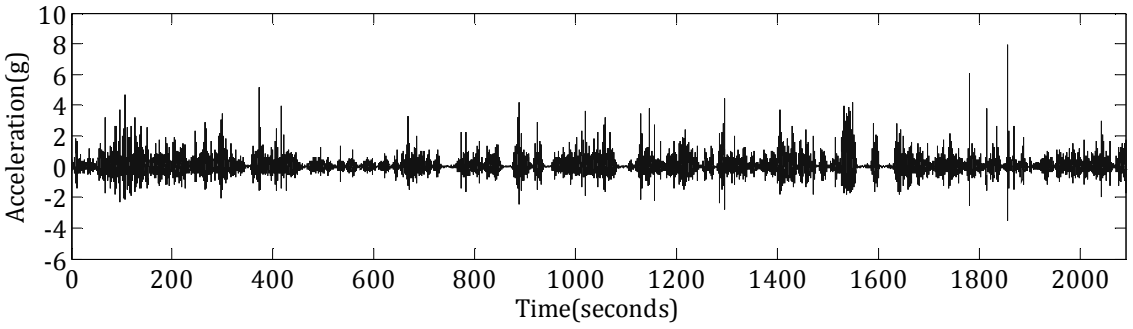

Figure 40: Vibration signal recorded on journey 1

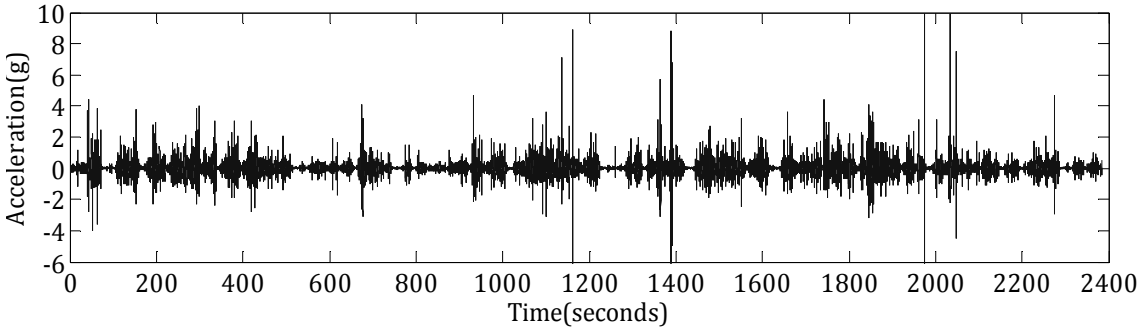

Figure 41: Vibration signal recorded on journey 2

Whilst the first journey may underestimate the severity of the journey, the second journey may be an over estimate. As a consequence there is a lack of confidence in the use of either signal. In order for there to be some level of confidence, multiple journeys on the distribution route must be recorded and evaluated, to approximate an 'average' journey. The data acquisition requirement for this method is time consuming and expensive and is therefore impractical for most products.

4.2.2 Two Way Split Spectra

Splitting the simulation PSD to form two spectra created from the lower and higher amplitude portions of vibration was first proposed by Young et al (1998). The method has further been used in a number of subsequent studies (Singh et al, 2006a; Chonhenchob et al, 2012). These studies created the two spectra based on the 70% low data and 30% high level data. A different study took a '*more stringent approach'* and split the spectra 80-20% (Wallin, 2007).

This method partially alleviates the issues relating to the established method by enabling testing to be carried out at a high acceleration level for a period of the test. This goes some way towards recreating the high level data that is modulated during. Additionally, it produces a signal that when considered as a whole is non-stationary and non-Gaussian. In reality the simulated signal is Gaussian and stationary for substantial periods of the total test. Importantly, the method is again based on averaged data and therefore a moderated signal is still produced, with the variation between high acceleration shock events and low level vibration not simulated accurately.

4.2.3 Three Way Split Spectra

An advance on the two way split spectra, a three way split, has been proposed. Here the signal is split into three parts leading to spectra of the lower 70%, intermediate 25% and top 5% of data. Arguably, this approach allows for better simulation of the overall vibration acceleration distribution and, in particular, the higher level events (Kipp, 2008b). Although in essence it still produces Gaussian, stationary signals for the greater part of the simulation.

Additionally, simulating all high level events consecutively could lead to unrealistic predictions of product fatigue or threshold level damage.

4.2.4 Shock on Random

Shock on random combines the established method with shock superposition. A PSD of the signal is used to create a random, stationary signal with a Gaussian distribution, representing the average vibration. Shock events recorded from the distribution journey are then integrated at random points within the signal, thereby allowing a signal with a non-Gaussian distribution to be produced and the high level shock events to be simulated (Kipp, 2001).

The benefit of this method is that it allows the input of realistic high level shock events in a manner similar to how they occur during actual vehicle vibration, therefore allowing for the impact that shock events have on product damage or on the activation of product damage.

Although the method allows for the non-Gaussian nature of the signal to be presented, the question of how many shocks and when they are imposed has to be asked. In order to confidently recreate the shock events on a particular distribution journey, it would be necessary to record vibration on several journeys to ensure an accurate view of the distribution journey is obtained. This exercise would be time consuming, costly and therefore inefficient.

4.2.5 Kurtosis Control

The established method produces a vibration signal with a kurtosis of 3. In section 3.4 the kurtosis of vehicle vibration was shown to be much higher. By applying Kurtosis control, the amplitude of higher acceleration events can be increased, resulting in a higher signal kurtosis. The generated signal would therefore have a similar acceleration distribution to vehicle vibration, although the sequence is statistically stationary. Van Baren (2005) describes a method of kurtosis control entitled 'Kurtosion' where a simulated signal is formed based on a given PSD, RMS acceleration and kurtosis parameter. The kurtosis parameter is used to increase the spread of the simulated signals acceleration PDF.

4.2.6 Modulated RMS Distribution

The RMS acceleration distribution of a vehicle vibration can be seen in Figure 42(c). Here the highly non-stationary nature of the vibration is evident. RMS modulation, randomly applies the statistical RMS acceleration distribution of the original vibration signal to create a non-Gaussian and non-stationary simulation signal constructed from short-time, stationary segments with a Gaussian distribution (Rouillard, 2007b).

Rouillard and Sek (2010) presented the development of the Statistical Vibration Synthesizer (SVS) module that can be incorporated into existing controllers and simulation tables, to create a modulated RMS simulation. The module randomly amplifies the table's drive signal to match the RMS acceleration distribution of the signal being simulated. A screen shot of the controller in use is provided in Figure 42. The computer system shows the real time: drive signal (a), PSD (b), RMS acceleration distribution of the simulated signal (c), RMS acceleration level (c) and the signal's PDF (d).

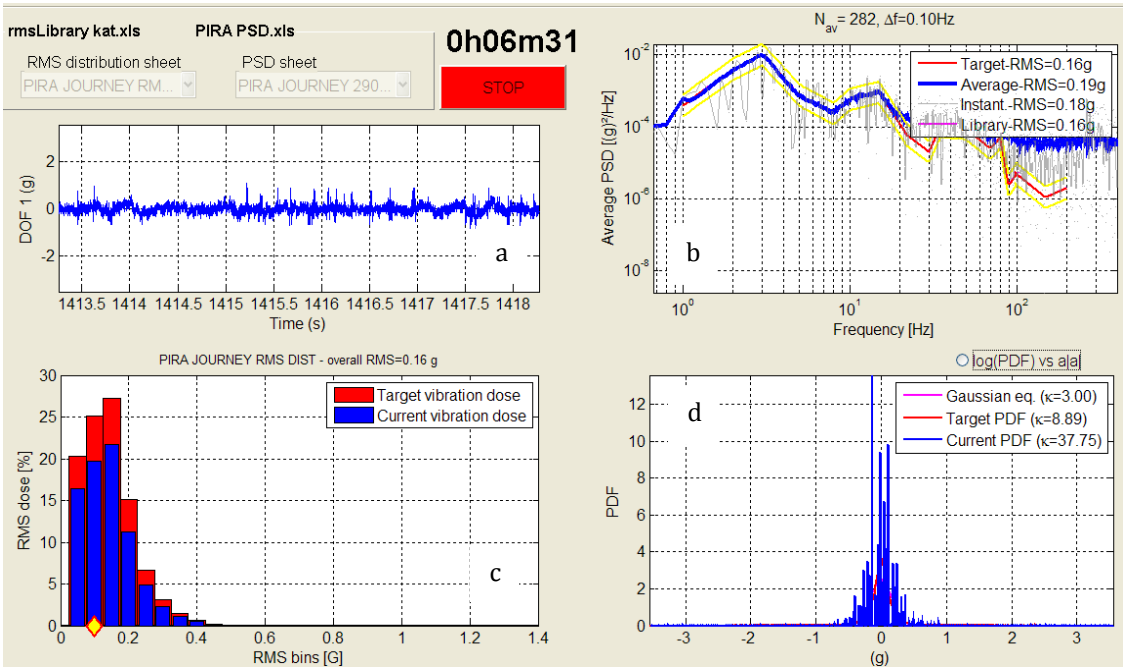

Figure 42: Screenshot of the SVS module computer system, showing real time (a) drive signal (b) PSD (c) RMS acceleration distribution (d) PDF

Results in Rouillard and Sek (2010) showed that the simulation produced through the SVS module correlated well with the original signal.

The main limitation of this method is that of controller capability which limits the speed at which the RMS acceleration level can be changed and hence the duration for which it is held. Furthermore, an accurate measure of the RMS acceleration distribution and the PSD that describes the distribution journey is required.

4.3 Concluding Remarks

In order to optimise a packaging solution, a high level of confidence in the method of simulation is required. The established method of vibration testing for distribution packaging creates a simulation that is based on the average frequency and amplitude content of vehicle vibration. It then reduces test duration using an acceleration method based on fatigue theory. This has been shown to result in a simulation which, in contrast to vehicle vibration, is stationary with a Gaussian

distribution, and therefore does not create a realistic simulation. Thus the limitations of the established method can result in conservative packaging design.

Simulation approaches suggested in recent and past literature highlight the inefficiencies of the established method and suggest methods of improvement. Many of these approaches use the same theory as the established method, but in addition utilise an improved statistical representation. This includes: the two way split spectra; three way split spectra; RMS modulation; and, shock on random. All of these approaches combine the established method with some form of additional statistical consideration.

Unfortunately, although it is suggested that these improved approaches are superior to the established method, there is little evidence of their benefits through application in physical testing and therefore they lack the user confidence that the established method possesses. In order to gain confidence in these improved simulation methods and additionally evaluate their use, correlation studies measuring actual product damage need to be carried out. The results of such studies are presented in Chapter 5.

5 AN EXPERIMENTAL COMPARISON OF THE DAMAGE CORRELATION OF SIMULATION METHODS

The objective is to understand how the various simulation approaches previously reviewed correlate with each other and with a benchmark time replicated journey. For the purpose of the study a single damage mechanism of scuffing is considered. Scuffing is used because it is generally accepted to be a cumulative form of damage. Previous work by Shires and White (2011) have generated and validated a design for a scuffing measurement rig. By measuring one overarching damage mechanism, the process of calculating damage is simplified.

5.1 Experimental Method

A continuous time record for a reference journey was used as the benchmark of this study, the damage produced by the time replication simulation was then compared with the damage produced by simulations created using the following simulation approaches:

- modulated RMS Distribution (Rouillard and Sek, 2010)
- two Way Split Spectra (Wallin, 2007)
- three Way Split Spectra (Kipp, 2008b)
- single Level PSD (established method non-time compressed)
- accelerated Single Level PSD (established method) – where K = 2 and time compression of 5 (Kipp, 2000)
- accelerated Single Level PSD (established method) – where K = 4.7 and time compression of 5

The reference journey was recorded on a Ford Luton Box van travelling at an average speed of 64 km/hr (40 mph) along a 32 km mix of roads in the city of Bath, UK (summary journey record shown in Figure 43). The data were sampled continuously at a rate of 2000 Hz. The resulting vibration signal was then filtered between 1 - 200 Hz.

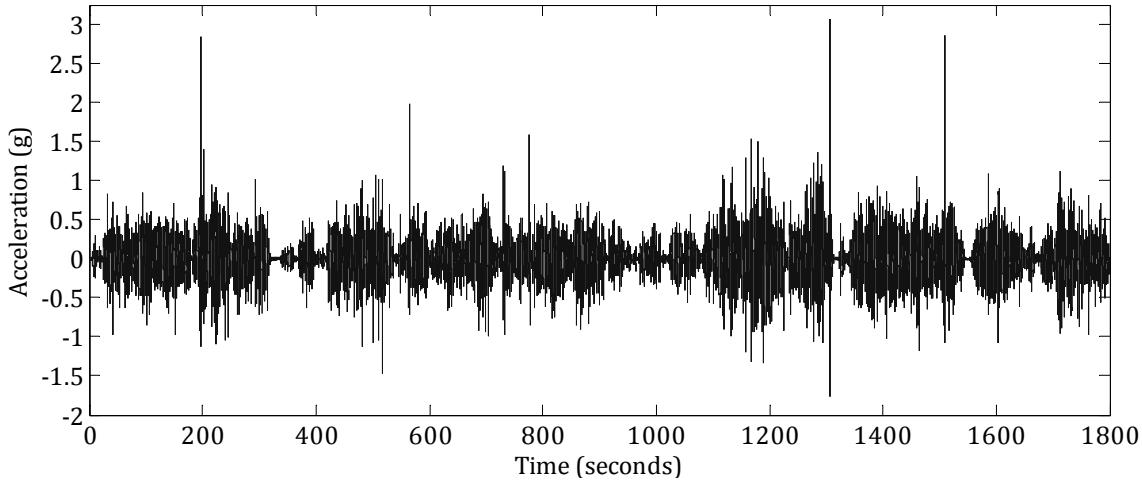

Figure 43: Time history for reference journey

The distribution of the RMS acceleration for one second samples was calculated. One second samples were taken from the signal with an overlap of N-1 data points, where N is the number of data points in a one second sample. An example of the sampling process is shown in Figure 44, where the first sample of length N includes data points 1 to N, the frame is then moved to provide an overlap of (N-1) so the second sample includes data points 2 to N+1. Overlapping the signal samples allows any variations in the RMS acceleration to be captured, so that a complete representation of the RMS acceleration distribution can be produced.

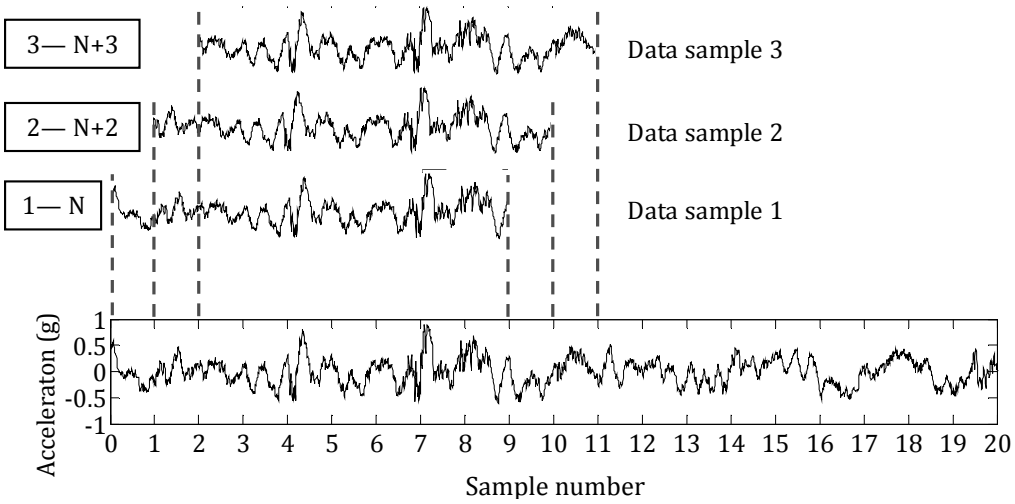

Figure 44: Example of data sampling with window length (N) with an overlap of (N - 1)

The RMS acceleration distribution for the vibration signal in Figure 43 is displayed in Figure 45, illustrating the percentage occurrence of RMS acceleration levels for one second samples. The percentage occurrence of RMS acceleration intensities is given in Table 8. The variation in the RMS acceleration distribution highlights the non-stationarity of the time history signal.

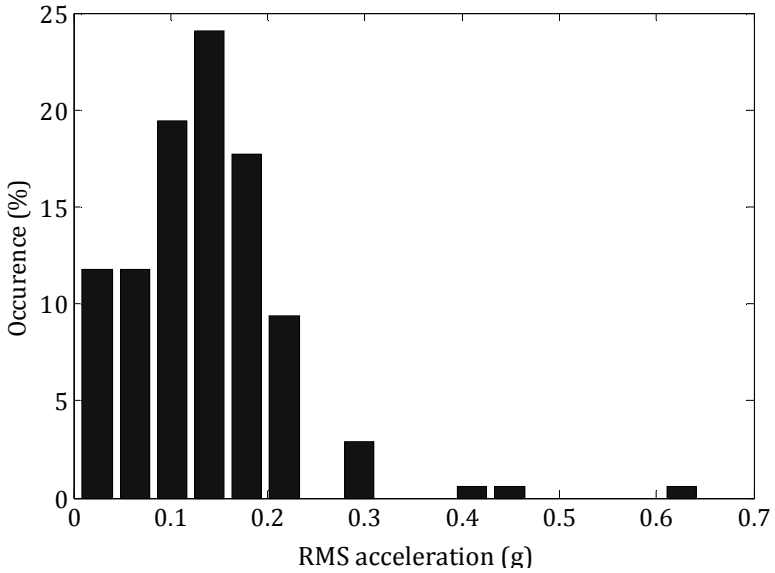

Figure 45: RMS acceleration distribution for reference journey

The signal's overall PSD, is then calculated as the average of each signal segment's PSD.

$$PSD = \frac{1}{n} \cdot \sum_{i=1}^{n} PSD_i \tag{20}$$

Where:

n = the number of signal segments, which is equal to the length of the signal minus the overlap used (N – 1)

i = 1, 2, 3, ..., n

To simplify the PSD, it is described using a reduced number of points that represent its overall shape. The average PSD for the signal is illustrated in Figure 46. The PSD breakpoints are given in Table 9.

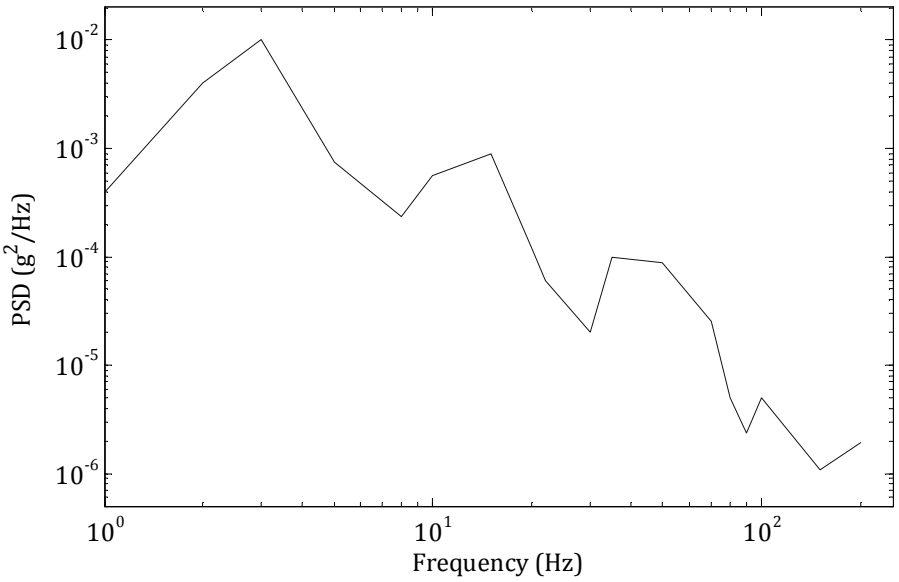

Figure 46: Average PSD for reference journey

Table 8: RMS acceleration distribution with levels in order of test

RMS ACCELERATION (g)	RMS ACCELERATION OCCURENCE (%)
0.294	2.9
0.140	24.1
0.063	11.8
0.178	17.7
0.449	0.6
0.626	0.6
0.410	0.6
0.217	9.4
0.1017	19.4
0.0247	11.8

Table 9: PSD break points

FREQUENCY (Hz)	PSD (g^2/Hz) (x10^{-5})
1	39.8
2	397
3	1020
5	75.0
8	23.4
10	56.3
15	89.2
20	12.0
22	6.06
30	2.02
35	10.0
50	8.80
70	2.50
80	0.502
90	0.237
100	0.496
150	0.108
200	0.194

Vibration tests were conducted using a Team servo hydraulic vibration testing machine (Team Corporation, Burlington, USA) controlled by an M&P VibPilot Controller (M&P International, Hannover, Germany). Tests were created using the simulation techniques and the test conditions summarised in Table 10.

Table 10: Simulation methods with RMS acceleration levels and test durations

N^O	TEST METHOD	RMS ACCELERATION (g)	DURATION (Minutes)
1	Time Replication	0.17	30
2	Modulated RMS	See Table 8	30
3	Two Way Split Spectra 80-20%	0.16 & 0.25	30
4	Three Way Split Spectra 75-20-5%	0.16, 0.22 and 0.39	30
5	Single Level PSD	0.17	30
6	Accelerated Single Level PSD (x5) K = 2	0.37	6
7	Accelerated Single Level PSD (x5) K = 4.7	0.23	6

5.2 Design of the Scuff Rig

The damage mechanism of scuffing was measured using a purpose built scuffing device. The design and validation of the scuffing device has been described previously (Shires and White, 2011). Details of the design and its validation are also given here for completeness.

The principles sought in the design of a vibration response device are:

1. it should have a measurable response to vibration input, within the range of vehicle vibration (1 – 200 Hz);

2. it should simulate a response to vibration seen in the distribution of packaged goods such as scuffing or bruising;

3. its response to vibration should vary with both input intensity and input duration in a repeatable and measurable way.

The device exploits the transfer of ink from a printed to a non printed surface as a result of relative surface motion in response to vibration, which closely relates to print scuffing in packaged goods distribution.

Parts (a) to (c) of Figure 47 illustrate the evolution of the rig design. A printed sheet of board is mounted on mass W1 and an unprinted sheet of board on mass W2. The masses are held together under pressure such that the printed and unprinted boards are in contact. The masses are mounted on different stiffness springs such that they move relative to each other in response to vibration. Figure 47(b) represents a simplification of the system in Figure 47(a) in that one mass is rigidly coupled to the vibration input. However, both systems present two concerns:

- They may be under-damped compared with packaged goods.

- They will be prone to complex off-axis vibration responses.

Off-axis vibration might be controlled by using linear guides, but these would increase the design complexity, may inhibit system response to low vibration levels and may present a design challenge in avoiding unwanted structural resonances.

Replacing the springs with foam cushions increases system damping (and arguably similar to cushioned packaged goods), but compressive creep in the contact pressure cushion could result in change in contact pressure and poor repeatability.

The design in Figure 47(c) rotates Figure 47(b) by 45 degrees and replaces the springs with a cushion material such that the contact pressure results from the normal component of the test mass (the cushion above the weight applies only slight pressure to prevent bouncing or chattering). The component of the mass parallel to the inclined plane was matched to the cushion such that the mass and cushion corresponded to an optimised cushion design (Goodwin and Young, 2011). The system will be less prone to error from small levels of compressive creep in the support cushion as the pressure is set by the mass.

A schematic of the device is shown in Figure 48 and images of the constructed device are shown in parts (a) to (d) of Figure 49.

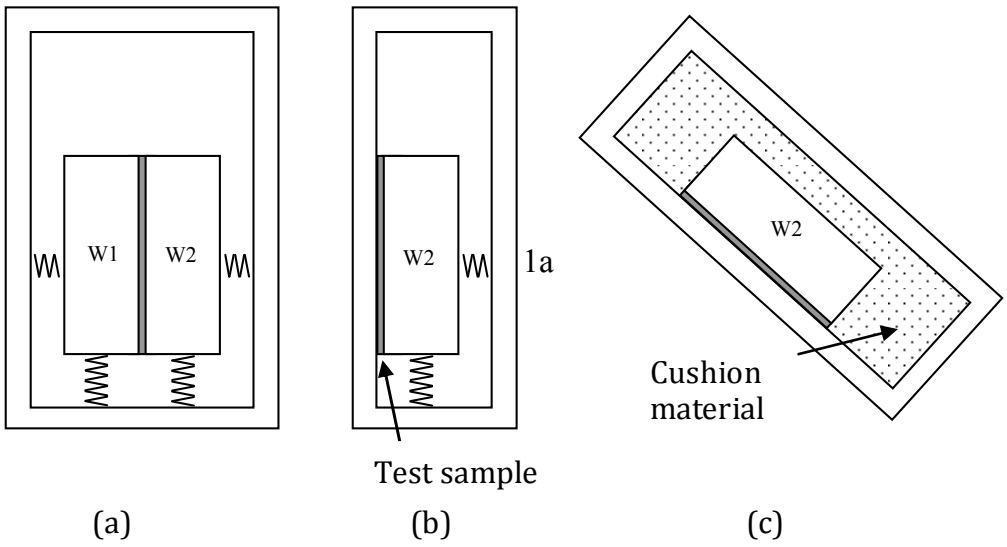

Figure 47: (a) – (c) Possible designs of test rig

Cushion material is positioned in the box, as in Figure 48 so the mass responds to vibration input in a manner similar to a packaged item with cushion shock protection. A foam block polyethylene (PE), with a closed cell density of 75 kg/m^3 was used to provide cushioning. The foam was selected based on the mass used to optimise cushion performance (and the scuffing potential).

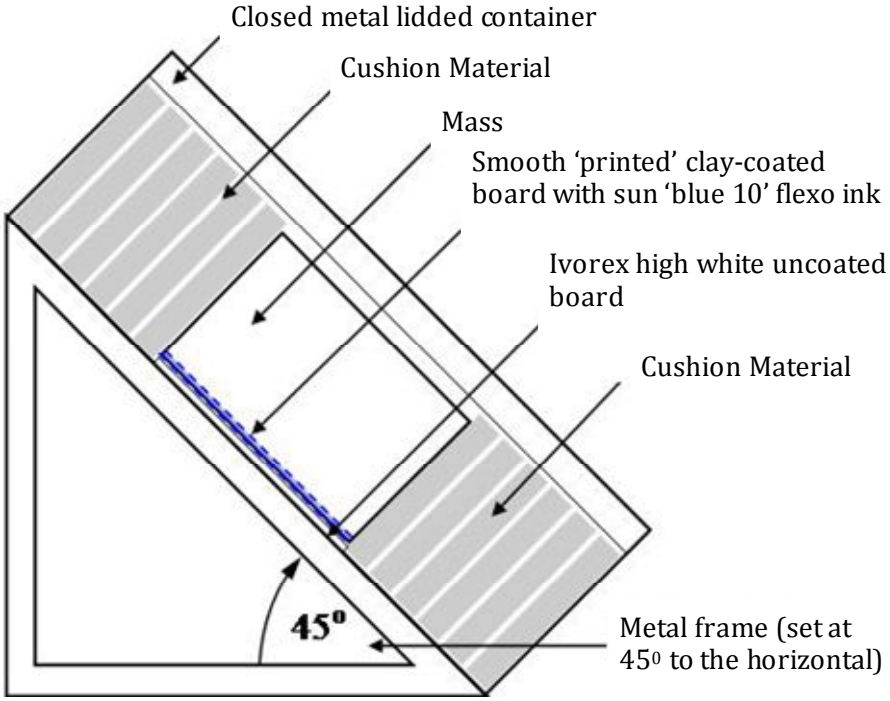

Figure 48: Scuffing test rig schematic

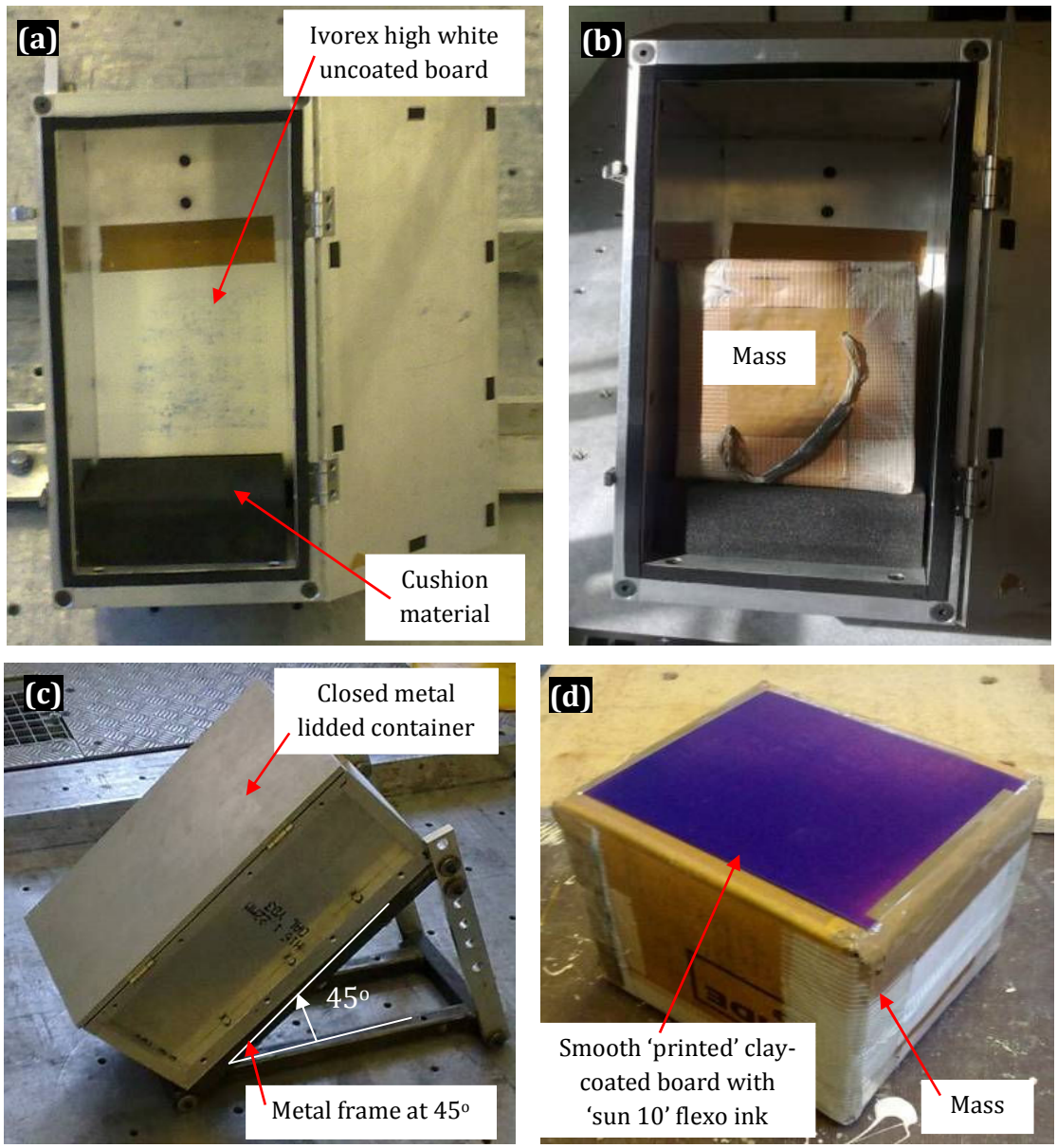

Figure 49: (a) Metal box with Ivorex card attached, with foam cushion (b) Cubic mass loaded in metal box, (c) Inclined metal box fixed to vibration table, (d) 25kg mass with smooth 'printed' clay-coated board with 'sun 10' flexo ink

5.3 Quantifying the Level of Scuffing

Following a test, the degree of scuffing is measured by summing the total blue content of all the pixels on the Ivorex card (Figure 50).

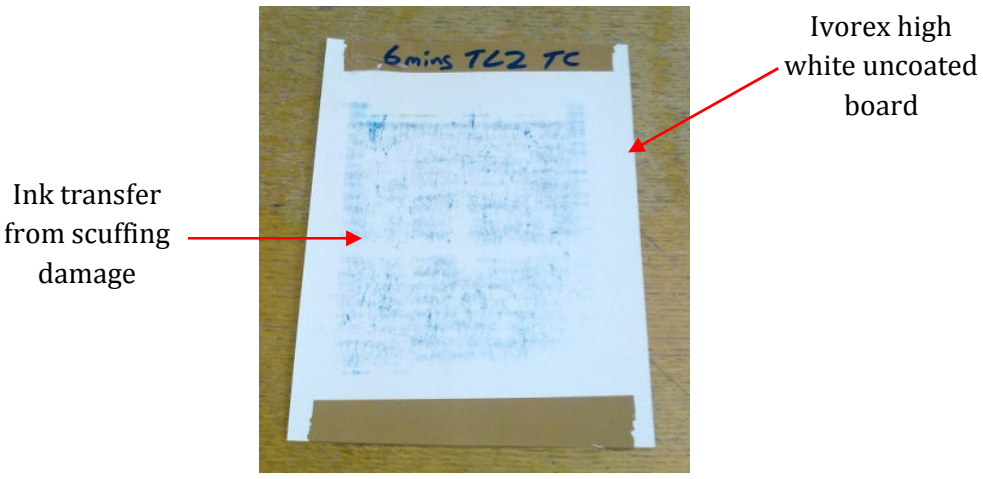

Figure 50: Ivorex card with scuffing after simulation

A computer program was used to count the blue pixels. This process was:

1. Scan the Ivorex card as a glossy photo with a resolution of 600 dpi.
2. Load scans on PC as a PDF and enlarge so that the entire PC screen is filled with the scuff damaged area.
3. Crop the scanned image so that it includes only the 15 cm x 15 cm area that was in contact with the mass.
4. Save cropped area as a Jpeg file.
5. Determine the percentage scuffing executed using Matlab code. The process is:
    a. Load the saved Jpeg file, automatically displaying the image as a count for red, green and blue (rgb) for each pixel.
    b. Sum the b count of all pixels to find the total blue value (B).
    c. Calculate the percentage scuffing, which is the reduction in the total blue pixel count (B) in proportion to the total blue pixel count for a blank white Ivorex card of the same size (C).

$$\left(1-\frac{B}{C}\right)\times 100 = Scuffing \tag{21}$$

The level of blue ink transferred indicates the severity of the test i.e. the higher the level of blue transferred the more severe the test (Shires and White, 2011).

5.4 Validation and Repeatability of Scuffing Rig

The rig was subject to a range of investigative tests to assess its response to vibration intensity and vibration time and repeatability.

The scuff rig was checked for repeatability by repeating a test at one intensity and duration ten times. The image analysis method was checked separately for repeatability by scanning and analysing the same sample ten times. The test gave repeatability better than 95% and the image analysis better than 99%.

The pattern ink transferred to the Ivorex board reflected localised pressure variability from the machining of the adjacent parts. This pattern could be eliminated by mounting the samples on resilient backing material, but the progression of scuffing was substantially slower. For practical purposes the scuffing pattern was therefore accepted, but this represented a possible barrier to inter-laboratory repeatability.

5.5 Scuff Correlation between Simulation Methods

The high level of repeatability through use of the rig meant that each simulation method was tested once only. Time replication (band 1, Figure 51) resulted in 0.59% additional blue as a result of scuffing. Both the modulated RMS (band 2, Figure 51) and, the accelerated single level PSD with a time compression of 5 and K = 2 (band 6, Figure 51), produced a similar level of damage to the time replication with 0.56% and 0.64% respectively. The three way split spectra produced the largest over test and the single level PSD produced the greatest under test at

0.81% and 0.1%, respectively. The variation in each test (simulation methods 2 – 7, Table 10) with respect to time replication (simulation method 1, Table 10) is shown in Figure 52.

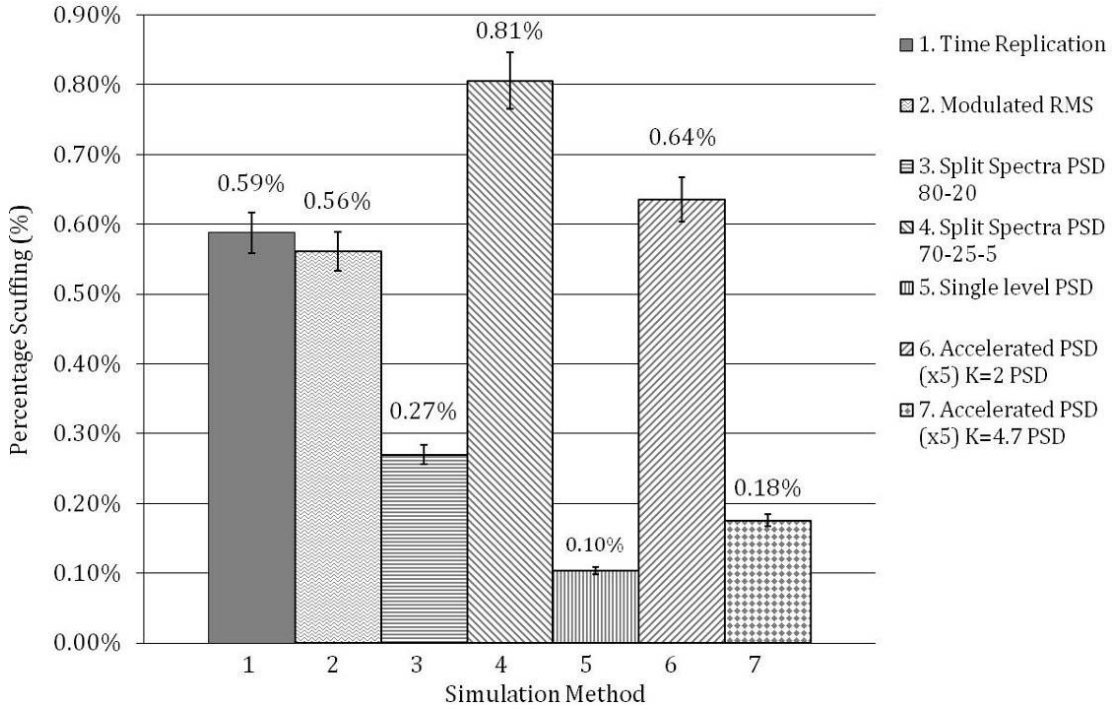

Figure 51: Percentage scuffing for the simulation techniques

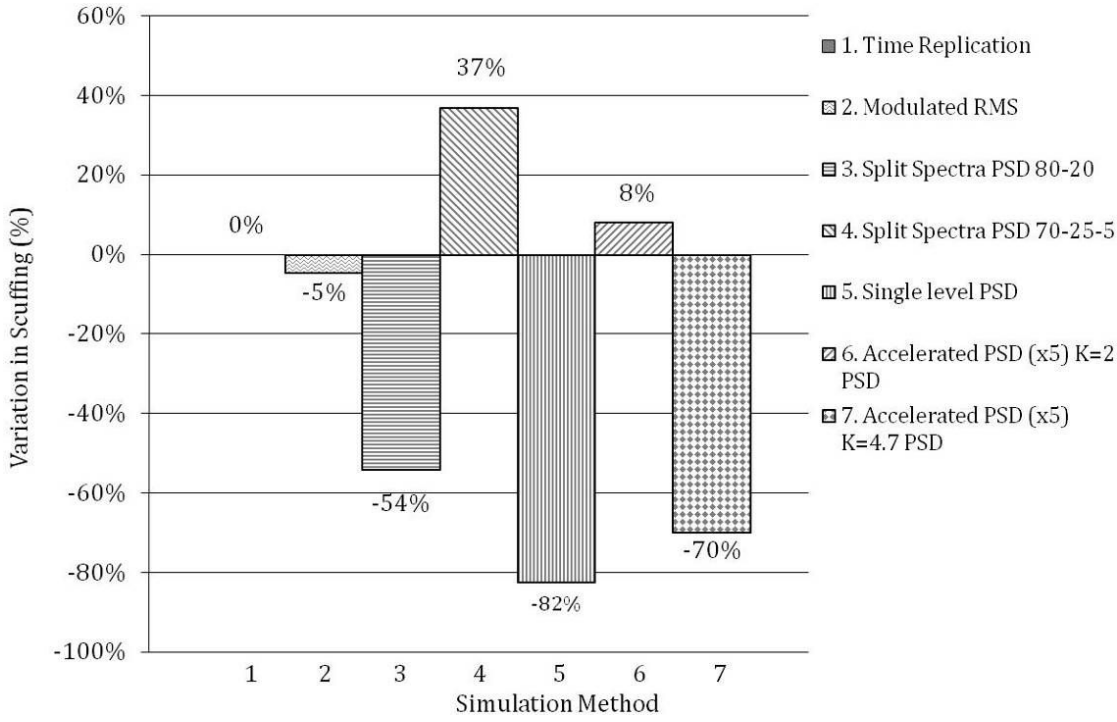

Figure 52: Percentage variation in scuffing for each simulation method compared to time replication

The results are consistent with the theoretical modelling of Shires (2011) who predicted that single level (non-time compressed) tests would represent an under test and that time compressed tests based on an assumed value of $K = 2$ would have a much lower error than expected from a comparison of average journey and test levels.

5.6 Concluding Remarks

The level of scuffing damage produced, varied between simulation techniques. The simulation approaches that gave best correlation with the benchmark time replication were the Modulated RMS and the established method using an accelerated test with $K = 2$.

The greatest error in a test resulted from the single level, non-time compressed approach and the single level time compressed test using a value for $K = 4.7$. These produced a significant under test, resulting in 82% and 70% less scuffing than time replication, respectively. Also of importance is the variation in scuffing produced between the two accelerated tests where $K = 2$ and 4.7, respectively. This indicates that the selection of K can induce significant errors in the packaging testing and that therefore careful consideration of the value selected should be given.

The results suggest that by using a more complete decomposition of the signal e.g. the RMS modulation method, rather than the two way or three way split spectra, error in the simulation can be reduced, and therefore, a more accurate representation of the vehicle vibration can be created. Both the two way and three way split spectra tests resulted in significant error, this is because the two way split test excluded the higher level events, and, the three way split over tested the higher 5% of the signal.

Whilst many approaches have considered the variation in signal RMS acceleration, they have not considered the variation in signal frequency content at difference RMS acceleration levels. The frequency content of a signal can have a significant effect on the product response due to resonance (section 3.5). Therefore, while the

RMS modulation approach produced a small amount of error (5% less scuffing damage than the time replication) it may still be improved upon by considering the variation in frequency content associated with the RMS acceleration levels.

Furthermore, each of these approaches considers only vibration with a Single Degree of Freedom (SDOF), along the vertical axis. In reality vehicle vibration has multiple degrees of freedom (MDOF). It is therefore necessary to consider the effect of vibration along the additional linear axes and vibration around the rotational axes, on product damage. A case study evaluating the need for MDOF testing has been carried out.

6 EVALUATING THE NEED FOR MDOF TESTING

The random and varying nature of a road surface means that vehicles and their corresponding payloads experience MDOF vibration, including along three linear axes: longitudinal (X); lateral (Y); and, vertical (Z); and, around three rotational axes: pitch; roll; and, yaw. These are illustrated in Section 3.6, Figure 27.

Current packaging test standards – ISTA, ASTM, EU, BS, Chinese and Japanese etc; simulate vehicle vibration using a SDOF in the vertical direction. The reasoning behind this is that the acceleration along the vertical axis is generally much greater and therefore considered to be more significant than in either the lateral, longitudinal or rotational axes.

This assumption is supported by the empirical comparisons of vehicle linear tri-axial vibration, given in section 3.6, which showed vibration acceleration to be predominant along the vertical axis, with longitudinal and lateral vibration being markedly less significant. This is most evident in the frequency range 1 – 20 Hz (Singh et al, 2006). A recent study concluded that in the frequency range 1 – 10 Hz, the neglected acceleration when using a vertical excitation only, was not significant. However, above this range the additional acceleration from the application of multiple axis vibration is significant (Bernard et al, 2011).

Figure 53 gives an example recording of the tri-axial vibration measured in a delivery vehicle. It is evident that the magnitude of the vibration and shock along the vertical axis is much greater than that along either the lateral or longitudinal axes.

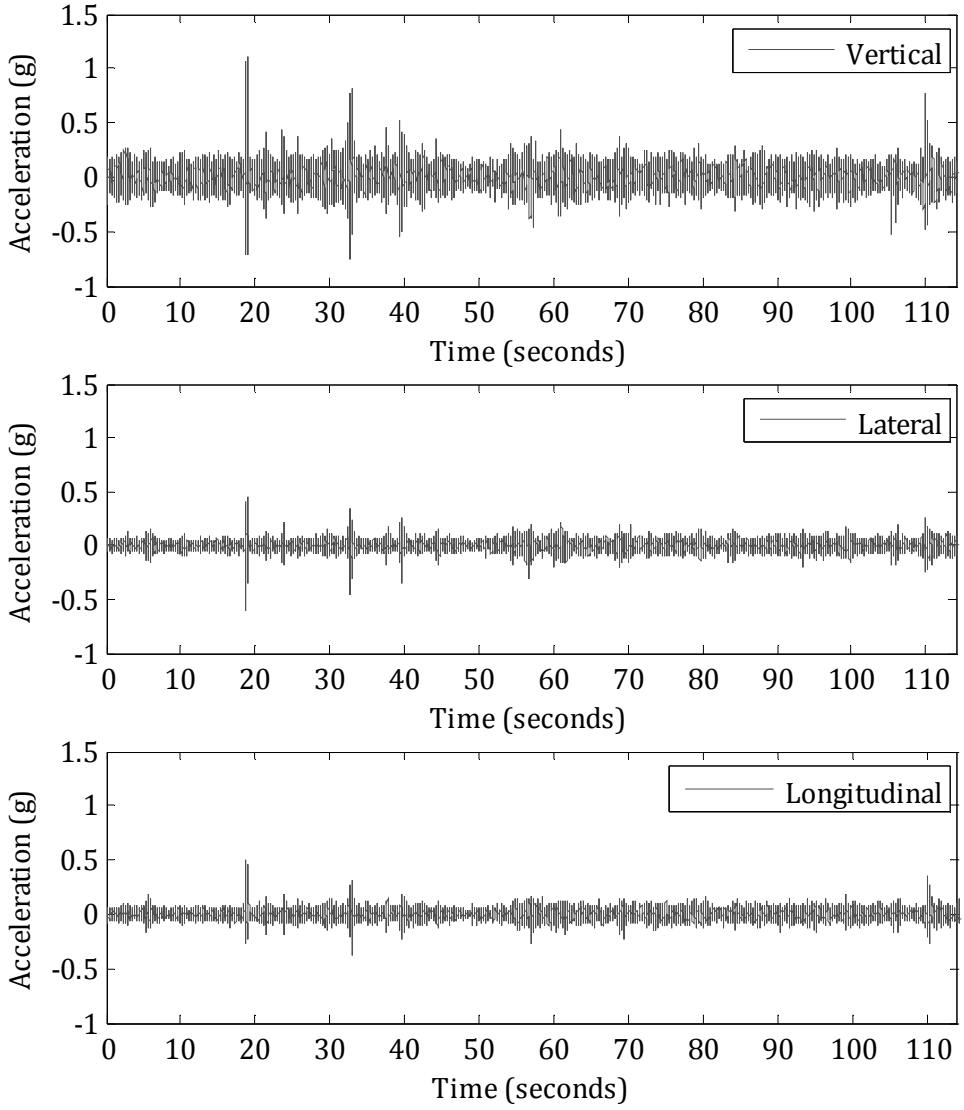

Figure 53: Vertical, lateral and longitudinal vibration signal

The acceleration power of the vibration on each axis is displayed in Figure 54 using the PSD of each signal. When comparing the PSDs the power within the vibration (where power is measured as the vibration acceleration squared (g^2)) along the vertical axis can be seen to be much greater than that along the lateral and longitudinal axes, specifically in the range 1 - 20 Hz. Above this range the variation in the power is less significant. Also evident in Figure 54 is the location of the key frequencies for each of the axes. The vehicle has three predominant resonant frequencies, which were discussed in section 3.5. The first of these can be seen in Figure 54 at around 2 Hz, the second frequency is then visible in the

vibration of all three axes around 10 - 20 Hz, the discretisation of the spectra makes the exact location of the peaks hard to specify exactly.

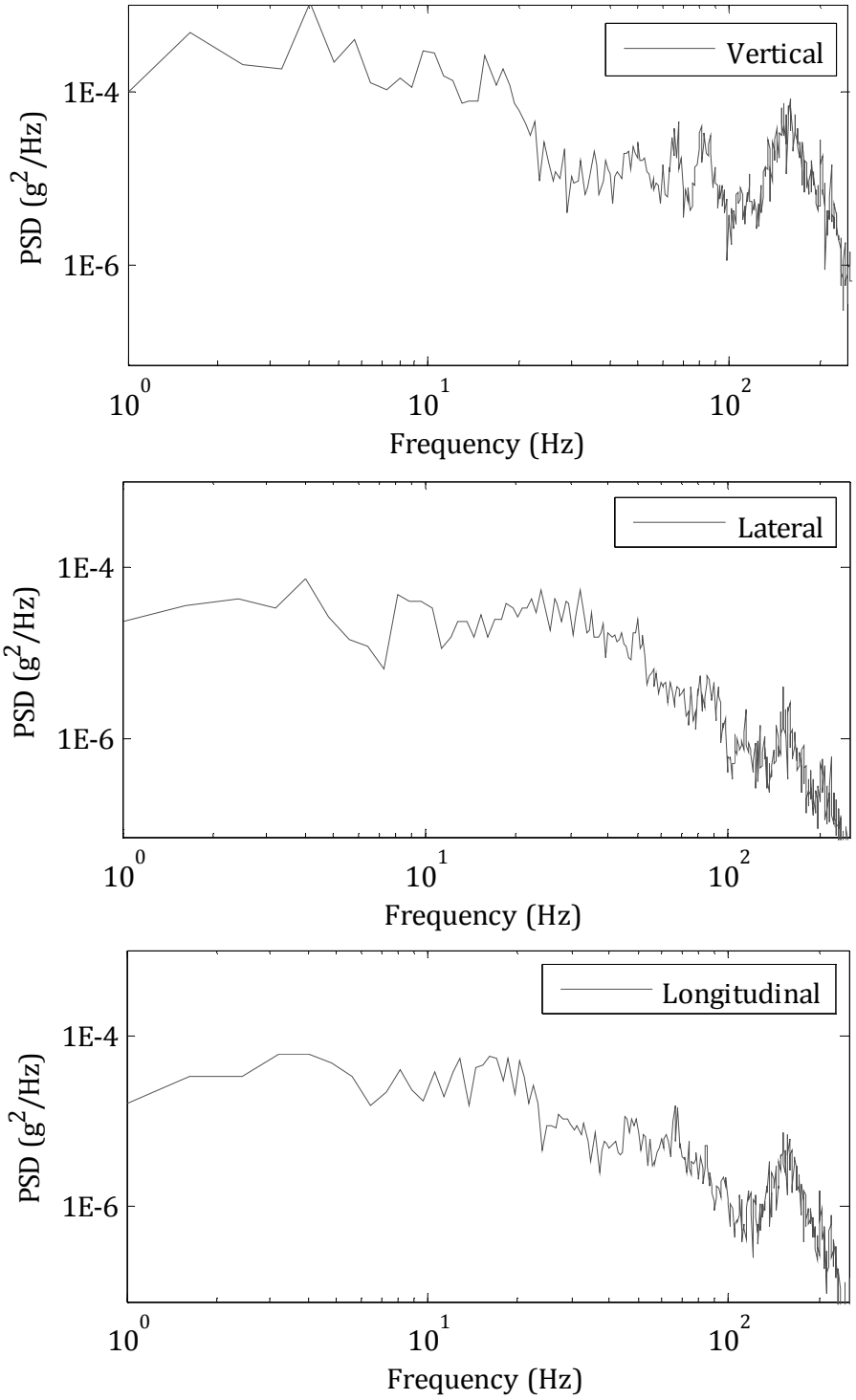

Figure 54: PSD of the vertical, lateral and longitudinal vibration

Although the vibration power along the lateral and longitudinal axes appears minor in comparison with that in the vertical axis, the total of their combined effect

should be considered as they may cause or accelerate damage when simulating the vertical axis only.

Consider for example a loosely stacked product. In this situation the lateral and longitudinal vibration may lead to stack instability, resulting in the load falling and causing impact damage, or, being subjected to excessive sideways or rotational movement. It is therefore important to consider the MDOF movement of a distribution vehicle and whether or not single axis testing is appropriate for approximating a distribution journey. A case study using the damage mechanism of bruising is presented in order to evaluate the need for MDOF testing.

6.1 Evaluating the Need for Multi Axial Vibration Testing

During this study the necessity of MDOF testing has been evaluated, using the test product of apples and the damage mechanism of bruising. This is a common form of damage in fruit and has been used to evaluate vehicle vibration in previous studies (Vursavus and Ozguven, 2004; Timm et al, 1996; Singh and Xu, 1993).

There are three aims to this study:

1. quantify and compare the damage caused to the test product under SDOF and MDOF time replication simulation;

2. using the results from the time replication tests, analyse the ability of the established method to recreate damage, using both SDOF and MDOF testing;

3. evaluate the use of the established method with test acceleration, using both SDOF and MDOF simulations, to recreate MDOF damage.

From these results a conclusion can be drawn as to whether or not MDOF testing is required.

6.1.1 Experimental Methodology

Simulations were created using data collected from a Riverford Organic © home delivery vehicle travelling around the cities of Bristol and Bath, UK, on both residential B roads (30 mph) and national speed limit A roads (60 mph). The vehicle used was a Ford Luton box van with a leaf spring suspension. Vertical vibration was recorded via three accelerometers located on the vehicle floor, one over the left hand side rear wheel and two on either side of the rear of the vehicle. The locations of the three accelerometers were selected to enable the calculation of the vehicle's pitch and roll and are shown in Figure 55. Because the longitudinal, lateral and yaw components are very small in comparison with the vertical, pitch and roll components (Bernad et al, 2011), they have been ignored for the purpose of this study.

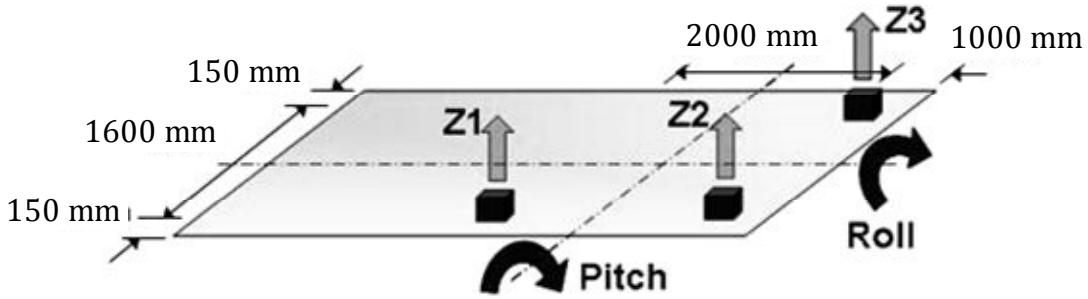

Figure 55: Locations of accelerometers of the vehicle floor and rotational measurements

6.1.2 Simulation Method

Simulations were created using the following approaches:

1. Time history reproduction
2. Established method without test acceleration
3. Established method with test acceleration

Figure 56 shows the 30 minute time history signal used on the Multi-Axial Simulation Table (MAST rig) to simulate the vertical vibration. For each test the

signal was run twice, resulting in a total duration of one hour. The pitch was calculated as the difference between position Z1 and Z2 divided by the distance between them; and, the roll was calculated as the difference between position Z2 and Z3 divided by the difference between them, so that:

$$Pitch = \frac{Z_1 - Z_2}{2} \qquad \text{and,} \qquad Roll = \frac{Z_2 - Z_3}{1.6}$$

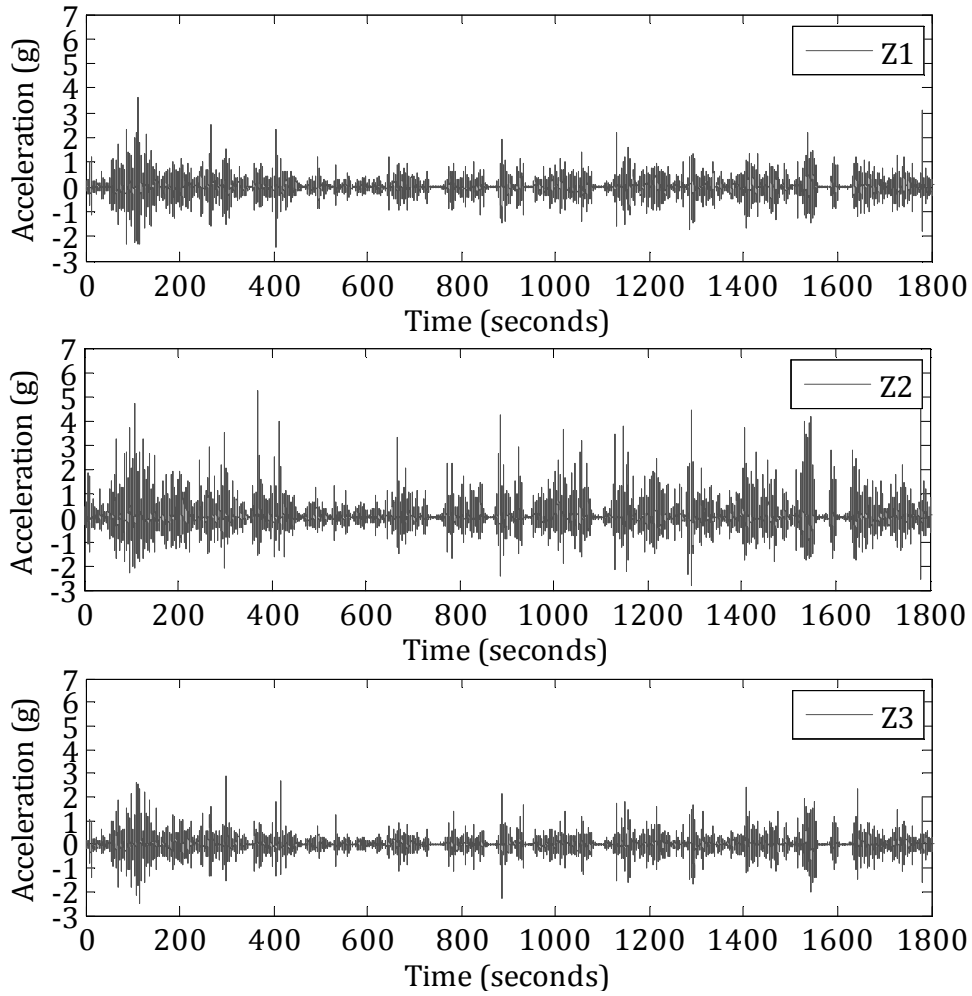

Figure 56: Time history vertical vibration signal, Z1, Z2 and Z3

The established method, used to create the simulations is detailed in section 4.1, using K = 2 to accelerate testing by a factor of 4 (reduced to 15 minutes).This ensured that the overall RMS acceleration did not exceed the maximum RMS acceleration of the original signal.

6.1.3 Measuring Product Damage

There are many mechanisms of damage for packaged-products e.g. scuffing, denting or compressing, which can be described qualitatively, but cannot easily be translated to a quantitative measure. To allow a more accurate evaluation of different simulation techniques it is important to have a method of quantifying product damage to remove subjectivity in the classification of the damage. For this purpose the Equivalent Bruise Index (EBI) was used.

The EBI provides a method of doing this by classifying apple bruising by measuring the diameter of bruises (Peleg, 1985). Thus, a numerical value can be given to the level of specimen damage, which can then be used to compare the severity of different simulation methods. This method was used in a previous study to quantify damage to green Golden Delicious apples (Vursavus and Ozguven, 2004). Using green rather than bi-coloured apples reduced the error in damage grading (Leemans et al, 2002). In this study it is used on Granny Smith apples. To calculate the EBI, the percentage of apples with bruising relating to each Degree of Damage (DoD) is multiplied by the rating index (R) associated with that DoD shown in Table 11.

$$EBI = \sum_{l=1}^{5} DoD_l(\%)R \tag{22}$$

where l equals 1 to 5, relating to the DoD's given in Table 11.

Table 11: DoD classification and rating index (Peleg, 1985)

RATING INDEX (*R*)	DEGREE OF DAMAGE (DoD)	SINGLE BRUISE DIAMETER(mm)	EQUIVALENT DIAMETER OF AGGREGATE BRUISES (mm)
0.0	None (1)	0.0	<12
0.1	Trace (2)	<12	12 – 19
0.2	Slight (3)	12 – 19	19 – 25
0.7	Medium (4)	19 – 25	25 – 32
1.0	Severe (5)	>25	>32

In addition to the EBI, the total area of bruising (Total Bruise Area (TBA)) for each tray of apples is also determined.

6.1.4 Test Product Conditioning

The transport packaging used in this study was single walled corrugated trays supplied by Riverford. Each case contains 42 apples. An example test tray can be seen in Figure 57.

Figure 57: Riverford home delivery tray and load example, used during testing

Prior to testing, the apples were stored for 2 days in a room at ~16 deg C. Afterwards, all apples were checked for bruising, the diameters of any bruises were measured and the EBI was calculated for each tray. After testing all the trays were stored for 5 days in a room at ~16 deg C, to allow any new bruising to develop. After this time, each tray's EBI was calculated. For each test a new tray of 42 apples weighing approximately 6 kg was used. For each of the six different simulations three different packaging configurations were used: a single column that is not shrink-wrapped; a single column of 5 trays shrink-wrapped (Figure 37); and, 4 columns of 5 trays shrink-wrapped to simulate a unitized load. These three packaging configurations were selected to provide insight into the effect that different packaging configurations had on specimen response to MDOF vibration and whether particular loading configurations may require MDOF testing.

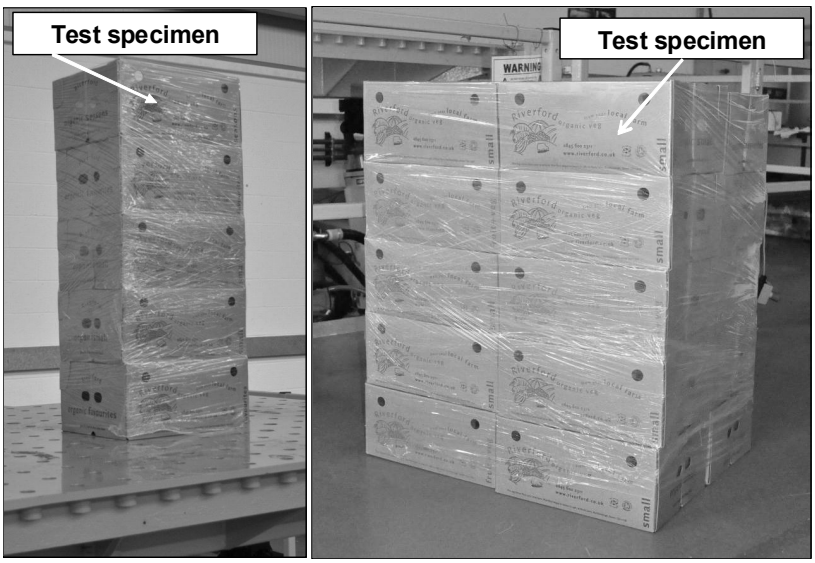

Figure 58: Single column unitized and four columns unitized

During testing, the test specimen was located within the uppermost layer of the stack. Evidence from a previous study showed that the response of packaged products to vibration is amplified upwards through the stack and that therefore the top of the stack is subject to the most severe vibration (Berardinelli et al, 2004). All lower level trays were filled with 6 kg of potatoes to mimic the loading of apples. In addition to the different stacking arrangements a test was undertaken with a reduced number (eleven) of apples to simulate loose loading and therefore simulate increased specimen movement. These trays were then packaged in the same configuration as shown in Figure 57.

6.2 Results

The EBI calculated for each test tray is given in Table 12, where both the pre testing and post testing EBI's are stated. These were used to calculate the increase in EBI. Similarly in Table 13, the pre testing Total Bruise Area (TBA), post testing TBA and the increase in TBA are presented.

Throughout the different tests, the EBI varied from 19.2 for the SDOF time history simulation to 56.9 for the MDOF Gaussian simulation.

The EBI calculated in Table 12 together with the TBA calculated in Table 13, are presented in graphical form in Figure 59. This Figure shows the similarity between the results using each method to calculate the damage.

Table 12: EBI calculation for different test regimes

TRAY No	CONFIGURATION	TEST	PRE TEST EBI	POST TEST EBI	INCREASE IN EBI
1	Single Column – Loose	SDOF time history	60.2	89.6	**29.4**
2		SDOF established method	33.0	84.2	**51.2**
3	Single Column – Shrink-wrapped	SDOF time history	39.8	66.6	**26.8**
4		SDOF established method	51.6	101.8	**50.2**
5		MDOF time history	38.1	81.4	**43.2**
6		MDOF established method	59.1	116.0	**56.9**
7	Four columns – Unitized	SDOF time history	44.0	63.2	**19.2**
8		SDOF established method	36.4	64.5	**28.1**
9		MDOF time history	34.1	64.3	**30.2**
10		MDOF established method	31.8	88.2	**56.4**

Table 13: Total bruise area for test regimes

TRAY No	CONFIGURATION	TEST	PRE TBA (mm^2)	POST TBA (mm^2)	INCREASE IN TBA (mm^2)
1	Single Column – Loose	SDOF time history	5023	7225	**2202**
2		SDOF established method	3079	6614	**3535**
3	Single Column – Shrink-wrapped	SDOF time history	2697	4306	**2488**
4		SDOF established method	3973	9278	**5304**
5		MDOF time history	3761	7797	**4036**
6		MDOF established method	4731	10266	**5536**
7	Four columns – Unitized	SDOF time history	2603	5091	**1609**
8		SDOF established method	2818	4366	**1548**
9		MDOF time history	3367	6032	**2665**
10		MDOF established method	2525	6916	**4391**

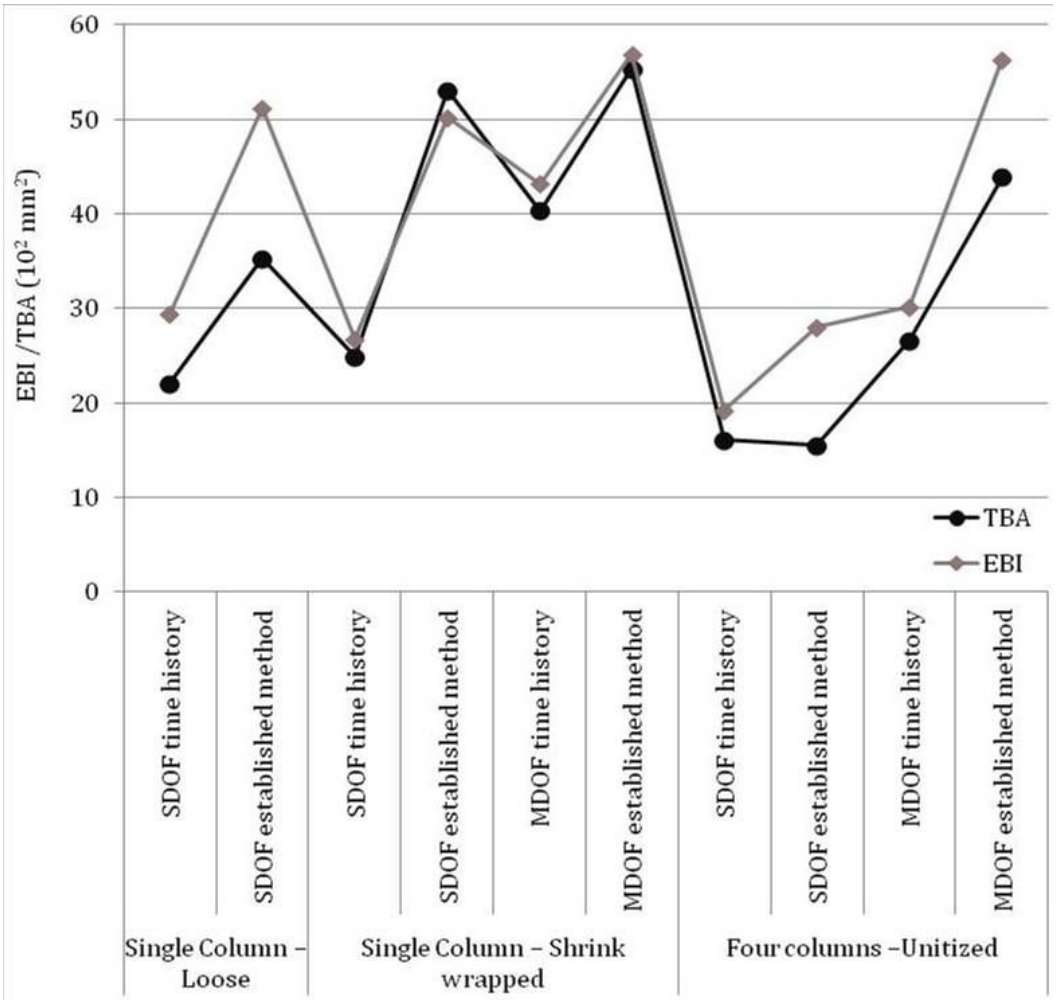

Figure 59: EBI and TBA (x10^3 mm^2) for each simulation method and loading configuration

The EBI of the individual apples in tray 5 (MDOF time history) and tray 3 (SDOF time history) is given in Figure 60 (a) and (b), respectively. There is a clear variation in the apple EBI. This is due to their respective location within the tray, with apples in the bottom layer suffering greater bruising than apples in the top layer. To therefore get a clear overview of the bruising damage the EBI of all of the apples within each tray is considered in order to reduce error in the calculation that may arise due to the use of a sample of apples form each tray.

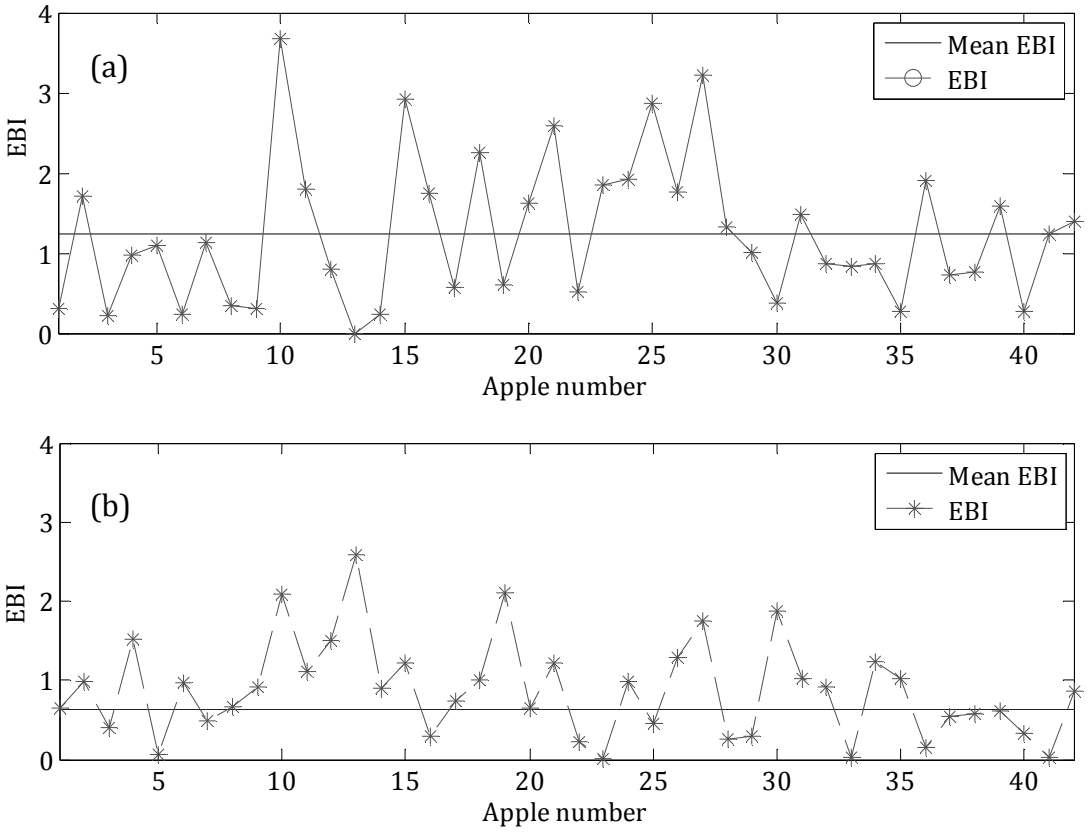

Figure 60: EBI for each apple for (a) tray 5 and (b) tray (3)

Because damage is being measured on a non uniform product, it is expected that there will be error in the results, due to changes in the apple structure, firmness, size, etc. Therefore, the results from this study can be used as a comparison of test severity but cannot be used as an accurate measure of precise damage.

6.2.1 Comparison of the Different Packaging Configurations

The results show that by unitizing several columns of trays the level of product damage is greatly reduced. This was true for the SDOF and MDOF time replication and the SDOF established method. Application of the MDOF established method produced high levels of damage in both configurations. This comparison is shown in Table 14.

Table 14: Reduction in EBI between single column and unitized load configurations subjected to various simulation methods

CONFIGURATION	EBI SINGLE COLUMN	EBI UNITIZED	REDUCTION IN EBI
Time History – SDOF	26.8 (3)	19.2 (7)	26%
Time History – MDOF	43.2 (5)	30.2 (9)	30%
Established method– SDOF	50.2 (4)	28.1 (8)	44%
Established method – MDOF	56.9 (6)	56.4 (10)	0%

6.2.2 Comparison of SDOF and MDOF Simulation

In addition to the variation of damage due to stack configurations, there is also a sizeable increase in the level of damage recorded when using MDOF simulations in comparison with those involving a SDOF. In both configurations single column and unitized, the apples subjected to time history MDOF showed 60% more damage (Table 15). The specimens subjected to SDOF and MDOF Gaussian simulations varied from an increase of 13% for the single column to 100% increase for the four column unitized load.

Table 15: Increase in EBI from real time and established method simulations using SDOF and MDOF

CONFIGURATION	EBI FOR SDOF	EBI FOR MDOF	INCREASE IN EBI
Time History - Single column unitized	26.8 (3)	43.2 (5)	61%
Established method - Single column unitized	50.2 (4)	56.9 (6)	13%
Time History - Four columns unitized	19.2 (7)	30.2 (9)	57%
Established Method - Four columns unitized	28.1 (8)	56.4 (10)	100%

6.2.3 Comparison of Time History and Gaussian Simulations

In general, the tests conducted using Gaussian signals tended to produce more damage than those conducted using time history signals, with the variation between the two being greatest when considering SDOF simulations.

Table 16: Comparison of EBI between time history and Gaussian simulations for a single column

DEGREES OF FREEDOM	EBI		VARIATION IN EBI
	TIME HISTORY	GAUSSIAN	
SDOF	26.8 (3)	50.2 (4)	87%
MDOF	43.2 (5)	56.9 (6)	32%

6.2.4 Comparison of Simulation Methods with Accelerated Testing

In comparison with the time history and the Gaussian simulations, the accelerated tests produced significantly more specimen damage, as shown in Figure 61. It was considered that this may be due to the test acceleration used i.e. time acceleration of 4 and k = 2 create an over test.

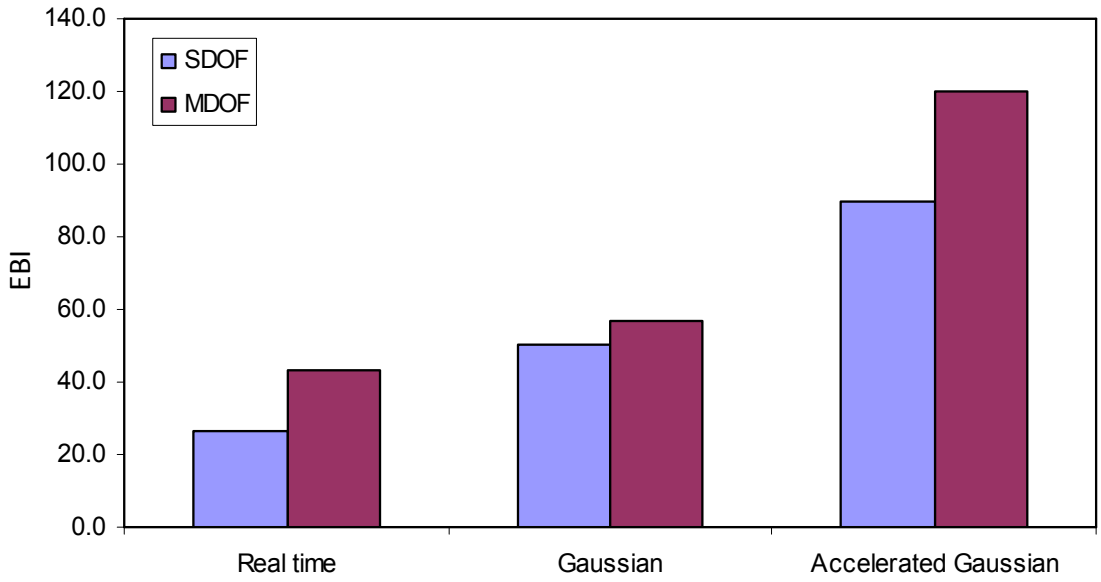

Figure 61: Comparison of the three different simulation techniques

To evaluate, additional testing was carried out where specimens were subjected to two hours of time history simulation using SDOF and MDOF models. By then comparing the time accelerated test results with those from the two hour test, the test acceleration would be equivalent to a time acceleration of 8 and k = 3.

The results, of Table 17 show that with the increase in duration the damage also increased to a level similar to that seen with the accelerated testing. This would

suggest that a higher value of k is required for these apples. Therefore, these results show some correlation in the use of accelerated Gaussian testing and actual time history for specimen damage.

Table 17: Comparison of time history the simulations with the accelerated Gaussian equivalent simulations

DEGREES OF FREEDOM	TIME HISTORY EBI		ACCELERATED GAUSSIAN EBI
	1 HOUR	2 HOUR	
SDOF	26.8 (3)	62.5	89.5
MDOF	43.2 (5)	89.9	91.1

6.3 Discussion

Specimens placed in the more stable load of four unitized columns incurred noticeably less damage. During testing, the single column configuration showed visually more movement, with additional sway movement that had not occurred in the more stable four column arrangement. Although there was additional movement, the percentage increase in damage between the two packaging configurations was similar.

There were three aims for the study, each of these is now defined and discussed.

1. *Quantify and compare the damage caused to the test product under SDOF and MDOF time replication simulation.*

   In both loading configurations the time replication simulation using MDOF produced a significantly higher level of damage, with the EBI for the MDOF increasing by 61% for the single column and 57% for the unitized load configuration. This indicates that if time replication testing were used, a SDOF approach would result in an under test of the packaging.

2. *Using the results from the time replication tests, analyse the ability of the established method to recreate damage, using both SDOF and MDOF testing.*

When comparing the established method without test acceleration results with the corresponding time replication tests it can be seen that the established method produced an over test in all cases. On comparing the results from the SDOF established method simulation to the MDOF time replication simulation it can be seen that similar levels of damage were recorded in both cases. Although the SDOF established method simulation appears to produce additional damage not seen in the SDOF time history, it does tend to produce a comparative level of damage to what would be caused by the actual vehicle movement (MDOF time history).

3. *Evaluate the use of the established method with test acceleration, using both SDOF and MDOF simulations, to recreate MDOF damage.*

   Initial testing, using the established method with test acceleration of 4 and k = 2, showed that, on average, more damage occurred than when using the MDOF time replication. Thus it provided a severe over test. However, when comparing the damage with that produced from the time history simulations of a longer duration (two hours instead of one hour) with corresponding test acceleration of 8 and k = 3, the damage produced by both the SDOF and MDOF accelerated Gaussian signals was similar to that of the MDOF time history.

6.4 Concluding Remarks

From the testing it can be concluded that the MDOF simulation produced more damage than the SDOF, in all cases. This suggests that simulating only the vertical vibration of the vehicle provides a significant under test. What is also interesting to note is that the SDOF established method simulated a similar level of product damage to that of the MDOF time history simulation in both load configurations.

Furthermore, the significance of MDOF vibration was found to be dependent on packaging configuration, with a less stable configuration being most affected by the MDOF movement. The results from this testing suggest that when designed

correctly, a single axis vibration simulation can represent MDOF vibration of a distribution vehicle.

This study also indicated that the degree of test acceleration and the value of k are product dependent. Therefore, in order to carry out test acceleration with confidence the appropriate acceleration and value of *k* must be known. However, establishing the correct value of *k* for a particular packaged product would require significant test time and evaluation.

Therefore, the improved simulation approach presented in this Thesis will be designed, at present, for SDOF vertical axis application without test acceleration.

It is noted that as testing was carried out on a single product, the results cannot be directly transferred for all products, though it does provide a good guide. In the case of food and drink distribution, where products are packaged in a more protective manner than the apples used in this study, thereby minimising the movement between products, the additional damage caused by movement in axes other than the vertical would be greatly reduced by comparison.

7 TIME-FREQUENCY ANALYSIS

Analysing a non-stationary and non-Gaussian vibration signal using only a frequency domain technique, such as Fourier transforms, does not account for the events within the signal that make it non-stationary or non-Gaussian. Rather, it will represent the signal as an average. Consequently, any simulation produced based on this information, will be stationary and have a Gaussian distribution. Thus, it will not be representative of the true nature of vehicle vibration. This leads to errors in the simulation and a need for conservatism in packaging design to account for this.

By using an analysis technique that identifies and illustrates changes in the frequency domain with respect to time, features characteristic of a signal's non-stationary and non-Gaussian nature can be detected. Three techniques: Short Term Fourier Transform (STFT); the continuous wavelet transform (CWT); and, the discrete wavelet transform (DWT) are discussed.

7.1 Short Term Fourier Transform (STFT)

The STFT, also known as the Gabor Transform, applies the DFT to continuous sections of a signal, allowing that signal's frequency content to be analyzed over localities in time. The equation for the STFT is given by:

$$STFT\{x(t)\} \equiv X(\tau,\omega) = \int_{-\infty}^{\infty} x(t)w(t-\tau_m)e^{-i\omega t}dt \tag{23}$$

where $X(\tau, \omega)$ is the Short term Fourier Transform for the series of windowed function, $x(t)w(t - \tau)$, of the subject function, $x(t)$, at a localized time point, $\tau_m = m\tau_o$ where τ_o is the time spacing between successive DFT calculations and m is an integer 1 to the number of DFT calculations required, this is dependent on the length of $x(t)$. The Fourier Transform of the windowed function for τ and ω is then determined.

When the STFT is used in this Thesis a rectangular window of length N is used, which surrounds the time point τ. An example of the application of the rectangular window is given in Figure 62 (a) to (d), in this example N is equivalent to one second and there is zero overlap between windowed function. The rectangular window in (b) is applied to the function $x(t)$ in (a), the resulting windowed functions for τ_1 and τ_2 are then given in (c) and (d), respectively.

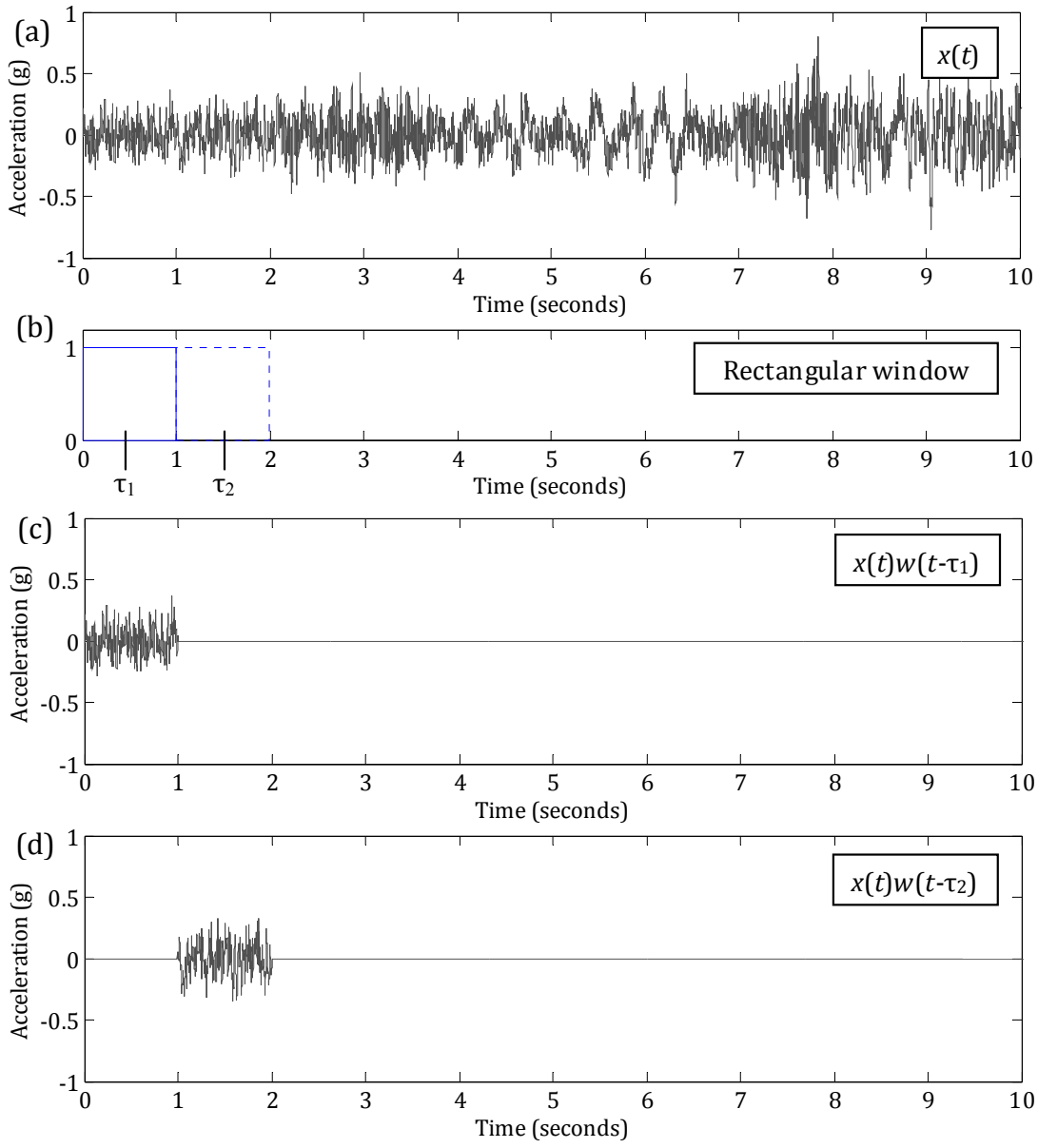

Figure 62: Example application of the rectangular window for the STFT

The temporal resolution afforded by the STFT means that variations in the frequency domain can be seen over time. Although the technique uses a stationary

signal processing method, because of the sliding window the overall technique is non-stationary (Akansu and Haddad, 2001).

Gabor (1945) observed that *'...although we can carry out the analysis with any degree of accuracy in the time direction or in the frequency direction, we cannot carry it out simultaneously in both beyond a certain limit*'.

The limitation of this is that a compromise between time and frequency resolution is required (Mallat, 1999). Therefore, in order to improve frequency resolution, the time over which the frequency content is calculated needs to be increased, leading to a reduction in the temporal resolution and vice versa. This relationship exists for all transforms. However, the STFT has the additional limitation that the resolution is fixed throughout the signals frequency range. For vehicle vibration, where the predominant frequencies are low, having high frequency resolution at low frequencies is important. Additionally, discrete transient events, also prevalent in vehicle vibration, mean that high frequency events tend to occur over short-time periods and therefore high temporal resolution is required at high frequencies.

Although the STFT allows for some improvement in the representation of vehicle vibrations, it is of limited use. To ensure all events are captured correctly, a transform that allows resolution variation is required.

7.2 Wavelet Analysis

Daubechies (1992) states that *'the wavelet transform is a tool that cuts up data, functions or operators into different frequency components, and then studies each component with a resolution matched to its scale'.*

Wavelet analysis is used in many applications because of its effectiveness when detecting variations in signals. It is used in the decomposition of both electrocephalagraph (EEG) and electrocardiogram (ECG) signals to identify transients with respect to both the time and frequency domain (Adeli et al, 2003; Sahambi, 1997). Further applications include fault diagnostics in mechanical

machinery and crack identification in structures (Liew and Wang, 1998; Jing and Liangsheng, 2000).

Wavelet analysis enables the identification of a signal's frequency content with respect to time. It does this by continually comparing the signal to a number of wavelet functions of varying length and frequency. The correlation between the function and the signal is then expressed through a coefficient. The higher the value of the coefficient, the better is the correlation between the signal and the function at the given frequency.

The wavelet functions are all formed from a single base mother wavelet ($\psi(t)$). The variation in the time frame (length) and frequency of the wavelet functions is then obtained by expanding and compressing this mother wavelet.

Common mother wavelets include: Daubechies db2, db6 and db10 (Daubechies, 1990), where the numerical value refers to the number of vanishing moments; Haar; Morlet; and, Mexican Hat, each of which are real or complex functions. These mother wavelets are illustrated in Figure 63 (Addison, 2002).

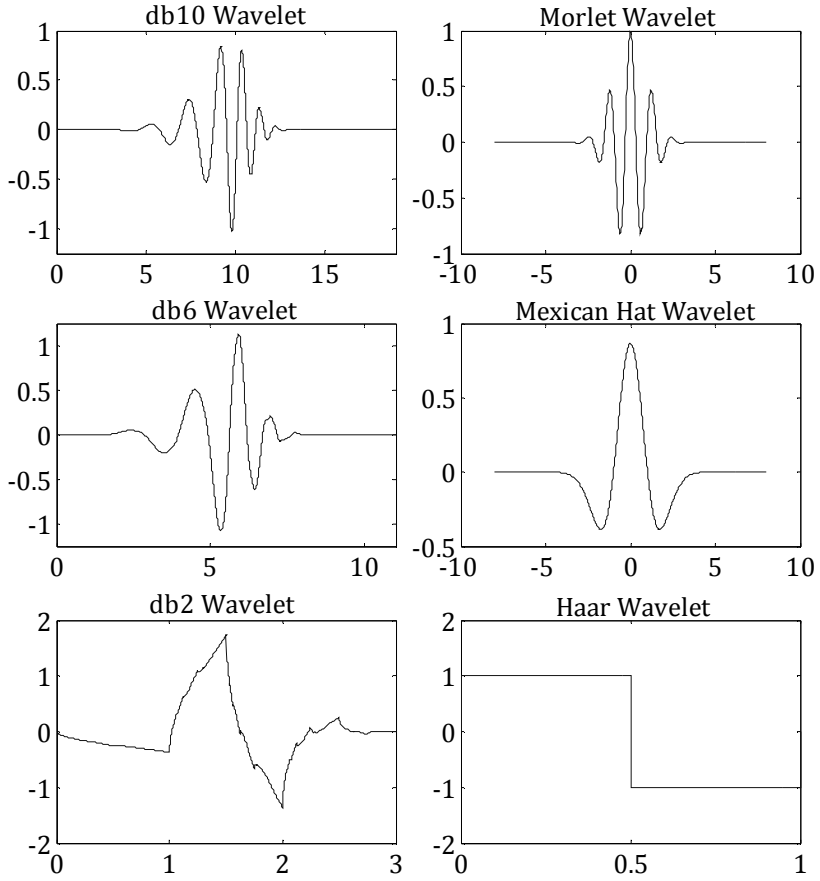

Figure 63: Mother wavelet functions

The degree of expansion or compression of the mother wavelet is determined by a scaling parameter, *a,* which is inversely proportional to the frequency. A translation parameter, *b*, then determines the location (time) of the analysis. So that the wavelet function with translation, b, and scaling parameter, a ($\psi_{a,b}(t)$) can be defined as:

$$\psi_{a,b}(t) = \frac{1}{\sqrt{|a|}}\psi\left(\frac{t-b}{a}\right) \tag{24}$$

The term a-1/2 normalises the energy within the wavelet across the different scales, keeping the energy of each wavelet function $\psi_{a,b}(t)$ equal to that of the mother wavelet function $\psi(t)$.

Examples of a compressed wavelet, and an expanded wavelet, being compared to a vibration signal are given in Figure 64. The scale (a_1) of the compressed wavelet is lower than the scale (a_2) of the expanded wavelet. Additionally, they both have different translation parameters (b_1 and b_2).

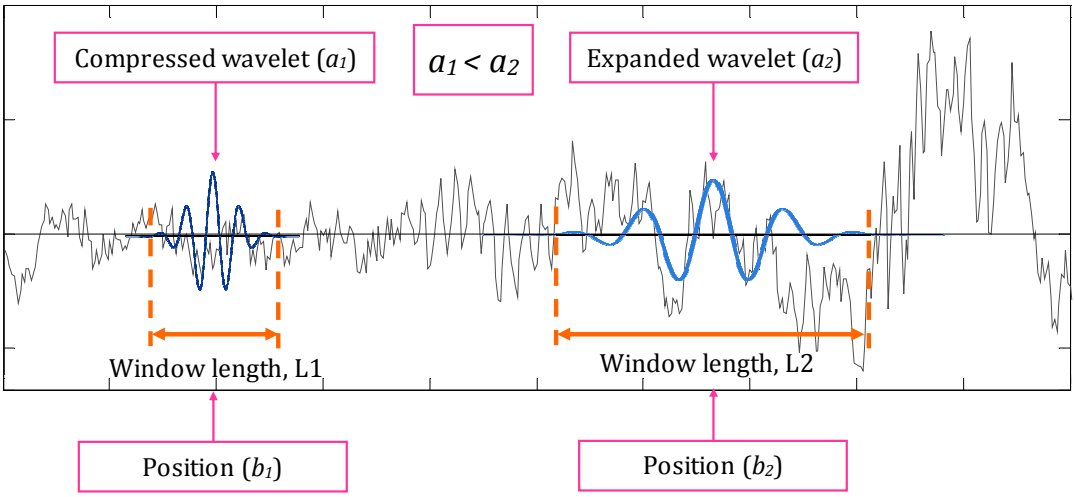

Figure 64:Examples of a compressed and an expanded wavelet, with different translation parameters

In Figure 64, it is apparent that the expanded wavelet's window length (L2) is much larger than that of the compressed wavelet (L1). This means that the expanded wavelet will carry out analysis over a larger time frame and will therefore have a lower temporal resolution than that of the compressed wavelet.

This compression and expansion of the wavelet allows the resolution of the analysis to vary. This is a benefit of wavelet analysis over STFT, as it enables a lower frequency resolution but a higher temporal resolution when analysing high frequencies (low scales), and conversely, it affords a higher frequency resolution but lower temporal resolution at low frequencies (high scales).

This property of wavelets is useful when analysing signals such as vehicle vibration, where low frequency vibration tends to be predominant and continual throughout the signal, while high frequency events tend to occur over short durations. This change in resolution and how it relates to the time and frequency resolution has been expressed in Figure 65. In the figure it is apparent that as the frequency of the wavelet increases, the scale (a) and the frequency resolution decreases, but the time resolution increases.

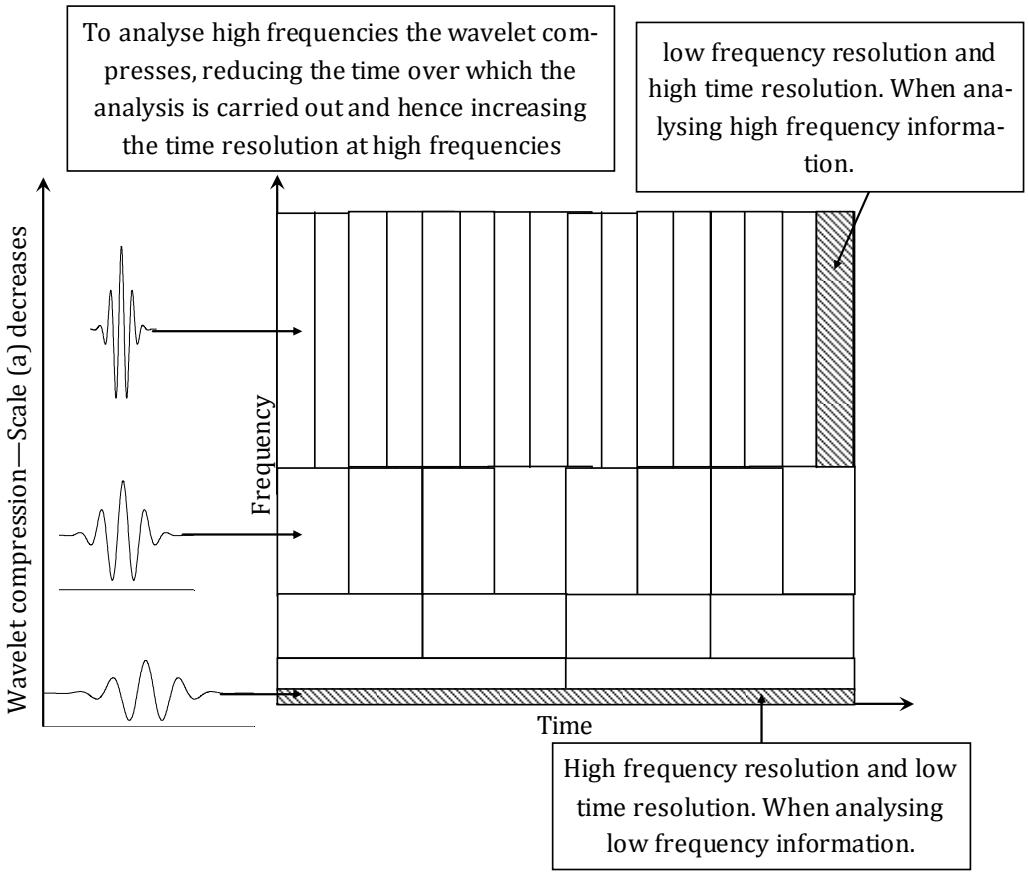

Figure 65: Wavelet analysis time and frequency resolution

7.2.1 The Continuous Wavelet Transform (CWT)

When using a real wavelet function, the continuous wavelet transform (CWT) is found by calculating the convolution of the complex conjugate of the wavelet transform ($\psi_{a,b}(t)$) and the time domain signal ($x(t)$) using the equation:

$$CWT_x^{\psi}(b,a) \equiv C(b,a) = \frac{1}{\sqrt{|a|}} \int_{-\infty}^{\infty} x(t) \psi\left(\frac{t-b}{a}\right) dt = \frac{1}{\sqrt{|a|}} \int_{-\infty}^{\infty} x(t) \psi_{a,b}(t) dt \quad (25)$$

Where $C(b,a)$ is the wavelet coefficient at position b and scale a. Typically a discretised version of the CWT is used:

$$CWT_x^{\psi}(b,a) \equiv C(b,a) = \frac{1}{\sqrt{|a|}} \sum_{a=1}^{S} \sum_{b=1}^{L} x(t) \psi\left(\frac{t-b}{a}\right) \quad (26)$$

where the wavelet coefficients are calculated for a number of scales $a = 1,2,3,..., S$, at positions $b = 1,2,3,..., L$, where S is a limiting number of scales and L is the length of the signal.

Note that if the wavelet function is complex, then the wavelet coefficients are found as the convolution of the time domain signal with the complex conjugate of the wavelet function.

The wavelet coefficients for an example vibration signal are illustrated in Figure 66. The real Morlet mother function, which is discussed later in this chapter, has been used in the CWT equation (Equation 25) to calculate the absolute wavelet coefficients. Where scales, a, used are all integer values from 1 to 128 and positions b, are all integer values from 1 to 4100, where one second is equivalent to 1500 data points. Changes in coefficients have been identified, a description of the events within the signal they relate to and the information they provide the user, has been given.

From Figure 66 the variation in the signal's frequency content throughout the range of scales can be seen. With low frequency components being present throughout the length of the signal and higher frequency events tending to only appear for short time frames. Shock events within the signal are clearly seen within the wavelet analysis as high value coefficients.

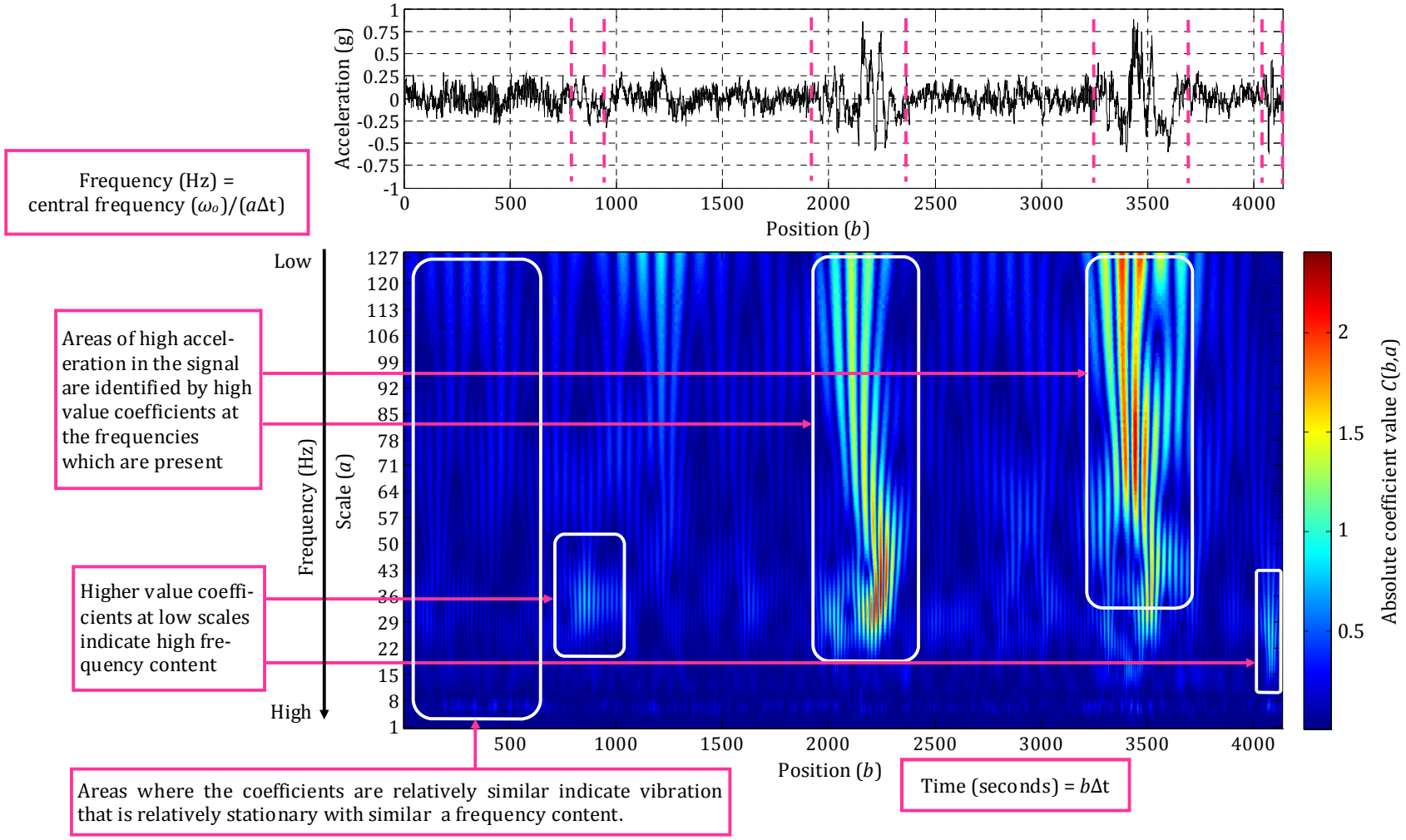

Figure 66: Example of wavelet coefficients and how they are used to indicate changes within the vibration signal

7.2.2 Selecting a Mother Wavelet Function

As there are many mother wavelet functions the most appropriate one for use with vehicle vibration signal analysis needs to be selected. To examine the variation between the different wavelet mother functions, CWT has been used to analyse a vehicle vibration signal, using the mother functions illustrated in Figure 63. The vehicle vibration used is taken from part of a journey recorded on the Ford Luton home delivery vehicle. The results from the different analyses are displayed in Figure 67 and Figure 68. These demonstrate the variation in the appropriateness of the different wavelet mother functions, for identify different features within a signal. The results show quite clearly that both Daubechie's db10 and, the Morlet mother function, are the most suitable for analysing the vibration signal as they detect the variations in frequency content more precisely. The Haar, Mexican hat and Daubechie's db2 mother functions, do not illustrate the variation in the frequency content at each position clearly. Indicating that when considering using a CWT within a new simulation technique either: Daubechie's db10; db6; or, the Morlet mother function should be used.

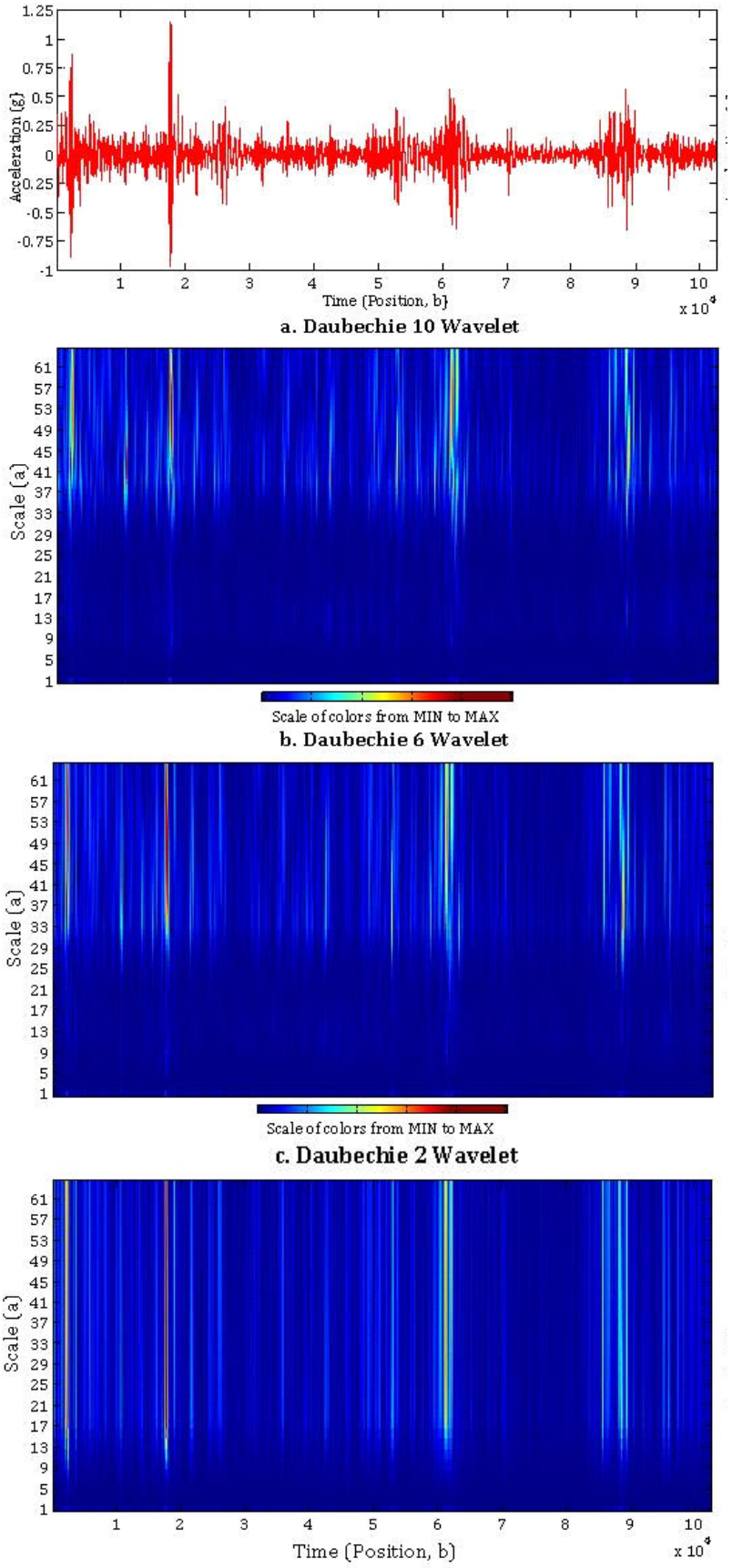

Figure 67: (a-c) Comparison of Wavelet Transforms

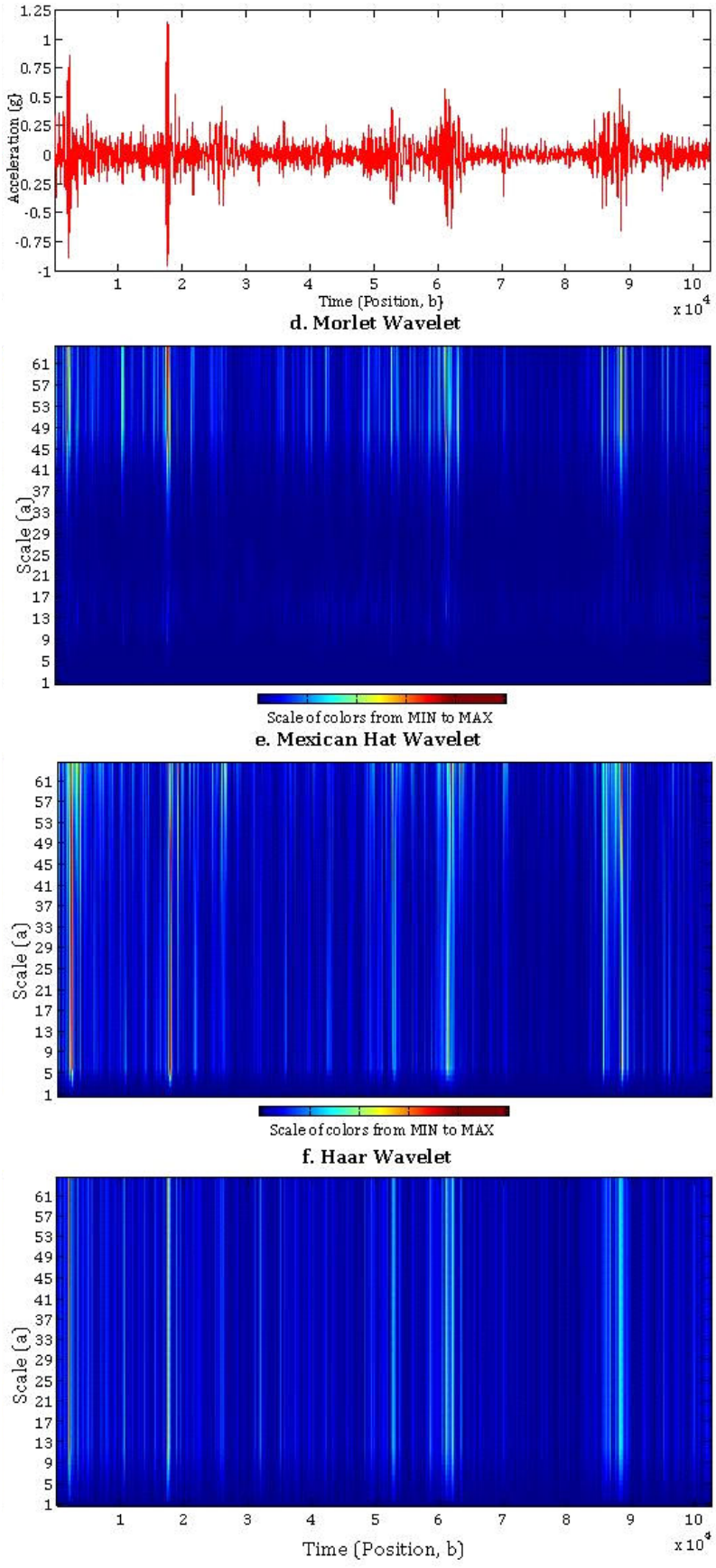

Figure 68: (d-f) Comparison of Wavelet Transforms

In order to identify and capture features within a signal using wavelet analysis, the mother wavelet selected should identify the key features of the signal being analysed.

Nei et al (2008) states that the Morlet function has relatively high performance for both time and frequency resolution. Because in this application wavelet analysis is being used to identify short duration transients in the signals, high resolution in the time domain is important. Furthermore, Lin (2001) successfully used the Morlet wavelet to identify impulses within a signal. A key feature of vehicle vibration is discrete high level shock events (similar to impulses), and, in Figure 67, the Morlet transform managed to clearly identify variations in the frequency content of the example vehicle vibration signal. Therefore the Morlet transform is appropriate for use in this study.

The Morlet function is a complex wavelet, its equation is given by:

$$\psi(t) = \frac{1}{\sqrt[4]{\pi}} \left(e^{i\omega_o t} - e^{-\frac{\omega_o^2}{2}} \right) e^{\left(-\frac{t^2}{2}\right)} \tag{27}$$

Where ω_o is the central frequency of the mother wavelet and the second term in the brackets is the correction term, this corrects for the non-zero mean of the complex sinusoid of the first term. From Equation 27 it can be seen that the Morlet wavelet is a complex wave ($e^{-i\omega t}$) masked by a Gaussian envelope ($e^{-t\hat{}2/2}$).

When using the Morlet wavelet to analyse real signals, such as vehicle vibration, only the real part of the Morlet wavelet is required (Tang et al, 2010). The equation for the real Morlet wavelet is:

$$\psi(t) = \frac{1}{\sqrt[4]{\pi}} e^{-\frac{t^2}{2}} \cos(\omega_o t) \tag{28}$$

where $\omega_0 \geq 5$. This is because when ω_0 is greater than or equal to 5 the error in the mean from zero is negligible and therefore the correction term in Equation 27 is no

longer required. From this point, when referring to the Morlet wavelet, the real Morlet wavelet is being considered.

7.2.3 The Discrete Wavelet Transform (DWT)

Whilst the CWT affords many advantages, it also suffers some limitations. In particular Akansu and Haddad (2001) state that, *'...the continuous wavelet transform suffers from two drawbacks: redundancy and impracticality'*. The redundancy issue arises from the overlapping of data when using the CWT and the extensive computation time and power make the CWT impractical in many situations. The Discrete Wavelet Transform (DWT) addresses these issues by sampling the CWT scales (*a*), thereby reducing the number of scales and hence reducing the computing time and removing redundancy. The scale (*a*) and translation (*b*) parameters then become $a = a_o^{-j}$ and $b = a_o^{-j} k b_o$, respectively, where *j* = 1,2,3,..., J and *k* = 1,2,3,..., K and *a* > 1 and *b* > 0:

$$\psi_{j,k}(t) = a_o^{j/2} \psi\left(a_o^j t - k b_o\right) \tag{29}$$

For the DWT the $a_o = 2$ and $b_o = 1$. This gives the equation for calculating the DWT as:

$$DWT(a,b) = DWT\left(2^{-j}, 2^{-j} k\right) = 2^j \int_{-\infty}^{+\infty} \psi\left(2^j t - k\right) x(t) dt \tag{30}$$

The signal is then decomposed into J levels. At each level the DWT separates the signal into two parts using a high pass and low pass filter. A high pass filter retains frequency information above the cut off frequency, f_c and attenuates frequency information below f_c. Conversely, the low pass filter retains the frequency information below f_c and attenuates frequency information above f_c. The cut off frequency, $f_c = f_s/2^j$, where $f_s = 1/\Delta t$, and is the signal's sampling frequency.

When using the DWT, at each level (*j*) the result from the high pass filter is stored and the result from the low pass filter is then filtered further. The process continues until the limiting number of levels (J) is reached, this filtering process is

shown in Figure 69, where the high pass filter is denoted by *H* and the low pass filter by *L*. Following the application of the DWT, the original signal $x(t)$ can be described as the combination of the signals from the high pass filters (d_1, d_2 … d_n) and the final level's low pass filter signal (a_J), where J is the number of levels used.

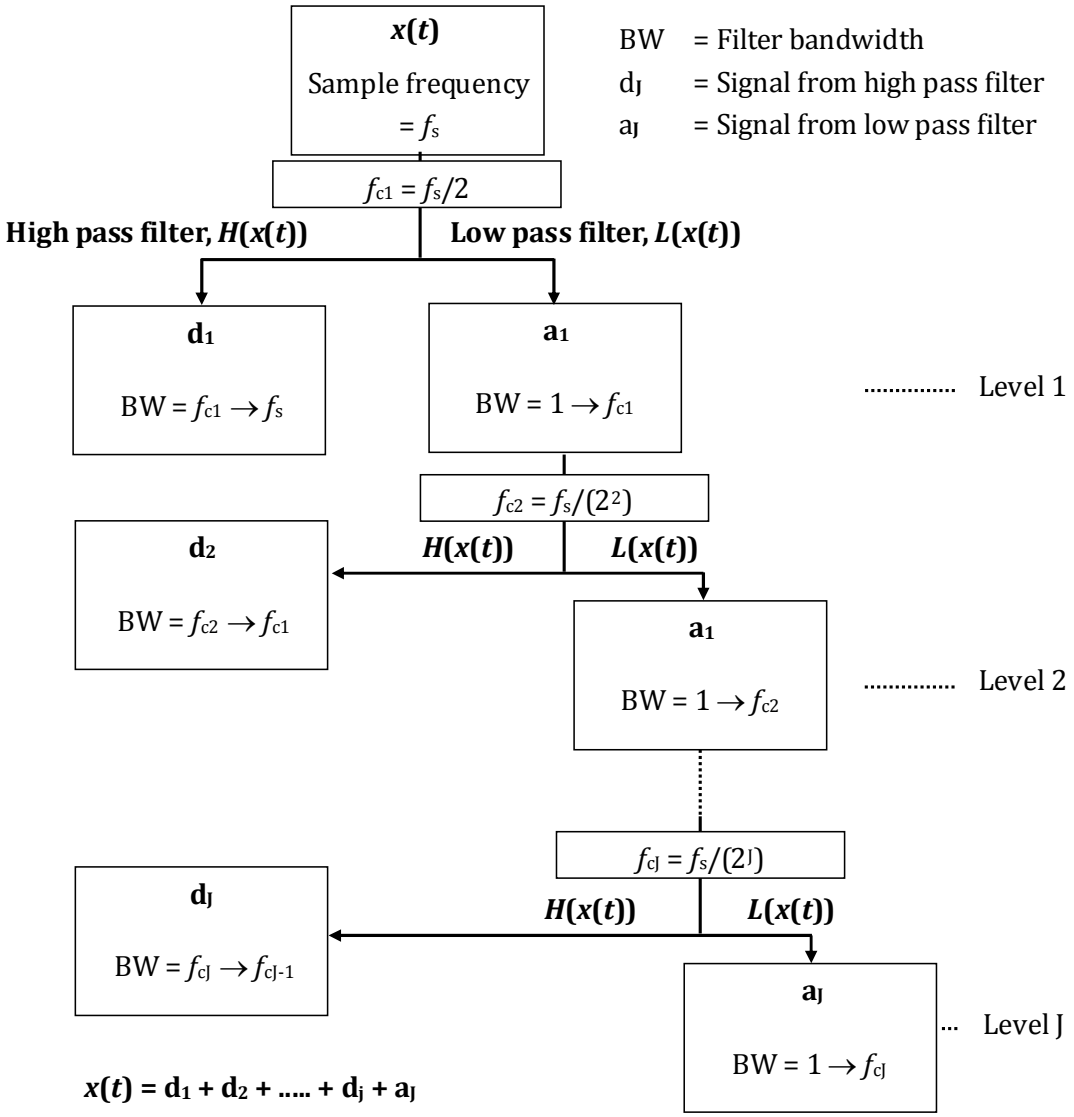

Figure 69: Example of the DWT filter bank for n levels

An example of a signal that has been passed through a high pass and a low pass filter, with a cut off frequency of 50Hz, is shown in Figure 70. It is clear that by applying a low pass filter the high frequency events within the signal are removed and conversely for the high pass filter the low frequency events are removed. The signal resulting from the application of the high pass filter corresponds to d_j in

Figure 69 and the signal resulting from the application of the low pass filter corresponds to a_j.

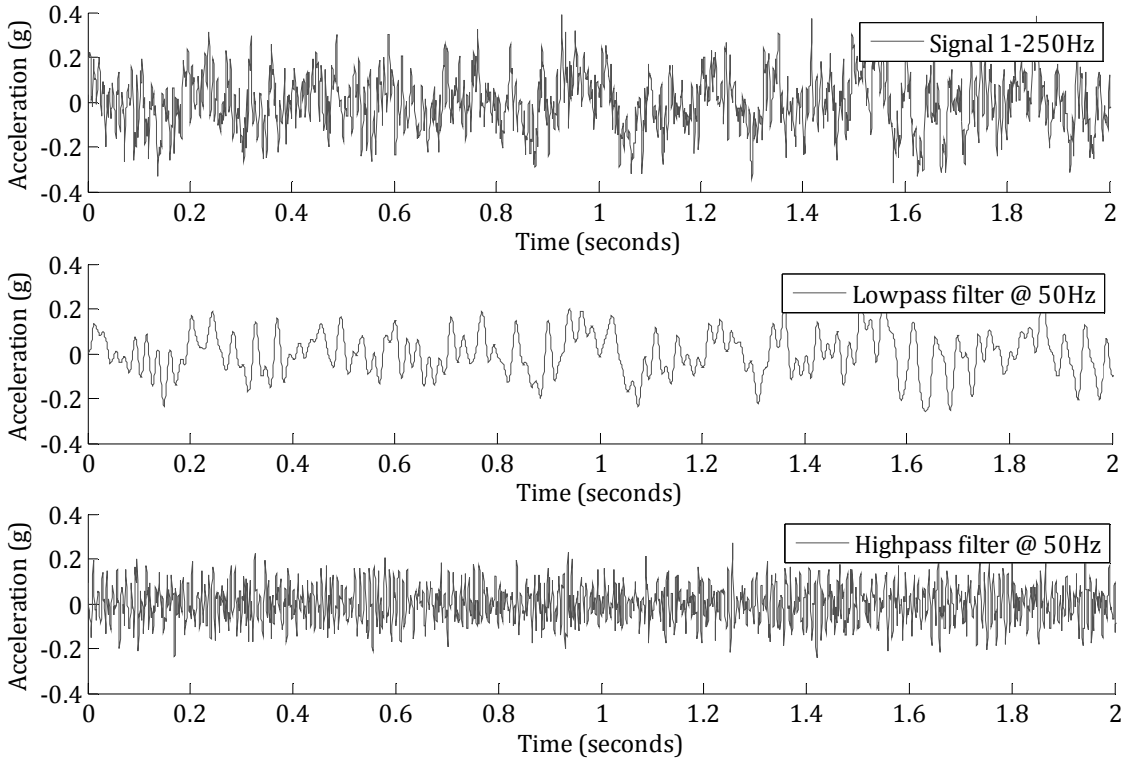

Figure 70: Example use of low pass and high pass filters with a cut off frequency of 50Hz

Nei et al (2008) used the discrete wavelet transform (DWT) with J = 8, to create a method of shock superposition for vibration testing, thus an 8 level DWT was carried out. The study found that the signal's discrete shock events were visible within levels 3 – 5. It was therefore recommended that when creating a simulation signal, short time segments within the signal should be amplified within the frequency range covered in levels 3 - 5, enabling a more accurate representation of both the amplitude and frequency variations throughout the signal. It was also recommended that the location and frequency of these amplified events, within the signal, be determined by their appearance and positioning within actual vehicle vibration.

7.3 Comparison of Time-Frequency Analysis Techniques

The signal in Figure 71 has been used to compare STFT, CWT and DWT analysis techniques. The signal was recorded in an empty Ford Luton box van during a home delivery journey in the city of Bath, UK. It has a sample time of 0.000585 seconds and has been passed through a band pass filter of range 1 - 250 Hz.

The STFT analysis of the signal is displayed in Figure 72. This was calculated using the following properties:

- Size of FFT: 2^{11}
- STFT Segment size: 2^{11}
- Sample frequency: 1710 Hz
- Overlap of segments: 0

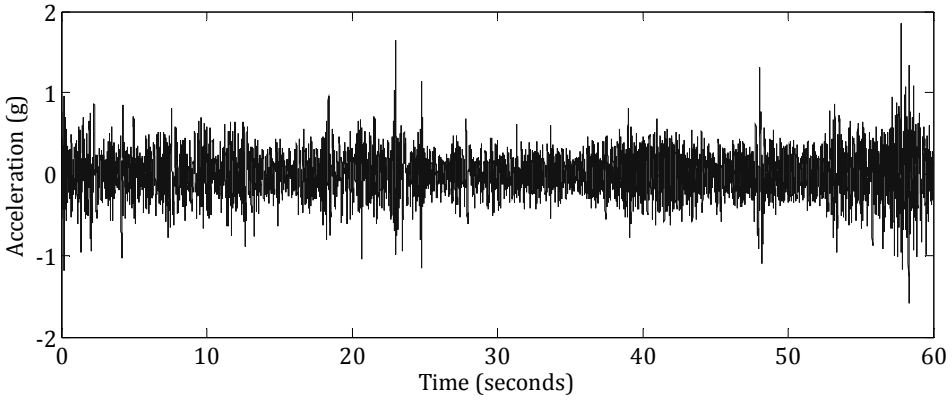

Figure 71: Example vehicle vibration signal to carry out comparison of time-frequency analysis techniques

The CWT and the DWT evaluations are displayed in Figure 73 and Figure 74, respectively. These analyses were carried out using the Matlab Wavelet Toolbox. The CWT was undertaken using the Morlet mother function and 128 scales, whilst the DWT was carried out using the Daubechies db6 mother wavelet function and was decomposed to 12 levels.

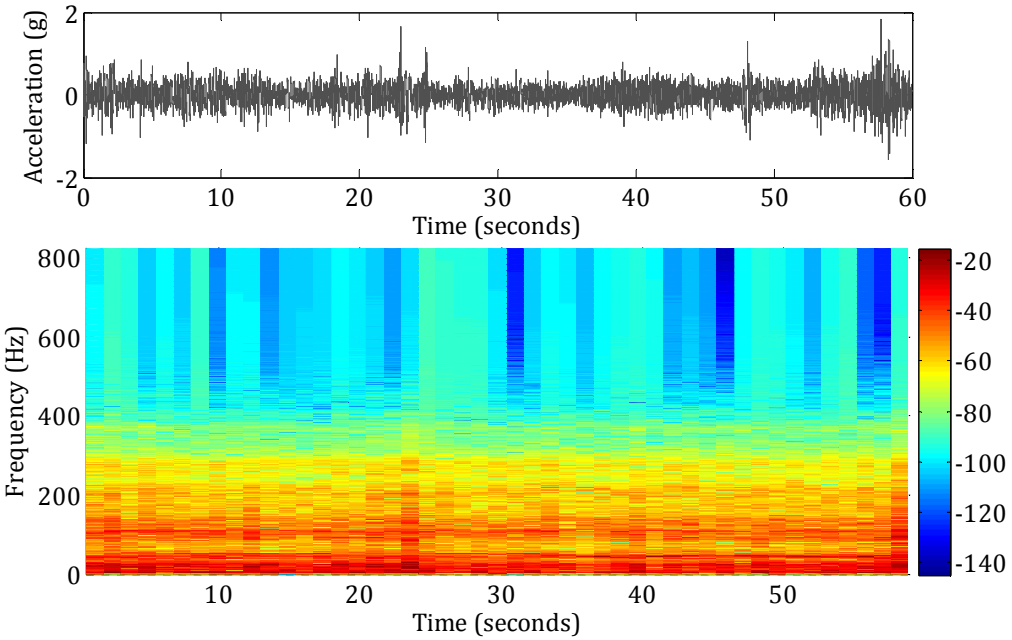

Figure 72: STFT of the signal given in Figure 71

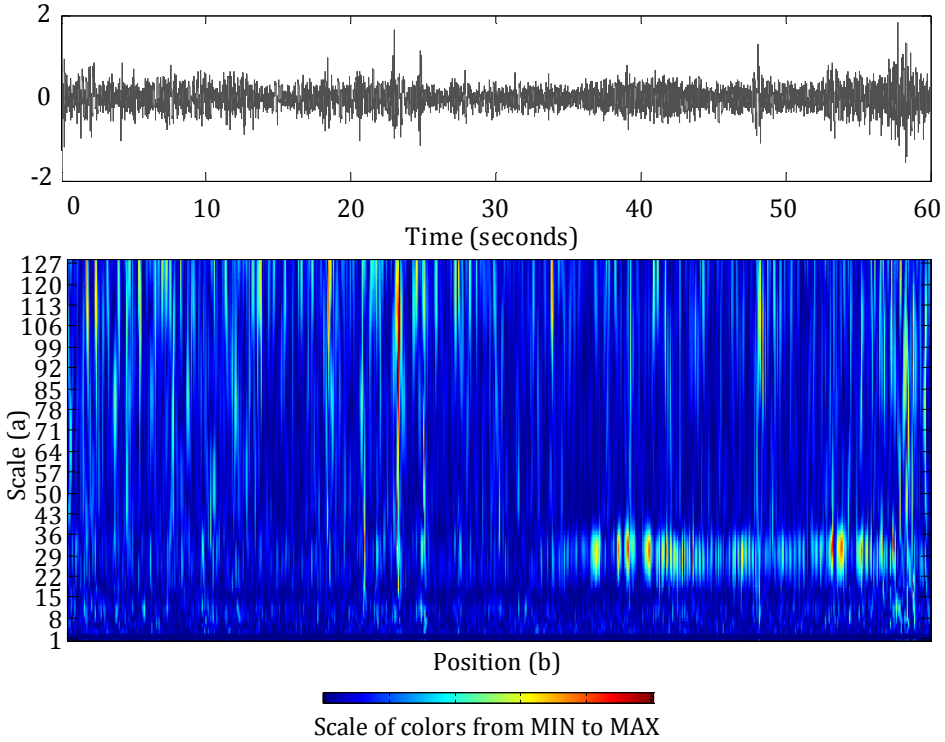

Figure 73: CWT of signal given in Figure 71 using the Morlet transform

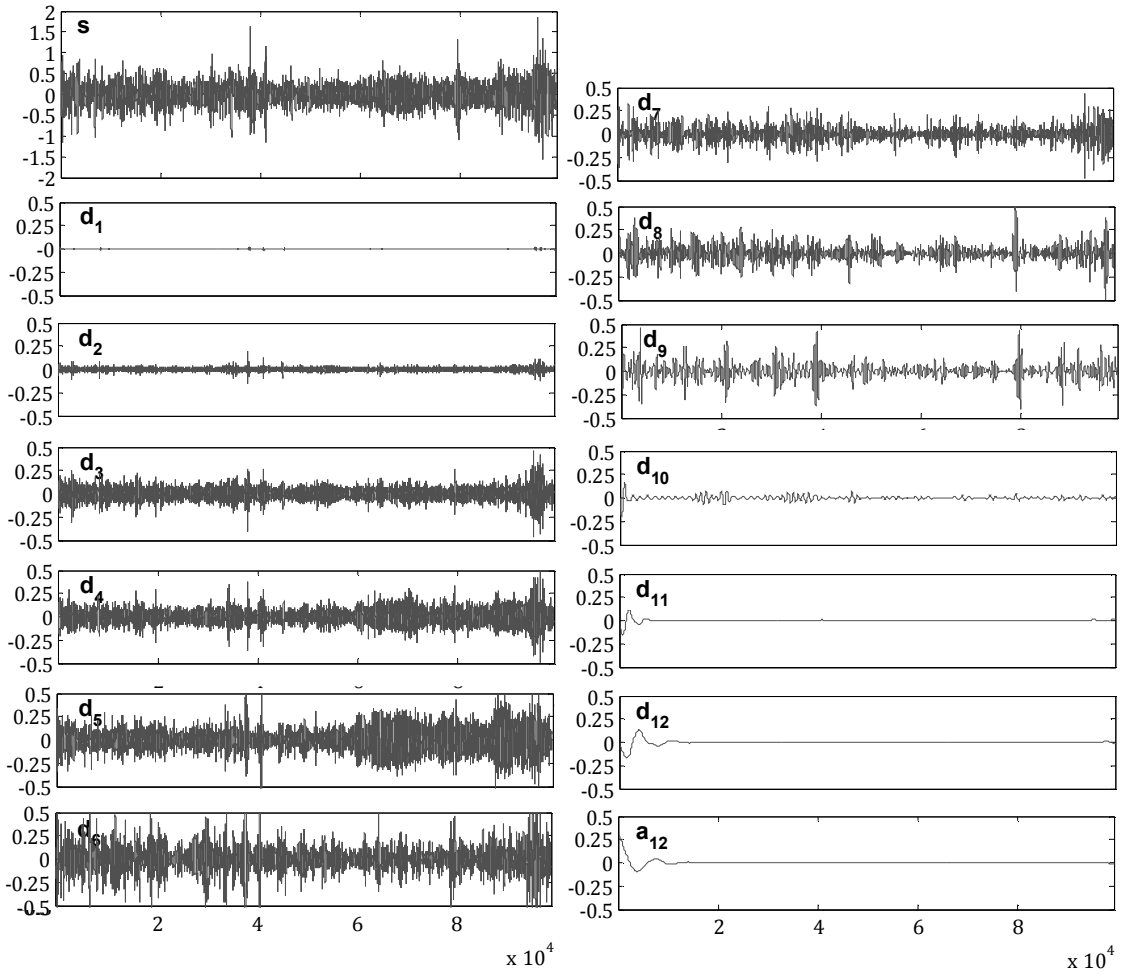

Figure 74: DWT of signal given in Figure 71 using Daubechie db6

By analysing vehicle vibration using a time-frequency technique it is possible to identify variations in the signal's intensity and frequency content over time. This allows for transients within the signal to be identified. In both Figure 72 and Figure 73, the high acceleration transient events, present in the signal in Figure 71 at approximately 47 and 58 seconds, are quite clearly visible. This is particularly true when considering the result from the continuous wavelet analysis, where high value coefficients are visible at these time points, throughout the full range of scales (1 to 128).

The DWT benefits from a reduced requirement of computational time and capabilities when compared with the CWT. This makes the DWT useful when evaluating vehicle vibration. Unfortunately, the DWT does suffer from some limitations. Firstly, the frequency resolution of the DWT is much lower than that of

the CWT due to the reduced number of levels used. Therefore, by using the CWT a more detailed view of the frequency variations in the signal can be obtained.

7.4 Concluding Remarks

The ability of time-frequency analysis techniques to identify transients and varying frequency content in vehicle vibration has been presented. It has been shown that whilst the STFT identifies variation in the signal, it is limited in resolution. This prevents it from fully recognising the short-time transient events present in vehicle vibration and also the accurate variation in frequency content variation. In contrast, the varying time and frequency resolution afforded by the CWT enables these events to be more accurately described.

The use of CWT is desirable in the analysis of non-stationary and non-Gaussian signals, such as vehicle vibration. Whilst the CWT is appropriate for analysing the signal and identifying variations in the frequency content and amplitude, its use within an approach for simulating vehicle vibration, is not so straight forward. This is mainly due to the way in which it analyses the signal. When inverting the CWT the original time history signal is returned, this therefore presents no obvious way in which several vibration signals can be considered in parallel to create an average representative simulation. Additionally it does not allow for the signal to be represented in a manner that is useable on most simulation rigs.

Vehicle vibration is unpredictable and highly unrepeatable. A key benefit of the established method is that it lends itself to journey averaging, enabling the inclusion of data from several journeys, giving the resulting simulation statistical significance. Additionally, this method also lent itself to application on existing laboratory simulation controllers, and, facilitated test acceleration. It is therefore apparent that while the CWT alone cannot be used to form a simulation approach, it can be used in conjunction with the established method to create a more suitable simulation approach.

Because of this, a new approach of simulating vehicle vibration, that utilises the CWT, has been developed.

8 A TIME-FREQUENCY APPROACH FOR SIMULATING VEHICLE VIBRATION

It is apparent that in order to identify signal transients when analyzing a non-stationary and non-Gaussian signal, a time-frequency analysis method should be adopted. In section 7.3, it was recognized that time-frequency wavelet analysis, provides the most suitable method for identifying these signal transients.

In section 4 the RMS modulation approach, developed by (Rouillard and Sek, 2010), was evaluated. A random non-stationary vehicle vibration can be described as a sequence of zero-mean Gaussian segments. This allows the signal to be defined by a series of RMS acceleration levels and '*vibration doses*' (durations) (Rouillard, 2007a). The resulting simulation has a varying RMS acceleration characterized by a given statistical distribution. This method evolved from previous work, which evaluated the non-stationary and non-Gaussian characteristics of vehicle vibration, with particular attention to the statistical content of vehicle vibration signals (Rouillard, 2007a; Rouillard and Sek, 2000).

In the correlation study, presented in section 5, the RMS modulation method was shown to correlate well with vertical vibration time replication, producing only a small error (5% under test), when considering the damage mechanism of scuffing.

As the RMS acceleration varies the signal's average PSD is uniformly scaled. Therefore while the method simulates the RMS acceleration distribution of a signal it does not account for variations in frequency content. By not accounting for the change in frequency content at different RMS acceleration levels, important frequency responses seen in time replication may be missed and this therefore may be a source of error.

It has been concluded, that by creating a simulation approach that analyzes the change in spectral shape along with the RMS acceleration distribution, a more

accurate representation of vehicle vibration can be formed. In order to analyse the change in spectral shape over time a time-frequency analysis tool based on the wavelet transform may be used.

Because the CWT retains the signal's information, when inversed it reproduces the original time-domain signal. Because of this, used independently, it only presents a more appropriate method of analyzing a signal to identify transient events. Therefore, it does not offer a suitable method of producing a simulation which is both usable on existing controllers and is statistically significant e.g. create a simulation from multiple and averaged data so that it contains events that are likely to occur in real life. This limitation, along with consideration of the work carried out by Rouillard and Sek (2010), has led to the construction of a simulation approach which employs a combination of time-frequency and frequency analysis tools.

The method presented uses an iterative approach to decompose a non-stationary signal, with a non-Gaussian distribution, in to approximately stationary and Gaussian parts of varying amplitude and duration. Each of these parts can be represented as a PSD and duration. By then applying these parts at random, a simulation signal, that has a similar RMS acceleration distribution, kurtosis, and average PSD to the original signal, can be formed. By incorporating the use of frequency analysis, the resulting simulation is usable on existing laboratory controllers, and has the potential for both signal averaging and test acceleration, if required.

A detailed explanation of the development of the wavelet decomposition method is now given, followed by a worked example of the method.

8.1 The Wavelet Decomposition Method for Simulating Vehicle Vibration

The wavelet decomposition method involves a two-level iterative approach. At each stage wavelet analysis is used to decompose a vibration signal into two parts: that which falls within a Gaussian envelope (low level vibration) and that which exceeds the Gaussian envelope (high level vibration). These two parts are referred to respectively, as the Gaussian approximation and the non-Gaussian part.

On the first iteration the original vibration signal is decomposed, on proceeding iterations, the non-Gaussian part resulting from the previous iteration is then decomposed.

Once a limiting number of iterations M have occurred, or the non-Gaussian part produced has a kurtosis below an acceptable value, the first level of iterations stops and the final non-Gaussian part becomes the $M+1^{th}$ Gaussian approximation.

In order to then refine each of the Gaussian approximations, the distribution of each (1 to M+1) is evaluated. If an approximation's kurtosis is above an acceptable value, a second level of iteration takes place. This second level of iteration is used to reduce the size of the signal parts, enabling the creation of smaller more stationary parts with distributions closer to Gaussian.

At the end of the iterative process, the signal has been decomposed in to a number of parts that have approximately Gaussian distributions, which when reconstructed together would reform the original vibration signal.

Because each part is approximately stationary with an approximately Gaussian distribution, they can each be defined relatively accurately by their PSD and duration. A simulation signal can then be created by randomly simulating each part. When simulated together, the parts form a simulation signal that is non-stationary and non-Gaussian with the same average PSD, average RMS acceleration and duration as the original signal.

A flow diagram illustrating the wavelet decomposition method is given in Figure 75. A detailed explanation of each step is then given.

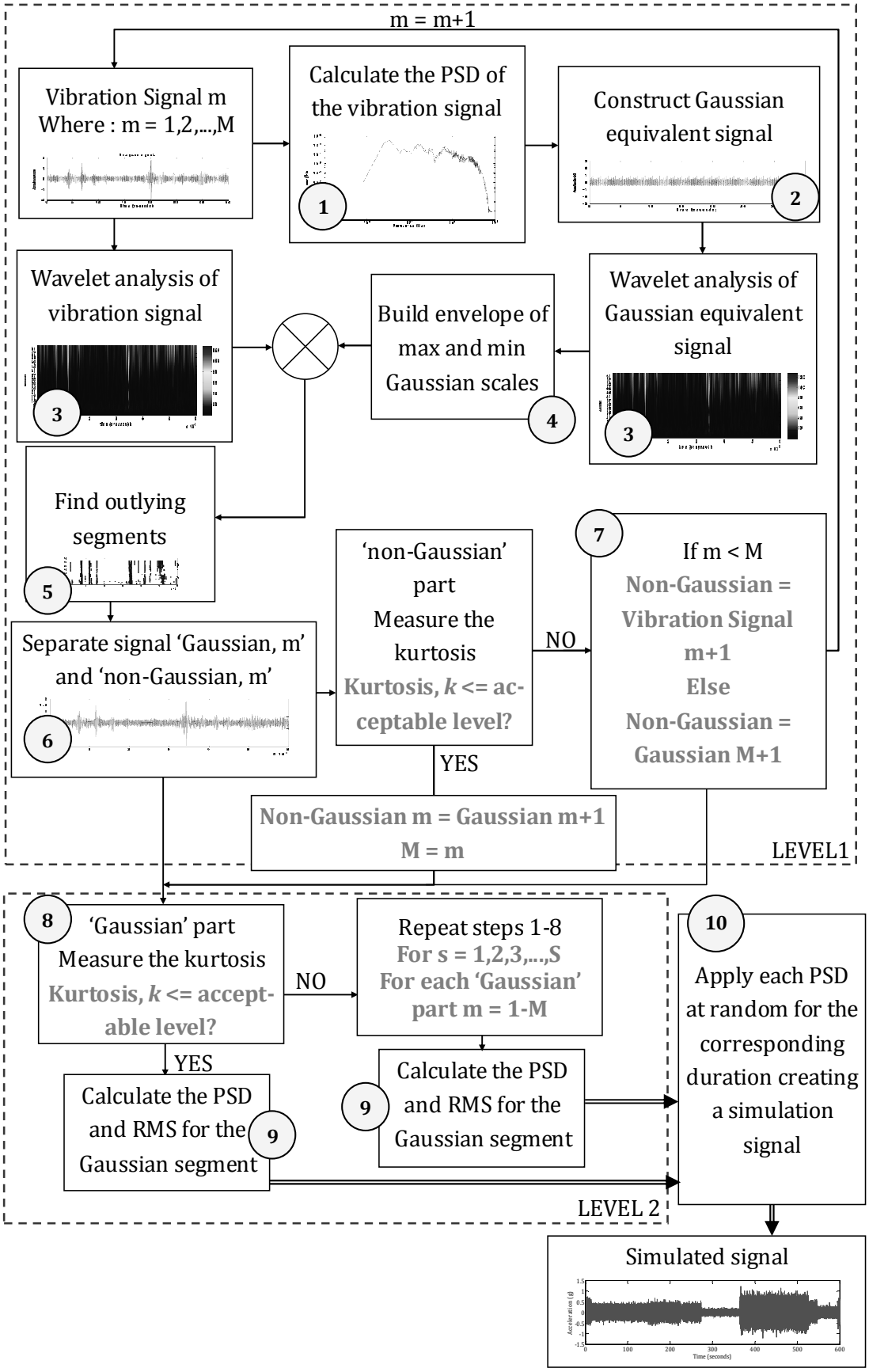

Figure 75: Flow chart illustrating the process of decomposing vibration signal using wavelet analysis

Matlab has been used to construct a code for creating simulations using the wavelet decomposition method. The associated code is included in Appendix V.

In the first level of iteration (Figure 75) M iterations take place, where m = 1, 2, 3, … M, represents the current iteration number. The value of M is decided by one of two factors, either:

1. M = a limiting number of iterations, e.g. a maximum 3 iterations are carried out.

2. Or, M = the number of iterations until the high level vibration part, that exceeds the Gaussian envelope, has k <= the acceptable limit.

Step 1 of the wavelet decomposition method calculates the average PSD ($S_m(f)$) for the vibration signal. When:

- For the first iteration (m = 1), the vibration signal, $y_1(t)$ = original vibration signal

- For any subsequent iterations (1 < m ≤ M), the vibration signal, $y_m(t)$ = the non-Gaussian part, $y_{NGm-1}(t)$.

The average Fourier spectrum, $Y_m(f)$, can be calculated using an adaption of Equation 12. In order to find the DFT, $Y_m(f_k)$, of a non-periodic signal, $y_m(t)$, the DFT would need to be calculated over the entire signal so that the sample size N would be equal to the length of the signal. To therefore reduce the size of the DFT, an average DFT for the signal is calculated. This is done by calculating the DFT for each segment of the signal (length N data points) as it falls within a window. In order to get the most accurate average, windowed segments should overlap by N-1 data points, giving the equation:

$$Y_m(f_k) = \frac{1}{Q}\sum_{q=0}^{Q-1}\sum_{r=0}^{N-1} y_m(t_r + t_q)e^{-i(2\pi f_k t_r)} \tag{31}$$

where:

$f_k = k\Delta f$, DFT frequency (Hz)

$k = 0, 1, 2, ..., N$

$\Delta f = \frac{1}{N\Delta t}$, frequency bandwidth (Hz)

$y_m(t_r + t_q)$ is the input signal at position $(t_r + t_q)$.

$t_r = r\Delta t = 0, 1, 2, ..., N-1$

$t_q = q\Delta t = 0, 1, 2, ... Q-1$, the time point to move sampling window to.

Q = Number of data points in the signal $(y_m(t))$ – $(N-1)$ = number of signal segments of length N averaged to form the average DFT. $(N-1)$ is the overlap of segments used.

Because of aliasing of frequencies above the Nyquist frequency, f_N (as discussed in section 3.1.9), the DFT frequency, f_k represents the frequencies:

$$f_k = \begin{cases} \frac{k}{N\Delta t} Hz & k \leq \frac{N}{2} \\ \left(\frac{k}{N\Delta t} - \frac{1}{\Delta t}\right) Hz & k > \frac{N}{2} \end{cases}$$

To remove the negative frequencies the Fourier spectrum $Y_m(f)$, has been truncated after the $(N/2)^{th}$ value, creating a one-sided spectrum of only positive frequencies.

The average PSD is then calculated from the average Fourier spectrum (Garcia-Romeu-Martinez, 2008):

$$S_y(f) = \frac{2\Delta t}{N} |Y_m(f)|^2 \quad (32)$$

Where $Y_m(f)$ is now the one sided Fourier spectrum and the multiplication of 2 compensates for using the one-sided spectrum of length $N/2$.

Step 2 creates a signal from the PSD, $S_y(f)$, this signal has the same average PSD, overall RMS acceleration and duration as the vibration signal. But because the signal is constructed from average data, it will ultimately be stationary (it will have a constant RMS acceleration), and it will have a Gaussian distribution. Therefore the simulation signal produced from the PSD will have the same average frequency distribution as the original signal and the same overall RMS acceleration, but it will not recreate the non-stationary nature and the non-Gaussian distribution of the original vehicle vibration. Hence why a signal simulated from the PSD is referred to in this Thesis as the equivalent Gaussian signal.

A Gaussian signal is created by inverting Equation 32 and utilising Equation 13 for the inverse DFT. Firstly, the PSD is inverted giving the one sided Fourier spectrum:

$$Onesided(X(f)) = \left(\sqrt{\frac{S_y(f)N}{2\Delta t}}\right)e^{iP} \tag{33}$$

Because when calculating the PSD, the signal's phase information is lost, a random phase, between 0 and 2π must be added to form the complex one sided Fourier spectrum ($X(f)$).

$$Onesided(X(f)) = |X(f)|e^{jPhase} \tag{34}$$

Where:

Phase = a random phase array.

The two sided DFT ($X_m(f)$), is then constructed by concatenating the one sided Fourier spectrum with its complex conjugate ($X^*(f)$) .

A time domain signal segment of time length $N\Delta t$ can then be constructed by applying the inverse DFT.

In order to then obtain a time domain signal with the same duration as the original vibration signal ($y_m(t)$), L, the process in step two needs to be repeated n times, where:

$$n = \frac{L}{N\Delta t}$$

The resulting n signal segments are concatenated to form a time domain signal $x_m(t)$, of duration L, the same duration as $y_m(t)$. An example of a vibration signal and its equivalent Gaussian signal is given in Figure 76.

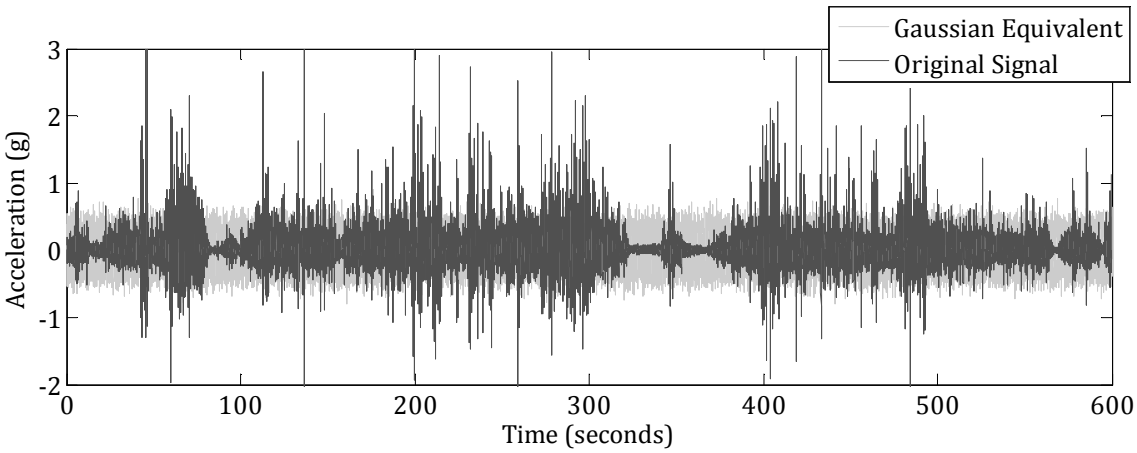

Figure 76: Comparison of original signal and its Gaussian equivalent

Step 3, wavelet analysis is performed on both the vibration signal and the equivalent constructed signal. The CWT (Equation 25) is used with the Morlet mother wavelet function, ψ defined by Equation 28, to calculate the wavelet coefficients of both signals, $X_m(t)$ and $Y_m(t)$.

$$X_m(b,a) = \frac{1}{\sqrt{|a|}} \int x_m(t) \psi\left(\frac{t-b}{a}\right) dt \tag{35}$$

A 'Gaussian' envelope is then constructed from the maximum and minimum coefficient values at each scale (a) of the constructed signal's wavelet coefficients:

$$Max(i) = \max(X_m(B,i))$$

$$Min(i) = \min(X_m(B,i))$$

where:

$i = 1, 2, \ldots, A$

A is the total number of scales

B = all positions, b.

An example of the Gaussian envelope is given in Figure 77. In *Step* 4, this envelope is compared with the vibrations signal's wavelet coefficients for all positions (b), and in *Step* 5 any coefficients that exceed the Gaussian envelope's maximum or minimum values are identified, these coefficients are termed outliers.

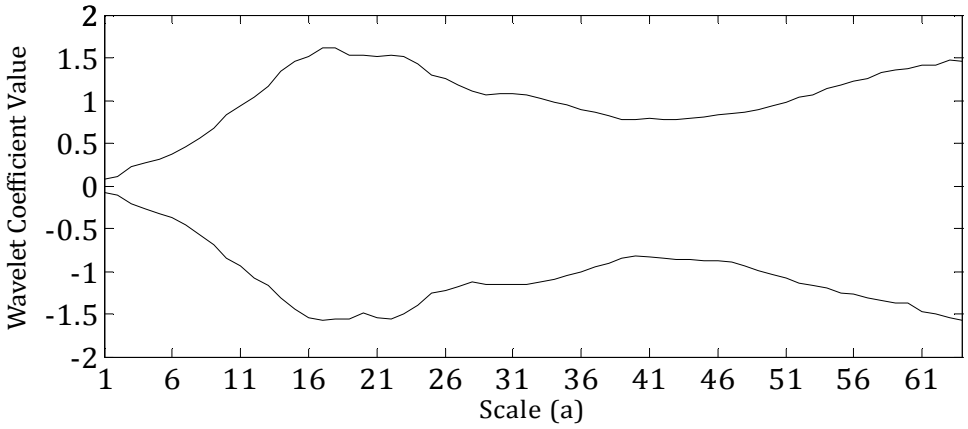

Figure 77: Example of the Gaussian envelope

Step 6, the segments surrounding positions that exceed the envelope are then extracted from the vibration signal. The size of the segment is determined by the frequency resolution required. As vehicle vibration is typically analysed within 1 – 200 Hz, a minimum segment size of one second is desirable to reduce calculation errors.

Figure 78 shows the results of the decomposition of the vibration signal shown in Figure 76, using a segment size of one second and a frequency resolution of 64 scales.

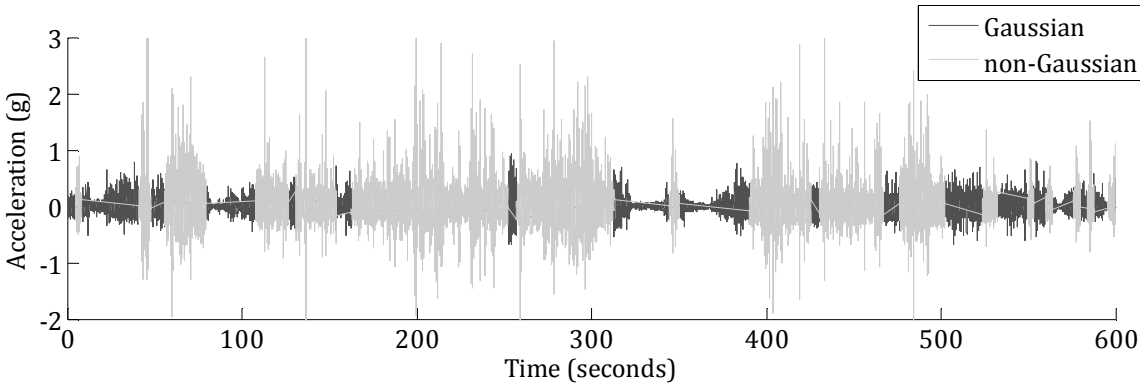

Figure 78: Decomposed signal showing Gaussian and non-Gaussian parts of the signal

Both the low amplitude vibration (Gaussian approximation) and the high amplitude vibration (non-Gaussian part) have been concatenated and are shown separately in Figure 79 parts (a) and (b), respectively.

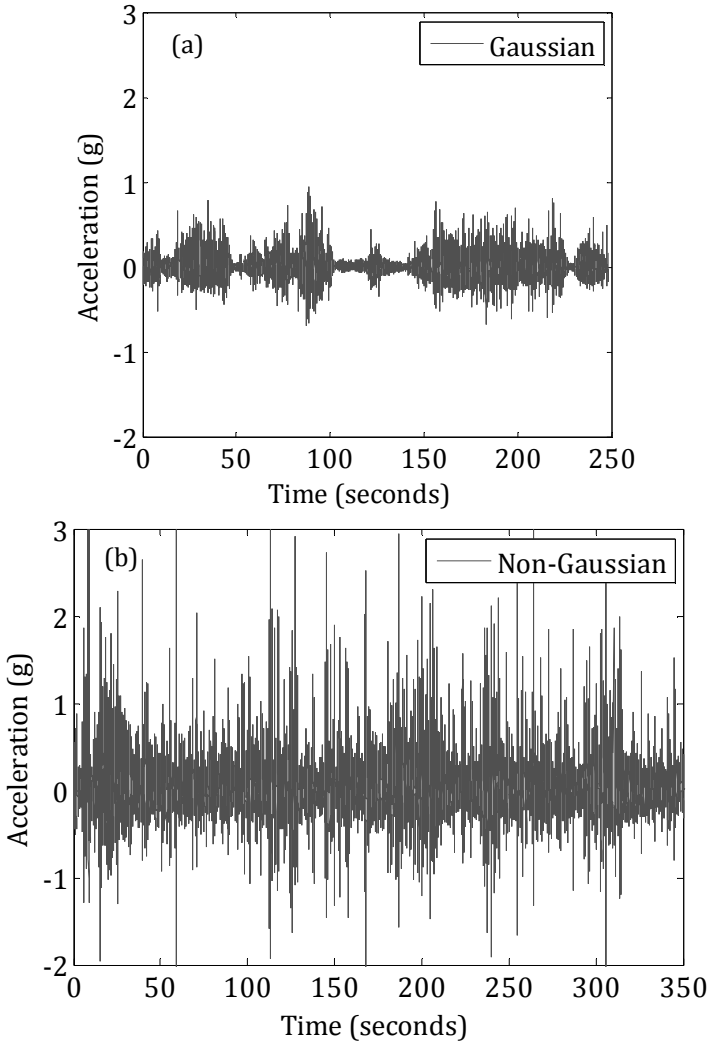

Figure 79: (a) Gaussian approximation and (b) non-Gaussian part of the signal

While the extreme high level events have been removed from the Gaussian approximation, its non-Gaussian distribution and non-stationary nature is still evident. The RMS acceleration distribution of the Gaussian approximation is given in Figure 80. The wide spread of the distribution demonstrates its non-stationary nature.

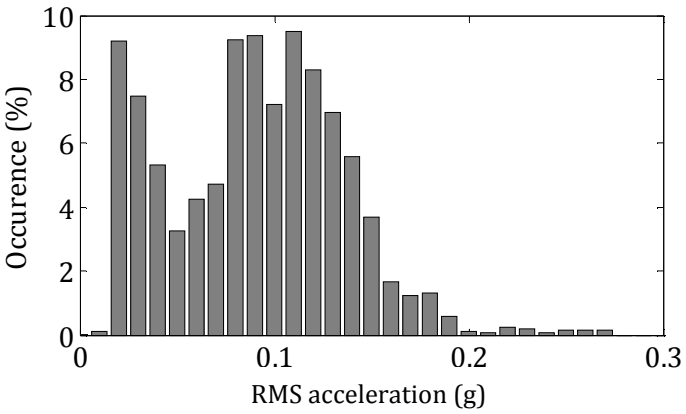

Figure 80: RMS acceleration distribution of Gaussian approximation of original signal

Step 7, once decomposed, the kurtosis of the non-Gaussian part of the signal is calculated. In this example the kurtosis of the Gaussian approximation and non-Gaussian part is 6.7 and 13.3, respectively. Therefore the iterative process is repeated.

Two further iterations have been carried out (M = 3). Figure 81 shows the Gaussian approximations produced through this decomposition. In total the signal has been decomposed in to M + 1 parts, where m = 1 to 3 are Gaussian approximations through the iteration process and m = 4, is the remaining non-Gaussian part.

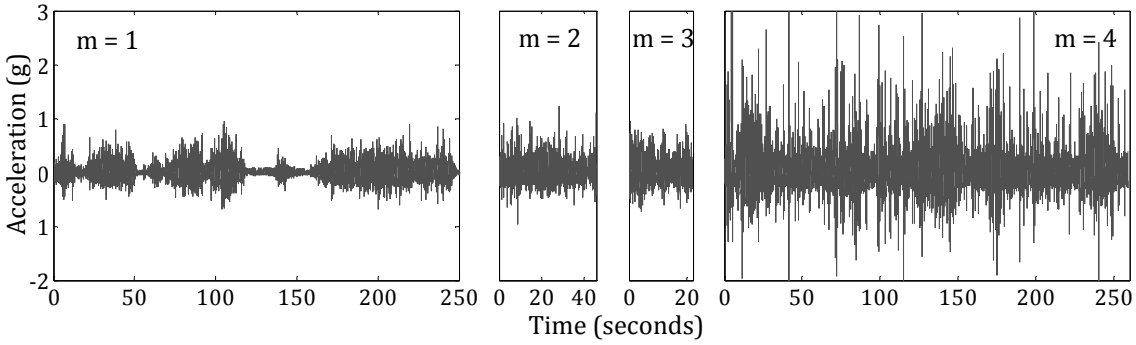

Figure 81: Original signal decomposition parts

The kurtosis and overall RMS acceleration of each of the four parts is given in Table 18. The RMS acceleration of each Gaussian approximation increases with each iteration (*m*). The kurtosis of the first and last iteration, are highest because, on the first decomposition, the signal's extremely low intensity vibration events are captured within the Gaussian envelope. Similarly, the last part (*m* = 4) contains all of the high level shock events that exceed the Gaussian envelope, therefore resulting in a high kurtosis.

Table 18: Kurtosis and RMS acceleration of decomposed signal parts

PART (*m*)	KURTOSIS (*k*)	OVERALL RMS ACCELERATION (g)
1	6.8	0.11
2	5.4	0.15
3	4.5	0.17
4	12.4	0.25

In *Step 8*, the kurtosis of each of the Gaussian approximations is calculated. If the kurtosis for an approximation exceeds the acceptable level, then that approximation is decomposed further, using a second level of iteration that repeats *Steps 1 – 7*. If the kurtosis is below the acceptable level the segment is not decomposed further.

The second level of decomposition was carried out using a limiting number of 2 iterations per Gaussian approximation. Each part is referenced with its first level of iteration (*m*) and second level of iteration (*s*) iteration, in the form *m*,*s*. In total the signal was decomposed into eleven parts.

Further decomposing the signal reduced the kurtosis of Gaussian approximations, and enabled a wider spread RMS acceleration distribution to be created, which better represented the original vibration signal. The kurtosis, RMS acceleration and duration of all parts from the second level of iteration, are given in Table 19.

Table 19: Kurtosis, RMS acceleration and duration of the signal parts from second level decomposition

PART NO	FIRST LEVEL ITERATION (*m*)	SECOND LEVEL ITERATION (*s*)	KURTOSIS (*k*)	OVERALL RMS ACCELERATION (g)	DURATION (seconds)
1	1	1	6.3	0.05	92
2	1	2	4.2	0.09	48
3	1	3	4.9	0.13	133
4	2	1	3.3	0.11	2
5	2	2	5.4	0.15	44
6	3	1	4.1	0.13	3
7	3	2	4.4	0.17	19
8	4	1	5.9	0.15	77
9	4	2	5.2	0.19	14
10	4	3	9.3	0.19	5
11	4	4	10.4	0.29	162

In *Step* 9 the PSD of each Gaussian approximation has been calculated and in *step 10* each PSD has been applied at random for the corresponding duration, to create a simulation signal that represents the original vibration signal. The wavelet decomposition signal (simulated signal) for this example is shown in Figure 82. The variation in intensity is in marked contrast to that produced when using the single level PSD approach, which is used in *Step 2* with an example in Figure 76.

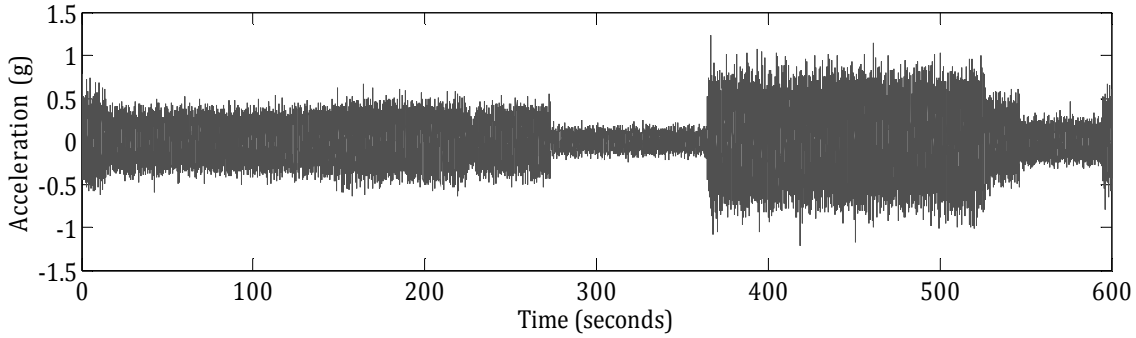

Figure 82: Wavelet decomposition method simulated signal of original signal in Figure 76

8.1.1 Evaluation of the Simulated Signal

A comparison between the maximum and minimum acceleration levels for each of: the original signal; the signal produced using the single level PSD approach; and, the simulated signal from the wavelet decomposition method, is given in Table 20.

Table 20: Maximum and minimum acceleration levels for each simulation and the overall RMS acceleration

SIGNAL	MAXIMUM ACCELERATION (g)	MINIMUM ACCELERATION (g)	OVERALL RMS ACCELERATION (g)	KURTOSIS (*k*)
Original Signal	3.83	-2.66	0.18	16.2
Signal level PSD	0.81	0.89	0.18	3.0
Simulated Signal	1.24	-1.22	0.18	5.0

The simulated signal improves on the single level PSD by providing more extreme maximum and minimum acceleration levels, that better match those of the original signal. As the wavelet decomposition method uses averaging, the magnitude of the maximum and minimum acceleration levels is less than that of the original signal. The maximum and minimum acceleration of the simulated signal could be modified to better match those of the original signal by carrying out a further level of iteration, enabling the production of smaller signal parts. But, consideration should be given to the minimum part length allowed, so that an over test is not created through the simulation of high level vibration events that are extremely unlikely to occur during distribution.

The RMS acceleration distribution for one second samples of the simulated signal has been calculated and is presented in Figure 83, alongside the RMS acceleration distribution of the original signal.

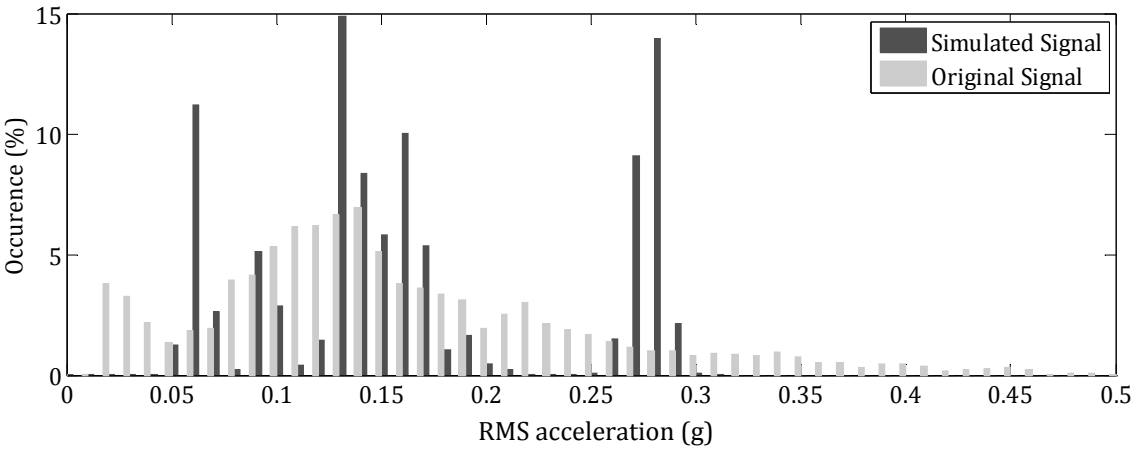

Figure 83: RMS acceleration distribution of original signal and the simulated signal

As defined in section 3.1.7, for a signal to be stationary it must have a constant RMS acceleration. In Figure 83 it is clear that the amplitude of the simulated signal's RMS acceleration varies significantly, indicating that the signal is non-stationary. The spread of the distribution does not match that of the original signal and appears to be more concentrated than the original at particular levels. The concentration around 0.27g to 0.29g is caused by the simulation of part 4,4, which contains all of the high level events from the signal. To reduce the size of part 4,4, and hence increase the spread of the RMS acceleration distribution above 0.2g, a smaller segment size during decomposition would be required. Unfortunately, reducing the segment size introduces further limitations which are discussed later. Also apparent is the exclusion of RMS acceleration levels below 0.05g in the simulated signal's distribution, which is caused by averaging used when creating the Gaussian signals. This part of the distribution could be better simulated better by the use of further iteration to reduce the size of Gaussian parts.

The average PSD of both the simulated signal and the original signal are given in Figure 84. The close match between the two signals is evident, showing that overall, the simulated signal represents well the original signal's frequency content and amplitude.

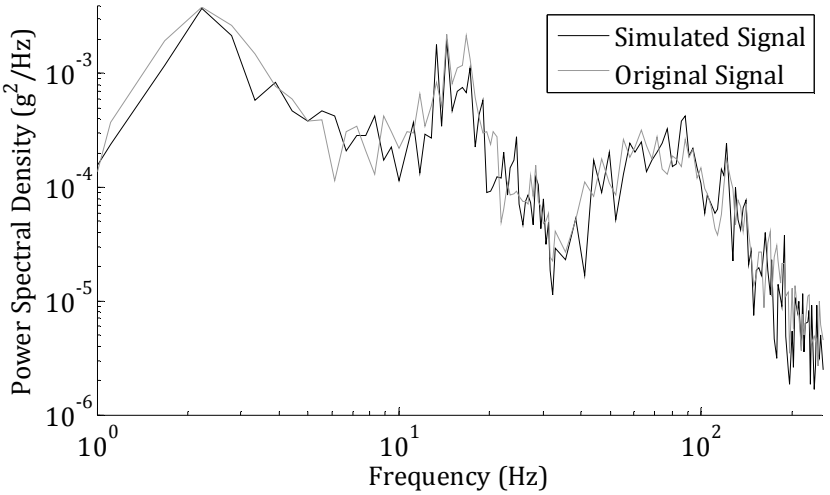

Figure 84: PSD of the original signal and simulated signal

With the wavelet decomposition method now detailed, a pseudo code flow diagram and a worked example are now given.

8.1.2 Wavelet Decomposition Method Pseudo Code

The ten steps corresponding with Figure 75 and the steps previously discussed have been illustrated using a pseudo code flow diagram, given in Figure 85, Figure 86 and Figure 87.

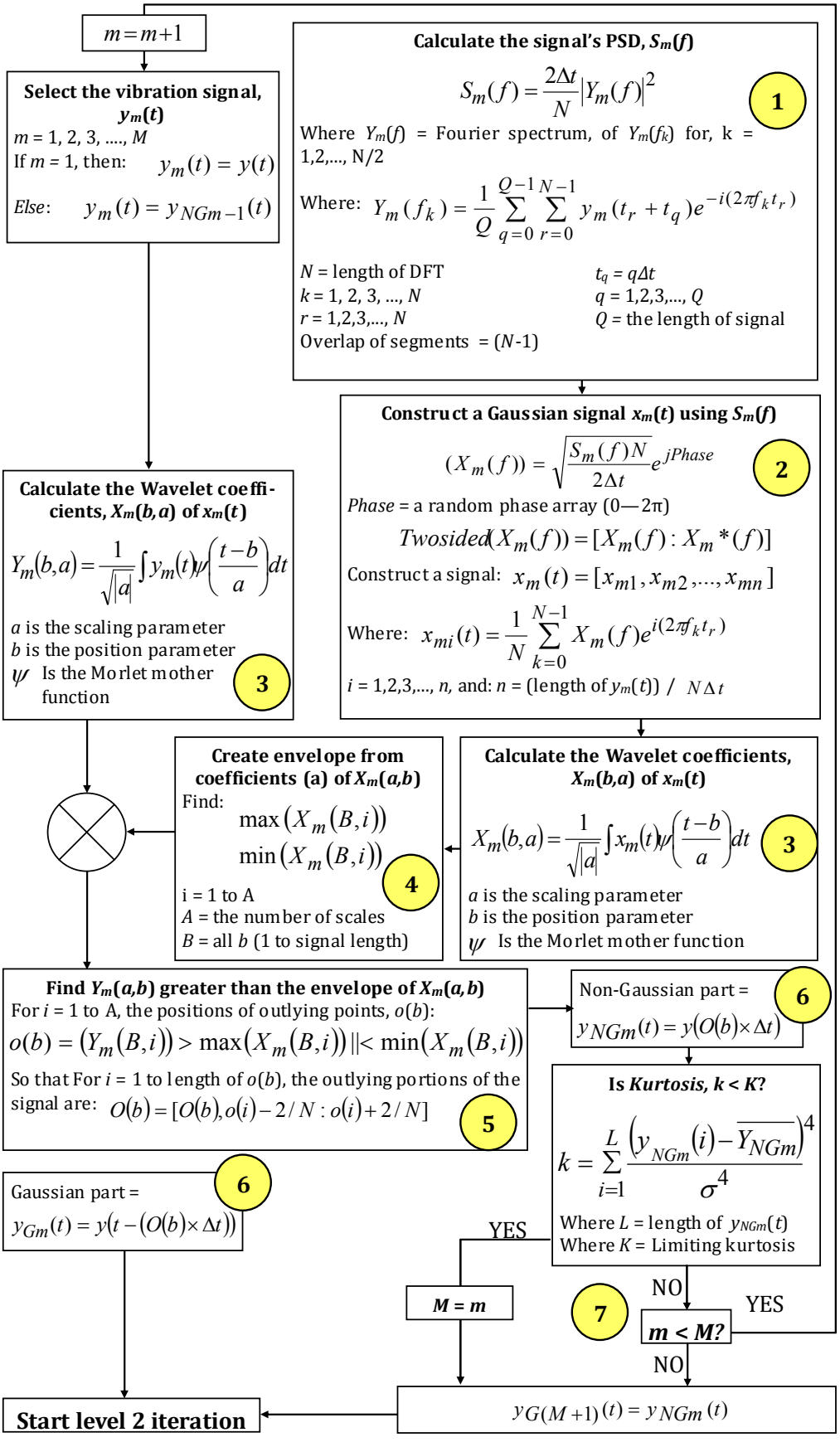

Figure 85: Pseudo code flow diagram of wavelet decomposition method (level 1 iteration)

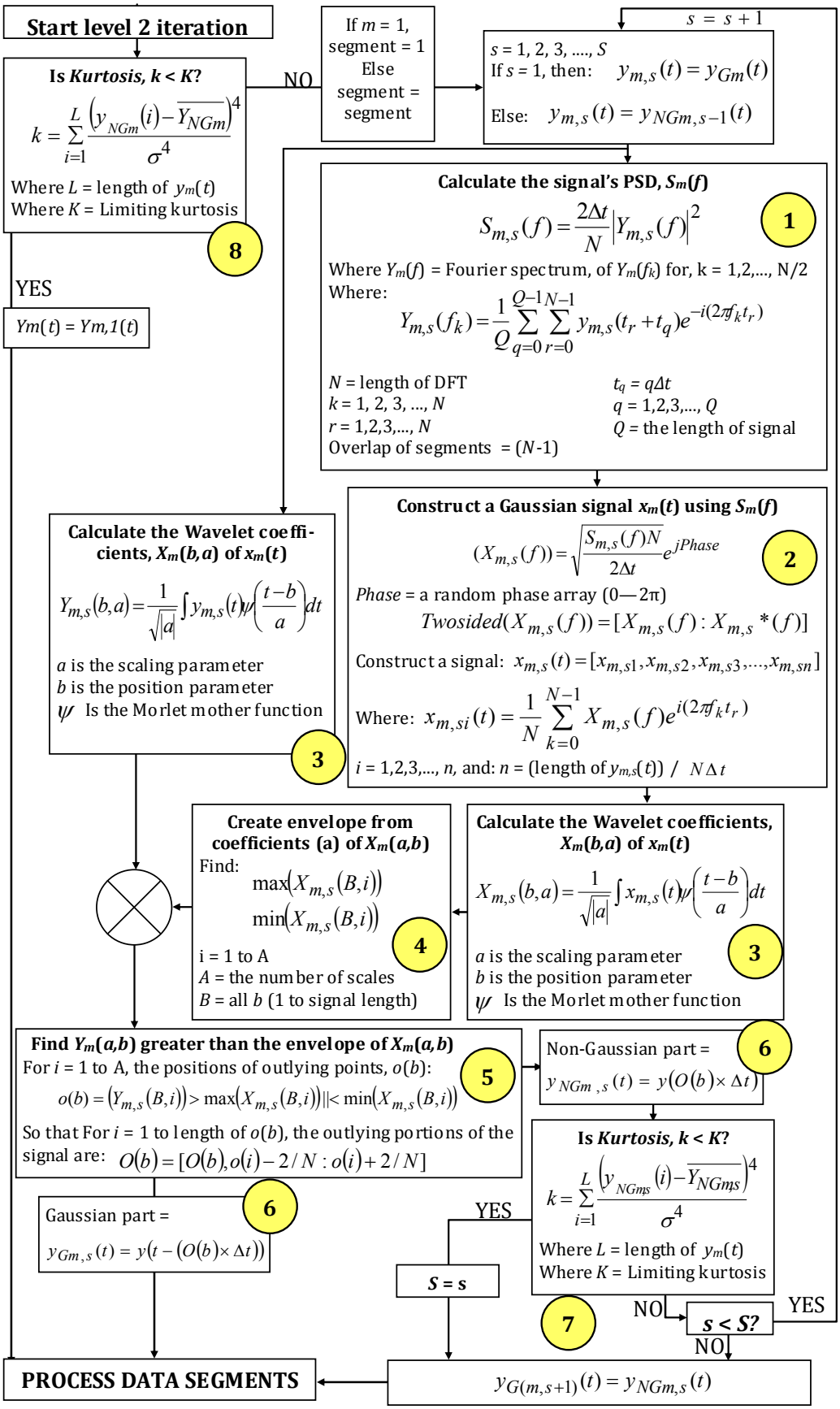

Figure 86: Pseudo code flow diagram of wavelet decomposition method (level 2 iteration)

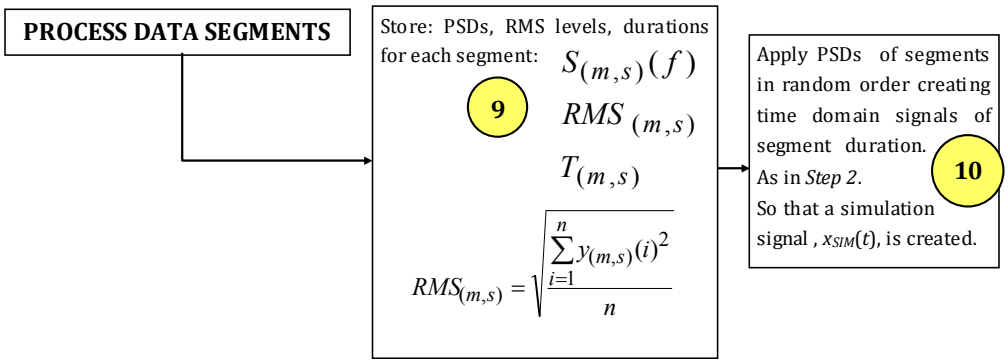

Figure 87: Create simulation signal, from data segments, for use on vibration table

8.2 Illustrated Use of the Wavelet Decomposition Approach

To illustrate the proposed method and its relevance, an example vehicle vibration from a supermarket home delivery vehicle is used. The data was collected using a Lansmont Saver 9x30 field data recorder. This was located on the floor of the vehicle above the kerb side rear tyre, as this is the position that tends to receive the worst case vibration (Figure 88).

Figure 88: Home delivery vehicle with location of Saver 9x30 unit

The vibration from the journey was measured in one minute samples with zero spacing to allow for continuous data sampling. A four minute portion of the journey was used to form an example of the analysis process. The time history vertical vibration signal is shown in Figure 89.

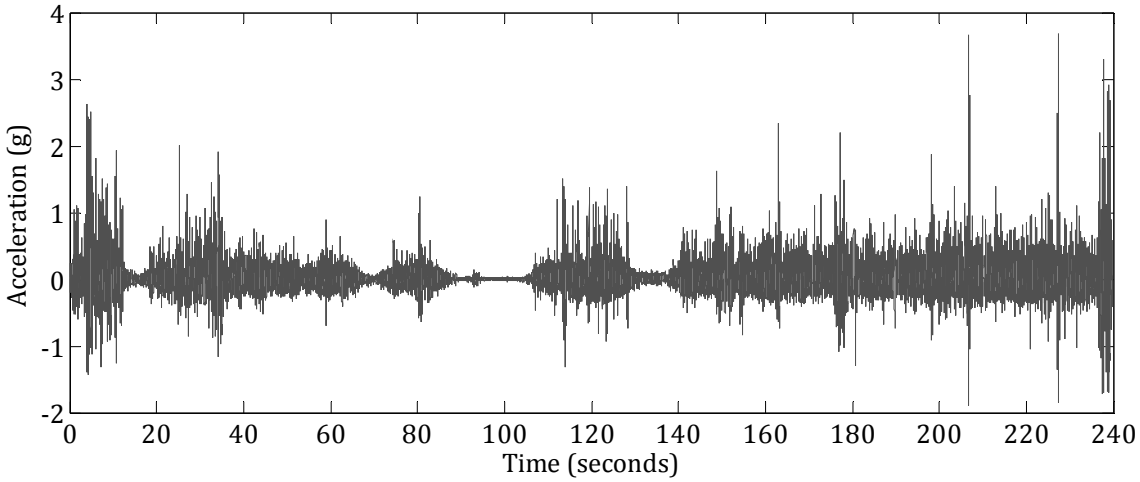

Figure 89: Time history vibration signal

8.2.1 Worked Example of the Ten Step Wavelet Decomposition Method

The nine steps of the wavelet decomposition method are presented respect to the vibration signal given in Figure 89.

Step 1 - ***Calculating the PSD:*** The signal's PSD, given in Figure 90, illustrates the average frequency content of the signal.

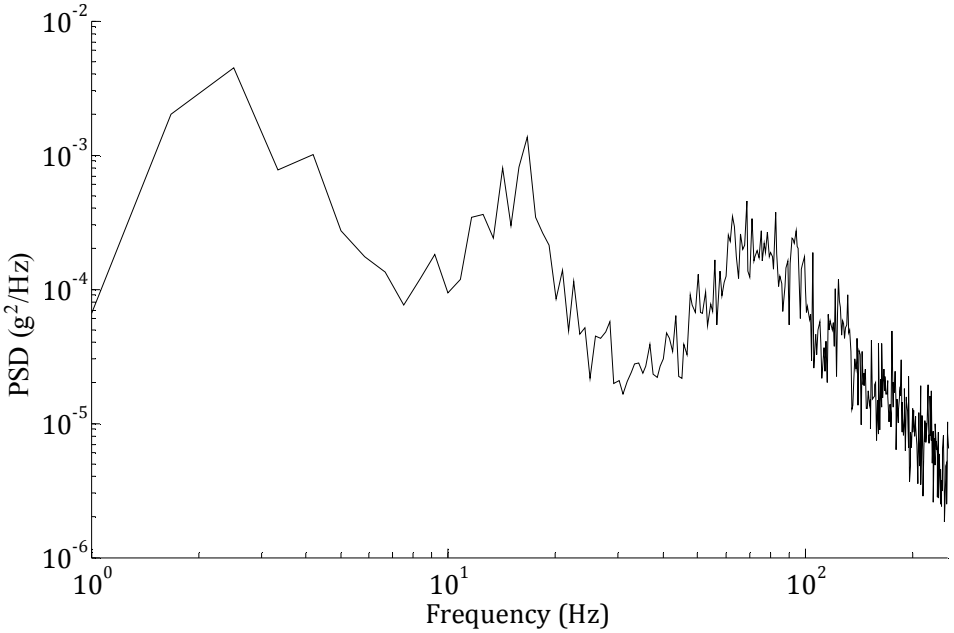

Figure 90: PSD calculated for the vibration signal

The RMS acceleration distribution of one second samples of the signal is given in Figure 91, the variation in the RMS acceleration distribution indicates that the signal is non-stationary.

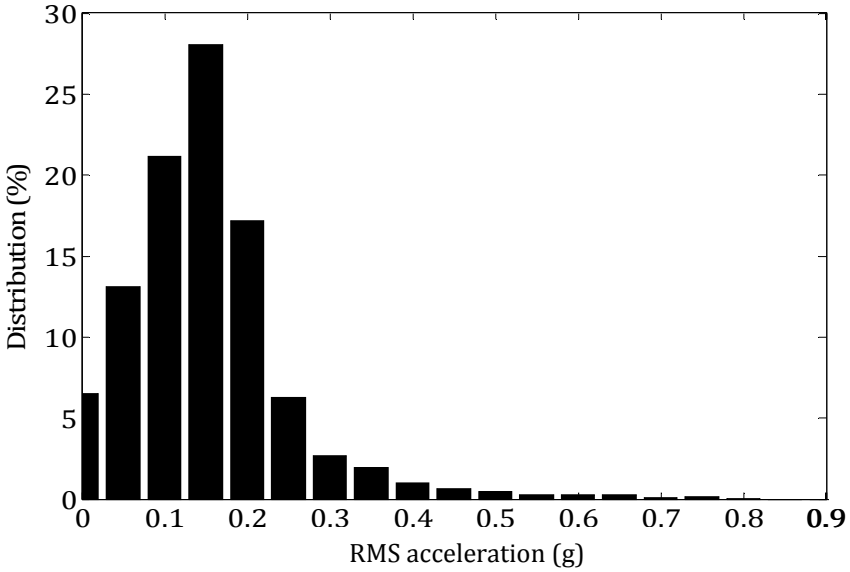

Figure 91: RMS acceleration distribution

Step 2 - ***Constructing a Gaussian equivalent signal:*** By taking the signal's PSD (Figure 90) and applying a random phase array, a Gaussian signal with the equivalent power content of the original signal is constructed (Figure 92).

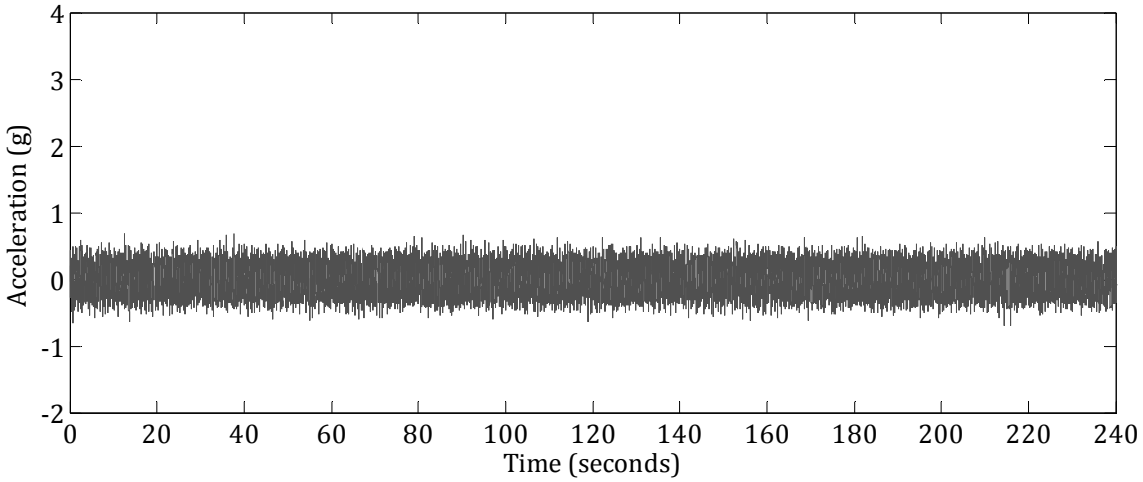

Figure 92: Simulated Gaussian signal

Step 3 - ***Perform wavelet analysis on vibration signals:*** The Morlet mother function is used to carry out wavelet analysis. A scalogram indicating the variation in the vibration signal's wavelet coefficients is given in Figure 93. The wavelet coefficients for the Gaussian signal are also calculated.

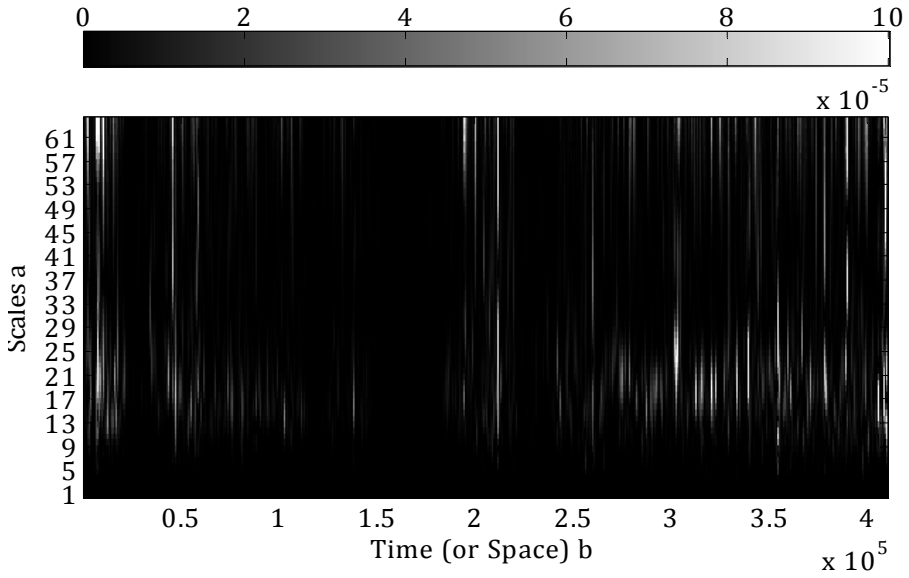

Figure 93: Wavelet analysis of vehicle vibration signal

Step 4 - ***Create Gaussian envelope:*** By finding the maximum and minimum wavelet coefficients for each scale (a) a filter can be created. This filter of the maximum and minimum Gaussian signal coefficients is shown in Figure 94.

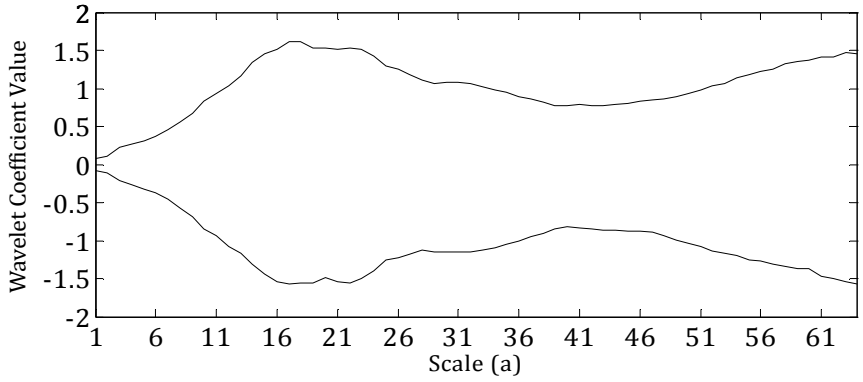

Figure 94: Limiting Gaussian envelope to identify outliers

Step 5 - ***Compare vibration signal's wavelet coefficients with the Gaussian envelope:*** The envelope containing the maximum and minimum Gaussian signal wavelet coefficients are compared with the vibration signal's wavelet coefficients. Coefficients that exceed the envelope are identified as points in Figure 95.

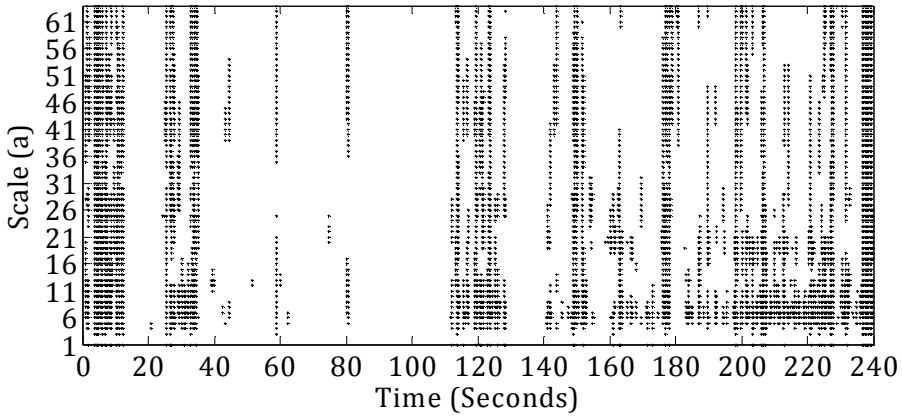

Figure 95: Outliers identified using the Gaussian envelope

Step 6 – ***Remove non-Gaussian segments from the vibration signal:*** Segments of the signal surrounding the position (*b*) of the outlying coeffient are extracted. Here a segment length of one second has been used to allow for accurate frequency content calculations down to 1 Hz. Figure 96 indicates the segments of the vibration signal extracted to form the non-Gaussian part, with the remaining parts forming the Gaussian approximation.

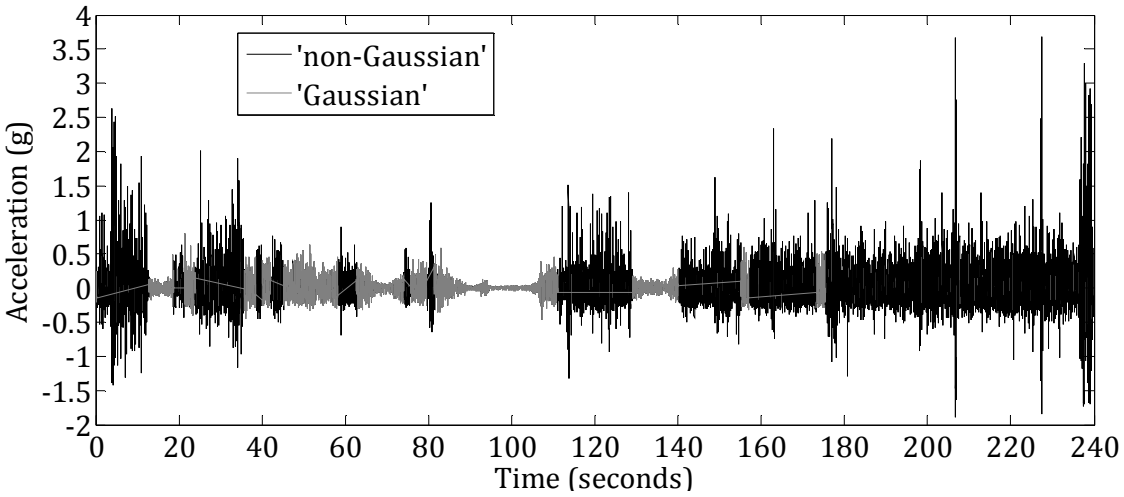

Figure 96: 'Gaussian' and 'non-Gaussian' segments of the signal

Step 7 - ***Evaluate the non-Gaussian signal part:*** The kurtosis of the Gaussian approximation is 6.5. In this example a limiting value of k = 4 has been set. Because the kurtosis exceeds this, the iteration process *Steps 1-6* are repeated with the non-Gaussian part being used as the vibration signal.

The process is repeated until all the data fits within a Gaussian approximation or a limiting number of iterations is reached. For this example, M = 3.

Step 8 - ***Evaluate the Gaussian approximations:*** The original vibration signal has therefore been decomposed into four Gaussian approximations, during the first level of iteration. The duration, overall RMS acceleration and kurtosis for each part is given in Table 21.

Table 21: Statistics for each Gaussian approximation produced during the first level of iteration

ITERATION NUMBER	DURATION (Seconds)	RMS ACCELERATION (g)	KURTOSIS, *k*
1	86	0.082	6.5
2	45	0.154	4.6
3	20	0.166	4.2
4	89	0.251	12.5

While the values of kurtosis for segments 2 and 3 are relatively close to that for a Gaussian distribution (kurtosis of 3), the kurtosis of segments 1 and 4 are not. In

particular, segment 4 has a much higher kurtosis of 12.5. The reasoning for this is that segment 4 (the fourth Gaussian approximation) is actually formed from the final non-Gaussian part, from the first level of iterations. It therefore contains all of the shock events from within the original signal and their surrounding vibration, which did not fit within a Gaussian approximation. If the original signal contains high level shock events, the wavelet decomposition method will always result in one final Gaussian approximation that is highly non-Gaussian, this is a limitation of the method and is discussed further in section 8.4.

The PSD of each part is given in Figure 97. The variation in spectral shape between the four segments is noticeable, particularly in the shape of the second spectral peak at around 15 Hz.

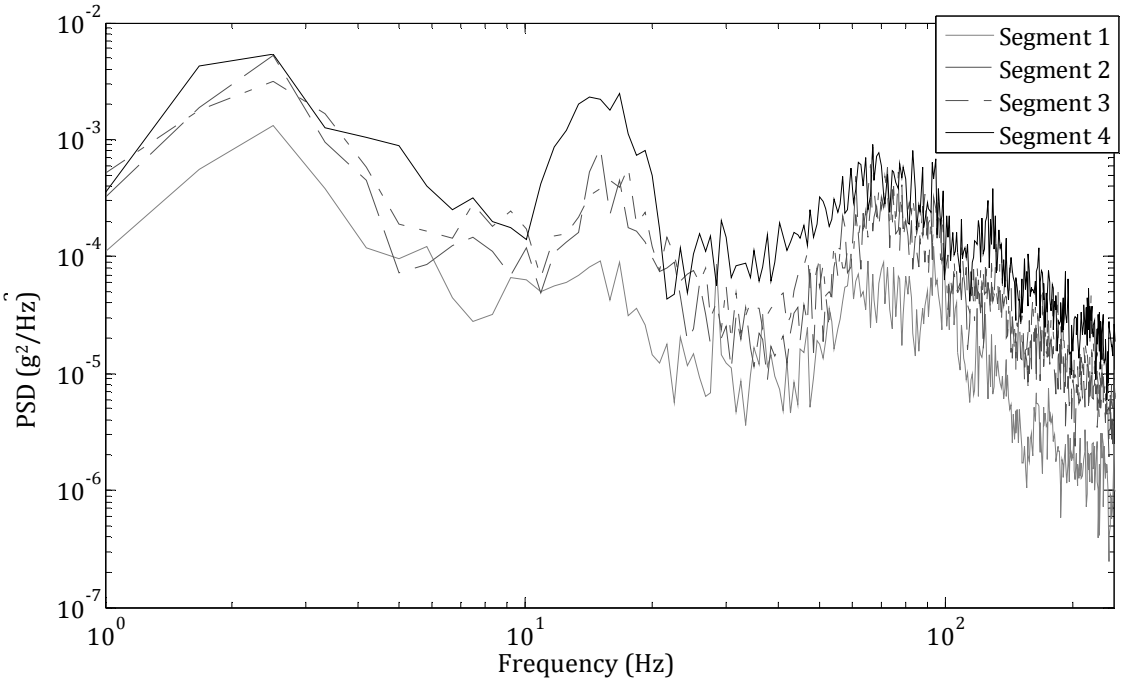

Figure 97: Average PSD of the 'Gaussian' segment for each iteration (level 1)

Because the kurtosis of each Gaussian approximation exceeds the liming value of 4, each segment is subjected to a second level of iteration to decompose it into smaller parts with distributions closer to Gaussian.

Steps 1-7 are repeated for a specified number of iterations (S = 2) or, until the non-Gaussian part is approximately Gaussian ($k < 4$).

For this simulation, two iterations are made during the second level of decomposition because of the reduced data set being used (four minute duration). Carrying out further iterations would create undesirable small duration data segments, which would present a problem due to the limitations of laboratory controllers for simulating vibration for such short durations.

The second level of iteration resulted in eight Gaussian segments. The duration, RMS acceleration and kurtosis relating to the vibration segments are given in Table 22. As with the first level of iteration, whilst the majority of segments have a kurtosis relatively close to the Gaussian value of 3, the final segment (8) has a much higher kurtosis. This is again due to the final segment containing all of the shock events from within the original signal and is a limitation of the wavelet decomposition method. This is discussed further in Section 8.4

Table 22: Statistics for each Gaussian part from second level of iteration

PART NO	1ST LEVEL ITERATION (m)	2ND LEVEL ITERATION (*s*)	DURATION (Seconds)	RMS ACCELERATION (g)	KURTOSIS (*k*)
1	1	1	41	0.037	5.2
2	2	2	5	0.113	3.7
3	3	1	40	0.108	4.2
4	4	2	5	0.130	4.0
5	1	1	39	0.156	4.6
6	2	2	20	0.166	4.2
7	3	1	9	0.164	5.6
8	4	2	81	0.259	12.2

Step 9 - ***Convert each segment into PSD and RMS acceleration value****:* In order to create a simulation, the PSD for each segment has been calculated.

Step 10 - ***Create a simulation signal:*** To create a simulation signal, each segment's PSD is applied in a random order and an equivalent signal is created. The resulting simulation signal is shown in Figure 98. Overall, this is both non-Gaussian and non-stationary.

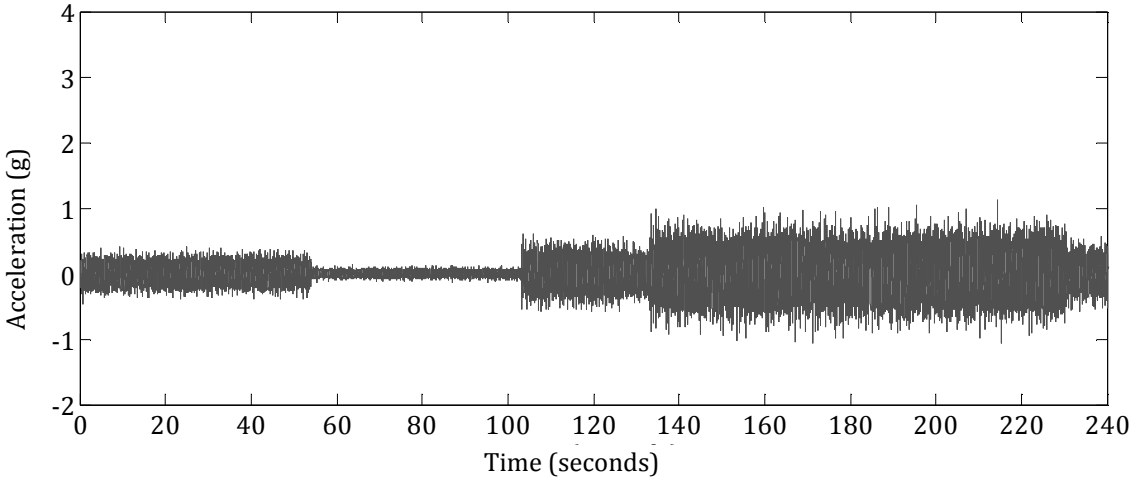

Figure 98: Wavelet decomposition method - simulation signal

8.3 Evaluation of the Wavelet Decomposition Method

By applying the wavelet decomposition method to a non-Gaussian and non-Stationary vibration signal, it is possible to decompose the signal and represent it as a series of stationary Gaussian parts. To assess the appropriateness of the method, comparisons between the PSD, RMS acceleration distribution and acceleration distribution, of the original vibration signal (Figure 89) and the simulation signal (Figure 98) are given in Figure 99, Figure 100 and Figure 101, respectively.

From these results, it can be deduced that the power distribution of the simulated signal shows good correlation with the power distribution of the original signal. The RMS acceleration distribution of the simulated signal correlated well with the original signal in the range 0 - 0.3g. But above 0.3g it did not recreate the distribution. By increasing the number of iterations made during the second level of decomposition, and/or reducing segment size, a more accurate representation of the RMS acceleration distribution could be gained. By carrying out relatively low resolution decomposition (i.e. a low number of iterations) there will still be an aspect of signal averaging and therefore the method will produce a slightly moderated simulation. Following the second level of iteration this stage the kurtosis of most segments was approximately 4, but for others (such as segment 8)

the kurtosis was much higher. These segments could therefore benefit from further analysis. In this example, a limit to the number of segments was imposed so as to avoid skewing the results of the process by creating too small a segment size for accurate frequency analysis.

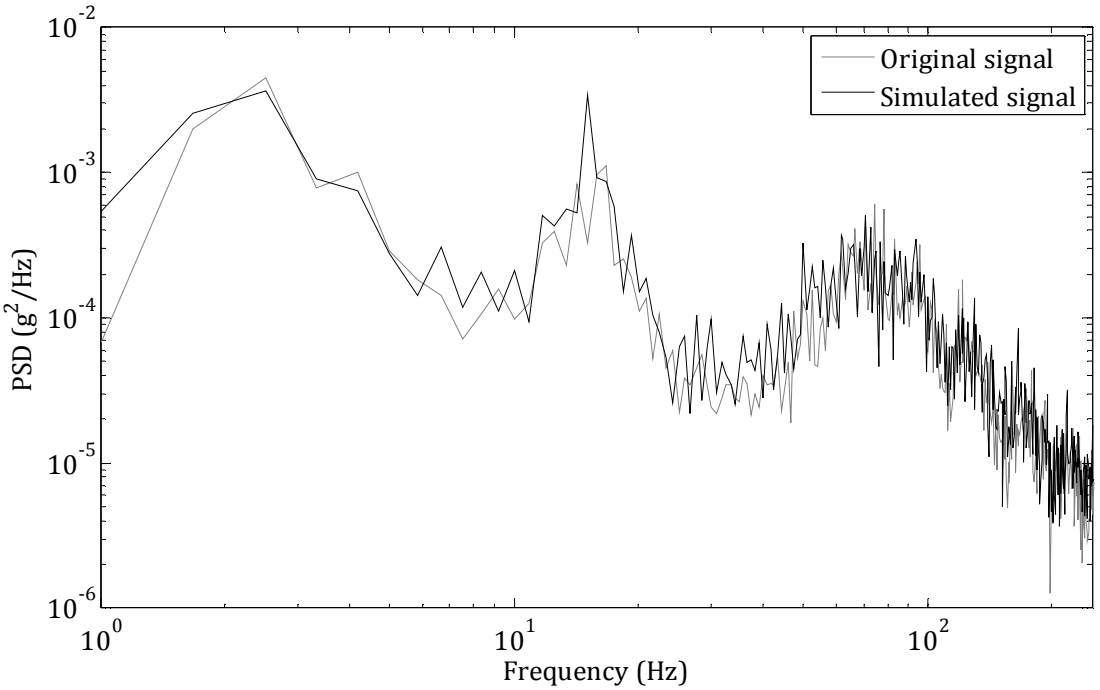

Figure 99: Average PSD comparison of original vibration signal and simulation signal

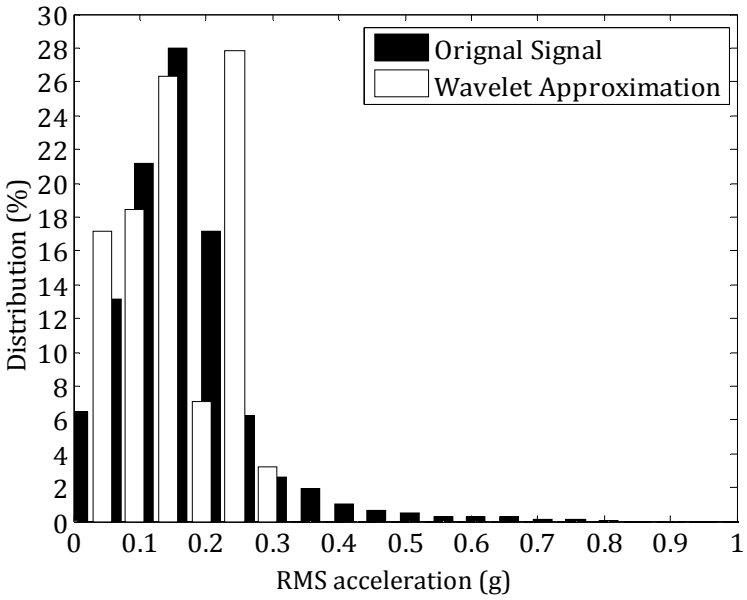

Figure 100: RMS acceleration level distribution comparison of original and simulation signal

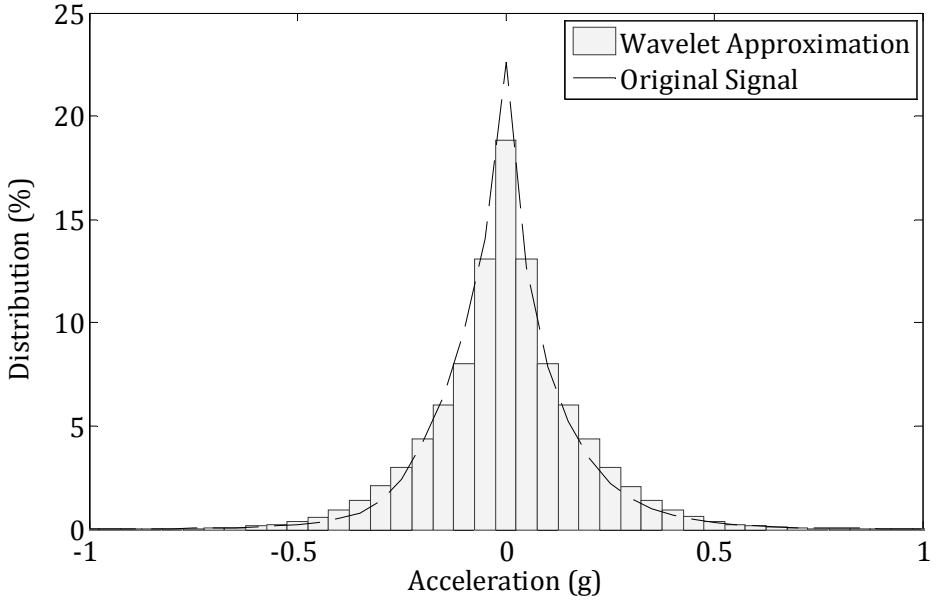

Figure 101: Acceleration level distribution comparison of original and simulation signal

8.4 Benefits and Limitations of the Wavelet Decomposition Method

Being usable on existing controllers is a key requirement of any new simulation method. The wavelet decomposition method produces a simulation that recreates a vehicle vibration's non-stationary and non-Gaussian nature, in a manner that can be applied to existing controllers. The wavelet decomposition method represents a signal as a series of PSDs of varying duration. These PSDs can be applied at random on any existing simulation table controller, to create a series of random vibration segments, which together build a non-stationary and non-Gaussian representation of the original signal.

The series of Gaussian approximations, resulting from a signal's decomposition, are assumed to be stationary with a Gaussian distribution. Segment 4, from the first level of decomposition shown in Table 21, has a kurtosis of 12.5, this means that it has a non-Gaussian distribution. Additionally, the short duration, high acceleration shock events interspersing the vibration, make the segment non-stationary. Further iteration of this segment may result in several parts that have a distribution closer to Gaussian, but due to the nature of vehicle vibration the final

Gaussian approximation, which contains the discrete high level shock events, will always exist.

Whilst the nature of the vibration limits the accuracy of the Gaussian approximations, the segment size used in the decomposition of the signal also has an effect. To enable accurate frequency analysis of each Gaussian approximation, a minimum segment size used for decomposition needs to be enforced. For the purpose of analyzing vehicle vibration it is suggested that when decomposing a signal, the minimum size of any segment removed from the signal is one second. This then allows for frequency analysis from 1 Hz. This limit on the minimum segment size means that when analysing signals high amplitude shock events of sometimes millisecond duration, will be incorporated within a segment with much lower amplitude vibration. These segments will have highly non-Gaussian distributions, thereby strengthening the limitation that the wavelet decomposition method will always produce one Gaussian approximation that is highly non-Gaussian.

Although the aforementioned limitation exists, the wavelet decomposition method offers much improvement on the current established method, by allowing the non-stationary and non-Gaussian nature of actual vehicle vibration to be simulated.

Furthermore, due to the complexity of the wavelet decomposition method, a large memory capacity is required. This is particularly true for long duration distribution journeys where it may be more appropriate to divide a journey into parts for analysis. Limitations in computing capacity can limit the frequency resolution of the wavelet analysis, which is defined by the number of scales used. The fewer scales used, the low is the frequency resolution and therefore the less definition in the signal decomposition.

Although there are limitations to this method, the results of this study have shown that the wavelet decomposition method can be used to decompose a non-Gaussian, non-stationary vehicle vibration into stationary parts each with an approximately Gaussian distribution.

Furthermore, the use of PSDs in creating the simulation means that it is easily adaptable for test acceleration using the existing approach.

8.5 Evaluating the Wavelet Decomposition Method using Damage Correlation

Correlation studies are an important part of validating a simulation method, as they allow a method to be validated using real measured damage. Therefore, to evaluate the ability of the wavelet decomposition method for simulating vehicle vibration, a damage correlation study using the damage mechanism of scuffing has been carried out using the same time history presented in Figure 43, section 5. The damage produced using the wavelet decomposition method was then compared with the damage produced by other simulation approaches.

In order to further validate the method, an additional vibration time history of a more severe distribution journey is also evaluated. The damage produced using both vibration profiles shows good correlation between the wavelet decomposition method and the time history replication.

8.5.1 Methodology

Testing was carried out using the vehicle vibration signal defined in section 5. The vibration signal time history, RMS acceleration distribution and PSD are illustrated in Figure 43, Figure 45 and Figure 46, respectively.

Wavelet decomposition has been carried out in Matlab using the code provided in Appendix V. During the first level of decomposition the time history signal was decomposed into 12 parts, which were further decomposed in to a maximum of 3 parts. In total, the signal was decomposed into 21 parts. The RMS acceleration, kurtosis and duration of each part is presented in Table 23.

Table 23: RMS acceleration, kurtosis and duration of each signal segment

SEGMENT	KURTOSIS, *K*	RMS ACCELERATION (g)	DURATION (Seconds)
1	4.9	0.150	495
2	4.4	0.235	59
3	3.2	0.249	2
4	3.2	0.260	3
5	3.7	0.270	13
6	3.3	0.303	4
7	3.1	0.255	2
8	13.5	0.335	21
9	5.0	0.130	525
10	4.2	0.221	11
11	4.8	0.262	4
12	4.6	0.223	4
13	3.3	0.218	12
14	4.1	0.279	43
15	4.9	0.148	489
16	4.4	0.237	60
17	3.3	0.250	8
18	3.6	0.268	16
19	3.3	0.303	4
20	3.6	0.235	3
21	13.2	0.338	21

By randomly applying each the PSD of each segment, for the appropriate duration, the simulated signal shown in Figure 102 (b) was produced.

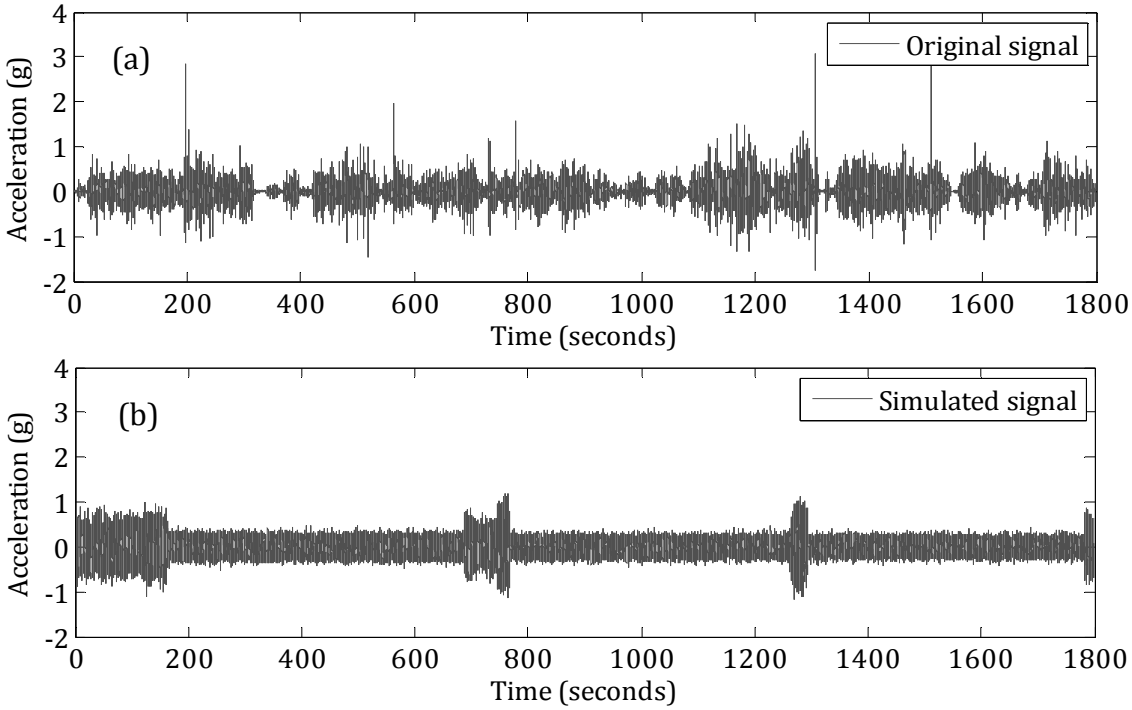

Figure 102: (a) Original vibration signal (b) Simulation signal using wavelet decomposition

The scuff rig defined in section 5.1 was used to evaluate the accuracy of the Wavelet decomposition method and to allow comparison with other simulation approaches.

Testing was carried out twice using two samples of smooth printed clay-coated board with sun 'blue 10' flexo graphic ink. The first sample, sample A, was from the batch produced during the testing carried out in section 5.5, therefore the scuff damage produced during test A can be compared with the results in section 5. The second sample, sample B, was produced using a slightly different consistency of sun 'blue 10' ink and cannot therefore be compared with previous results.

8.5.2 Evaluation of the Simulated Signal

Although the simulated signal does not fully resemble the original signal, it does replicate some of the variation in acceleration levels which are characteristic of vehicle vibration. A comparison of the overall kurtosis and RMS acceleration of the original signal and the simulated signal is given in Table 24. The error between the overall RMS acceleration is 0.002g, which is relatively small and would therefore

suggest good correlation between the overall amplitude of the two signals. The simulated signal has a kurtosis of 5.6, which signifies a non-Gaussian distribution. The kurtosis of the original signal is 7.4. The variation between the two is due to averaging in the wavelet decomposition method.

Table 24: Kurtosis and RMS acceleration of the original and the simulated signal

SIGNAL	KURTOSIS, *k*	RMS ACCELERATION (g)
Original	7.4	0.158
Simulated	5.6	0.156

The PSD of the original signal and the simulated signal is given in Figure 103.

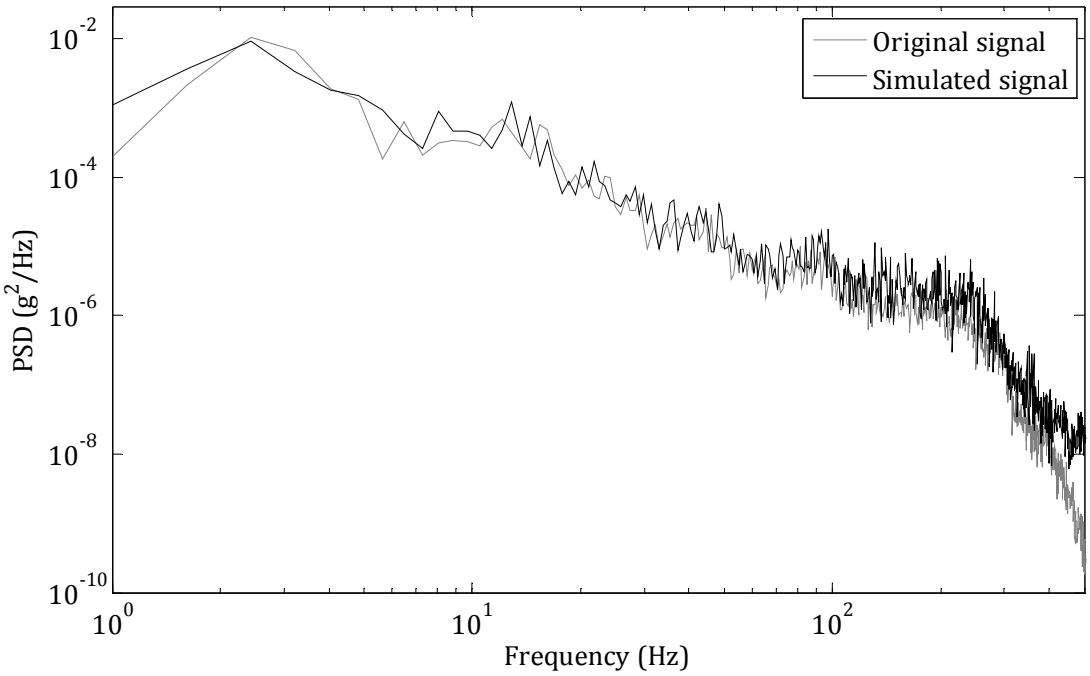

Figure 103: PSDs for original time history signal and simulated signal using wavelet decomposition

The shape of the simulated signal's PSD correlates with the original vibration signal's PSD, with only a small amount of error between the two, this error is presented in Figure 104. Only the frequency range 1 - 30 Hz is shown as the error in frequencies above this is comparatively low. The error in the PSD is greatest in the low frequency range (1 – 10 Hz), this is because the power within the low frequency range is much greater than that at higher frequencies. Therefore as a

percentage, the error within the low frequency range is much smaller than that at higher frequencies.

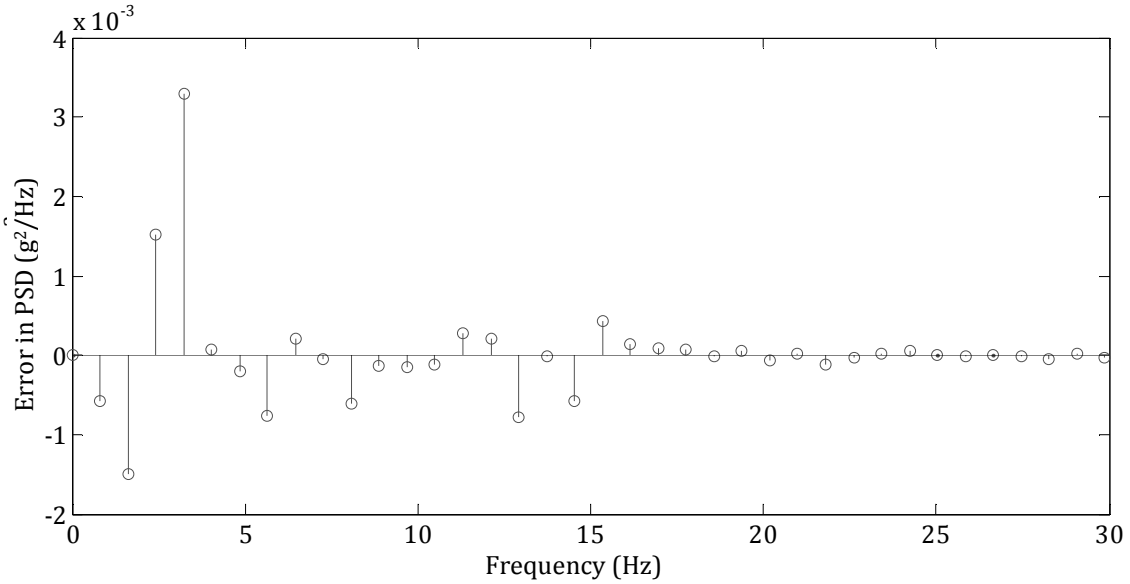

Figure 104: Error in simulated signal's PSD by comparison to original vibration signal's PSD

The RMS acceleration distribution for one second samples of both the original signal and the simulated signal are given in Figure 105.

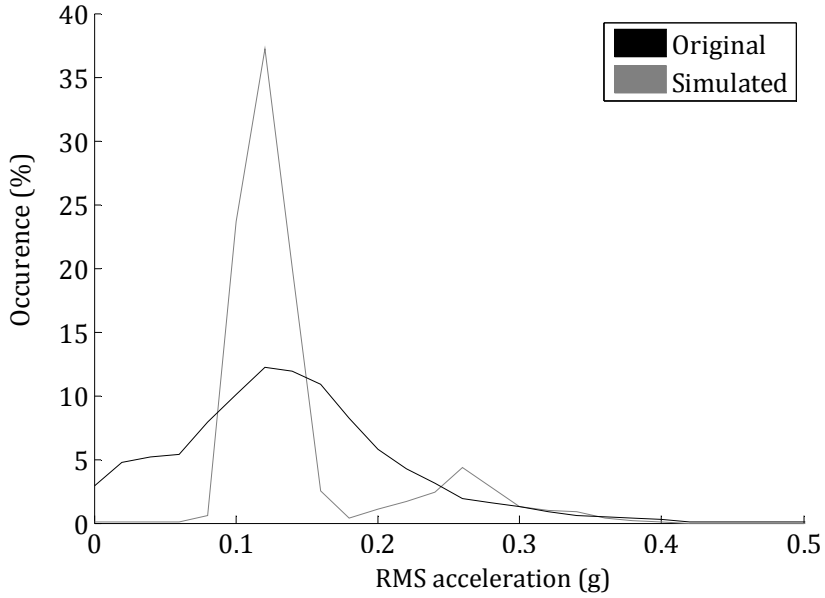

Figure 105: RMS acceleration distribution for original time history signal and simulated signal using wavelet decomposition

The RMS acceleration distributions shown in Figure 105, indicate that the RMS acceleration of both signals varies significantly, illustrating the non-stationary nature of both signals. The simulated signal has a prominent peak at around 0.1g with zero distribution below 0.08g. Both, the concentration around 0.1g and, the lack of lower RMS acceleration levels, is a result of averaging during simulation, which removes the extreme high and low events.

Segment 1 from Table 23 is shown in Figure 106. It has duration of 495 s, an RMS acceleration of 0.150g and kurtosis of 5.

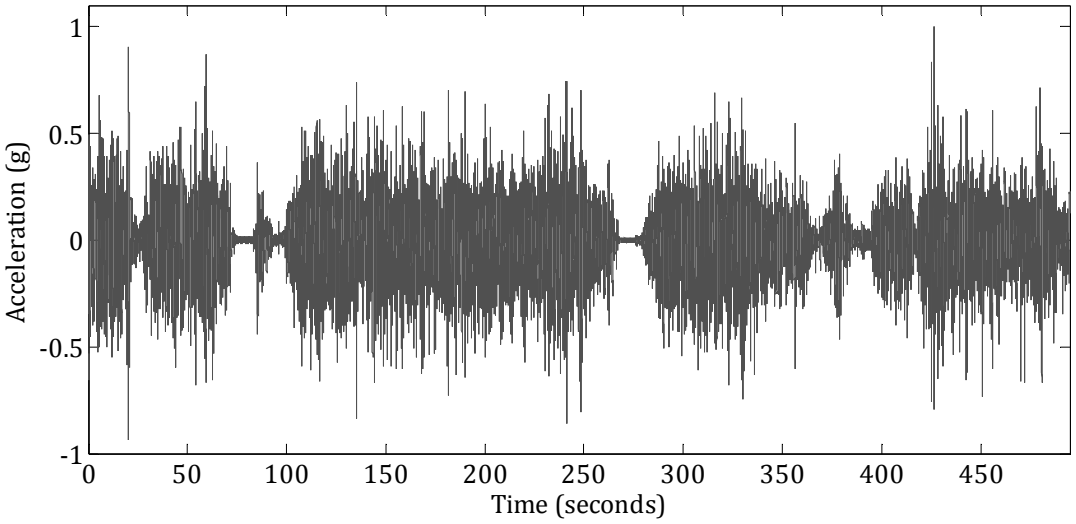

Figure 106: Segment one from wavelet decomposition method

Using the segment in Figure 106 as an example, it is clear, visually, that the segment is non-stationary due to its continually varying acceleration. The presences of high acceleration shock events and a kurtosis of 5 further indicate that this segment has a non-Gaussian distribution. Decomposition of this segment by a further level of iteration would enable the segment to be decomposed into smaller more Gaussian and stationary segments. It is thought that doing this would create an RMS acceleration distribution that is less concentrated resulting in a more representative spread distribution, though it has not been proven.

8.5.3 Results

The percentage of scuff damage produced from a time replication simulation and wavelet decomposition method is shown for Test A in Table 25, and, for Test B in Table 26.

Table 25: Test A percentage scuff damage using time replication and wavelet decomposition

TEST (A)	SIMULATION APPROACH	PERCENTAGE SCUFFING	INCLUSION OF 5% ERROR		VARIATION FROM TIME REPLICATION
			MAX	MIN	
1	Time Replication	0.60%	0.63%	0.57%	-
2	Wavelet Decomposition Method	0.56%	0.59%	0.53%	-7%

Table 26: Test B percentage scuff damage using time replication and wavelet decomposition

TEST (B)	SIMULATION APPROACH	PERCENTAGE SCUFFING	INCLUSION OF 5% ERROR		VARIATION FROM TIME REPLICATION
			MAX	MIN	
1	Time Replication	0.71%	0.75%	0.67%	-
2	Wavelet Decomposition Method	0.80%	0.84%	0.76%	13%

8.5.4 Comparison of Results Using other Simulation Methods

The resulting level of scuff damage, using sample A, is presented in Figure 107 with the results from the previous correlation study.

The results show good correlation between the first and second time replication simulation with, 0.59% and 0.60% scuff damage, respectively. The level of scuff damage produced using the wavelet decomposition method correlates well with both time replication tests with the error in the level of scuff damage being 5% and 7%, respectively.

When compared with the other simulation approaches, the wavelet decomposition method shows the highest correlation with the modulated RMS approach.

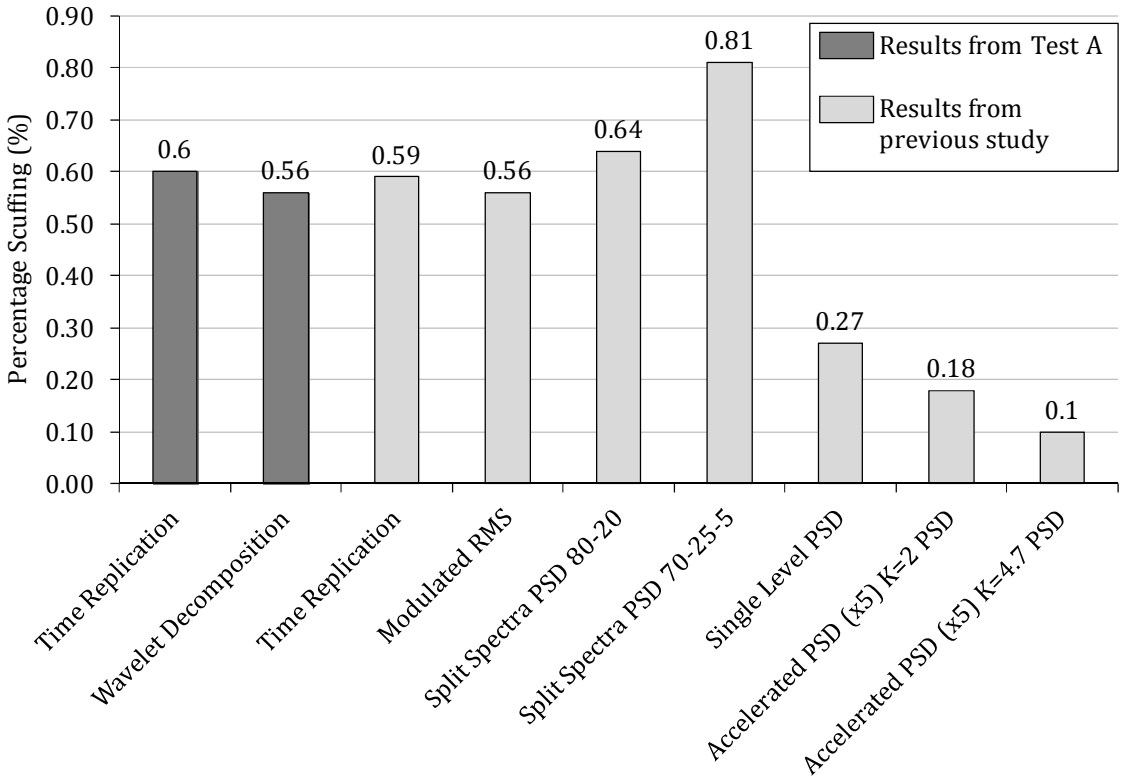

Figure 107: Percentage level of scuff damage for different simulation approaches

Overall, the samples used in Test B produced a higher level of scuff damage in both tests. This was due to the change in consistency of the ink used. When compared to Test A, Test B produced a slight over test of 13%.

In both tests, the wavelet decomposition method was shown to correlate well with vertical vibration time replication, with Test A producing a slight under test of 7%, and Test B producing a slight over test of 13%.

The level of damage produced from the wavelet decomposition method in Test A correlated well with the RMS modulation approach. However, the results in Test B correlated better with the accelerated PSD where the time was compressed by 5 and k = 2, producing over tests of 13% and 14%, respectively.

This variation in results could be due to test errors as it was shown by Shires et al (2010) that the scuff rig had a confidence limit of 95% with an error margin of 5%. This error is typically produced by the method of measuring the scuffing. This variation in the over and under test may therefore be due to test error. To evaluate

the method further, the Wavelet decomposition method has been used to simulate an additional journey. The results from this testing are now presented.

8.5.5 Simulating an Alternative Journey Using Wavelet Decomposition Method

To further validate the use of the wavelet decomposition method, additional analysis and experimentation has been carried out on an additional, more severe journey. The time history vehicle vibration is given in Figure 108. Using the wavelet decomposition method, a simulation signal was produced.

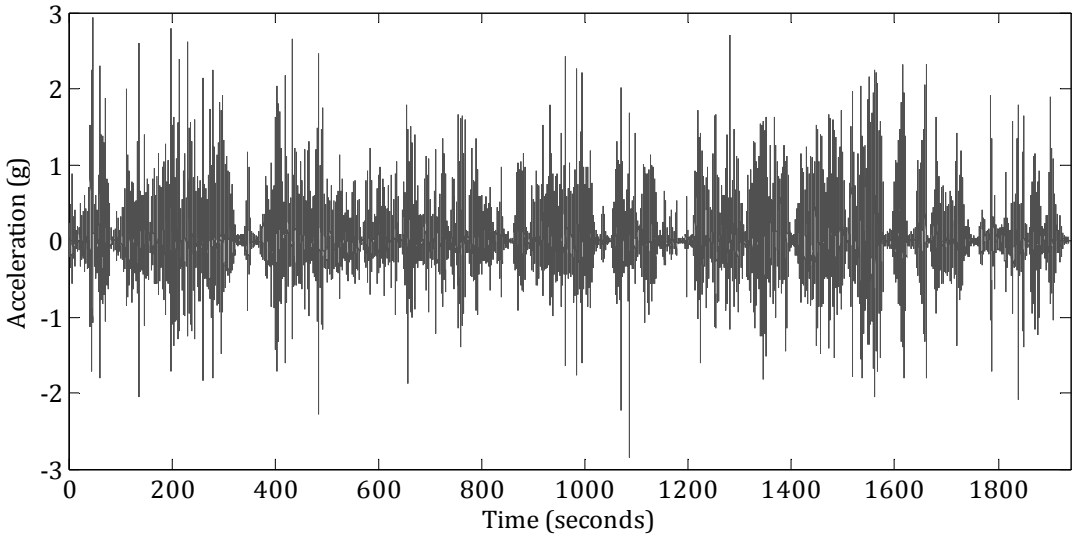

Figure 108: Time history vehicle vibration signal

8.5.6 Comparison of Results

The percentage scuff damage produced using the wavelet decomposition method and time replication of the time history, is shown in

Table 27. In Test C the wavelet decomposition method correlates well with the time replication with only 8% error in the level of scuff damage. Similar to Test B, the wavelet decomposition method produced an over test in comparison with the time replication simulation.

Table 27: Percentage scuff damage produced for the simulation methods

TEST (C)	SIMULATION APPROACH	PERCENTAGE SCUFFING	INCLUSION OF 5% ERROR		VARIATION FROM TIME REPLICATION
			MAX	MIN	
1	Time Replication	1.15%	1.21%	1.09%	-
2	Wavelet Decomposition Method	1.24%	1.30%	1.18%	8%

8.6 Concluding Remarks

Throughout this chapter the wavelet decomposition method has been explained in detail and the process of producing a simulation has been described. It has been shown, through theoretical evaluation, that by simulating the original signal as a series of Gaussian approximations of varying RMS acceleration and spectral content, the method manages to recreate part of the signal's non-stationarity and non-Gaussian distribution.

The wavelet decomposition method has been proven for both example time histories to correlate well with time replication simulation. In Test A the percentage error in damage correlated well with RMS modulation, in Tests B and C the percentage error correlated better with the single level PSD where the time was compressed by 5 and $k = 2$.

In two out of the three simulations the wavelet decomposition method produced a slight over test in comparison to the single axis time history replication.

When considering vehicle vibration, which is known to be highly non-stationary and non-Gaussian, being able to distinguish points within the signal which make it so, is beneficial within the analysis process. By making use of time-frequency analysis, the wavelet decomposition method is able to decompose a non-Gaussian and non-stationary signal into its approximately Gaussian and stationary parts. Shown here and within sections 8.2 and 8.3 is that the simulation produced through the random synthesis of these parts is, overall, non-stationary in both the

time (evident in the varying RMS acceleration distribution) and frequency domain (evident in the changing shape of the PSD) and, has a non-Gaussian distribution (evident in the measure of kurtosis). This allows a signal's characteristics in the time and frequency domain to be considered together, which is in contrast to the established method.

The example given in this study has shown how the wavelet decomposition method is used to create a simulation representative of actual vehicle vibration. However, the RMS acceleration distribution of the simulated signal deviated from that of the original signal. If the Gaussian approximations, produced during the second level of iteration, were decomposed further, it is possible that a simulated signal with an RMS acceleration distribution, matching better that of the original signal, could be formed, though this has not been proven.

Through theoretical work, the wavelet decomposition method's ability to replicate the statistical content of vehicle vibration has been examined and proven. In order to evaluate the method's appropriateness in recreating the extent of product damage during distribution, a correlation study measuring damage has been carried out and is now discussed.

9 APPROXIMATING VEHICLE VIBRATION AND ROAD ROUGHNESS USING COMPUTATIONAL VEHICLE MODELS

The use of a vehicle model to approximate a vehicle's vibration response to that of a given road profile in order to create a representative test for distribution packaging was first proposed by Rouillard (2008). In this chapter a simplified quarter vehicle model and a known road profile were used to calculate the vehicle's response. Doing so allows for variations in: the vehicle's payload; suspension; tyre stiffness; and, speed; to be accounted for when producing a simulation test.

Over the last two decades various vehicle models have been proposed which vary in detail and complexity, including quarter car, half car and full vehicle models (Rajamani, 2012; Pacejka, 2006). Vehicle models are constructed from an array of mass-spring-dampers placed in series and in parallel which model the vehicle's suspension and tyre systems. The complexity of these vehicle models varies depending on the accuracy and detail of the model and information required from it. Specialised computer programs exist for the simulation of vehicles, including: Adams©, which is a multi-body dynamic simulation program enabling the user to construct complex vehicle models for vehicle simulation and optimisation; Vehiclesim©, which is a programme that specialises in vehicle simulation; and, Mathworks Simulink©, which contains toolboxes from which the user can construct a vehicle model.

For the purpose of this work, the vehicle model is only required to simulate the vehicle movement and not to optimise the model, additionally the model must be compatible with Matlab programming. Therefore Simulink has been used to create vehicle models. Both the full vehicle and quarter vehicle models are now discussed.

9.1 Review of Vehicle Models

For the purpose of this research, both the full car model and quarter car model have been considered. The benefits and limitations of each are discussed, in order to provide reasoning behind the use of either for the purpose of generating a simulation regime for packaging distribution. An appropriate vehicle model has then been developed for the purpose of creating an improved simulation regime and also for the purpose of generating road roughness profiles from vehicle vibration data.

9.1.1 Full Vehicle Model

A full vehicle model is the most complete, allowing the user to approximate the full motion of the vehicle along all of its linear and rotational axes. The complexity of this model is dependent on the detail of the vehicle. For instance, in contrast to a car, which has a single body, a semi-trailer (where a coupling system connects the driver's cabin and trailers) has more degrees of freedom and constraints making it much more complex. This can be seen in the vehicle models shown in Cheng and Cebon (2008) and Miege and Cebon (2005).

For the purpose of this study, where the input to the vehicle model is the vertical displacement of the road profile, the lateral, longitudinal and yaw components of the vehicle cannot be considered. Therefore by using a full vehicle model to simulate the vehicle's vibration response, vibration in only the vertical, pitch and roll axes can be calculated to evaluate an MDOF response of the vehicle. In order to do this accurately, the road roughness must be provided for each point of vehicle contact with the road and must be in phase. Incorrect recording of the road profiles or timing of their application can lead to great errors in the calculation of the vehicle's pitch and roll.

As only the vertical vibration of the vehicle is considered in the established method and the wavelet decomposition method, only the vertical component of the vehicle model used is required.

For this purpose, the main benefit of the full vehicle model is that it allows the vibration response across the vehicle body to be calculated, thus enabling the consideration of load position and distribution on the vehicle floor. This in turn would allow for a vibration tests to be constructed suiting the position of the load within the vehicle.

The variability in parameters and movement in load and position is hard to predict and therefore, by using the full vehicle model, uncertainties in the vibration response can exist.

9.2 Quarter Vehicle Model

Rather than consider each wheel and suspension connection separately, the vehicle is represented as two mass-spring-damper systems with the average parameter values for the unsprung mass and suspension and tyre system, and, a quarter of the vehicle mass. The simplicity of the model means that the varied response across the vehicle cannot be calculated, only a vehicle average.

The quarter vehicle model is shown in Figure 109. It comprises of two mass-spring-damper systems in parallel, these correspond to the sprung mass (suspended vehicle), M_V, and unsprung mass (wheel system), M_T. Both of the masses are constrained to move only vertically, with displacements x_2, and x_1, respectively. The vertical input to the tyre from the road surface is x_0. The suspension stiffness and damping parameters are denoted by K_S and C_S, respectively, and the tyre stiffness and damping is denoted by K_T and C_T, respectively. By generating the equations of motion for the quarter vehicle model it is possible to estimate the vehicle's response to a given road input.

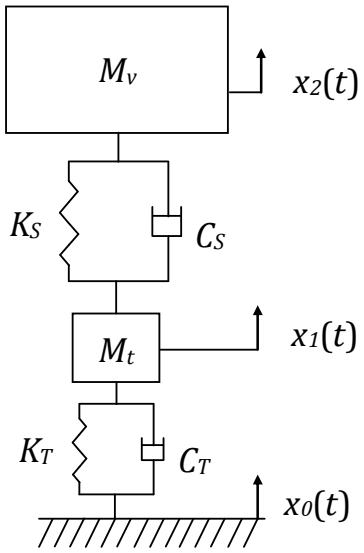

Figure 109: Quarter vehicle model

For the quarter vehicle model given in Figure 109 the equations of motion are derived as:

$$M_V \ddot{x}_2 + C_S(\dot{x}_2 - \dot{x}_1) + K_S(x_2 - x_1) = M_V g = F_1 \quad (36)$$

$$M_T \ddot{x}_1 + C_S(\dot{x}_1 - \dot{x}_2) + K_S(x_1 - x_2) + C_T(\dot{x}_1 - \dot{x}_0) + K_T(x_1 - x_0) = M_T g = F_2 \quad (37)$$

Incorporating a quarter vehicle model within a new test regime removes the need for in situ vibration data acquisition and therefore significantly reduces data collection times.

9.3 Simulink Quarter Vehicle Model

A quarter vehicle model has been constructed using a Simulink block diagram. The model and its subsystems are shown in Figure 110, Figure 111 and Figure 112. The input to the model is a vector of the road's vertical displacement at each sample time (*dt*). The output is then the vehicle's vertical acceleration of the sprung mass (*ddx*$_2$). Tyre damping (C_T) has not been included in the vehicle models.

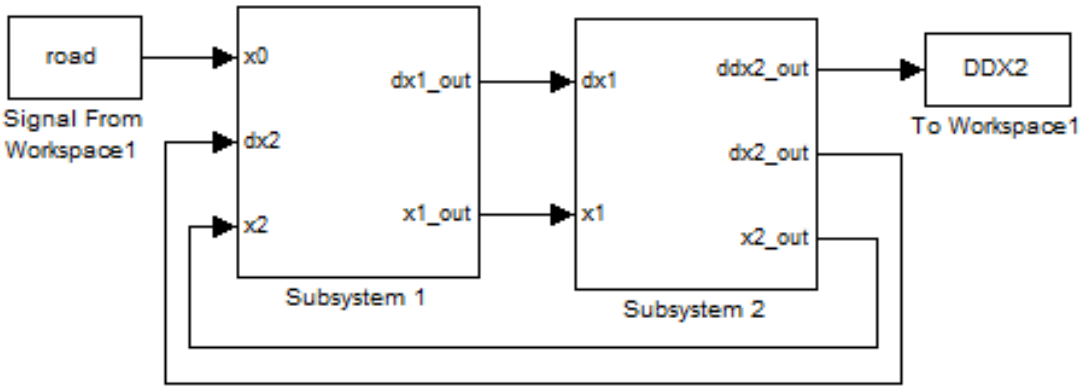

Figure 110: Simulink quarter vehicle model

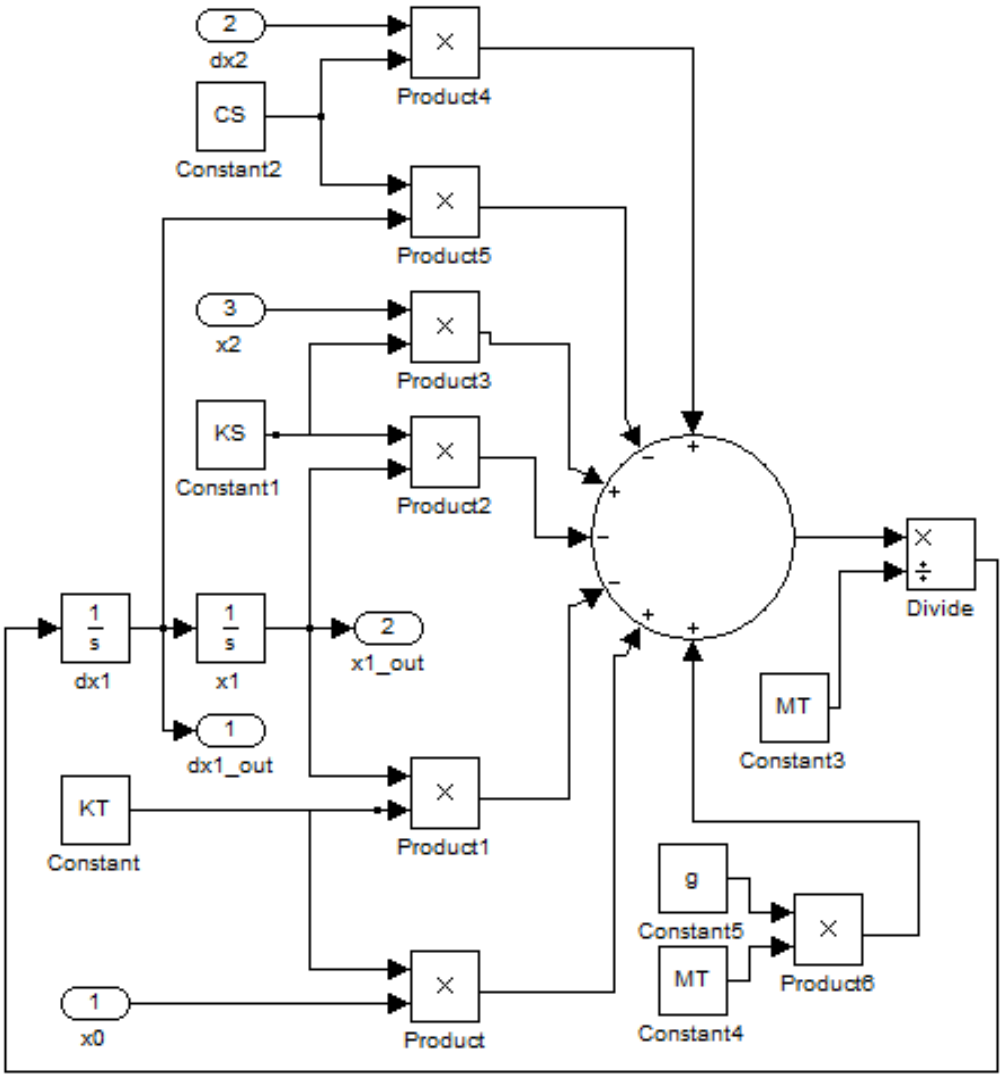

Figure 111: Simulink quarter vehicle model subsystem 1 from Figure 110

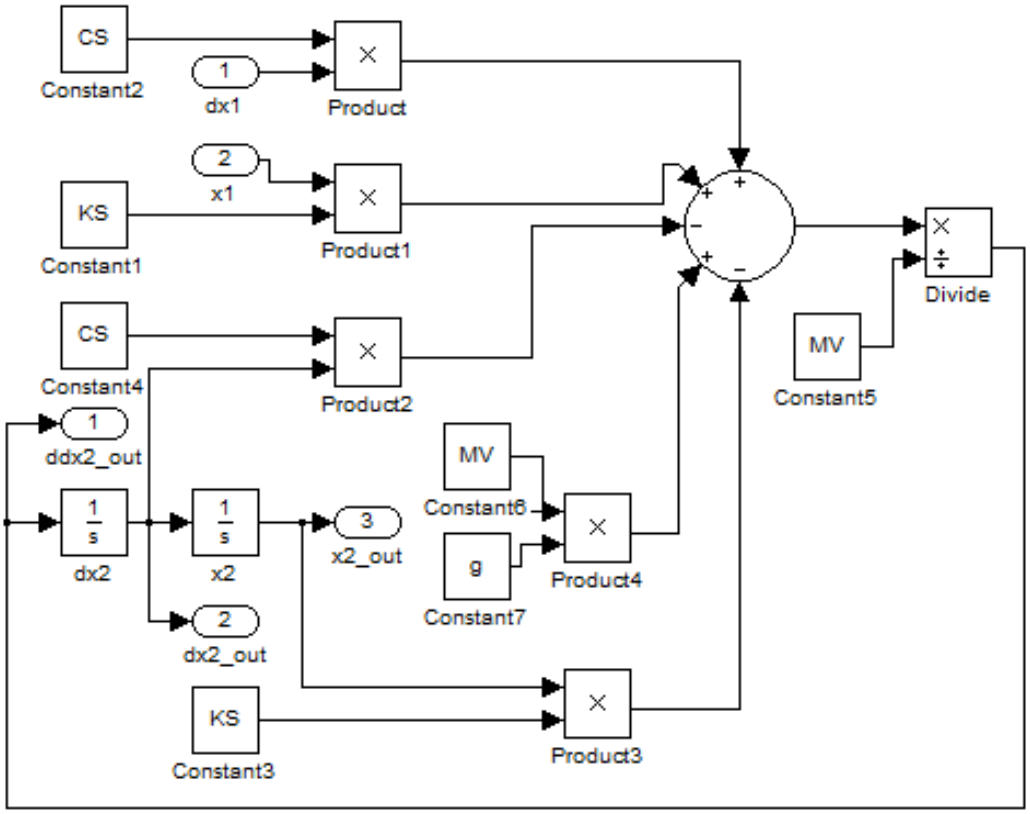

Figure 112: Simulink quarter vehicle model subsystem 2 from Figure 110

9.4 Using the Inverse Quarter Car Model to Approximate Road Profiles

In addition to approximating the vehicle response, the inverse of the vehicle model can be used to approximate a road profile from vehicle vibration. This can be done by inverting the vehicle's equations of motion making the relevant parameters the subject:

$$\frac{M_V \ddot{x}_2 + C_S \dot{x}_2 + K_S x_2 - K_S x_1 - M_V g}{C_S} = \dot{x}_1 \tag{38}$$

$$\frac{M_T \ddot{x}_1 + C_S(\dot{x}_1 - \dot{x}_2) + K_S(x_1 - x_2) + C_T \dot{x}_1 + K_T x_1 - C_T \dot{x}_0 - M_T g}{K_T} = x_0 \tag{39}$$

By using the inverse model, a vehicle vibration profile from a specific distribution route can be used to approximate the vibration profile of any other vehicle travelling along that distribution route. This allows for a change in distribution vehicle and/or payload to be accounted for without the need for additional in-situ data acquisition.

A Simulink model which solves Equations 38 and 39 has been created, to allow the calculation of an approximate road profile. The structure of the model and its subsystems is given in Figure 113, Figure 114 and Figure 115, respectively.

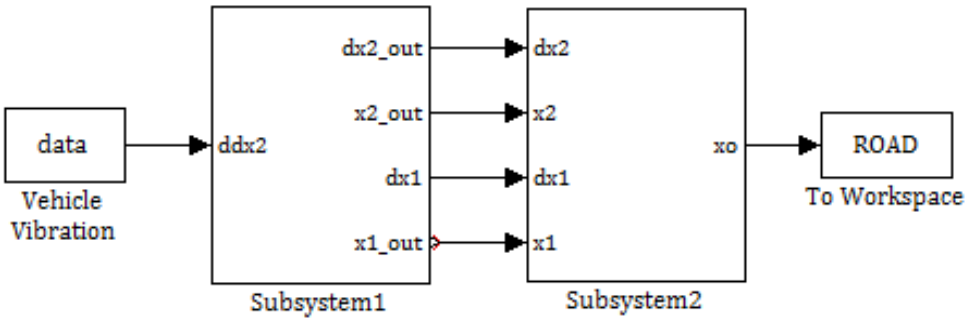

Figure 113: Simulink Inverse vehicle model

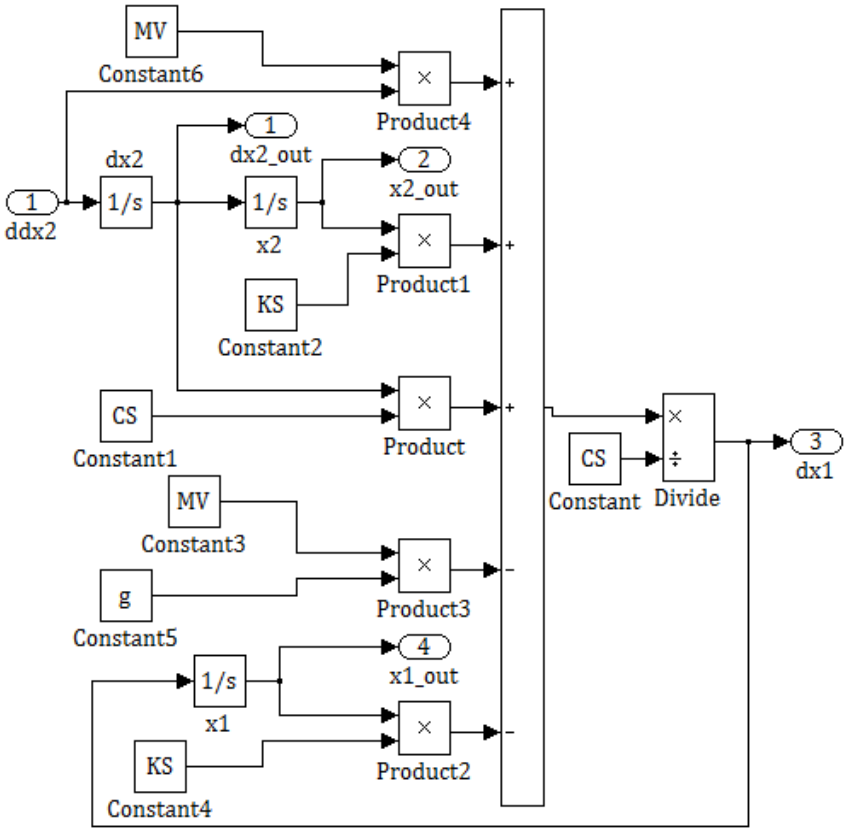

Figure 114: Simulink inverse quarter vehicle subsystem 1

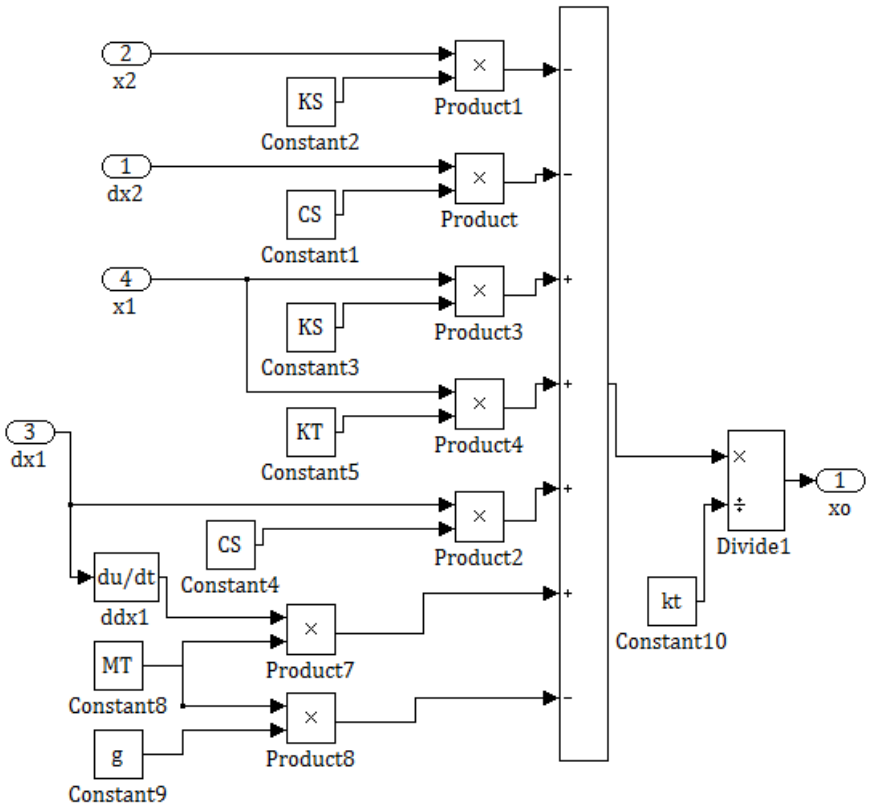

Figure 115: Simulink inverse quarter vehicle subsystem 2

When using the model the initial conditions for each of the parameters are set as zero, so that when time, $t = 0$:

$$x_2 = \frac{dx_2}{dt} = \frac{d(dx_2)}{dt^2} = 0 \qquad x_1 = \frac{dx_1}{dt} = \frac{d(dx_1)}{dt^2} = 0$$

$$x_0 = \frac{dx_0}{dt} = 0$$

These assumptions lead to errors in the resulting road profile approximation. This error dissipates with time. An example of the error induced by calculating a road profile from a given vehicle vibration (Figure 116) using the inverse vehicle model the approximate road profile is calculated (Figure 117), the quarter vehicle model is then used to calculate the approximate vehicle vibration (Figure 118). The error arising between the original vehicle vibration and the approximated vibration calculated using the vehicle model, is shown in Figure 119.

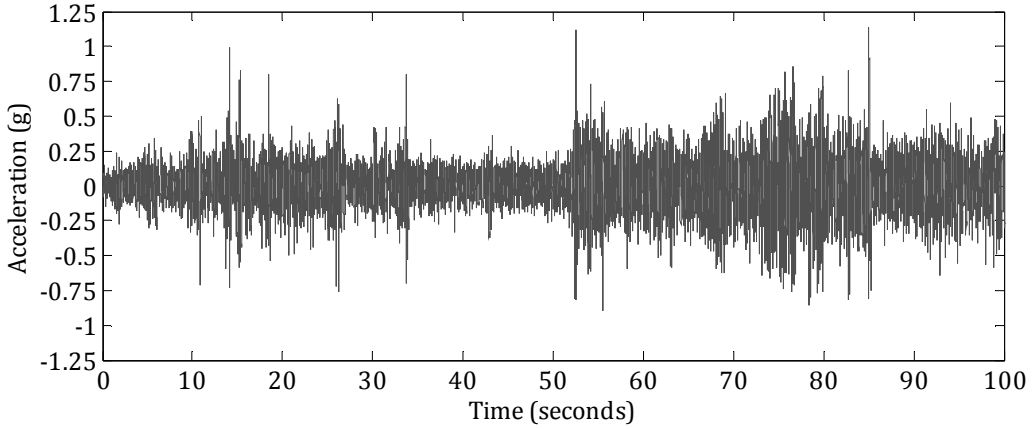

Figure 116: Example vehicle vibration

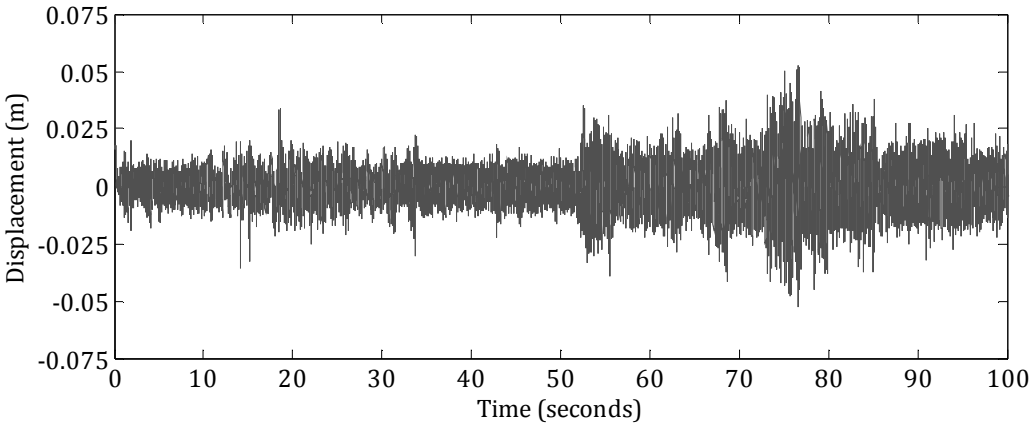

Figure 117: Approximate road profile calculated using the inverse quarter vehicle model

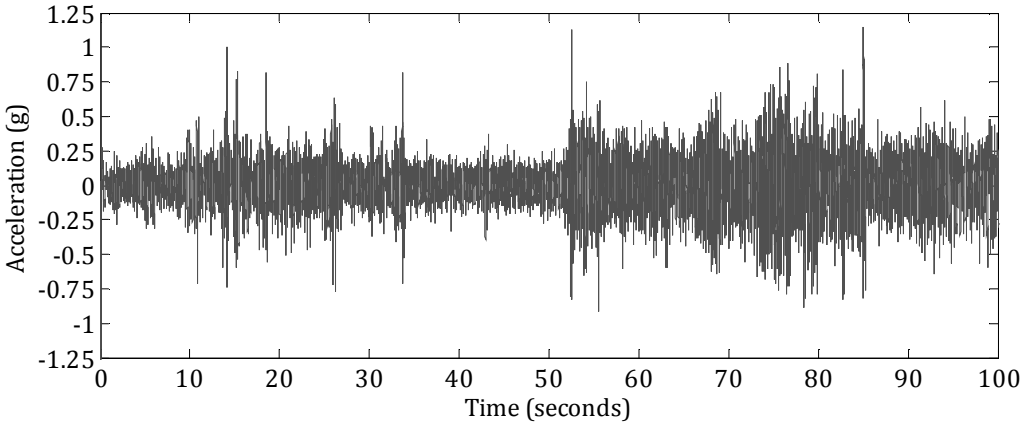

Figure 118: Approximate vehicle vibration calculated using the quarter vehicle model

In Figure 119 a large initial error is visible, this is caused by the approximation of the initial conditions leading to a significant over approximation causing an over shoot in the approximated vehicle's response, though this error dissipates, after which the error is insignificantly low.

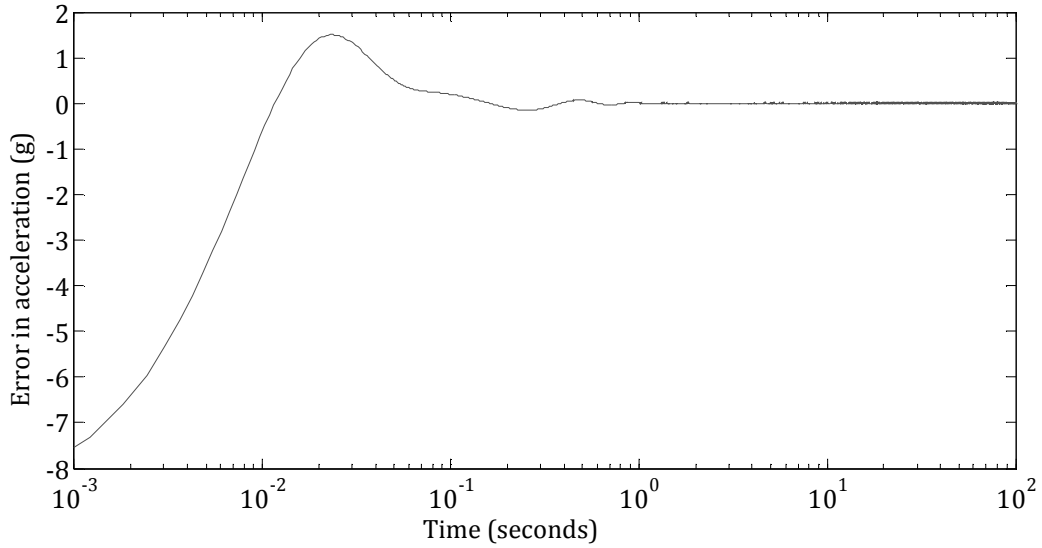

Figure 119: Amplitude of error in the calculated vehicle vibration for time history vibration in

The PSD for both the original vibration and that simulated by the quarter vehicle model, are given in Figure 120. The simulated vibration's PSD correlates well with the original signal's PSD.

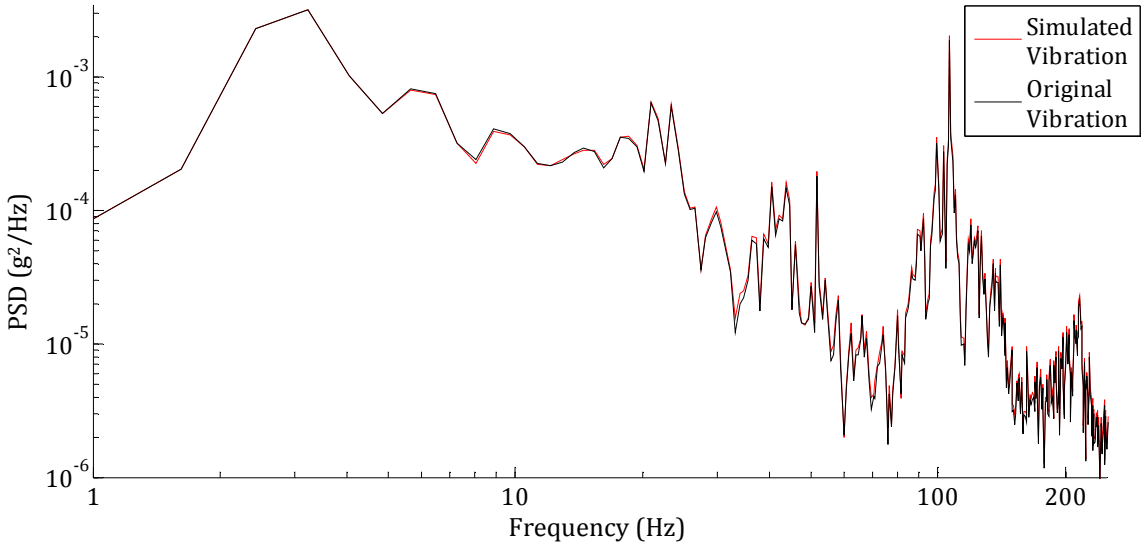

Figure 120: PSD of original vehicle vibration and vehicle vibration simulated through vehicle model

The error between the original and the simulated signals' PSDs is given Figure 121. The error in the low frequency range (1 -10 Hz) is extremely low. Above 30 Hz the error is significantly higher, with the highest error, of approximately 35%, at approximately 74 Hz.

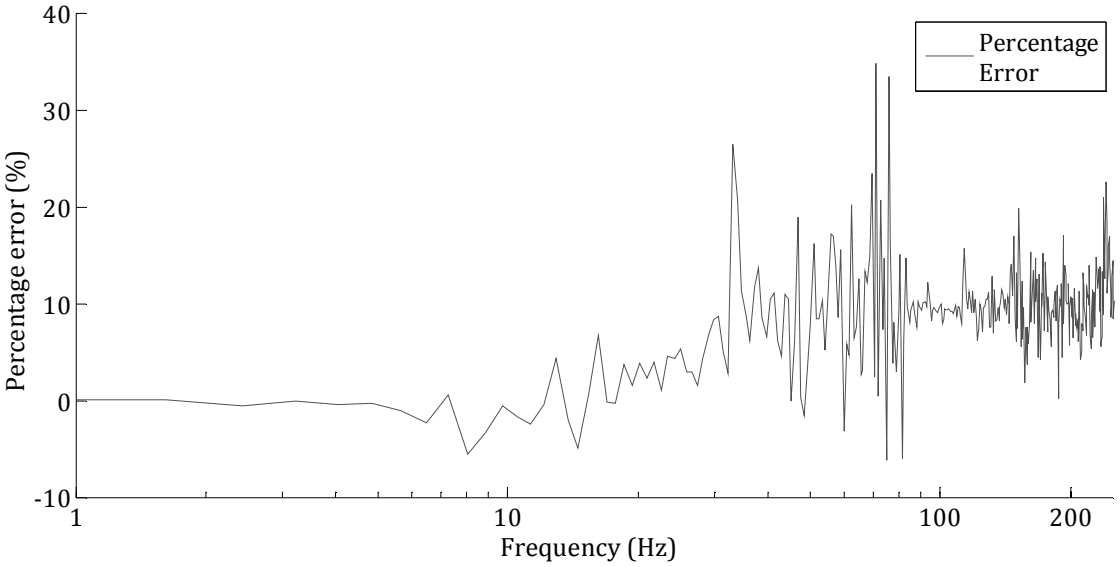

Figure 121: Percentage error between original signal's PSD and simulated signal's PSD

The simulated signal showed good correlation with the original signal. The model is therefore suitable for use in the journey database. Though consideration of the initial error should be given and this part of the signal removed before further analysis.

9.5 Quarter Vehicle Model Benefits and Limitations

Although basic, the quarter vehicle model has a number of benefits. Firstly, unlike the full vehicle model, where several road profile inputs are required, the quarter vehicle model only requires one. This not only simplifies the process of road profile data collection but also reduces the computational power required to calculate the vehicle motion. Secondly, by only having one output, the memory requirement is significantly reduced compared with that of the full vehicle model. Thirdly, fewer vehicle parameters are required and, by using the average of the vehicle parameters, the significance of possible errors in the calculation of individual vehicle parameters is reduced.

Whilst there are benefits to using a quarter vehicle model, there are also several limitations that must be considered. The simplicity of the quarter vehicle model requires the following assumptions to be made:

• *Vehicle parameters are deterministic* - In reality vehicle parameters can vary due to: manufacture tolerances; vehicle age; vehicle condition; the distribution payload; and, the varied and complex interaction of the vehicle with the road surface. For instance, spring stiffness and damping can differ from the manufacturer's value as a result of wear or production tolerances. Additionally, it is now common for suspension characteristics on vehicles to be designed specifically for the product they are carrying, resulting in parameters varying between vehicles.

In the quarter vehicle model, the tyre's contact with the road surface is modelled as a point which is in continual contact with the road surface. In reality the way in which the tyres interact with the road is much more complex. The constant change in contact area and surface pressure, along with uncertainties in the static pressure and extend of the wear of tyres, can lead to stochastic variations in the tyre stiffness that are difficult, if not impossible, to predict.

Vehicle mass can also vary significantly due to loading and unloading of products. Additionally, the placement of products in the vehicle for distribution can lead to variations in vehicle response across the vehicle floor. By using a quarter vehicle model these variations are either difficult or impossible to consider.

• *The vehicle is symmetrical* – Because the quarter vehicle model uses parameter averages, a uniform load is assumed throughout the vehicle. It is rarely the case that the vehicle's centre of gravity will fall directly in the centre of the vehicle and, the suspension system have the same characteristics left to right and front to back. Therefore, in reality, the vehicle's response varies across the vehicle floor, with the vibration at the rear on the kerb side of the vehicle typically being the most severe.

• *Limited to low frequency range estimation* - The quarter vehicle model allows the calculation of the first and second natural frequencies, arising from the suspension and wheel system, respectively. The third natural frequency, caused

by the structural floor/body of the vehicle, cannot be simulated through a quarter vehicle model. In order to evaluate this third natural frequency a more complex model would be required, for which further vehicle parameters pertaining to the vehicle's construction would be required. Typically, this frequency falls within the range 50 – 60 Hz, with a much smaller modal participation factor than the first two frequencies. It is therefore considered to have little effect on product damage. The repercussions of this are evident when a vehicle's vibration response during a specific distribution journey is used to approximate another vehicle's response on that same journey. The low frequency content of the approximated vehicle response will reflect that of the simulated vehicle, whilst the high frequency content will not be considered and therefore will reflect that of the original vehicle. The significance of this depends on the frequency response of the packaged product being evaluated.

9.6 Sensitivity Analysis of the Quarter Vehicle Model

In order to be able to simulate a vehicle's vibration response to different road inputs, the vehicle's parameters are required. As stated earlier, the assumption that the parameters are deterministic is not correct. Therefore, it is likely that errors will arise in the simulated vehicle response due to the incorrect selection of vehicle parameters. In some cases the use of incorrect parameters has little or no effect on the vehicle response, but, in other cases these errors can be large and may significantly alter the simulated response. It is therefore necessary to assess the effect that errors in parameters have on the estimated response. For the purpose of this study the Ford Luton Box van from a previous study is used as an example vehicle, with the correct vehicle parameters assumed to be those shown in Table 28.

Table 28: Ford Luton box van parameters

	PARAMETER	VALUE
M_V	Vehicle Mass	600 kg
M_T	Unsprung Mass	50 kg
K_S	Suspension Stiffness	95 kN/m
C_S	Suspension Damping	250 Ns/m
K_T	Tyre Stiffness	285 kN/m
C_T	Tyre Damping	60 Ns/m

Two measures can be used to evaluate the magnitude of the error: the vehicle's natural frequencies; and, the vehicle's transmissibility. The method of calculating both the natural frequencies and the transmissibility is now detailed.

9.6.1 Calculating a Vehicle's Natural Frequencies

The vehicle's first two undamped natural frequencies, relating to the suspension and wheel systems, can be found from the Eigen values of the equations of motion (Equations 36 and 37).

Firstly, the free vibration of the system needs to be considered, where $F_1 = F_2 = 0$, and x_1 and x_2 are assumed to have the same frequency and expressed in the complex form:

$$x_1(t) = X_1 e^{i\omega t} \tag{40}$$

$$x_2(t) = X_2 e^{i\omega t} \tag{41}$$

Substituting Equations 40 and 41 into Equations 36 and 37 gives:

$$\left[-\omega^2 M_V X_1 + K_S (X_1 - X_2)\right] e^{i\omega t} = 0 \tag{42}$$

$$\left[-\omega^2 M_T X_2 + K_T X_2 + K_S (X_2 - X_1)\right] e^{i\omega t} = 0 \tag{43}$$

In matrix format, Equations 42 and 43, can be expressed as:

$$\begin{bmatrix} \left(-\omega^2 M_V + K_S\right) & -K_S \\ -K_S & \left(-\omega^2 M_T + K_S + K_T\right) \end{bmatrix} \begin{bmatrix} X_1 \\ X_2 \end{bmatrix} = 0 \tag{44}$$

Rearranging Equation 44 in to the format $[K]\{X\}= \omega^2[M]\{X\}$ gives:

$$\begin{bmatrix} (K_S) & -K_S \\ -K_S & (K_S + K_T) \end{bmatrix} \begin{bmatrix} X_1 \\ X_2 \end{bmatrix} = \omega^2 \begin{bmatrix} M_V & \\ & M_T \end{bmatrix} \begin{bmatrix} X_1 \\ X_2 \end{bmatrix} \quad (45)$$

By multiplying both sides of Equation 44 by the inverse of the mass matrix, $[M]^{-1}$ the equation can be put in the form of the characteristic determinant $|A - \lambda \mathrm{I}|$, where:

$$A = [M]^{-1}[K]$$

$$A = \frac{1}{M_T M_V} \begin{bmatrix} M_T & 0 \\ 0 & M_V \end{bmatrix} \begin{bmatrix} K_S & -K_S \\ -K_S & K_S + K_T \end{bmatrix}$$

and, $\lambda = \omega^2$

From the characteristic determinant the Eigen values and therefore the natural frequencies (in Rad/s) can be found, where:

$$\omega_n^2 = \omega_1^2 \text{ or } \omega_2^2 \quad (46)$$

Using the parameters in Table 27, the first and second natural frequency for the Ford Luton box van were found to be 2.4 Hz and 17.5 Hz, respectively.

9.6.2 Vehicle Transmissibility

Transmissibility measures the energy transferred between the input of a system and its output. Using the Equations 36 and 37, the transmissibility can be calculated for the vehicle displacement (x_2) in relation to the road profile displacement (x_0). Rearranging Equations 36 and 37 and substituting in Equations 40 and 41, gives:

$$(-\omega^2 M_V + K_S + \omega C_S i) X_2 - (K_S + \omega C_S i) X_1 = 0 \quad (47)$$

$$-(K_S+\omega C_S i)X_2+(-\omega^2 M_T+K_T+K_S+\omega C_S i)X_1=(K_T+\omega C_T i)X_O \tag{48}$$

Using matrix multiplication, the transmissibility between the displacement of the vehicle, X_2, and the input X_0, can be found:

$$\begin{bmatrix} a & b \\ b & c \end{bmatrix}\begin{bmatrix} X_2 \\ X_1 \end{bmatrix}=[\mathrm{B}]\{\mathrm{X}\}=\begin{bmatrix} 0 \\ (K_T+\omega C_T i)X_0 \end{bmatrix} \tag{49}$$

Multiplying each side by the inverse of matrix B gives:

$$\begin{bmatrix} X_2 \\ X_1 \end{bmatrix}=\frac{1}{ac-b^2}\begin{bmatrix} c & -b \\ -b & a \end{bmatrix}\begin{bmatrix} 0 \\ (K_T+\omega C_T i)X_0 \end{bmatrix} \tag{50}$$

$$\begin{bmatrix} X_2 \\ X_1 \end{bmatrix}=\frac{1}{(-\omega^2 M_V+K_S+\omega C_S i)(-\omega^2 M_T+K_T+K_S+\omega C_S i)-(K_S+\omega C_S i)^2}$$

$$\ldots\begin{bmatrix} (-\omega^2 M_T+K_T+K_S+\omega C_S i) & (K_S+\omega C_S i) \\ (K_S+\omega C_S i) & (-\omega^2 M_V+K_S+\omega C_S i) \end{bmatrix}\begin{bmatrix} 0 \\ (K_T+\omega C_T i)X_0 \end{bmatrix}$$

The transmissibility of the vehicle is therefore found from:

$$\left|\frac{X_2}{X_0}\right|=\left|\frac{-b(K_T+iC_T\omega)}{ac-b^2}\right|$$

$$\left|\frac{X_2}{X_0}\right|=\frac{\sqrt{(K_S K_T)^2+\left(iC_S\omega K_T+iC_T\omega K_S-C_S C_T\omega^2\right)^2}}{\sqrt{\left((K_S-M_V\omega^2)(K_T-M_T\omega^2)-K_S M_V\omega\right)^2+\left(iC_S\omega(M_V\omega^2+M_T\omega^2-K_T)\right)^2}} \tag{51}$$

The transmissibility for the Ford Luton box van has been calculated and is given in Figure 122, where the peaks in the transmissibility can be seen at the first and second natural frequencies.

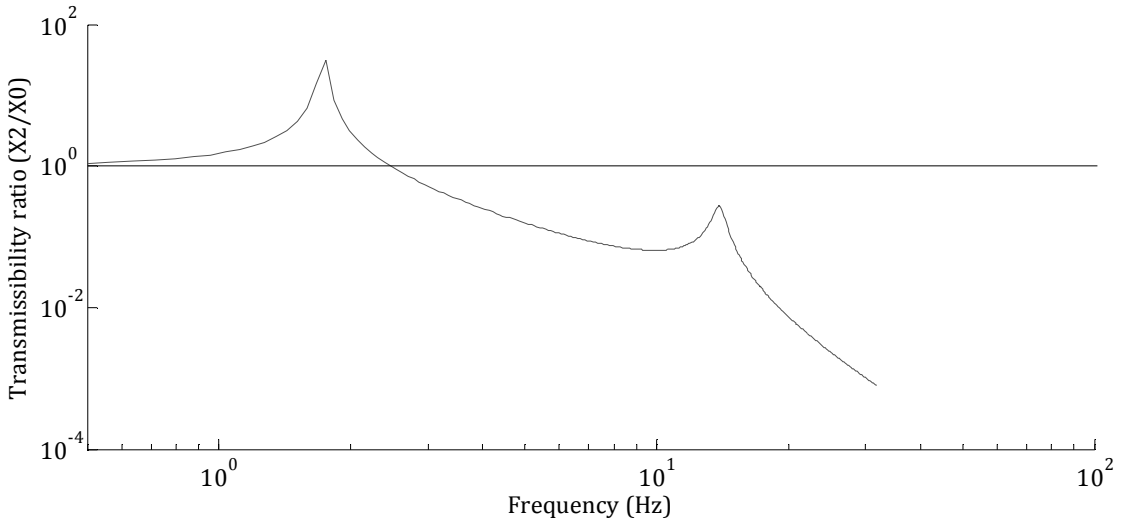

Figure 122: Ford Luton box van transmissibility (X_2/X_0)

9.6.3 Suspension Stiffness

The vehicle's suspension system acts to isolate the vehicle's structure from undesirable shock and vibration during transit. This protects the occupants and load from exposure to high level shock events and excessive vibration, and, protects the vehicle from excessive fatigue damage, without negatively affecting the vehicle's handling and stability.

The suspension stiffness can vary depending on the vehicle mass. Heavier vehicles require a stiffer suspension and therefore, for example, a semi-trailer will have a much stiffer suspension than a delivery van. Although a value for the suspension stiffness may be given by the manufacturer, or, estimated depending on vehicle type and payload, the stiffness may still vary depending on: the age of the vehicle; manufacturer's tolerances; or, vehicle alterations due to its special use. Therefore, when simulating a vehicle the possible error in suspension stiffness and its effect on the simulated response needs to be considered.

Figure 123 illustrates how changes in the suspension stiffness affect the vehicle transmissibility. It can be concluded that the stiffer the suspension, the higher the transmissibility ratio, particularly around the natural frequency. Increasing the suspension stiffness also increases the vehicles natural frequencies.

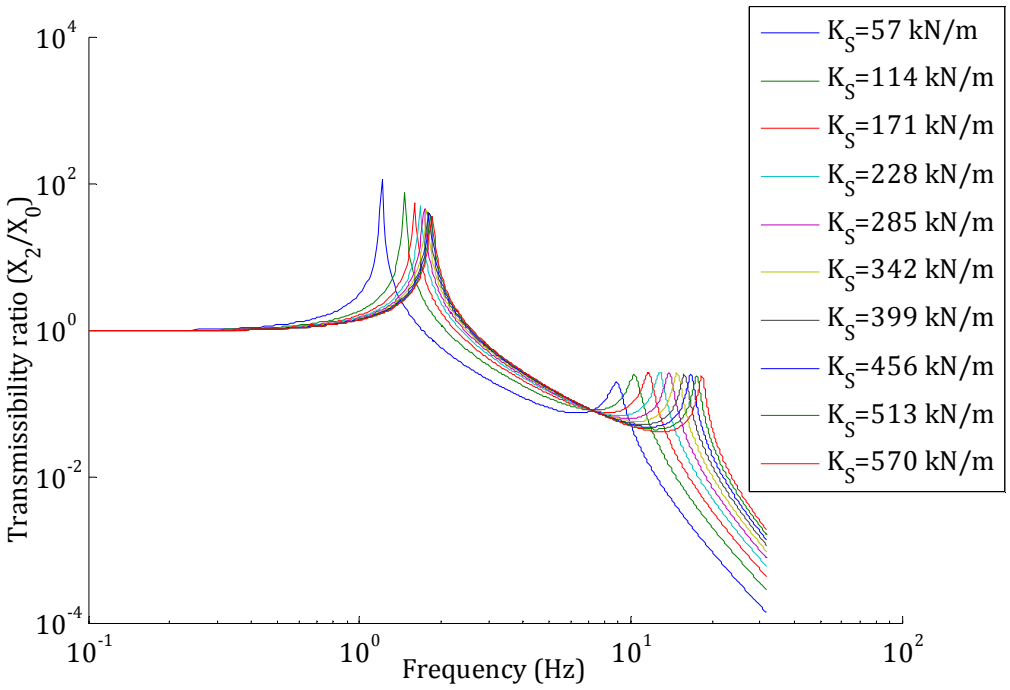

Figure 123: Transmissibility for vehicles with varying suspension stiffness, K_S

The error in both the first and second natural frequencies with respect to error in the suspension stiffness is proportional to an order six polynomial, where the constants are determined by the vehicle's parameters.

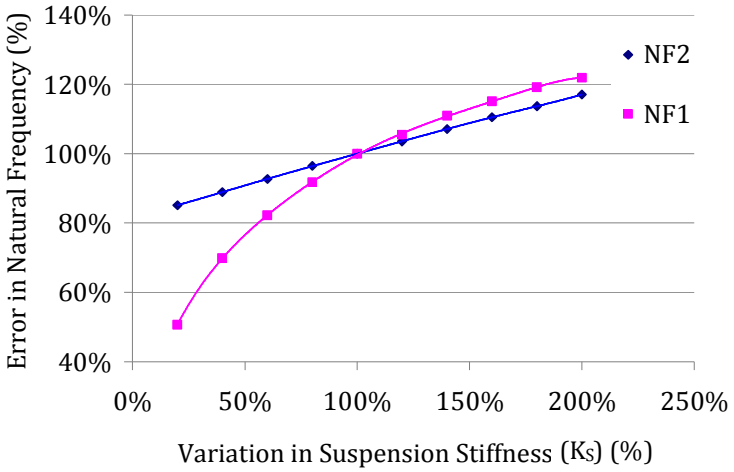

Figure 124: Percentage error in natural frequency due to error in suspension stiffness, K_S

An example of the change in vibration response for varying suspension stiffness is shown in Figure 125, where 100% is equivalent to 95 kN/m.

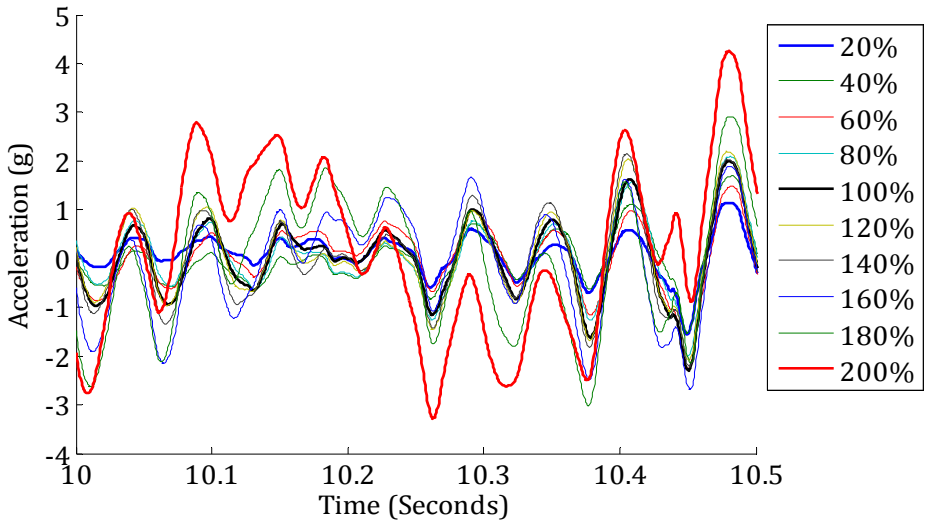

Figure 125: Sample Vibration signal for varying suspension stiffness, K_S

Figure 125 indicates that the greater the suspension stiffness, the more severe the vibration response, due to the suspension system not isolating the input excitation as effectively. Therefore, it can be concluded that error in the approximation of the suspension stiffness can lead to relatively significant error in the simulated vehicle response and hence, careful consideration should be given to the value of the suspension stiffness used in the vehicle model.

9.6.4 Suspension Dampers

In the suspension system, dampers are used to dissipate any high energy vibration occurring at and around the suspension's natural frequency, ensuring that high energy shock events caused by large displacements in the road surface are not transferred to the vehicle. The effect of varying the vehicle's damping on the transmissibility is illustrated in Figure 126. When the suspension damping is increased, the transmissibility peak at the suspension's natural frequency is reduced.

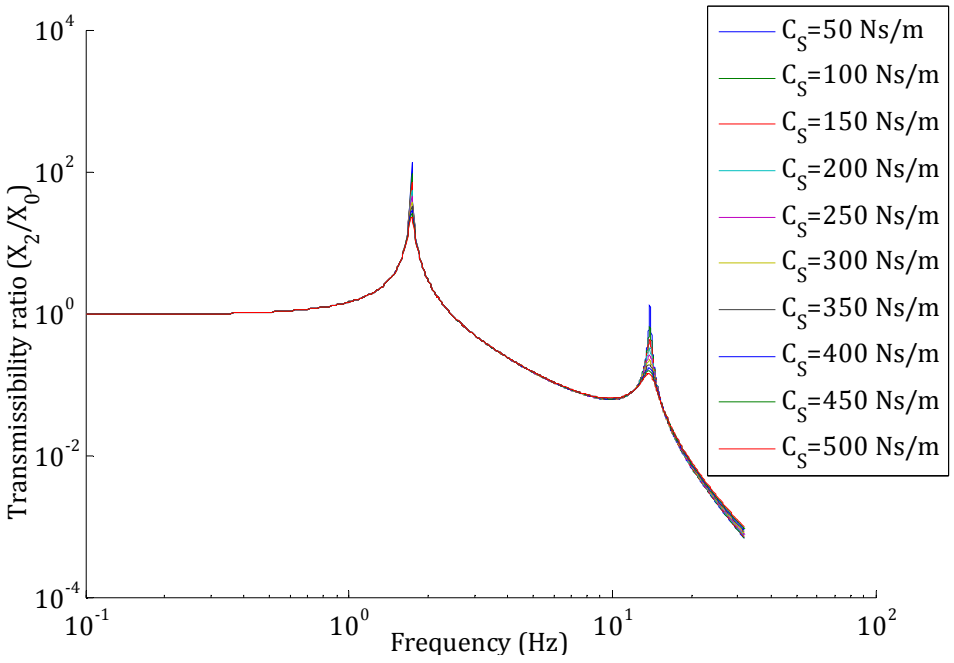

Figure 126: Transmissibility for varying suspension damping, C_S

When modelling a vehicle, as with the suspension stiffness, it is difficult to calculate the exact suspension damping, C_S, value. Therefore it is likely that when modelling a vehicle errors in the calculation will occur. When considering the percentage error in the transmissibility at both the first and second natural frequencies in relation the percentage error in C_S, the error relationship is a polynomial of order six where the values are dependent on the values of the parameters used.

9.6.5 Tyre Stiffness

Whilst the suspension removes the low frequency high amplitude events, the tyres remove high frequency low amplitude events, providing a more comfortable ride. (Garret et al, 2001). The tyres are inflated to a pressure at which they are able to support the static and dynamic loading of the vehicle. The higher the pressure the stiffer is the tyre and the more is the energy transmitted to the vehicle and as a result the more severe is the vibration. The effect of varying vehicle stiffness is illustrated using the transmissibility plot in Figure 127.

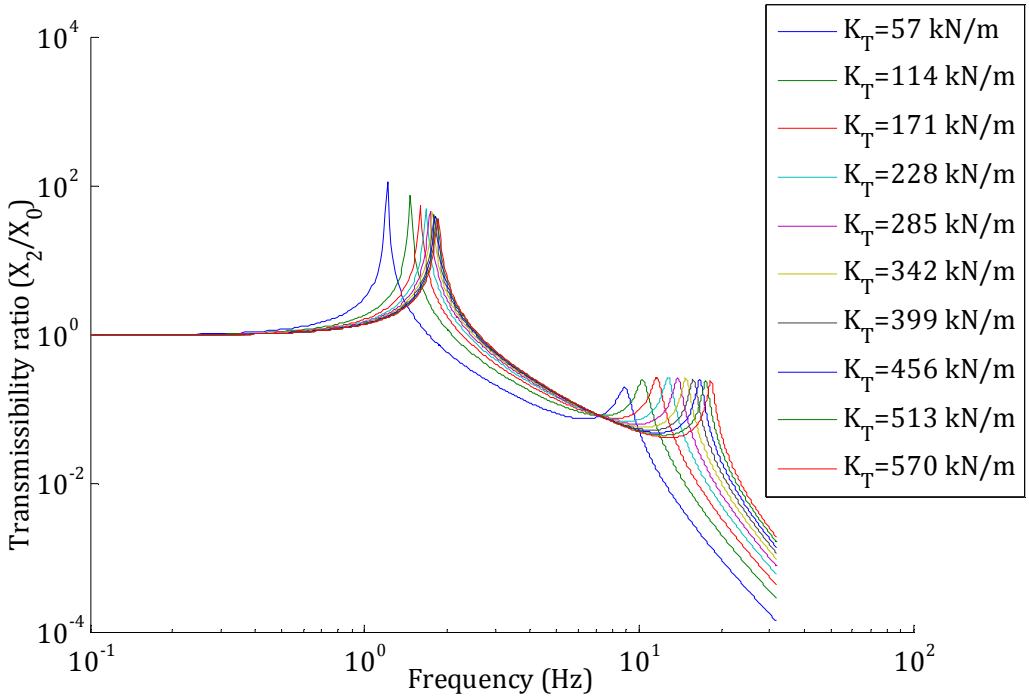

Figure 127: Transmissibility for varying tyre stiffness, K_T

9.6.6 Tyre Damping

The level of damping provided by the tyres is relatively low and therefore often neglected (Wong, 1993). A tyre's damping rate is also difficult to calculate due to constant changes in the tyre's shape, its road contact area and its stiffness. As a result, most vehicle models omit the tyre damping from calculations. In the quarter car model used in this study the tyre damping has been accounted for using a low nominal value with variations in this value having minimal effect on the vehicle response.

9.6.7 Sprung Mass

Altering a vehicle's mass affects its first natural frequency. This is typically in the range 1 – 5 Hz and arises due to resonance in the suspension system. Altering a vehicle's mass also affects the amplitude of its peak transmissibility. The variation in the transmissibility curve for the example vehicle is illustrated in Figure 128. The frequency of the first natural frequency is inversely proportional to the vehicle mass, whilst the amplitude of the transmissibility at the natural frequency is

proportional. Also evident, is that the vehicle's mass affects the amplitude of the transmissibility at the second natural frequency, with it being inversely proportional to the mass, but it does not affect the frequency.

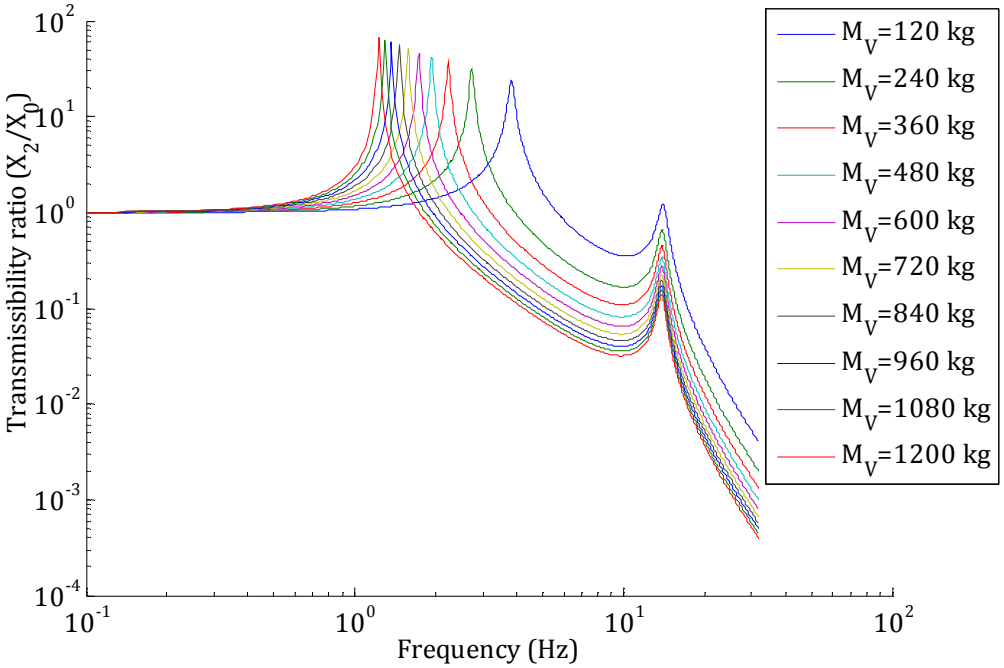

Figure 128: Transmissibility for varying vehicle Mass, M_V (kg)

The relationship between vehicle mass and the first natural frequency is illustrated in Figure 129. It can be said that the higher the mass (M_v) the less is the effect a change in the mass will have on the natural frequency.

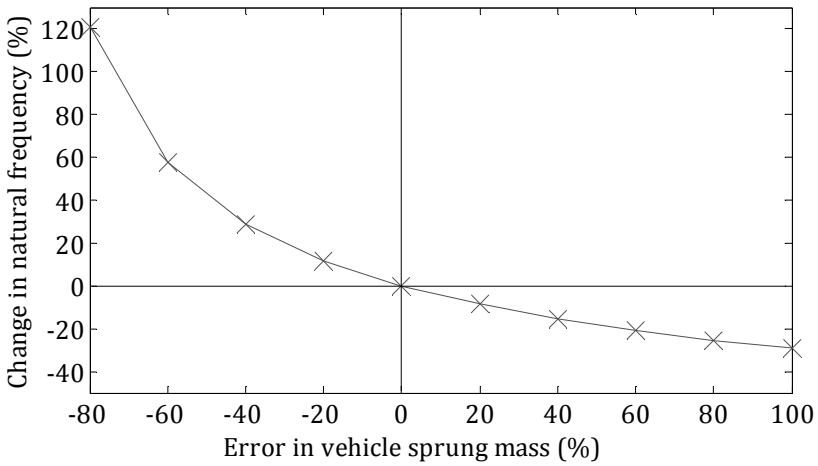

Figure 129: Variation in first natural frequency relative to the variation in vehicle mass, M_V

To consider how a change in vehicle mass affects a vehicle's response, the quarter vehicle model has been used to carry out a comparison of vehicle responses to a given road input. Figure 130, shows a two second sample from the vibration response. There is a clear variation in the vehicle's response, with a lower vehicle mass corresponding to greater amplitude of the vibration acceleration.

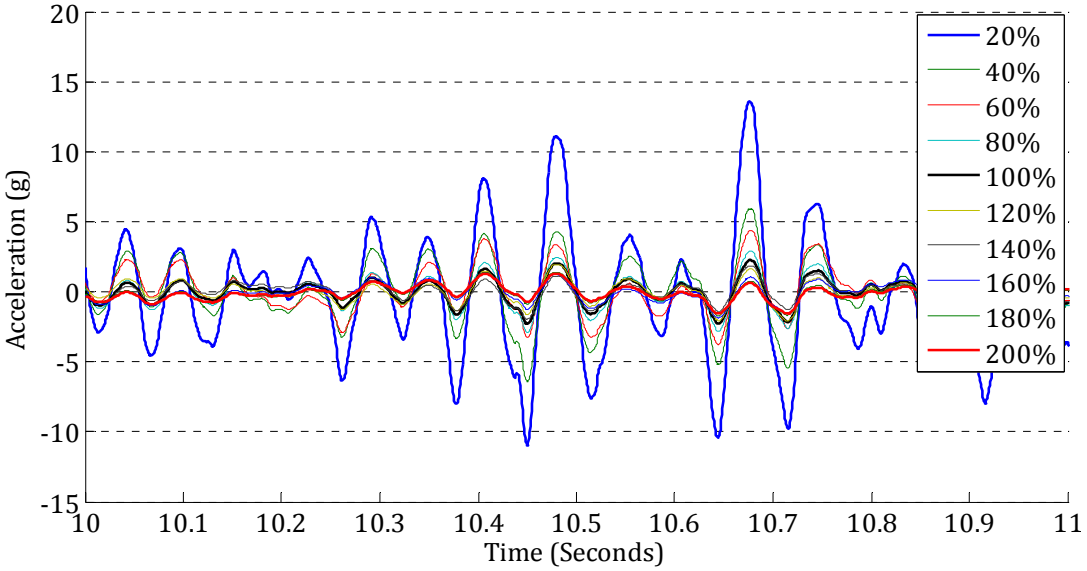

Figure 130: Sample vibration signal for varying mass, M_V

9.6.8 Payload

Vehicle payload can vary significantly between items of distribution, for example, a shipment of a high density product such as cola will have a significantly higher mass than a shipment of a less dense product such as potato crisps. Further variation in payload may occur during the distribution journey if several shipments are distributed on one route. The observable variation in vehicle response for varying vehicle mass, shown in Figure 130, highlights the importance of ensuring the correct payload is modelled.

The centre of mass of a vehicle will vary depending on the vehicle payload. Whilst the vehicle is empty, the centre of mass will not be located in the centre of the vehicle but will be positioned towards the front of the vehicle, where the engine is located. The effect of this can be accounted for in a full vehicle model and to some extent in the half vehicle model. However, with the quarter vehicle model, an

evenly distributed load is considered and as a result an average vibration is produced.

9.7 Unsprung Mass

A vehicle can be separated into two defined masses: the sprung mass (M_V), which accounts for all elements of the vehicle supported by the suspension e.g. the structural body of the vehicle; and, the unsprung mass (M_T), which includes all elements of the suspension system, the wheels and anything else that is connected to but not supported by these.

Variations in the unsprung mass have a significant effect on the second natural frequency. This is evident in the vehicle's transmissibility, shown in Figure 131, where an increase in the unsprung mass results in the amplification of the transmissibility peak and a decrease of the second natural frequency. Also evident, is the minimal effect that changes in the unsprung mass have on the first natural frequency and hence the low frequency response range of the vehicle (1 - 5 Hz).

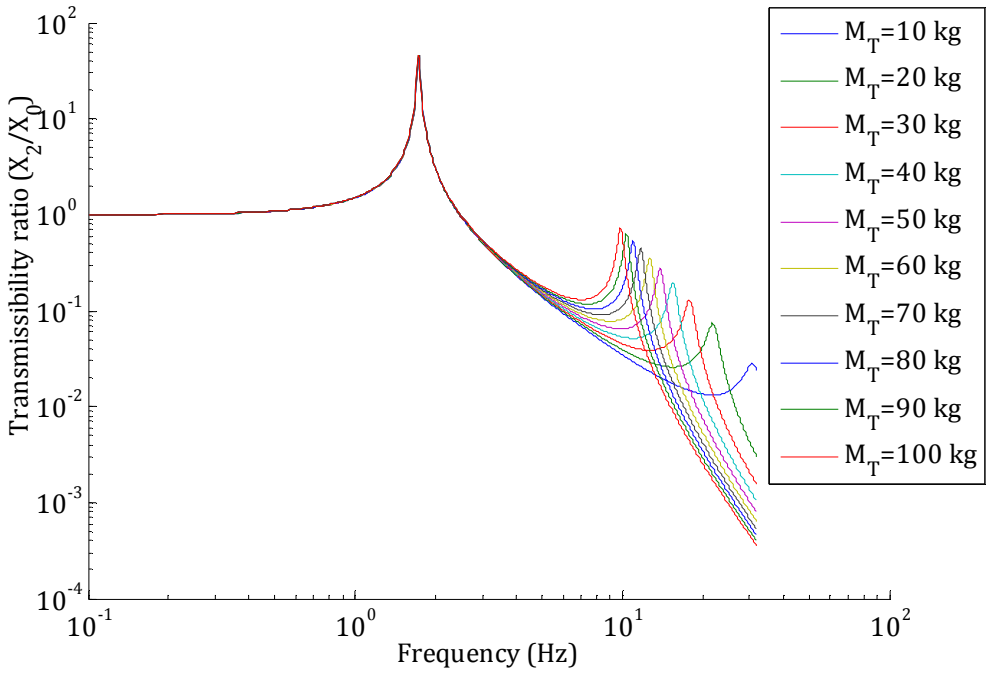

Figure 131: Transmissibility for varying unsprung mass, M_T (kg)

Further analysis of the unsprung mass, in relation to the vehicle response is shown in Figure 132. This shows the vehicle's vibration response over a one second period when the unsprung mass is, respectively: 20% of the actual value; the actual value; and, twice the actual value. In the transmissibility plots, the second natural frequency at each of these values can be seen to be approximately +30 Hz, 17 Hz and 11 Hz, respectively.

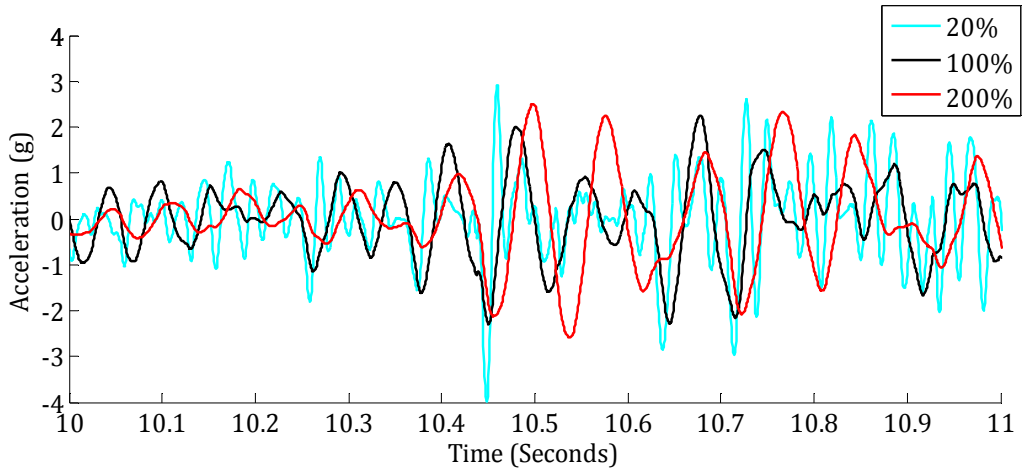

Figure 132: Vehicle response for varying unsprung mass, M_T (kg)

The existence of these frequencies is evident in the corresponding vehicle response, with the lower unsprung mass evidently having a much higher prominent frequency.

This highlights the potential problems that can occur when the unsprung mass used in the simulation is different from the actual mass. Because the unsprung mass is typically small in comparison with the vehicle's 'sprung' mass, proportionally, the effect of errors in its calculation can have a large impact on the predicted vehicle response.

9.8 Chapter Summary

For the purpose of this study an approximation of the vertical vibration response at a point on a vehicle, and conversely, the vertical displacement of the road

surface, is required. It was therefore decided that a quarter vehicle model would be adequate.

The 2 degree of freedom quarter vehicle model has then been presented and the equations of motion on which it is built have been stated. The quarter vehicle model was constructed using Mathworks Simulink©, so that the model could be integrated into the Matlab programming used to create vibration simulations.

The simplicity of the quarter vehicle model means that static values must be given to the vehicle's parameters. In reality, these parameters are complex and dynamic in nature and therefore, considering them as static values can generate errors in the calculated results.

To evaluate both the effect of changes in vehicle parameters and the effect of potential errors in the estimation of a vehicle's parameters on the calculated vehicle response, a sensitivity analysis of the quarter vehicle model was carried out. This analysis showed that:

- Increasing the suspension stiffness, increased the frequency of the vehicle's first and second natural frequency and also increased the severity of the vehicle response.
- Increasing the suspension damping reduced the severity of the vehicle's vibration response.
- Increasing the tyre stiffness resulted in an increase in the frequency of the first and second natural frequency and increased the amplitude of the vehicle response.
- Alterations to the tyre stiffness had little effect on the overall response due to its comparatively low value.
- Increasing the vehicle mass, increased the frequency of the first natural frequency, but, reduced the amplitude of the vibration response.

- Increasing the unsprung mass increased the frequency of the second natural frequency and reduced the vehicle's response at frequencies around and above the second natural frequency.

The sensitivity analysis has highlighted the need for careful consideration of vehicle parameters and vehicle load in order to minimise error in the calculated vehicle response.

10 CREATING A VIBRATION SIMULATION FOR A SPECIFIC DISTRIBUTION JOURNEY

The relationship between a vehicle's vibration response and its parameters is presented in the sensitivity analysis of the quarter vehicle model in Chapter 9. Changes to these parameters, including: suspension stiffness and damping; vehicle mass; payload; and, tyre stiffness; can alter the position of the vehicle's natural frequencies and noticeably alter the severity and nature of a vehicle's response.

In section 4.1 the current testing standards are presented. They utilise a standard data set to simulate all distribution journeys and therefore do not account for journey and vehicle variability. This results in significant differences in the vibration simulation leading to under or over testing of packaged products.

To create a vibration simulation that more accurately represents the nature of the intended distribution, representative vibration data is required. In the ISTA Standards, tests created to account for the actual distribution environment are called 'focused tests' which can be used if the representative data is available (ISTA, 2012). The inclusion of focused testing in the current standards emphasise the importance of accounting for the intended distribution environment in order to create accurate simulation tests.

The collection of vibration data covering all possible distribution routes and vehicles is uneconomical and time inefficient. Therefore, an alternative method of generating a more representative simulation, without the need for additional in-situ data collection, is required.

The solution proposed in this study, is to construct a database of historical road profile information collected during in-situ data acquisition. This historical data

can then be used to approximate an alternative distribution journey. An approximation of a given distribution vehicle's response to the road profile, is then calculated using a quarter vehicle model, like that discussed in sections 9.2 and 9.3.

By simulating the distribution vibration using the journey database and the quarter vehicle model, both the intended distribution vehicle and journey can be considered without the need for costly and time consuming in-situ data collection. The previous chapter discussed the creation of the vehicle model and this chapter presents the concept of a journey database for storing road profile data.

10.1 Data Acquisition

A key component of the journey database is the acquisition of road profile data, which is required in order to populate the database. Three methods of data acquisition have been identified. These are:

- **Using a Profilometer**

  A profilometer is *'...a "rolling straight-edge" that measures a pavement's longitudinal profile. As the unit is pushed along a roadway, it provides a trace of the road profile as well as locates, measures and records any bumps or depressions in the pavement surface...*' (Transportation, 2001). Modern profilometers measure the road surface displacement using a laser mounted vertically on a vehicle. An integrated accelerometer is then used to correct for the vehicle's vertical movement. They have been used in conjunction with computational quarter vehicle models to evaluate ride roughness (Sun et al, 2001). With access to a profilometer, road profile data can be collected during distribution journeys or during normal travel.

- **Using Archived Road Profile Data**

  Profilometers are used in many countries to monitor the condition of roads. In the UK this information is used to classify road condition. Unfortunately,

access to this data in the UK is not possible, although other countries such as Australia, store this data (Sek, 1996). With access to this data, road profiles can be sourced without the need for data collection.

A British Standard, BS7853, exists which provides displacement PSD spectra relating to varying severity of road roughness (BS7853, 1996). These spectra are shown in Figure 162, Appendix IV. They illustrate the displacement power (m^3/cycles) variation with Spatial frequency, n (cycles/m). Each line indicates a different road type, from: *A*, the smoothest; up to *H*, the roughest; allowing a random road profile to be produced based on historical data average. By constructing a road profile based on a single displacement PSD, the average vehicle response on a road type can be produced.

The limitation of using averaged data is that large discrepancies such as potholes and road damage will not be replicated. This method lends itself to use with the established method for simulating vehicle vibration.

- **Inverse Vehicle Model**

With the use of a computational vehicle model, historical vehicle vibration data can be converted into approximate road profiles. The journey speed information is then used to convert the road profiles to the spatial domain, so as not to limit the use of the road profile data for future journey approximations. Although this method enables database population without the need for additional data collection, using an inverse model means that assumptions about the vehicle are made, which can induce errors in the road profile approximation. A detailed description of the vehicle model used is given in Chapter 9 along with possible sources of error and their magnitude and effect on the calculated vehicle vibration response.

The data collection method used is dependent upon a number of factors, including: access to equipment; access to historical road profile data or vehicle vibration data; and, the accuracy required.

During this study, the inverse quarter vehicle model was used, because:

- access to equipment was limited to accelerometers, therefore a profilometer could not be used;
- historical vehicle vibration data was readily available;
- high accuracy of the vehicle vibration was required.

Therefore, although the displacement PSDs presented in the British Standards would provide the quickest method of obtaining road profile data, they do not provide an accurate representation of the large deviations apparent in the road profile which cause shock events. The acquisition of vehicle vibration data and the integration of the inverse quarter vehicle model into the journey database are now described.

10.2 Collecting Vehicle Vibration Data to Approximate Road Profiles

In order to use the inverse vehicle model, vehicle vibration data is required. To enable accurate measurement of the entire distribution journey, data was acquired continuously. The vibration was measured using single axis B&K ICP accelerometers which were hardwired to a National Instruments wireless DAQ (NI 9234) unit. Due to the large amount of vibration data collected, a wireless network connection was set up to transfer the vibration signal to a laptop computer for storage. In parallel with this, the vehicle's GPS location and speed profile were recorded using a wireless I-GOT-U GPS device.

The vehicle vibration was stored on the laptop using Labview's specially designed 'Data Assistant'. The signals were then analysed using Matlab.

Once filtered, the vibration data collected can be converted to an approximate road profile using the inverse quarter vehicle model defined in section 9.4. The road profile produced via this method is an approximation of the actual road profile and

not an exact match because of potential errors in the vehicle parameters used and the assumptions made when using the quarter vehicle model, as explained in section 9.5.

10.3 Data Segmentation and Classification

Once a road profile is obtained, the data must be suitably segmented, categorised and stored within the database.

Data Segmentation

The requirement for efficient and accurate use of the database creates the need for road profile information to be easily selected and accessible. To facilitate this, road profile data is decomposed into segments based on the type of road. Examples of UK road classifications are: motorways, A-roads, B-roads and unclassified roads. Examples of these different road types are shown in Figure 133, where the variation in the condition and construction of roads can be seen. Shown are examples of a Motorway (A), A-road (B), B-road (C), B-road residential road (D) and an unclassified road - country road (E). Road types A to D are paved whereas the country road (E) is not. There is a visible increase in the roughness of the road surface for the unpaved road. Because motorways and A-roads act as major arterial roads and are therefore subject to heavy use, they are maintained on a regular basis.

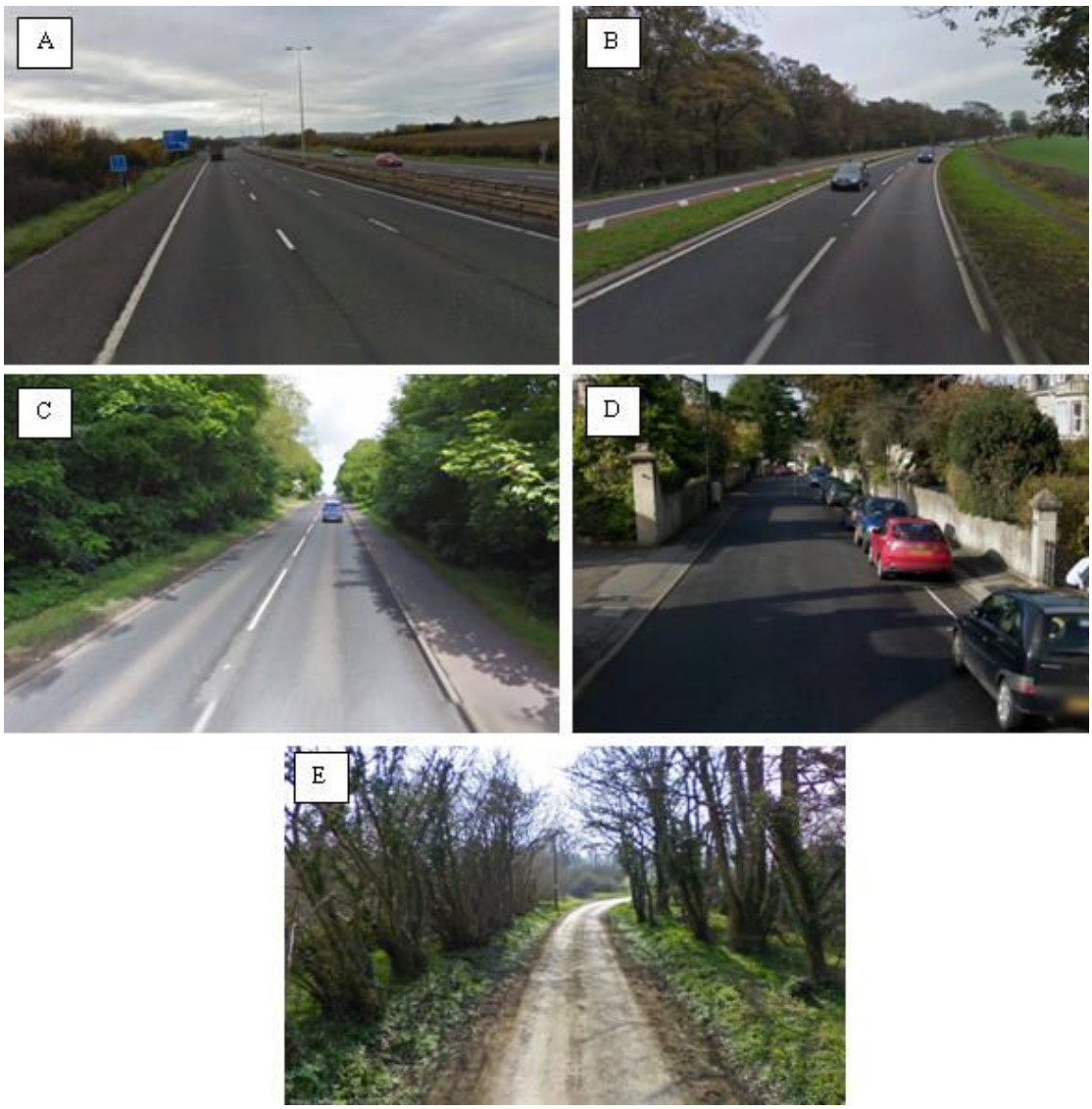

Figure 133: Road types (a) Motorway (b)A road (c) B road (d) B road - Residential (e) Unclassified - Country road (TAKEN FROM Google Streetview)

By evaluating the GPS data acquired with a vibration signal, the road types throughout a journey can be identified. This allows changes in road type throughout the journey to be identified. Therefore, the vibration signal can then be segmented based on road type. An overview of the segmenting process is now given.

1. The address for each GPS co-ordinate is found using a Google map URL command.

2. Using phrase and character recognition, the road type at each GPS location is determined.

3. A numerical value is then given to each GPS point based on the road type. The classifications are given in Table 29.

Table 29: Road classifications

ROAD TYPE	NUMERICAL VALUE
Motorway	1
A-road	2
B-road	3
Road	4
Street, Hill	5
Way, Walk, Drive, Vale, Place, Close, Terrace, Avenue, Lane, Grove, End	6
Unclassified (unrecognised address)	7

4. For all GPS locations where no address is found, the locations before and after that points are checked. If the locations are the same e.g. both road type 5, then a road type 5 is assigned to that GPS location. If the locations are different, then the user must decided, based on the previous and following road types, which road type to prescribe.

5. For each location where there is a change in the road type i.e. moving from motorway to A-road, the corresponding time stamp is found.

6. The time stamp for the start and end point of each road type is used to segment the vibration signal at the corresponding point. This results in the creation of a number of vibration signal segments. In order to accurately segment the vibration signal, the GPS unit and Vibration DAQ unit, must be calibrated to the same time.

7. The segments are then saved as individual data files.

Alternatively, if the GPS data is not available, the route taken can be analysed along with the journey time. This enables the distance travelled on different road types to be approximated.

Once the vibration signal has been segmented based on road type, the condition of the road on each segment needs to be considered.

Data Classification

The condition of roads can vary significantly within a country and between countries, due to age, construction, maintenance and frequency of use. One of the issues relating to the Accelerated PSD approach is that it assumes the road quality on all journeys is the same, making it likely to produce an inaccurate simulation. It is therefore wise to classify road profile data based on the road condition, enabling journeys to be constructed based on a higher level of detail, thereby giving greater accuracy in journey approximations.

A visual assessment of the journey could enable a basic judgement about the condition of each road. However, if this information is not available, then roads can be classified based on the severity of their displacement PSD.

To calculate the displacement PSD, the road profile must first be converted from the time to the spatial domain. This is done by multiplying the signal's time information by the corresponding vehicle speed acquired with the GPS data, resulting in the vertical road displacement (m) with respect to distance (m). The displacement PSD can then be found using Equation 52.

It should be noted that, typically, the vehicle speed is sampled every 5 seconds and the vehicle's vertical vibration sampled less than every 0.002s. It is therefore possible that some small amount of error will be introduced by calculating the spatial road profile in this manner. Therefore this method will provide an overall assessment of the road condition, but, this should not be considered an accurate representation of the road surface roughness.

The roughness of the road surface can then be classified by comparing the calculated displacement PSD with limiting spectra defined for different road conditions. Cebon (1999) provides maximum and minimum spectra defining the classification of road roughness from very good to very poor condition. These

spectra were taken from a proposal for an ISO standard for road roughness. The equation used to calculate these limiting spectra is given as:

$$S_u(\kappa) = \begin{cases} S_u(\kappa_0)\left(\dfrac{\kappa}{\kappa_0}\right)^{-n_1} & \dfrac{\kappa}{\kappa_0} \le 1 \\ S_u(\kappa_0)\left(\dfrac{\kappa}{\kappa_0}\right)^{-n_2} & \dfrac{\kappa}{\kappa_0} > 1 \end{cases} \quad (52)$$

where $S_u(\kappa)$ is the displacement PSD limit, n_1 = 3, n_2 = 2.25, κ_0 = 1/(2π) cycles/m and the limiting values of $S_u(\kappa_0)$ are given in Table 30.

Table 30: Values of $S(\kappa_0)$ in the corrected ISO standard (Cebon, 1999)

ROAD CLASS	$S(\kappa_0)$ (X10^{-6}) (m^3/cycle)
Very good	2 – 8
Good	8 – 32
Average	32 – 128
Poor	128 – 512
Very poor	512 – 2048

The resulting spectral limits are illustrated in Figure 134. By comparing the displacement PSDs of road segments with these limits, the severity of each road segment can be evaluated and classified as appropriate.

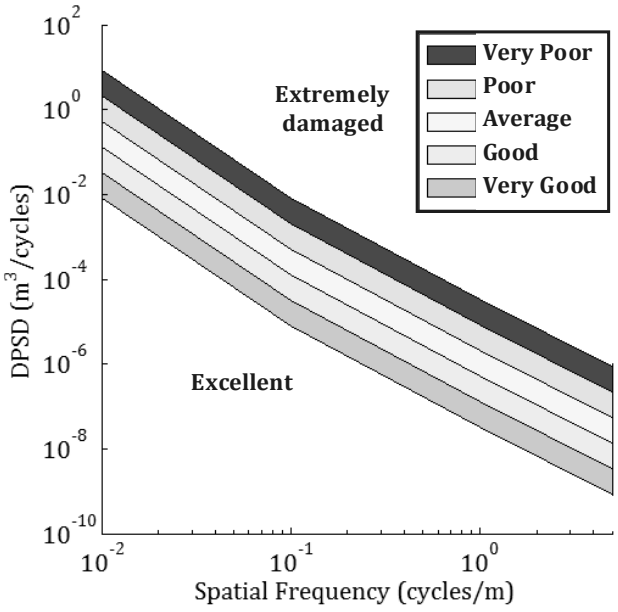

Figure 134: Classifications for spectral density of road height (Cebon, 1999)

Each road classification has been assigned a numerical value. These are given in Table 31.

Table 31: Road roughness classifications

NUMERICAL CLASSIFICATION	ROAD CLASS
1	Excellent
2	Very good
3	Good
4	Average
5	Poor
6	Very poor
7	Extremely damaged

A limitation of using the displacement PSD is that the data is averaged. This means that the large deviations in the road surface which cause shock events are not included. DfT (2012), states that a pothole is road damage greater than 40mm deep. If events of this magnitude are present within the road roughness profile then they may not be accounted for and could result in unrealistic damage. Therefore, in order to account for these events, the RMS displacement distribution for 1m segments of road should also be evaluated.

The process of road classification can be described as follows:

1. The displacement PSD, overall RMS displacement, RMS displacement distribution for 1 metre samples and kurtosis are calculated.

2. The displacement PSD is then compared with the limits given in Figure 134 and the road segments are then graded dependent upon where they fall within the limits. This is done by:

    a. Calculate the area under the road roughness displacement PSD

    b. Calculate the area under each ISO road roughness limit for the corresponding spatial frequency range

    c. Find which limits the road roughness falls between and classify the road condition accordingly.

3. The overall RMS displacement, RMS displacement distribution, high displacement events and kurtosis are then stored as a reference for each road segment.

An example of the classification process is given for the vertical vibration time history in Figure 135. This journey was on a residential road (road type 5) travelling at 30 mph. The road was newly paved and therefore in very good condition.

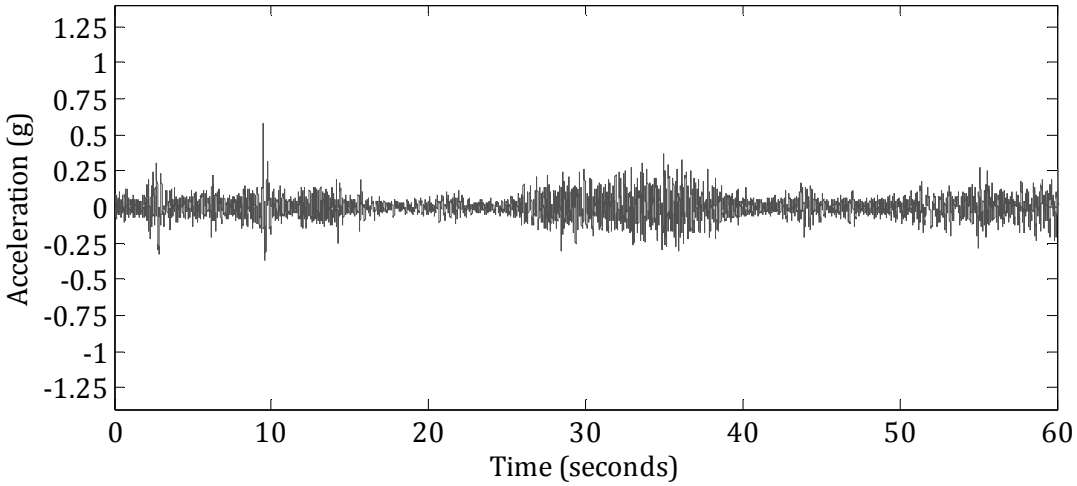

Figure 135: Vehicle vibration time history – sample 1

The inverse quarter vehicle model has been used to approximate the corresponding road profile. The road profile calculated is given in Figure 136. The smoothness of the road is evident in the relatively low vertical displacement of the road's roughness.

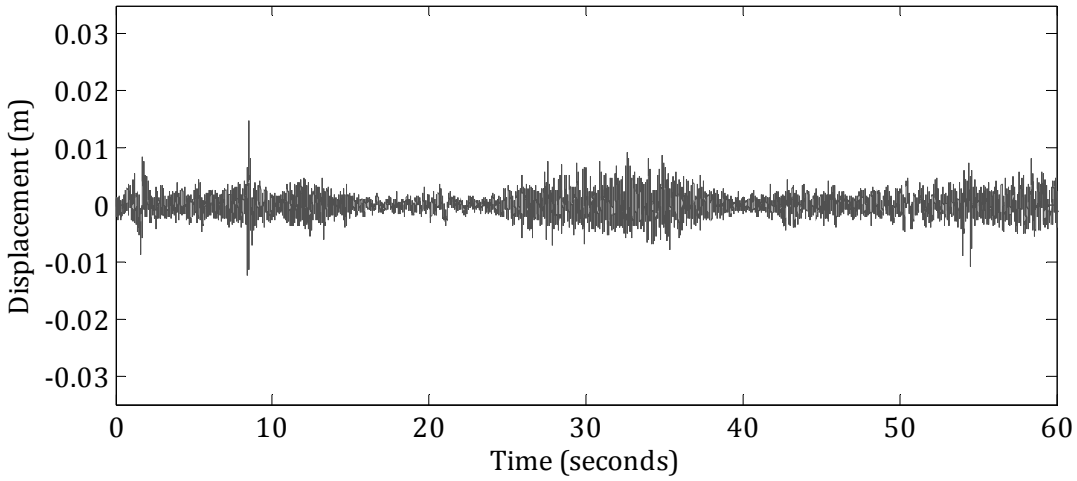

Figure 136: Approximate road profile of vehicle vibration in Figure 135 – sample 1

After converting the time history road profile into a spatial road profile (using the average speed of 30 mph), the RMS displacement distribution for 1m segments of the road surface was calculated and the displacement PSD for the road was also calculated. These are shown in Figure 137 and Figure 138 respectively. The RMS distribution highlights the low vertical displacement of the road surface and hence the smoothness of the road.

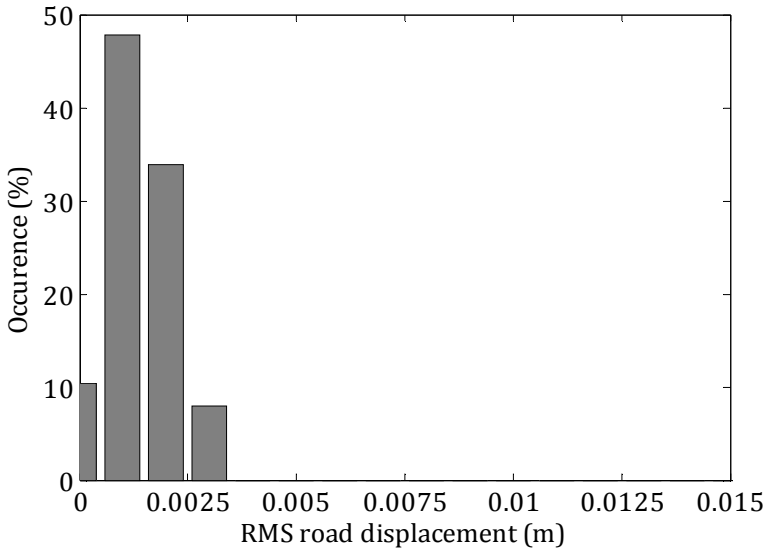

Figure 137: Percentage RMS displacement distribution of one second segments of road profile (Figure 136) – sample 1

The displacement PSD for the road profile was calculated and compared to the classification limits given in Figure 134. The road profile for the given road can be classed as very good, using the classification method set out.

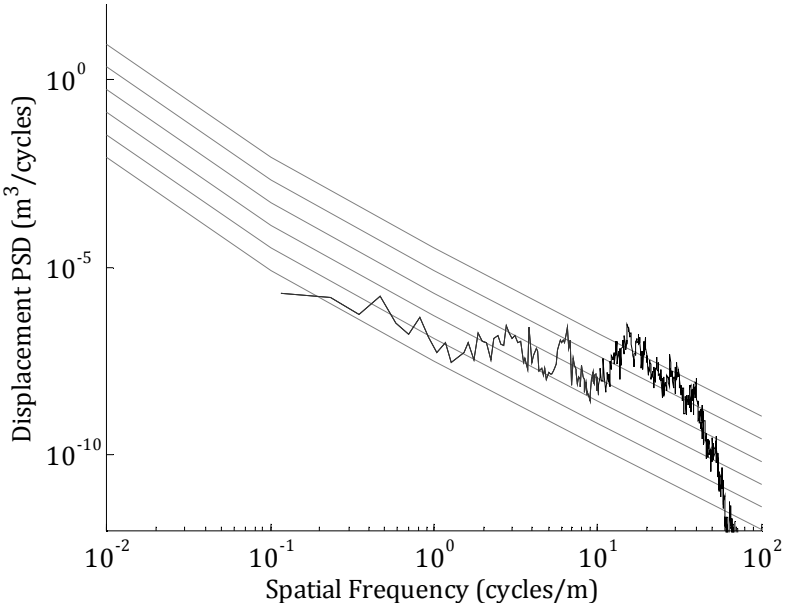

Figure 138: Comparison of the displacement PSD for the road profile (Figure 136) to the classification limits – sample 1

To provide a comparison of a very good classification road to an average, the road profile corresponding to a second vehicle vibration time history (Figure 139) has been calculated and evaluated. The road profile is given in Figure 140.

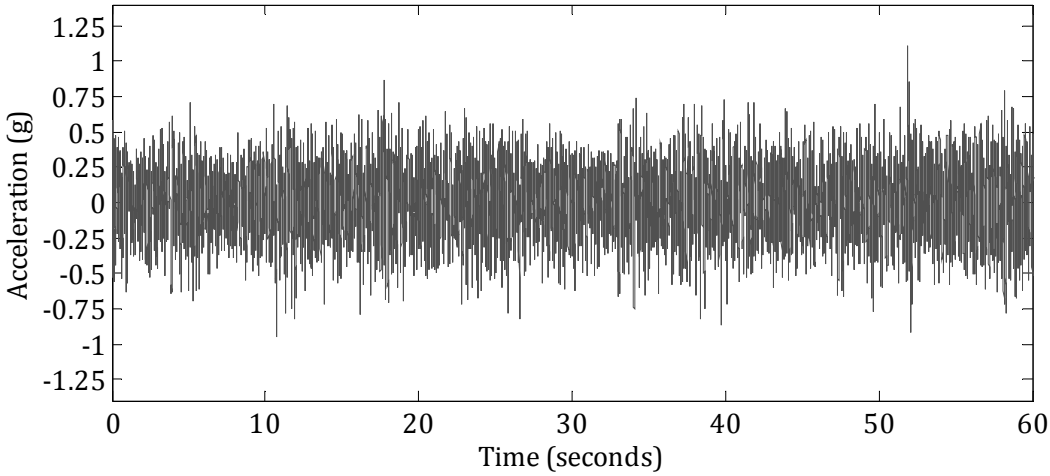

Figure 139: Vehicle vibration time history – sample 2

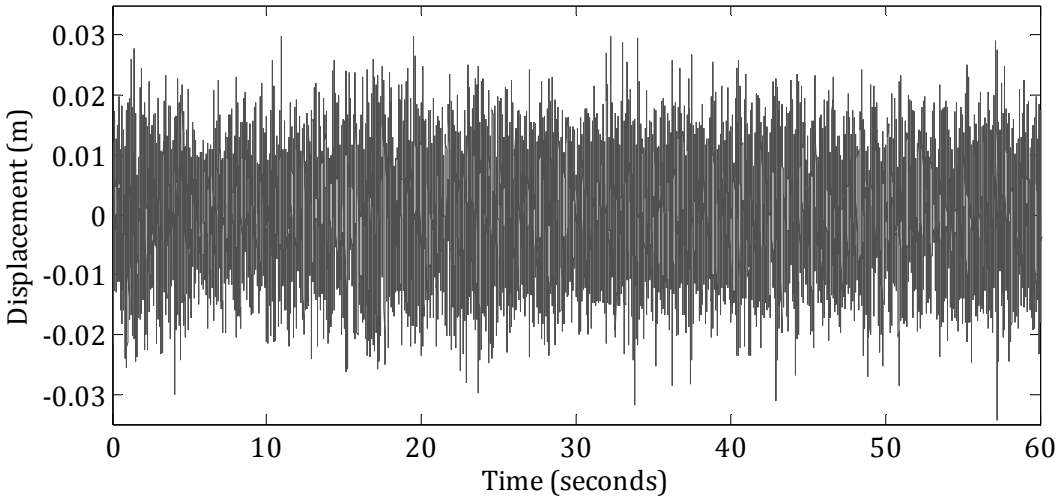

Figure 140: Approximate road profile of vehicle vibration in Figure 139 – sample 2

This vibration signal was recorded on a lane (Road Type 6) that would be classed as a country road, this road was paved but in mediocre condition. The speed limit on this road was 40mph, this journey was made using the same vehicle as the journey in Figure 135. The corresponding displacement PSD and the percentage distribution of the RMS displacement of segments of road are given in Figure 141 and Figure 142, respectively. By comparison the displacement of the road profile in sample 2 is significantly greater than that sample 1. This is evident in the difference between the RMS displacement for each, with the RMS displacement of sample 1 being 0.0016m and the RMS displacement of sample 2 being 0.0071m. The additional roughness of sample 2's road profile is also visible in the displacement PSD. When compared to the classification limits sample 2 can be said to be of average condition.

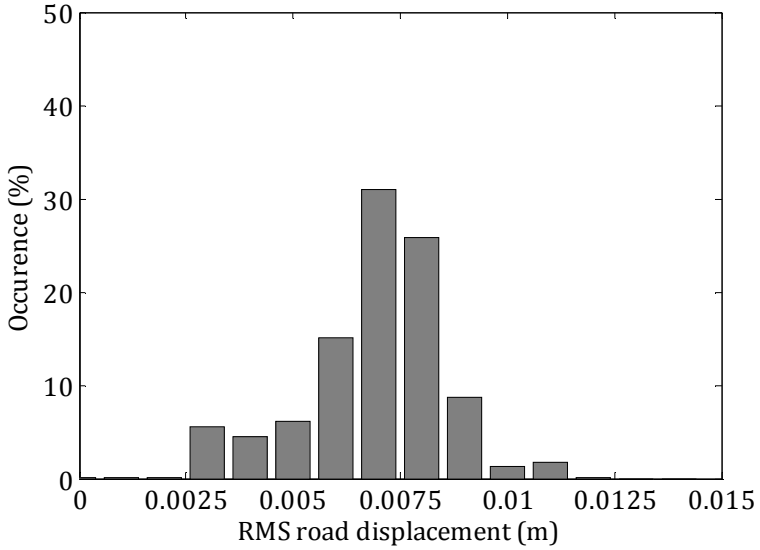

Figure 141: Percentage RMS displacement distribution of one second segments of road profile (Figure 140) – sample 2

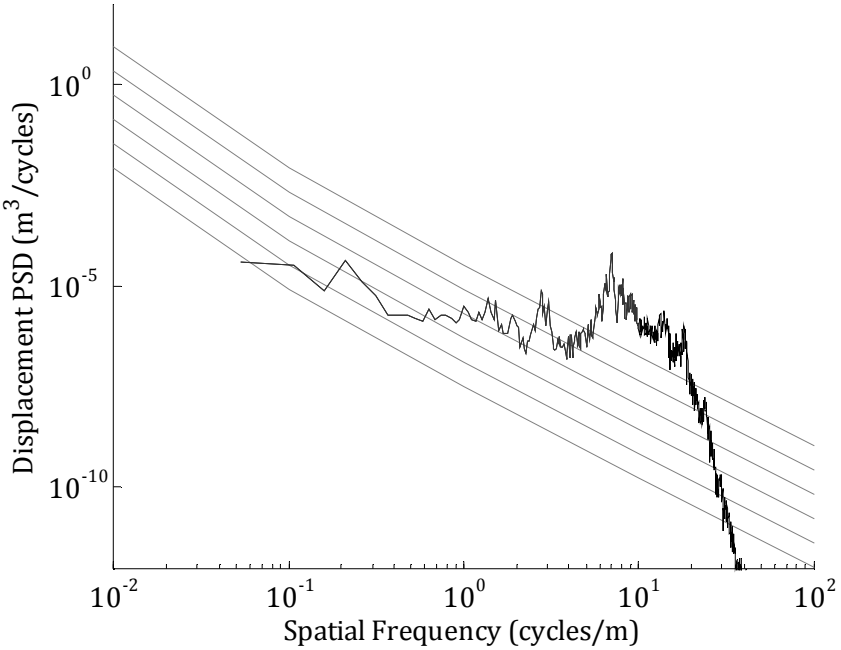

Figure 142: Comparison of the displacement PSD for the road profile (Figure 140) to the classification limits – sample 1

10.4 Storing Data in the Journey Database

By segmenting and classifying the road profile data as described, a simple hierarchical structured database can be used. The structure is illustrated in Figure

143. This structure allows the user to easily and efficiently select the right road profile information to use for future journey simulations. The highlighted example shows the selection of a UK motorway road profile that is in good condition.

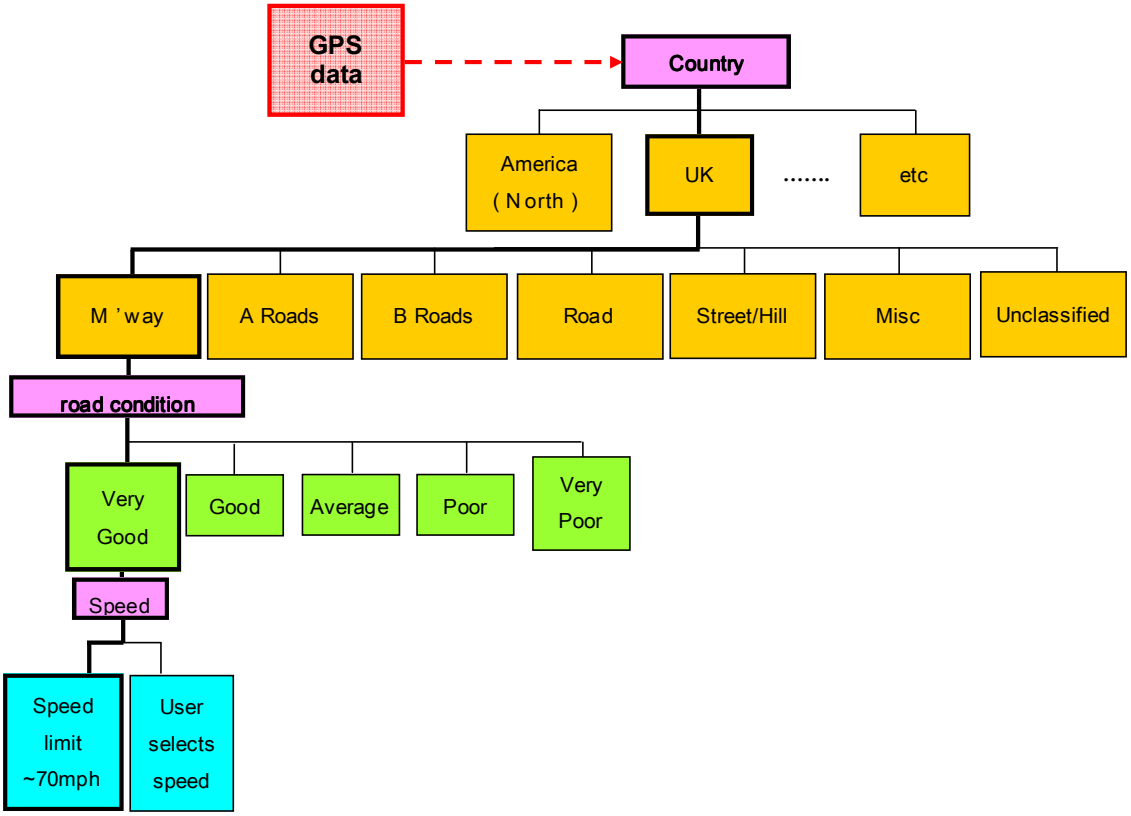

Figure 143: Hierarchical structure of 'Journey Database' data classification and storage

10.5 Populating the Journey Database

A method of populating the journey database, which brings together the aspects discussed in section 10.1, 10.2, 10.3 and 10.4, is illustrated in

Figure 144. This diagram illustrates several key stages in the population process including:

1. *Data collection* – vehicle vibration data and the related GPS data is acquired during in-situ data collection;

2. *Inverse vehicle model* – an approximate road profile is then obtained via an inverse vehicle model, using the vehicle's vibration profile as the input;

3. *Creating a spatial road profile* – by combining the speed profile with the calculated road profile a spatial approximation of the road profile can be calculated;

4. *Data classification* – road profiles are segmented, based on road type e.g. motorway, A-road, B-road, etc (numerical reference given in Table 29). These segments are then classified further, based on the road segment's condition (numerical reference given in Table 31);

5. *Journey database* – once classified, the road profiles are stored within the database from which a simulation journey can be built.

For the purpose of this Thesis a model journey database has been constructed, using vibration data acquired on home delivery vehicles. The quantity of data within this model database is given in Table 32, based on road type and condition. Due to the nature of the distribution journeys data was acquired on, no motorway data has been collected.

Table 32: Quantity of data available in the model journey database (in minutes)

ROAD TYPE	ROAD CONDITION							TOTAL TIME BY ROAD TYPE (minutes)
	1	2	3	4	5	6	7	
1	0	0	0	0	0	0	0	**0**
2	0	1	2	22	0	0	0	**25**
3	0	0	0	15	36	0	0	**50**
4	3	23	37	84	26	0	0	**173**
5	5	31	101	54	74	2	0	**266**
6	7	19	120	45	17	0	0	**208**
7	5	15	4	3	1	0	12	**41**
Total Time road condition (minutes)	**19**	**88**	**265**	**223**	**154**	**2**	**12**	**Total time = 762 minutes**

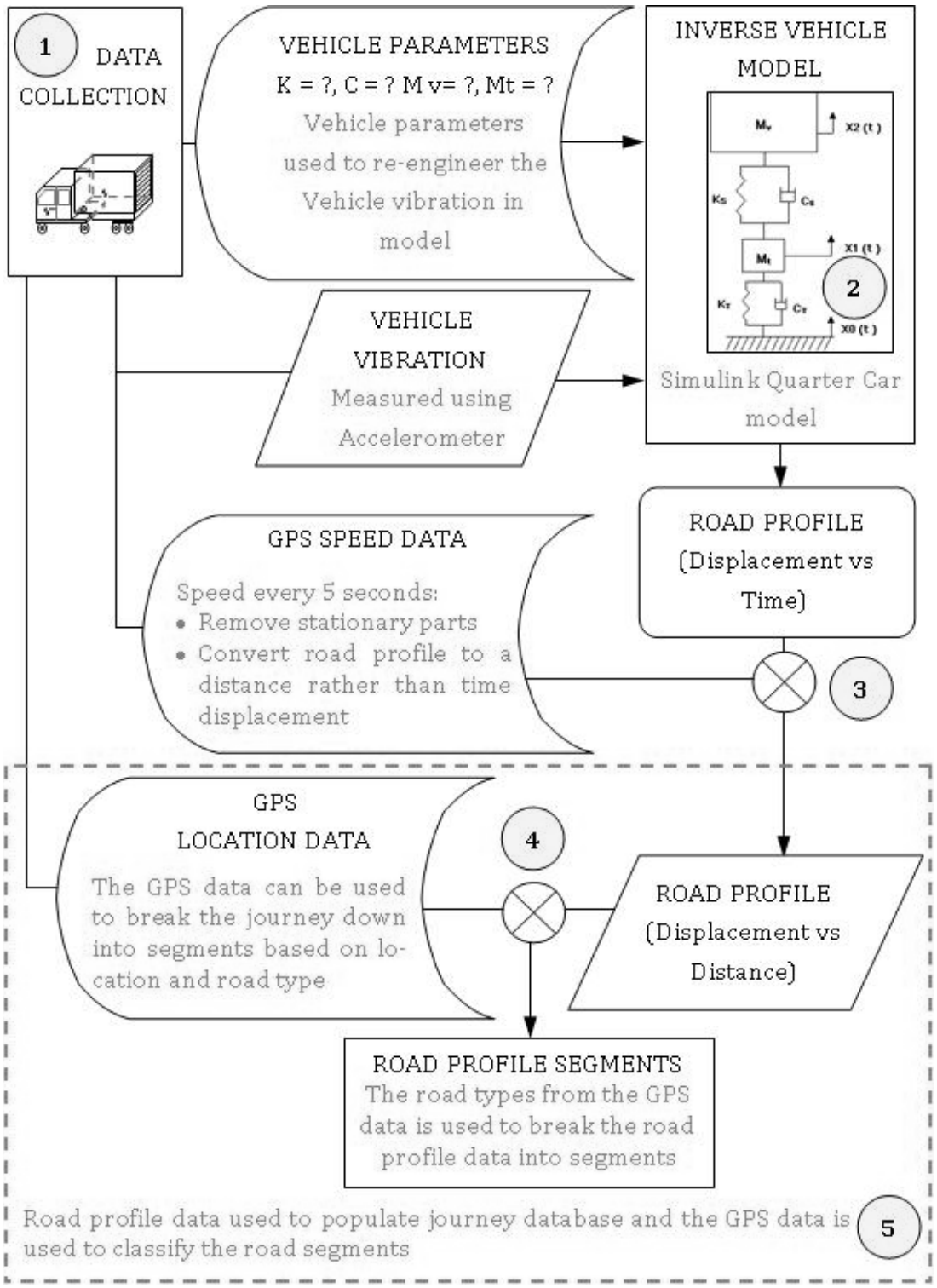

Figure 144: 'Journey Database' population

10.6 Building a Journey

In order to build a journey using the 'Journey Database', information on the intended distribution route is required. This can be achieved using one of the following options:

Option one: GPS information for the route including speed profile from a previous journey;

Option two: distribution route map with road speed limits;

Option three: estimates of the distance on each road type with intended speeds.

To enable the use of option one, a programme designed using Matlab was created. This programme requires the user to input the GPS data from the journey and produces a breakdown of the time spent on particular road types together with speed of travel. This method is described by the following steps:

1. GPS data is imported into Matlab, with the address of each GPS point being found using its longitudinal and lateral co-ordinates.

2. Character recognition is used to identify specific names relating to road types.

3. A numerical value is allocated to each GPS point or journey location based on the road type.

4. A second numerical value is allocated based on the speed of the vehicle at each GPS point.

5. An assessment is made as to the severity (roughness) of the road profile required. This can be done using regional or national statistics on the quality of roads. ONS (2011a) and ONS (2011b) rate the condition of roads by region in the UK based on a traffic light scale, where green relates to roads in good condition and red relates to roads that require maintenance.

6. The numerical road type values, selected roughness, along with the distance are then used to select the appropriate road profile segments to build an approximate spatial road profile of the journey.

7. The average speed data for each road type segment is then used to convert the road profile into a displacement time signal, resulting in an approximation of the distribution journey's road profile.

Table 33: Speed classifications

SPEED (km/hr)	NUMERICAL VALUE
1 - 5	1
5 – 10	2
10 – 20	3
20 – 30	4
30 – 40	5
40 – 50	6
50 - 60	7
60 – 70	8
70 – 80	9
80 – 90	10
90 - 100	11
100 +	12

Figure 145 illustrates the process of building an approximation of the distribution journey's road profile. There are four key stages highlighted in the diagram:

1. *Data collection* – the GPS data or the journey data is recorded.

2. *Journey Evaluation* – deconstruct the distribution journey to find the distance travelled on each road type.

3. *Building a journey* – the journey evaluation data is then used to select appropriate road profile segments from the journey database which approximate the distribution journey's road profile.

4. *Account for speed* – using either the speed profile information from the journey data or speed limits, the spatial road profile approximation is converted to displacement versus time.

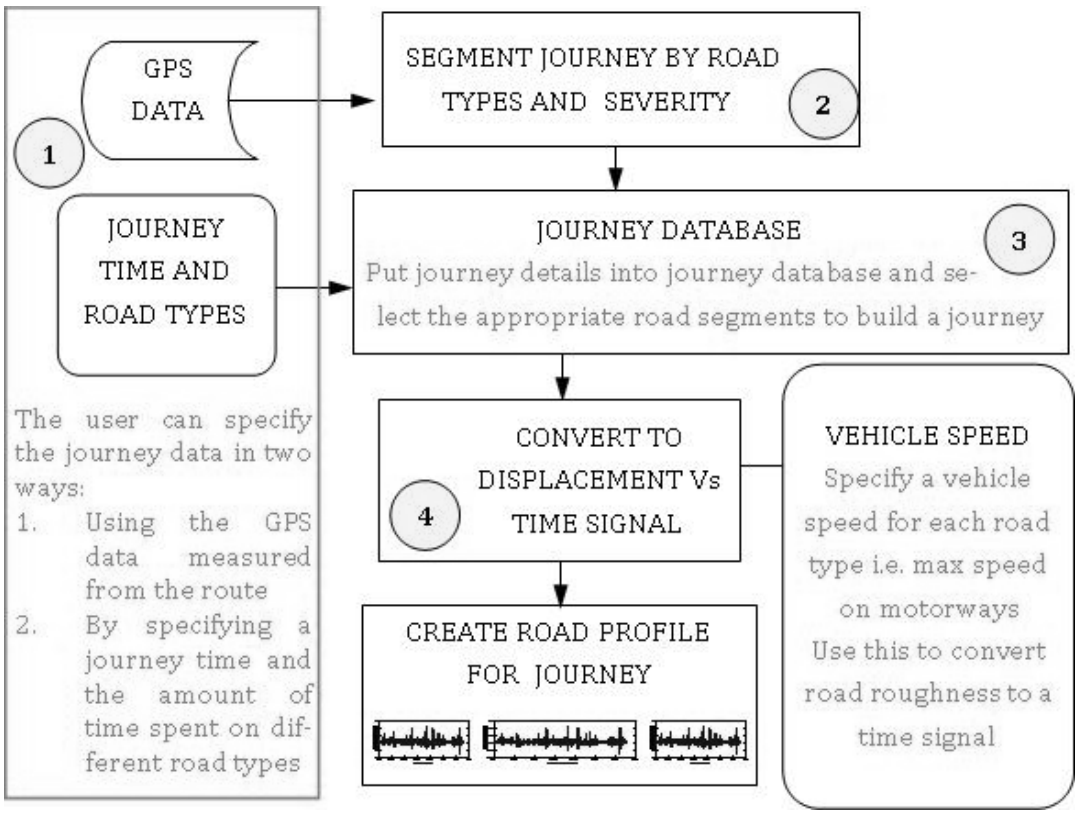

Figure 145: Building a journey

10.7 Creating a Vehicle Vibration Approximation

The road profile approximation from section 10.6 can be used as an input into a quarter vehicle model of the intended distribution vehicle in order to produce an approximation of the vehicle's vibration response. Creation of an approximation of the vehicle's vibration response is a three stage process, which is described below and presented schematically in Figure 146.

1. *Find or calculate vehicle parameters* - The vehicle parameters for the distribution vehicle need to be found. These are: sprung mass (M_V); unsprung mass (M_T); suspension stiffness (K_S); suspension damping (C_S); tyre stiffness (K_T); and, tyre damping (C_T). If the specific vehicle's parameters are not directly available, they can be approximated using one of three methods:

a. *Parameter approximation* - using only the vehicle's sprung mass and unsprung mass (these are typically specified by the manufacturer), the remaining vehicle parameters can be approximated using an estimate of the vehicle's natural frequencies.

The suspension and tyre stiffness K_S and K_T can be approximated by considering each as part of a SDOF mass spring damper system with an external force, $F = 0$ and no damping ($C = 0$). The equation of motion for a SDOF system can be defined as:

$$-M_V \ddot{x} + C\dot{x} + Kx = F \tag{53}$$

where x can be defined as $Xe^{-i\omega t}$ (Equation 40). By then rearranging Equation 53, the following relationships for approximating the suspension and tyre stiffness, can be found:

$$K_s = M_V \omega_1^2 \qquad \text{and} \qquad K_T = M_T \omega_2^2 \tag{54}$$

where $\omega_1 = 2\pi f_1$ and $\omega_2 = 2\pi f_2$ where f_1 and f_2 are the first and second natural frequency, these are typically in the ranges 1 – 5 Hz and 10 – 15 Hz, respectively.

By again considering the free vibration of the system ($F = 0$), an approximate value of the suspension damping coefficient (C_S) can be found as the roots of the characteristic equation:

$$-\omega^2 + \frac{C}{M}\omega + \frac{K}{M} = 0$$

$$\omega = \frac{C}{2M} \pm \sqrt{\left(\frac{C}{2M}\right)^2 - \frac{K}{M}}$$

When $C_C = \sqrt{4MK} = 2M\omega$ the system is critically damped. The suspension damping, C_S, can then be defined as:

$$C_S = \xi\sqrt{4M_V K_S} = \xi C_C \quad (55)$$

where ξ is the damping ratio, with a value between 0 to 1.

Because of the assumptions made when approximating the vehicle parameters this way, an iterative approach should be used in order to refine parameter values to ensure sensible results.

b. *Vehicle database* – Previously used vehicle data that is stored within a database allows the user to select a representative vehicle. Example vehicle parameters used in previous studies are given in Table 34. These parameter values provide a basis for the vehicle database.

For the purpose of this Thesis vehicle parameters have been estimated using method a, parameter approximation.

2. *Build distribution vehicle model* – The vehicle parameters are then used to create a quarter vehicle model in Matlab.

3. *Calculate approximation of vehicle vibration response* - By running the road profile through the quarter vehicle model, the approximate vehicle response can be determined.

Table 34: Vehicle model parameters

VEHICLE	QUARTER TRUCK (Cebon, 1993)	QUARTER CAR (Verros et al, 2005)	FULL CAR (Sun and Cui, 2001)	HALF CAR (Gao et al, 2007)	QUARTER CAR (Gobbi et al, 2006)	UPPER-LOWER LIMITS (Gobbi et al, 2006)	HALF CAR (Gopala and Narayanan, 2008)	HALF SEMI TRAILER (Law and Zhu, 2005)
M_V (kg)	3,900	375	1,200	1,794.4	229	-	730	3,930 (Cab) 15,700 (Trailer)
M_T (kg)	484	60	125	87.15 (Front) 140.4 (Rear)	31	-	40 (Front) 35.5 (Rear)	220 (Front) 1,500 (Middle) 1,000 (Rear)
K_S(kN/m)	878	15	50	66.8244 (Front) 18.615 (Rear)	25	0-80	19.96 (Front) 17.5 (Rear)	2,000 (Front) 4,600 (Middle) 5,000 (Rear)
C_S (Ns/m)	17,500	1,425	6,000	18,615	1,000	0-5,000 (Passive) 0-700,000 (Active)	1,290 (Front) 1,620 (Rear)	5,000 (Front) 30,000 (Middle) 40,000 (Rear)
K_T (kN/m)	1,490	200	400	101.115	120	0-700	175.5 (Front) 175 (Rear)	1,730 (Front) 3,740 (Middle) 4,600 (Rear)
C_T (Ns/m)	1,755	7	-	-	-	0-50,000	-	1,200 (Front) 3,900 (Middle) 4,300 (Rear)
Pitch Inertia (m4)	-	-	2,100	3,443.05	-	-	1,230	-
Roll Inertia (m4)	-	-	1,800	-	-	-	-	-

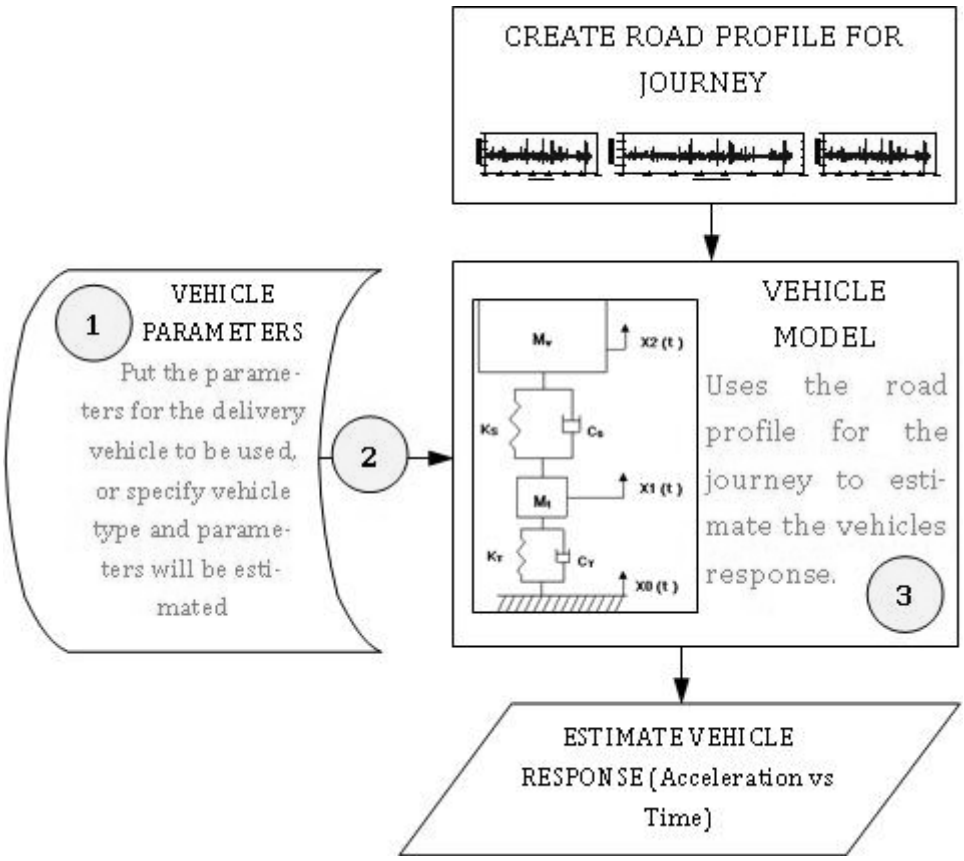

Figure 146: Creating a vehicle vibration approximation

10.8 Concluding Remarks

The journey database has been proposed as a method of creating representative vehicle vibration profiles, to simulate a specific distribution journey and vehicle. The three main aspects of the database have been discussed, these are: database population, data classification and journey simulation.

Three methods of data acquisition were presented. Of these, two methods allowed the accurate reproduction of the road surface roughness, these were: using a profilometer and using a inverse quarter vehicle model to approximate road profile from vehicle vibration.

During this Thesis the inverse vehicle model method has been presented. Although the method allows the non-Gaussian and non-stationary nature of the

road surface roughness to be presented, there are certain limitations pertaining to the use of the quarter vehicle model. Many of these limitations have been discussed previously in section 9 and relate to the error in simulating dynamic parameters as static values and additionally to approximation of these parameters. In many cases the exact suspension and vehicle dynamics are not known and therefore an approximation has to be made. The effect of errors, in the approximation of parameters, on the calculated vehicle response was evaluated in section 9.6.

The calculated road profiles are stored within the database. To enable simple and efficient selection, the road profiles are segmented and categorised based on the road type and condition. Road types are defined through the GPS data from the journey and the condition of the road is classified based on the displacement PSD and the RMS displacement distribution.

To then enable the simulation of a journey, either the GPS data or an approximation of road type and duration is used to assimilate data from the journey database. By classifying road profiles within the database by severity a more representative road profile can be built to suit the region of distribution's road conditions.

With a road profile approximating the distribution journey, the quarter vehicle model is used to simulate the distribution vehicle. The inclusion of the vehicle model enables the consideration of the actual distribution vehicle's dynamics. Altogether, this creates a vehicle vibration signal that is representative of the actual distribution journey and vehicle.

The concept of the journey database has been defined. In order to evaluate its ability approximate distribution journey vibration accurately, a case study, using a worked example is required.

11 AN IMPROVED TEST REGIME FOR VIBRATION TESTING OF DISTRIBUTION PACKAGING

By combining the journey database with the wavelet decomposition method, a complete test regime for simulating vehicle vibration for the testing of distribution packaging can be constructed. The process of constructing a simulation using the improved test regime is illustrated in Figure 147.

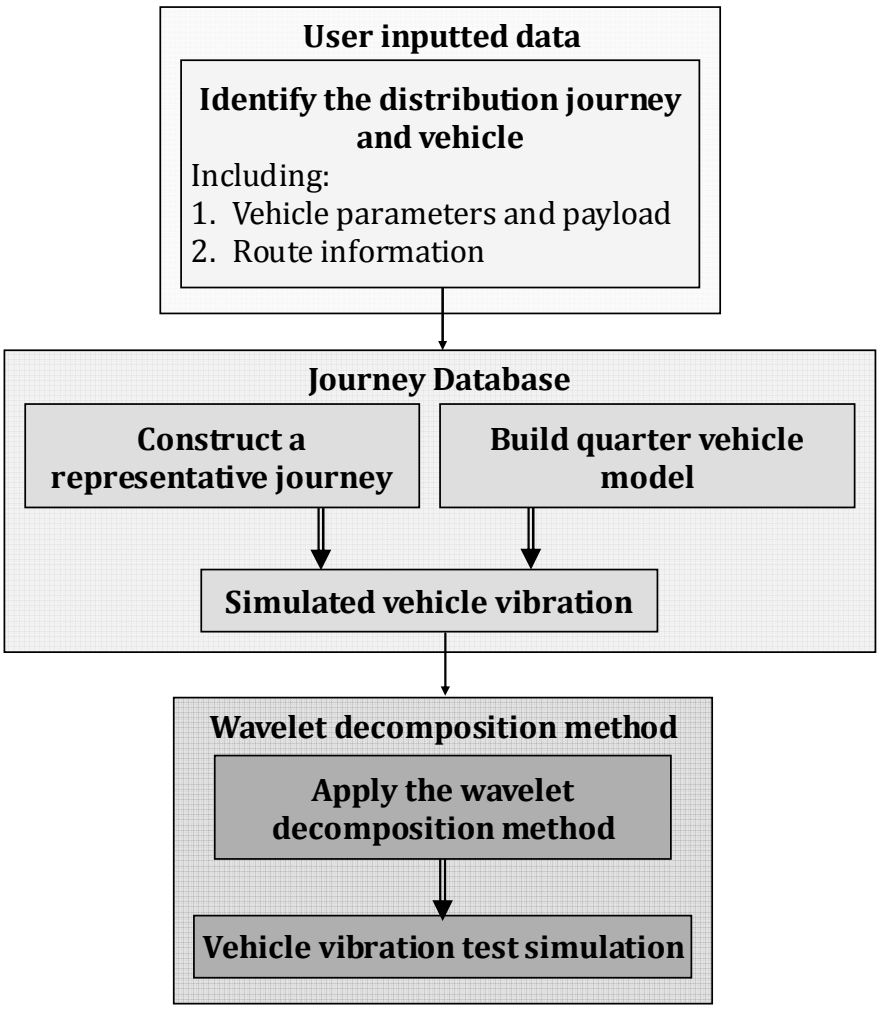

Figure 147: The process of constructing a simulation using the improved test regime

There are three key stages involved in the improved test regime, these are:

1. *User inputted data* – In order to create a test simulation the user must enter information regarding the distribution journey and vehicle, as explained in sections 10.6 and 10.7.

2. *Journey database* – A simulated vehicle response is then constructed using the journey database, by:

    a. Using the journey information to construct an approximation of the road profile for the distribution journey.

    b. The vehicle information is used to construct a quarter vehicle model of the distribution vehicle, whereby an approximation of the vehicle's response to the road profile can be constructed.

3. *Wavelet decomposition method* – A vibration test simulation is then created from the approximate vehicle vibration by applying the wavelet decomposition method.

11.1 Evaluating the Improved Test Regime

The journey database has been proposed as a method of creating a representative vehicle vibration profile for a given distribution journey and vehicle. In order to illustrate and evaluate the appropriateness of the journey database an example database has been used to construct a simulation based on a known distribution vehicle and journey. Once constructed, this simulation will be compared with a measured vibration profile from an actual distribution journey. Following this the wavelet decomposition method will be used to construct a test simulation using the vehicle vibration produced from the journey database. This will then be compared to the original vehicle vibration, evaluating the appropriateness of the improved test regime.

11.1.1 Constructing a Simulation Journey

The example distribution journey used in this study is that of a home delivery journey around parts of Staffordshire and Shropshire, UK. The simulated distribution journey was then created using vibration data measured on a distribution journey around Bath, UK. These areas are highlighted on the map given in Figure 148.

Figure 148: Location of distribution journey and location where journey database data was collected.

The distribution journey being simulated is then illustrated in Figure 149. The distribution vehicle that was used during the data collection in Bath, UK was a Ford Luton box van shown in Figure 88. The delivery vehicle used on the home delivery journey to be simulated was a Ford Transit short wheel base van.

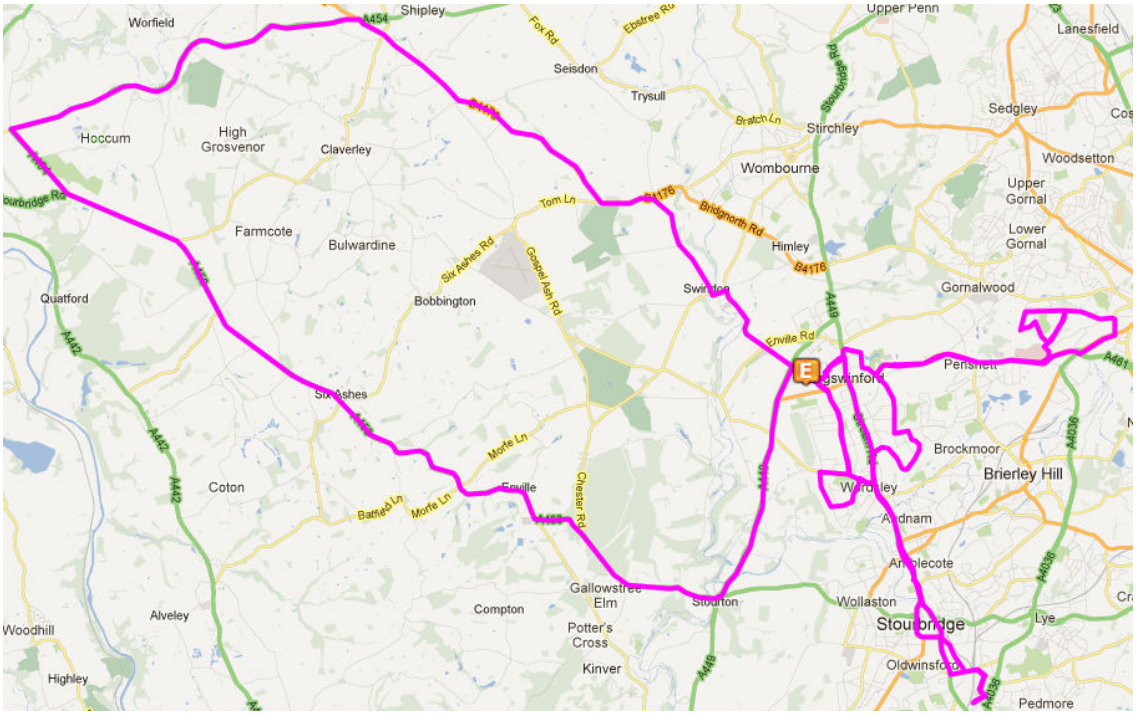

Figure 149: Distribution journey around Shropshire and Staffordshire

The vibration profile of the Ford Transit, on the distribution journey given in Figure 149 is given in Figure 150.

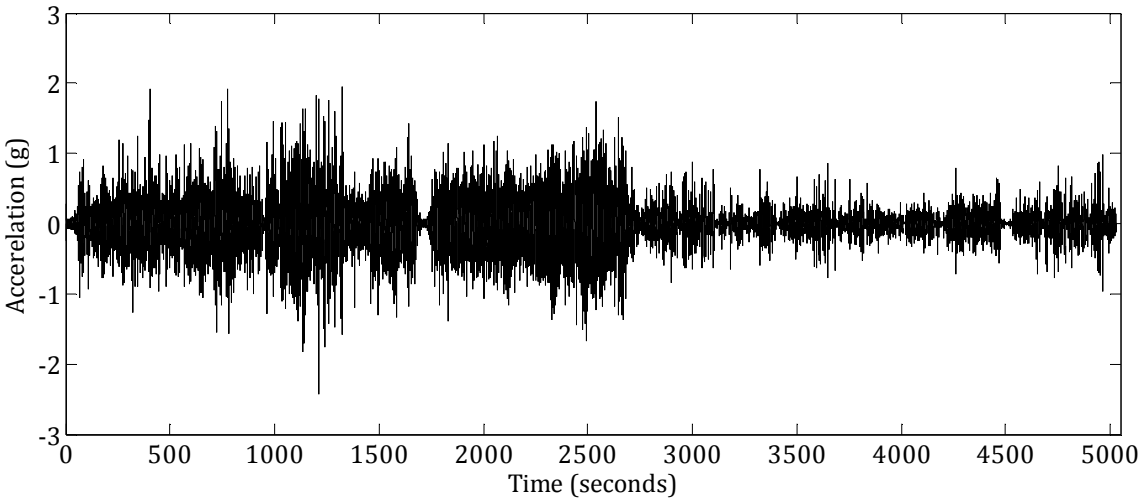

Figure 150: Time history vibration profile for Ford Transit van

The GPS data from the distribution journey was analysed using the specially designed Matlab code. The distance travelled on each of the road classifications was found, together with the speeds at which the vehicle travelled. This information is presented in Table 35.

Table 35: Break down of distribution journey classification

ROAD TYPE	DISTANCE (m)	TIME (secs)	SPEED																		Average Speed (km/hr)
			x<=10		10 < x <= 20		20 < x <= 30		30 < x <= 40		40 < x <= 50		50 < x <= 60		60 < x <= 70		70 < x <= 80		80 < x <= 90		
			No	Dist (m)	No	Dist (m)	No	Dist (m)	No	Dist (m)	No	Dist (m)	No	Dist (m)	No	Dist (m)	No	Dist (m)	No	Dist (m)	
1	0	0	0	0	0	0	0	0	0	0	0	0	0	0	0	0	0	0	0	0	
2	22092	1585	13	1081	8	687	10	695	9	768	40	2730	68	4260	125	8842	44	3029	0	0	**50**
3	0	0	0	0	0	0	0	0	0	0	0	0	0	0	0	0	0	0	0	0	
4	28226	2860	48	1562	52	2554	114	5774	136	6305	89	4400	78	4114	41	2436	14	1082	0	0	**36**
5	7496	935	42	1901	24	903	23	1135	31	1047	53	1838	14	673	0	0	0	0	0	0	**29**
6	670	215	24	78	5	102	11	359	3	131	0	0	0	0	0	0	0	0	0	0	**11**
7	2614	280	2	33	4	63	11	377	24	1260	15	881	0	0	0	0	0	0	0	0	**34**
8	0	0	0	0	0	0	0	0	0	0	0	0	0	0	0	0	0	0	0	0	
9	0	0	0	0	0	0	0	0	0	0	0	0	0	0	0	0	0	0	0	0	
10	0	0	0	0	0	0	0	0	0	0	0	0	0	0	0	0	0	0	0	0	
11	0	0	0	0	0	0	0	0	0	0	0	0	0	0	0	0	0	0	0	0	
12	0	0	0	0	0	0	0	0	0	0	0	0	0	0	0	0	0	0	0	0	
13	0	0	0	0	0	0	0	0	0	0	0	0	0	0	0	0	0	0	0	0	
Total (km)/ (MINS)	**61**	**98**																			

An approximate distribution journey was then constructed from the journey database, which contained vibration data from distribution journeys around Bath, in the Ford Luton box van. Information on the different road segments that were used to build a distribution journey is given in Table 36 and in Table 42 and Table 43. This information includes the road type, condition, the average expected speed and the duration of the vibration segment.

Table 36: Road classification of data in journey database

ROAD	ROAD TYPE	CONDITION	EXPECTED SPEED (km/hr)
University	5	Good	32
Bathwick Hill	4	Poor – Heavily potholed	48
City	4	Good	48
Wells Way	4	Average	48
Oldfield Park	5	Good	40
Oldfield Student	5	Average	32
Lower Bristol Road	3	Good	48
NSL (A4)	2	Good	80
Penn Hill Road	4	Good – Traffic calming	48
Weston	3	Poor	48
Royal Cresent	6	Very poor – Cobbled road	32
Lansdown	4	Good	48
Camden	5	Average – Traffic calming	32
Snow Hill	4	Good	32
Into City	4	Good	48

The parameters for both the Ford Luton Box van and the Ford Transit van have been approximated based on the measured frequency response and manufacturer quoted vehicle masses. These are given in Table 37, for a quarter vehicle.

Table 37: Approximation of the vehicle parameters

PARAMETER	FORD LUTON BOX VAN (35OL)	FORD TRANSIT (SWB) VAN
Sprung mass (kg)	604	438
Unsprung mass (kg)	50	45
Suspension Stiffness (kN/m)	149	117
Suspension Damping (kNs/m)	4	3
Tyre Stiffness (kN/m)	387	348

The vehicle vibration profile built using the journey database, to approximate the actual distribution journey, was then inputted into an inverse quarter vehicle model of the Ford Luton box van, to produce an approximate road profile. This road profile was then inputted into a quarter vehicle model of the Transit van to produce a test simulation. The resulting vehicle vibration profile, approximated from the vehicle model is given in Figure 151.

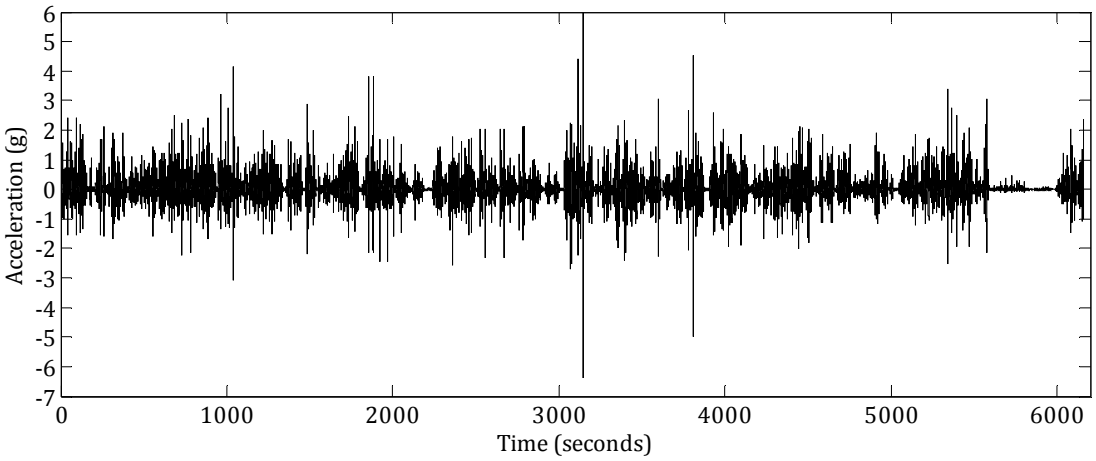

Figure 151: Simulated vehicle vibration using journey database

11.1.2 Comparison of Results

The overall RMS acceleration, kurtosis, and maximum and minimum acceleration level for both the original vehicle vibration signal and the simulated signal have been compared in Table 38. The RMS acceleration of the simulated signal is higher than the original with 6% error. Additionally, the kurtosis of the simulated signal is also higher than the original due to the variation in peak accelerations.

Table 38: RMS acceleration, kurtosis and minimum and maximum acceleration levels

Journey	RMS ACCELERATION (g)	Kurtosis, *k*	Maximum (g)	Minimum (g)
Original	0.1410	19	4	-2.4
Simulated	0.1489	31	6	-6.4

The RMS acceleration distributions of one second samples for the original and simulated signal are illustrated in Figure 152. The distribution appears similar, particularly above 0.15g. This shows good correlation between the two signals.

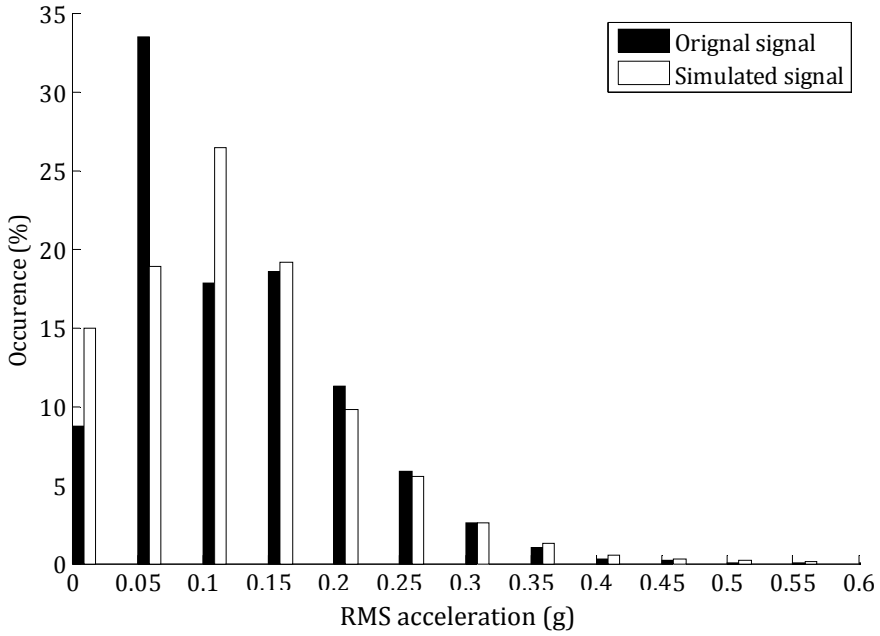

Figure 152: RMS acceleration distribution for the original signal and simulated signal

In Figure 153, the PSDs for both the original signal and the simulated signal are also shown to have good correlation.

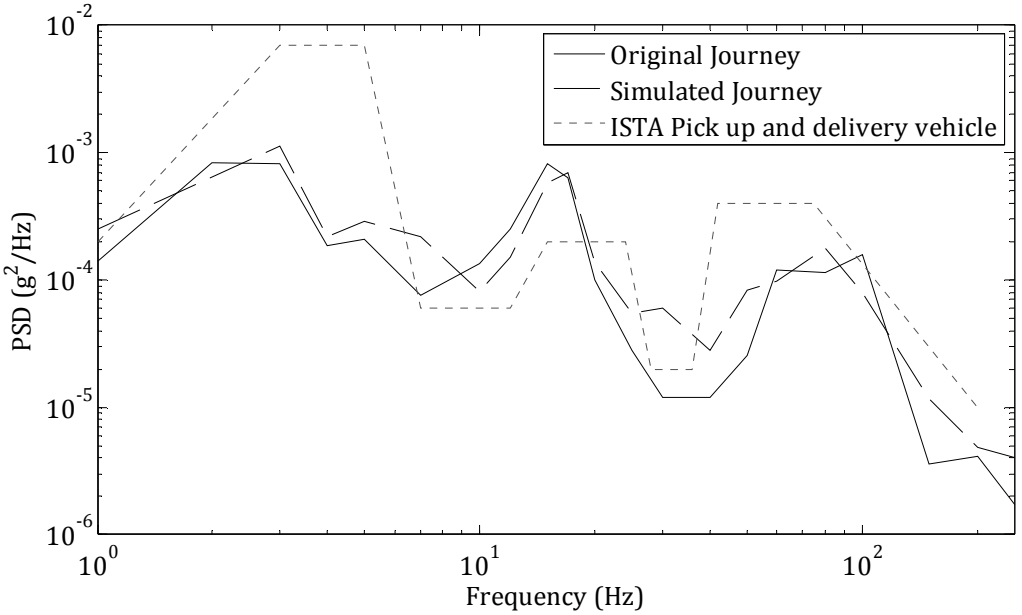

Figure 153: PSDs for the original signal and the simulated signal

Whilst the simulated signal's PSD does not match the original signals perfectly, the overall shape and amplitude is similar. Because of variations in road profiles, the assumed static vehicle parameters and the constant fluctuations in vehicle speed, it

would be difficult, if not impossible, to simulate a perfect match in the spectral shape.

For reference purposes, the PSD provided in the ISTA standards for the vehicle type relating to that used in this study, has been illustrated on Figure 153. This PSD shows a much higher frequency component in the low frequency range (1 – 7 Hz) and overall does not show good correlation to the actual vehicle vibration's PSD.

11.1.3 Comparison using Wavelet decomposition

The simulated vehicle vibration, created using the journey database, has been evaluated using the wavelet decomposition method. The simulation signal produced is illustrated in Figure 154. The signal's non-stationarity is evident.

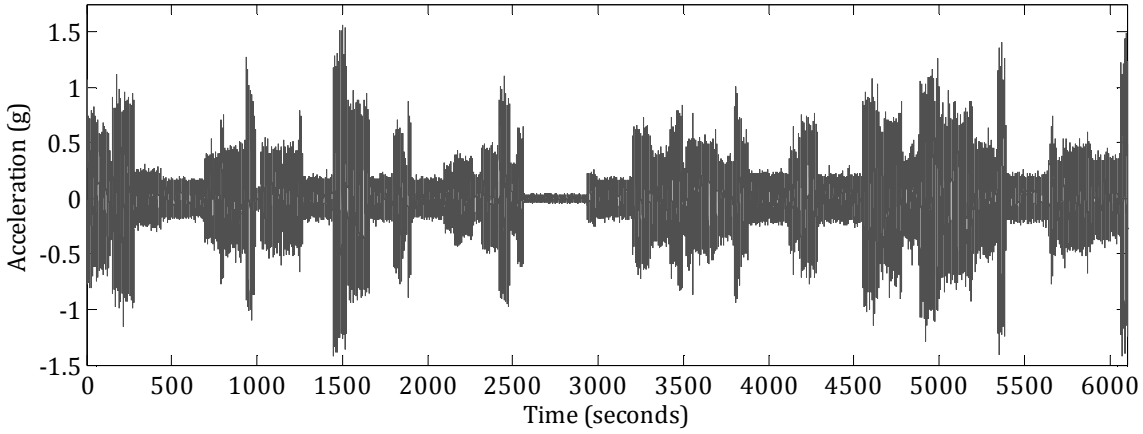

Figure 154: Simulated journey's wavelet decomposition simulation signal

In Table 38, the signal's RMS acceleration, kurtosis and maximum and minimum acceleration levels, are displayed alongside the original signals. The overall RMS acceleration is similar with only 3.5% error. The simulated signal's kurtosis signifies that the signal has a non-Gaussian distribution. The peak acceleration levels of the simulated signal are lower than the original signal's, this is due to averaging when creating the signal.

Table 39: RMS acceleration, kurtosis and minimum and maximum acceleration levels

Journey	RMS ACCELERATION (g)	Kurtosis	Maximum (g)	Minimum (g)
Original	0.1410	19	4	-2.4
Wavelet decomposition of simulated	0.1460	7.5	1.5	-1.4

The RMS acceleration distribution using one second samples for both signals, is displayed in Figure 155. It can be seen that the simulated signal's RMS acceleration distribution correlated very well with the original signals distribution.

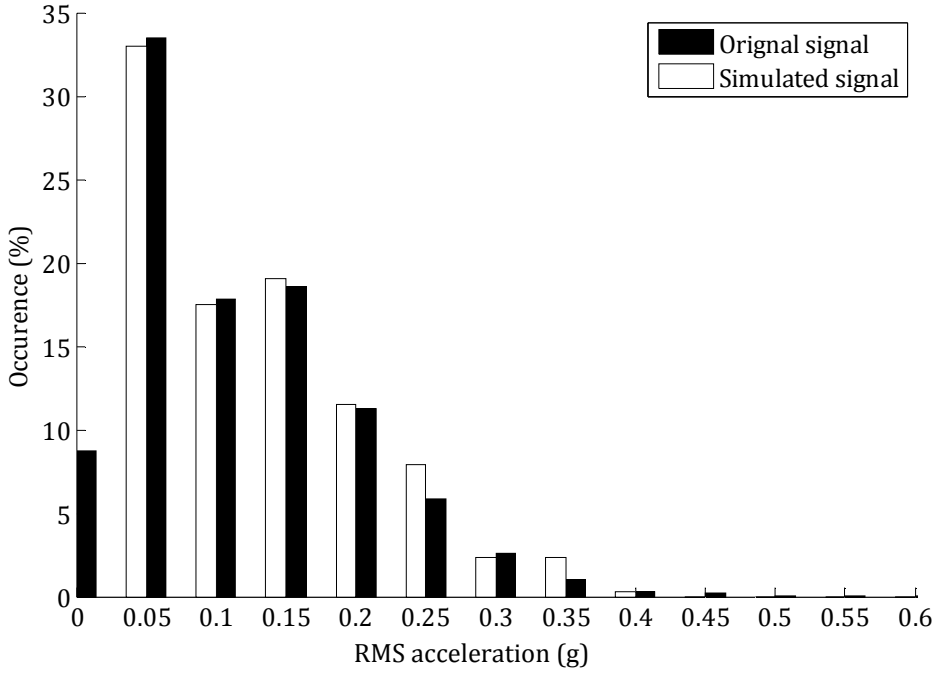

Figure 155: RMS acceleration distribution of the original signal (Figure 150) and the simulated signal (Figure 154)

The PSD of the simulated signal has also been compared with the original signal's PSD, this is illustrated in Figure 156. Although there is some disparity in the two spectra, the spectral peaks, in both spectra are similar, therefore the simulated signal provides a good representation of the original vehicle vibration.

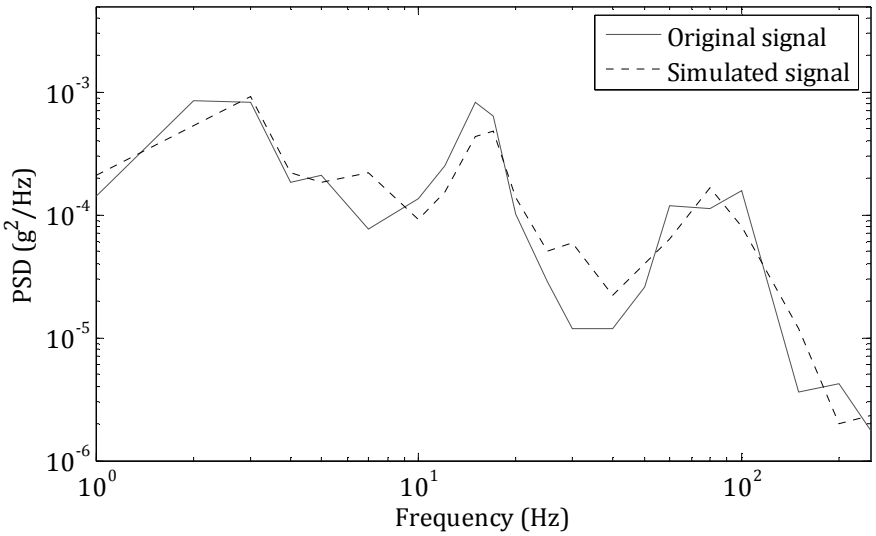

Figure 156: PSD of the original signal (Figure 150) and the simulated signal (Figure 154)

11.2 Concluding Remarks

Within this chapter, the improved test regime has been presented and demonstrated using a case study. The improved test regime includes: the journey database, which uses both the inverse quarter vehicle model and the quarter vehicle model; and, the wavelet decomposition simulation method.

In section 11.1.1 the journey database has been used to construct a representative vibration signal (Figure 151) for the specified distribution journey and vehicle (Figure 150). The simulated vibration has then been compared to the actual vibration signal, acquired during the distribution journey. It was found that the simulated signal match relatively well with the actual vibration signal, showing good correlation with its PSD and RMS acceleration distribution. This example therefore proves that the journey database can be used to construct a representative vibration profile. To further validate the journey database additional journey simulations are required.

Some discrepancies were seen within the journey database's simulated vibration signal. This was due to the presence of some high amplitude shock events within the journey database data. This could be removed by using lower sampling rates or filtering signals between a smaller bandwidth (currently 1 – 200 Hz is used).

Discrepancies between the actual vehicle vibration and the simulated vibration signals may also exist due to errors in the approximation of vehicle parameters.

Following the construction of a representative journey, the wavelet decomposition method was used to create a simulation for laboratory use (Figure 154). This simulated signal was compared to the original distribution journey (Figure 150) and was found to correlate well, with the spectral peaks of the simulated signal's PSD being at similar frequencies and amplitudes as the actual vehicle vibration's spectral peaks. Additionally, the RMS acceleration distribution of the simulated signal closely matched that of the actual vehicle vibration.

The wavelet decomposition method was also used in section 8.2 and section 8.5 to construct simulations. In both of these examples the PSD of the simulated vibration correlated well with that of the original vibration. But, in both examples, the RMS acceleration distribution of the simulated signal did not correlate as well as the simulation produced in this example. In both of the previous examples fewer iterations were carried out during the decomposition, hence a less detailed decomposition occurred. It is evident from the improvement in the correlation of the simulated signal in this example with the original signal, that increasing the number of iterations can improve the accuracy of the simulated signal.

12 CONCLUSIONS AND FUTURE RESEARCH

The aim of this Thesis was to create an improved method for simulating vehicle vibration for the testing of distribution packaging, with a particular focus on building a representative test regime generated from an understanding of road conditions and vehicle dynamics. A key constraint in the formulation of the new test regime was that the approach used to simulate the vibration must be usable on all existing laboratory controllers. The need for this research has been highlighted through the review of current literature and the evaluation of the established method.

To begin with, a comprehensive description of packaging enabled its importance to be conceptualised. It was concluded that, for distribution packaging, meeting the logistical and safety needs of the product/s is vital in creating a successful packaging solution. This is because distribution packaging not only facilitates distribution, but also provides the product with the necessary protection from the distribution environment. To support and expand on this conclusion, a detailed review of the distribution cycle and all its stages was presented. Vehicle vibration and shock, during distribution, were highlighted as key contributors to product damage. With an understanding of the damage potential, an overview of pre-distribution tests for packaging and the commonly used standards was presented, covering: drop/impact testing; climatic testing; compression testing; and, vibration testing.

Combining the protective requirements of the packaging solution with the need for sustainability, forces the need for the optimisation of packaging. In order to do this with confidence there is a need for accurate pre-distribution testing of packaging.

Focusing on the specific hazard of vehicle vibration and shock, the key characteristics of vehicle vibration were defined. This in turn enabled a detailed

critique of the established method of pre-distribution vibration testing, identifying the benefits and limitations of the method. Limitations included: the inaccurate representation of vehicle vibration as stationary with a Gaussian distribution; the use of global data to represent all journeys and vehicles; and, using a method of test acceleration not intended for distribution testing.

To eliminate the limitations of the current method, a review of improved simulation approaches, suggested in current literature, was carried out. A correlation study evaluating the ability of each of the approaches to recreate product damage was also completed. This showed that the modulated RMS approach correlated most closely with a benchmark time replication vertical vibration simulation.

The need for MDOF simulation was considered and a case study measuring product damage was performed. This revealed that in the majority of loading configurations SDOF testing was adequate.

Alternative methods of signal analysis, using both the time and frequency domain, were analysed in order to evaluate their ability to capture the characteristics of vehicle vibration. This analysis highlighted the variation in the frequency content of the signal over time. The findings from this research were then used to construct a new and improved simulation method, referred to as wavelet decomposition.

This method was created with the specific intent that it would be usable on existing laboratory controllers. Therefore the method enables a simulation to be defined as a series of stationary segments with Gaussian distributions, allowing each to be simulated from its PSD. When simulated in series, these segments then create a signal that is non-stationary and has a non-Gaussian distribution.

A correlation study was used to evaluate its effectiveness, with the results of this study showing that the wavelet decomposition method correlated closely with time history vertical vehicle vibration.

Following this, focus was drawn to the issue of global data sets in the current testing standards. A method for constructing a more representative simulation,

referred to as, the journey database, was then presented and evaluated in a final case study.

By combining the wavelet decomposition method with the journey database, a new improved pre-distribution vibration test regime was created.

The Research Questions developed in section 1.4 and how they have each been addressed are now considered.

12.1 Research Question 1

How can the effect of a vehicle's parameters and its journey conditions on the vehicle's vibration response be characterised?

Prior to answering this Research Question the characteristics of vehicle vibration had to be found. In this Thesis, vehicle vibration has been shown to be random, highly non-stationary and to have a non-Gaussian distribution. With this known, the first research question could be addressed.

The solution to this problem was to create an improved simulation method using time-frequency analysis. The method, referred to as wavelet decomposition, uses the Continuous Wavelet Transform (CWT) to decompose a vehicle vibration signal in to a number of approximately Gaussian parts (Gaussian approximations).

Each of the Gaussian approximations can then be defined by its PSD and duration. A simulation signal is then formed by randomly applying each of the PSD for the corresponding duration. This results in a simulation signal that overall is non-stationary with a non-Gaussian distribution.

By simulating vehicle vibration using the wavelet decomposition method, the signal's non-stationary nature and its non-Gaussian distribution can be simulated, with the additional advantage, that by simulating each Gaussian approximation

based on its PSD, the method is adaptable for: existing controllers; test acceleration; and, signal averaging.

Three key objectives were set in order to address this Research Question. These are now discussed.

- ***Objective 1 - Evaluate current packaging vibration test methods through comparison with actual vehicle vibration in order to enable the identification of critical parameters.***

To evaluate the current pre-distribution vibration test for packaging, referred to as the established method, both the techniques used within the method and the resulting simulation were analysed. Consequently it was shown that, using a frequency domain analysis technique and subsequently describing vehicle vibration using the average PSD, false assumptions about the nature and characteristics of vehicle vibration are made, namely, that it is stationary with a Gaussian distribution. Further, the method of test acceleration to reduce duration, which is based on fatigue theory, was also shown to make false assumptions about the nature of vehicle vibration. These include the assumptions that: it is a single level vibration; that all components of the packaged product have a single fatigue rate; and, that product damage is due to fatigue failure and not threshold level damage.

By then using the established method to simulate vehicle vibration, the resulting signal differs from the actual vehicle vibration both visually and statistically. The established method produces a Gaussian signal and therefore the high level discrete shock events, apparent in actual vehicle vibration, do not appear in the simulation. Furthermore, the simulated signal is also stationary.

Although the established method made many false assumptions and had limitations, it use of signal averaging and its allowance for the averaging of multiple signals, enabled the simulation to have statistical significance. Furthermore, the established method has gained user confidence through its use in past testing, and, can be applied to most current laboratory controllers.

It was therefore concluded that in order to accurately simulate vehicle vibration, the simulation technique should account for the signal's non-stationary and non-Gaussian nature, whilst still enabling the produced simulation to benefit from statistical significance and hence confidence in the simulation produced. It was also deduced that in order to gain user confidence in any new simulation approach, correlation studies to measure product damage are required.

- ***Objective 2 – Review improved methods that have been proposed for vibration simulation in order to establish their benefits and drawbacks.***

Improved simulation approaches that have been proposed in previous studies, were described. These included; time replication; shock on random; two way and three way split spectra; RMS modulation; and, kurtosis control. It was concluded that, whilst in theory each of these methods offered improvements on the established method, in order to fully evaluate their ability to simulate the damage caused by vehicle vibration, a correlation study using a specific damage mechanism should be performed.

A case study was carried out to enable a comparison of the level of damage produced using each approach. The damage mechanism of scuffing was evaluated and a specially designed rig was used to quantify the damage.

Results from this study showed that the RMS modulation approach correlated best with the time history simulation. This was an anticipated outcome because the RMS modulation method enabled the non-stationary and non-Gaussian nature of the vehicle vibration to be simulated, using the signals statistical distribution.

The use of SDOF testing to simulate the MDOF vehicle movement was evaluated. A study measuring the damage mechanism of bruising was carried out. The difference in the level of bruise damage between SDOF and MDOF tests for different load configurations was measured. Results from this study led to the conclusion that, in the majority of product load configurations, SDOF vibration testing along the vertical axis was sufficient for modelling product damage.

- ***Objective 3 - Propose a more realistic test simulation which incorporates the key characteristics of vehicle vibration.***

It is apparent that, in order to simulate vehicle vibration as realistically and accurately as possible its inherent non-stationarity and non-Gaussian nature should be accounted for.

The RMS modulation approach appeared to best recreate/match the vehicle vibration with confidence. It incorporates the RMS acceleration distribution and hence the signal non-stationarity, and, by creating a simulation signal constructed from randomly ordered Gaussian signal segments of varying RMS acceleration, is compatible with existing controllers.

All of the improved simulation methods discussed incorporated Fourier analysis to evaluate the frequency content of vehicle vibration. By doing this the spectral shape for the frequency content throughout the signal was constant, based on the signal average. In reality, as with the signal's RMS acceleration, the spectral shape may vary over time.

It was recognised that by using a time-frequency analysis technique, changes in the spectral shape could be identified. The Short Time Fourier Transform (STFT), Continuous Wavelet Transform (CWT) and Discrete Wavelet Transform (DWT) were considered and it was concluded that the CWT was the most appropriate for use in detecting changes in the spectral shape.

Whilst using wavelet analysis allowed for the spectral shape to be considered, it did not present a suitable method for creating an overall simulation approach. It was concluded it was necessary to create a simulation method which was compatible with existing controllers, which incorporated the benefits of the established method together with the improved simulation approaches. To ensure this, the use of Fourier analysis within the simulation method was also required.

With the requirements of the improved simulation approach identified, the Wavelet decomposition method was then created.

The Wavelet decomposition method allows for the RMS acceleration distribution of the signal to be simulated along with the change in spectral shape. This is important as certain vibration events may excite different frequencies. By not simulating the change in spectral content, the additional energy at these frequencies may be missed and hence any additional damage caused by these would not be seen during testing.

To evaluate the appropriateness of the Wavelet decomposition method a correlation study, using the scuffing rig, was carried out. By using this rig the results from the study could be compared with the previous results, from other improved simulation approaches.

The result showed that the Wavelet decomposition method correlated well with time history single axis simulation. In two out of three cases, the Wavelet decomposition method produced approximately 10-13% more damage than the time replication. The third case resulted in approximately 8% less damage than time replication.

By comparison, MDOF simulation created slightly more product damage than SDOF simulation. Therefore, by using a simulation method that provides a slight over test in comparison with SDOF time replication, the small amount of additional damage seen in MDOF vibration can be accounted for.

12.2 Research Question 2

How can the simulation of vehicle vibration for packaging testing be improved so as to create a more representative test regime?

It was established that vehicle vibration was caused by the vehicle traversing the rough road surface. The vehicle's response was then further characterised by the vehicle dynamics. The sensitivity of the vehicle's response to changes in its

dynamics resulted in vehicle vibration that is highly variable and unpredictable. Therefore, in order to define the nature and characteristics of vehicle vibration, the effect that changes in the vehicle dynamics and the initial road input have on the measured response, needed to be analysed. Ultimately, this allows the importance of changes in these parameters to be assessed.

The solution to this Research Question was to create a database of road profile data, which could be used in conjunction with a quarter vehicle model, of the intended distribution vehicle, to calculate an approximation of the vehicle vibration during a specific distribution route.

To build the journey database road profile information was determined from vehicle vibration data was using an inverse quarter vehicle model. The GPS data, collected during the vibration data acquisition, was used to segment the road profiles based on road type. Each road segment could then be further classified by evaluating its road roughness.

A method for simulating a journey was presented. Whereby, the GPS data for the intended distribution journey is evaluated in order to estimate the distance travelled on different road types, including: motorways; A-roads; B-roads; and, country lanes. Using this information, a road profile can be constructed by extracting relevant segments of data, stored within the journey database.

Once an approximation of the road profile is constructed, it can be used, along with the approximate vehicle speed, to simulate the specified vehicle's vertical vibration response.

The objectives set to answer this research question are now addressed.

- ***Objective 4 - Establish the key journey and vehicle parameters that characterise vehicle vibration and propose a method to account for their influence on vehicle vibration.***

In order to identify the vehicle and journey parameters that shape a vehicle's response, a review of previous experimental work that has been reported on in the

literature was carried out. Firstly, the road roughness input was evaluated. This included taking into account: road type; the presence of hazards; and, the geographical location. Road roughness is not globally consistent, but varies from country to country and region to region. Furthermore, the presence of hazards was shown to cause high level shock events in vehicle vibration and the random occurrence of these events meant that they are highly unpredictable. Road types and road construction were also shown to affect the road roughness, with asphalt roads providing a much smoother ride than laterite (unpaved) or concrete roads. This highlighted the need for the consideration of a distribution journey's location and the road types traversed, when creating a simulation test and further demonstrated the significant error induced by the use of a global data set.

Vehicle parameters that further shape a vehicle's vibration response were then considered, including: suspension stiffness and damping; tyre stiffness and damping; vehicle (sprung) mass; the vehicle unsprung mass; and, payload. The relationship between variations in these parameters was then further investigated using a theoretical quarter vehicle model. By analysing these parameters, the importance of their consideration when simulating a distribution vehicle's vibration was made apparent. Seemingly small changes in vehicle parameters affected the vehicle's natural frequencies and transmissibility of vibration and hence ultimately, affected the shape of the vehicle's response. Incorrect simulation of the vehicle's response, may lead to under or over excitation of the packaged product which consequently, will lead to the inaccurate assessment of damage. Although the vehicle's parameters can vary during distribution, static values can be estimated.

Vehicle speed is another parameter that can greatly affect the severity of the vehicle's vibration, where the greater the speed the more severe is the vibration. Whilst small fluctuations in the vehicle's speed will occur continuously, the vehicle average speed can be predicted based on legal speed limits and vehicle speed restrictions.

Whilst all of the parameters so far mentioned can be predicted, the quality of the driving is not easily determined as this is dependent on individual driver behaviour.

Finally, with the effect of journey and vehicle parameters determined, the method by which the vehicle vibration was acquired and measured was then considered. It was found that vehicle vibration was not consistent across the vehicle floor, with some locations providing more severe vibration than others. This meant that when acquiring vehicle vibration, the position at which it is measured must be considered. Additionally, the method by which the data is acquired, whether continuously or through sampling, and, the rate at which it is acquired were shown to affect the measured vibration.

The conclusion was that, whilst an improved simulation method increased the accuracy of the way in which the vibration was simulated, without consideration of the intended distribution journey and the distribution vehicle's parameters, the confidence in the vibration simulation provided was limited. Therefore, in order to increase the confidence in the overall improved test regime, consideration of these parameters must be made.

- ***Objective 5 - Create a database of vehicle vibration data and propose a method by which this data can be used to approximate an alternative distribution journey.***

Following the review of vehicle and journey parameters, it was evident that differences between journeys and vehicles can lead to significant variations in their vibration responses. This therefore meant that the use of a global data set to simulate all vehicles and journeys was not appropriate when accuracy in simulation is required. Because of this, it was decided that in order to create an overall improved test regime, it was necessary to predict a particular vehicle's response and a given distribution journey.

Constraints on time and finance meant that data collection for each distribution journey was not a viable option. It was therefore decided, that to account for

journey variations when simulating vibration, a database of road profile information that can be used to build a representative road profile for a given distribution journey would be created. The journey database provided a method that was not time consuming through reducing the amount of data acquisition required.

The database was populated using an inverse quarter vehicle model to approximate road profiles from a given vehicle's measured vibration. The approximate road profile of a journey was then segmented using the GPS data from the journey on which the vibration was acquired. This enabled the road profile to categorise based on the road type. These road profile segments were then further classified by measuring each segments road roughness.

This meant that when considering the vehicle vibration for a given distribution journey and vehicle a representative vehicle vibration could be calculated using a quarter vehicle model and a road profile built to approximate the distribution journey.

- ***Objective 6 - Create an improved test regime with an integrated vehicle model which allows for the established variations in vehicle and journey parameters to be considered.***

Whilst the journey database enabled the creation of a road profile to approximate the intended distribution journey, a computational quarter vehicle model was then enabled the simulation of the intended distribution vehicle's vibration response. This enabled the vehicle parameters for a particular distribution vehicle to be considered.

The journey database and vehicle model, together with the wavelet decomposition method, have provided an overall improved test regime. This enabled the construction of representative vehicle vibration simulations, improving the accuracy of the established method's simulation approach and data selection.

A case study was carried out, whereby, a given distribution vehicle's vibration on a given distribution route was simulated using the improved test regime. Firstly, the

journey database was used to construct an approximate vehicle vibration based on the distribution vehicle and the GPS data of the distribution route. The approximated vehicle's vibration was compared to the actual measured vibration signal and showed good correlation, matching well the actual vehicle's RMS acceleration distribution and average PSD.

A simulation was then produced using the wavelet decomposition method and the journey database's approximated vehicle vibration. The simulation also correlated well with the actual vehicle vibration.

This study showed that the improved test regime could be used to simulate a given distribution journey and vehicle.

12.3 Contribution to Knowledge

This Thesis has presented a new and improved method for simulating vehicle vibration for the pre-distribution testing of packaging. This test regime consists of two major components:

- *The journey database*

The journey database allows for the creation of a simulation that is representative of a given distribution journey and vehicle. Both the method of populating the database and the method of creating a journey have been presented.

1. Populating the journey database:

    a. An inverse quarter vehicle model has been developed so that the road profile for a given vehicle vibration, can be approximated.

    b. Road profiles are segmented using the journey's GPS data to identify changes in road type e.g. motorway, A-road, B-road, etc.

    c. The displacement PSD relating to each road profile segment is then used to classify the segment's roughness severity.

2. Building a simulation journey:

    a. Deconstructing the intended distribution journey to identify the distance travelled on each road type.

    b. Constructing an approximate road profile from the journey database, based on the intended journey's road types and severity.

    c. Calculate an approximate vehicle vibration for the intended journey and vehicle, using a quarter vehicle model of the distribution vehicle and the approximate road profile.

- *The wavelet decomposition method*

The wavelet decomposition method allows the representative vehicle vibration, calculated from the journey database, to be converted into a test simulation.

Wavelet analysis is used to decompose a signal into a series of Gaussian approximations. By randomly simulating each approximation using its PSD and duration, a simulation signal can be created. Similar to vehicle vibration, the simulated signal is non-stationary with a non-Gaussian distribution. By constructing the simulation from Gaussian segments, and simulating only the vertical vibration, the wavelet decomposition method meets the key constraints associated with existing controllers.

Vehicle vibration is highly non-stationary and has a non-Gaussian distribution. Therefore, applying the wavelet decomposition method will inevitably result in one segment that is highly non-stationary and has a non-Gaussian distribution. This segment will contain the vibration signal's high amplitude shock events. To ensure the wavelet decomposition method is usable for all existing controllers, this segment must be assumed to be stationary and to have an approximately Gaussian distribution, allowing it to be simulated from its PSD. This assumption means that the extreme high level shock events present within this segment will be averaged out and therefore not simulated. This is the main limitation of the wavelet decomposition method.

It should be noted that, because the wavelet decomposition method allows a signal to be decomposed into relatively small segments, the effect of averaging on the intensity of each segment will be significantly less than the effect of averaging on the existing method, where averaging is applied to the signal as a whole.

A further benefit of the wavelet decomposition method is that it allows for test acceleration, by accelerating the PSD of each segment, removing the need for long and arduous simulations.

12.4 Future Research

Several areas of future research have been highlighted. These include:

1. To further build confidence in the overall test regime further experimental work is required.

2. In order to create a more concise and complete journey database and to allow the more accurate creation of an approximate road profile, further data is required.

3. As tri-axial and multi-axial simulation tables become more readily available, it may be more appropriate to simulate vehicle vibration in more than one axis. Therefore, further work evaluating the need for MDOF and how it should be implemented within the test regime, would be required. This includes the implications for the vehicle model and how these would be addressed.

5. In addition, the desirability of test acceleration to reduce test duration, points to the need for evaluation of a suitable method of test acceleration that can be applied to the wavelet decomposition method. Each of these aspects is now discussed.

12.4.1 Further Experimental Work

The ability of both the wavelet decomposition method and the journey database to create improved simulations has been shown through case studies. In order to present a rounded view of the work a case study evaluating both in tandem is required.

Additional correlation studies using products each with a known overriding damage mechanism, should be carried out in order to further demonstrate the accuracy of the wavelet decomposition method and thereby build confidence in the technique.

12.4.2 Additional Data Acquisition

The current journey database is very limited and can therefore only be used to simulate distribution journeys within the UK that are carried out on limited road types and conditions. Therefore, in order to allow for more accurate representations of distribution journeys a more comprehensive journey database is required. Therefore further data acquisition is required to populate the journey database, this should include road profile data from different regions and countries, to account for variations in geographical locations.

12.4.3 The use of MDOF Simulation

The use of MDOF simulation has been discussed and evaluated in this Thesis. The conclusions were that SDOF simulation was sufficient to evaluate product damage during distribution, as long as products were packed in a uniform, stable configuration. The restriction of many existing controllers to the use of single axis testing has been a cause of limitation to the method of simulation. But, with increase in tri-axial and multi-axial simulation rigs, the option for MDOF testing is becoming more viable. Therefore, further research into the effect of MDOF vibration, simulating different combinations of axes e.g. tri-axial or vertical, pitch

and roll, would be beneficial in the further development of the simulation test regime.

The addition of MDOF testing also requires the evaluation of the Wavelet decomposition method in a multi axial configuration, and additionally, the consideration of how the multi axial vibration data is measured when calculated using the journey database and vehicle model.

A further requirement is the need to create a full vehicle model so that all axes can be simulated. This brings with it further complications such as additional parameter information requirements, such as: vehicles inertia and mass distribution.

12.4.4 Development of the Computational Vehicle Model

It has been mentioned that the use of MDOF vibration simulation would require the development of a full vehicle model.

Additionally, the quarter vehicle model could be further developed. This would allow for a more accurate simulation of the intended vehicle. This might include accounting for: tyre and suspension dynamics and variation, or, load fluctuations; this would increase the accuracy of the simulated vehicle vibration.

12.4.5 The use of Accelerated Testing

The established method uses test acceleration based on fatigue theory (section 4.1). The use of this method for accelerating the wavelet decomposition method needs to be examined. Additionally, alternative methods of test acceleration should also be evaluated, with damage correlation studies used to evaluate their appropriateness. Some examples of alternative test acceleration methods are now given.

- ***Use only the most severe amplitudes observed, hence cutting out some of the testing duration***

Vibration, below a certain amplitude, is assumed to cause negligible damage to the specimen and therefore can be removed from the test profile so as to reduce duration. This may seem a valid way of reducing test duration, but it does not consider the effects that the low amplitude vibration may have on the specimen once it has been damaged or 'compromised' by the high level vibration.

In future work this assumption should be tested using correlation studies in its evaluation.

- ***Find the conditions which lead to rapid damage and test at those levels, this again removes some of the test duration***

This is similar to that of the sine sweep test. The specimen is subjected to the range of frequencies from the measured environment at which it resonates for an extended period of time. This could be done by locating the frequency range over which the transmissibility is greater than one, creating a test simulation using only frequencies in that range.

This method of test acceleration would lead to an unrealistic simulation, since it subjects the specimen to the worst possible conditions it could experience, for an extended period of time. In reality, it may only be subject to such conditions for a very limited amount of time and hence, its effect would not be so great.

- ***Increase the frequency of the applied vibrations, hence 'compacting' the test.***

Farrar et al (1999) gives the following example of the use of this method *'…a component subjected to a low-frequency shipboard vibration environment say 20 H. sinusoidal. If the first mode of the component of interest were, for example, 300 Hz, then, depending on damping, an increase of a factor of 10 in the test frequency, without an amplitude change, would reduce the total test time by the same factor. Increasing the magnitude of the input signal appropriately could be used to further compress the test time….*'

'*Increasing vibration amplitude above the normal levels leading to a reduction in testing time*' and '*Use only the most severe amplitudes observed, hence cutting out*

some of the testing duration', are the most viable methods, as they both accelerate the tests whilst still providing a semi realistic simulation of the distribution environment. Both of these would need comparison with real-time simulation to see how accurate they are for use.

APPENDIX I. PUBLICATIONS RESULTING FROM THIS WORK

I.I. Journal Articles

K. Griffiths, D. Shires, W. White, Prof. P. S. Keogh, Dr B. J. Hicks (2012) Correlation Study Using Scuffing Damage to Investigate Improved Simulation Techniques for Packaging Vibration Testing. *Packaging, Technology and Science.* published online: 2nd July 2012

I.II. Conference Papers

K. R Griffiths, B. J. Hicks, P. S. Keogh, D. Shires (2010) Investigating the Suitability of Testing Standards for Simulating Vehicle Vibrations during Supermarket Home Delivery. *17th IAPRI World Conference on Packaging*. Tianjin, China. October 12th - 16th

K. R Griffiths , P. S. Keogh, B. J. Hicks (2011) Simulating the Transport Environment for Packaging Testing Using a Multi Degree of Freedom Method. *ISTA Transport Packaging Forum 2011.* Florida, USA. April 18th-21st

13 APPENDIX II. REFERENCES

AASHTO (2009) Rough Roads Ahead: Fix it Now or Pay for it Later [Online]. Available: http://roughroads.transportation.org/RoughRoads_FullReport.pdf. [Accessed: 8th September 2012].

Addison, P. (2002) *The Illustrated Wavelet Transform Handbook*. IoP Publishing Ltd. (Accessed 22nd May 2012).

Adeli, H., Z. Zhou & N. Dadmehr (2003) Analysis of EEG Records in an Epileptic Patient using Wavelet Transform. *Journal of Neuroscience Methods,* 123, 69 - 87.

Akansu, A. & R. Haddad (2001) *Multiresolution Signal Decomposition: Transforms, Subbands, Wavelets: Transforms, Subbands, and Wavelets*. Elsevier Academic Press. London, UK.

Association for Safe International Road Travel (ASIRT) (2004) Road Travel Report India [Online]. Available: www.asirt.org.

ASTM (2006) Standard Practice for Performance Testing of Shipping Containers and Systems ASTM D4169 – 09. Philadelphia, USA: ASTM.

Azzi, A., D. Battini, A. Persona & F. Sgarbossa (2012) Packaging Design: General Framework and Research Agenda. *Packaging, Technology and Science*. Online 31st January 2012

Bai, R. (2010) *Lenovo Packaging Specification 45J5387 - Packaging Cosmetic Requirements*. Lenovo Corporation

Barchi, G. L., A. Berardinelli, A. Guarnieri, L. Ragni & C. T. Fila (2002) Damage to Loquats by Vibration-simulating Intra-state Transport. *Biosystems Engineering,* 82, 305 - 312.

Barling, D., R. Sharpe & T. Lang. (2008) Re-Thinking Britain's Food Security [Online]. Available: http://www.soilassociation.org/. The soil Association. [Accessed: 10th June 2012].

Basquin, O. H. (1910) The Exponential Law of Endurance Testing. *Proceedings of American Society for Testing and Materials,* 19, 625 - 630.

Bech-Larsen, T. (1996) Danish Consumers' Attitudes to the Functional and Environmental Characteristics of Food Packaging. *Journal of Consumer Policy,* 19, 339 - 363.

Berardinelli, A., V. Donati, A. Giunchi, A. Guarnieri & L. Ragni (2004) Damage to pears caused by simulated transport. *Journal of Food Engineering,* 66, 219 - 226.

Bernad, C., A. Laspalas, D. Gonzalez, E. Liarte & M. A. Jimenez (2010) Dynamic Study of Stacked Packaging Units by Operational Modal Analysis. *Packaging, Technology and Science,* 23, 121 - 133.

Bernad, C., A. Laspalas, D. Gonzalez, L. Nunez & F. Buil (2011) Transport Vibration Laboratory Simulation; On the Necessity of Multiaxis Testing. *Packaging, Technology and Science,* 24, 1 - 14.

Bhave, S. (2010) *Mechanical Vibrations Theory and Practice*. India: Dorling Kindersley.

Bogsjo, K. (2006) Development of Analysis Tools and Stochastic Models of Road Profiles Regarding Their Influence on Heavy Vehicle Fatigue. *Vehicle System Dynamics: International Journal of Vehicle Mechanics and Mobility,* 44, 780 - 790.

Bogsjo, K., K. Podrorski & I. Rychlik (2012) Model for Road Surface Roughness. *Vehicle System Dynamics,* 50(5), 725 - 747

Boonruang, K., V. Chonhenchob, S. P. Singh, W. Chinsirikul & A. Fuongfuchat (2012) Comparison of Various Packaging Films for Mango Export. *Packaging, Technology and Science,* 25, 107 - 118.

Brundtland. (1987) Our Common Future: the report on the World Commission on Environment and Development. Oxford: The Brundtland Commission.

Bruscella, B., V. Rouillard, & M. Sek (1999) Analysis of Road Surface Profiles. *Journal Transport Engineering*, 125(1), 55 – 59.

BS7853 (1996) Mechanical Vibration: Road Surface Profiles Reporting of Measured Data. *British Standards.* BS 7853:1996

Cabinet Office Strategy Unit (COSU) (2008) Food Matters Towards a Strategy for the 21st Century [Online]. Available: http://www.cabinetoffice.gov.uk-/strategy/work_areas/food_policy.aspx.

Carter, C. R. & D. S. Rogers (2008) A framework of sustainable supply chain management: moving toward new theory. *International Journal of Physical Distribution and Logistics Management,* 38 (5), 360 – 87.

Cebon, D. (1999) Handbook of Vehicle-Road Interaction. lisse, Abingdon. Swets & Zeitlinger

Cheng, C. & D. Cebon (2008) Improving Roll Stability of Articulated Heavy Vehicles using Active Semi-Trailer Steering. *Vehicle System Dynamics,* 46, 373 - 388.

Chonhenchob, V., S. P. Singh, J. J. Singh, J. Stallings & G. Grewal (2012) Measurement and Analysis of Vehicle Vibration for Delivering Packages in Small-Sized and Medium-Sized Trucks and Automobiles. *Packaging, Technology and Science,* 25, 31 - 38.

Chonhenchob, V., S. Sittipod, D. Swasdee, P.Rachtanapun, S. P. Singh & J. Singh (2009) . Effect of Truck Vibration during Transport on Damage to Fresh Produce Shipments in Thailand. *Journal of Applied Packaging Research,* 3 (1), 27 - 38.

Coles, R. & M. J. Kirwan (2011) *Food and Beverage Packaging Technology*. Blackwell Publisher Ltd.

Council of Logistics Management (CLM) (1998) What's it All About?. Oak Brook, IL, USA.

Daubechies, I. (1990) The Wavelet Transform, Time-frequency Localization and Signal Analysis. *IEEE Transaction on Information Theory*. 23 (5) 961 - 1005

Daubechies, I. (1992) Ten Lectures on Wavelets. *CBMS-NSE Regional Conference Series.* Capital City Press.

Department for Environment, Food and Rural Affairs. (DEFRA) (2011) Food Statistics Pocketbook [Online]. Available: http://www.defra.gov.uk/statistics-/files/defra-stats-foodfarm-food-pocketbook-2011.pdf. York, UK. [Accessed: 23rd July 2012].

Department for Transport (DfT) (2012) Prevention and a Better Cure: Potholes Review [Online]. Available: http://www.dft.gov.uk/publications/pothole-review/. London, UK. [Accessed: 15th September 2012].

Department for Transport (DfT) (2010) Road Lengths (miles) by Road Type and Region and Country in Great Britain, Annual. London, UK.

Ek, M., G. Gellerstedt & G. Henriksson (2009) Paper Products Physics and Technology. *Pulp and Paper Chemistry and Technology*.

ERM (2003) Environmental Resources Management, Streamlined LCA study of apple packaging systems. Marks & Spencer Plc.

EUROPEN (2009) Packaging in the Sustainability Agenda: A Guide for Corporate Decision Makers. EUROPEN.

EUROSTAT (2008) Packaging waste data 2008, 1000 tonnes. Statistical Office of the European Union. [Accessed: 10th June 2012].

FAO (2004) Globalization of Food Systems in Developing Countries: Impact on Food Security and Nutrition. In *FAO Food and Nutrition Paper*. Rome.

Farrar, C. R., T. A. Duffey, P. J. Cornwell & M. T. Bement (1999) A Review of Methods for Developing Accelerated Testing Criteria. *Proceedings of the 17th International Modal Analysis Conference*, 3727, 608

Gabor, D. (1945) Theory of Communication, Part I: The Analysis of Information. *Journal of the Institution of Electrical Engineers - Part III: Radio and Communication Engineering,* 93 (26), 429 - 441

Garcia-Romeu-Martinez, M.-A., S. P. Singh & V.-A. Cloquell-Ballester (2008) Measurement and Analysis of Vibration Levels for Truck Transport in Spain as a Function of Payload, Suspension and Speed. *Packaging Technology and Science,* 21, 439 - 451.

Garcia-Romeu-Martinez, M. A. & V. Rouillard (2011) On the Statistical Distribution of Road Vehicle Vibrations. *Packaging, Technology and Science,* 24, 451 - 467.

Garret, T. K., W. Steeds & N. Newton (2001) *The Motor Vehicle*. Elsevier Butterworth-Heineman.

Gillespie, T. D. (1985) *Measuring Road Roughness and its Effects on User Cost and Comfort*. American Society for Testing and Materials. (Accessed: 1th June 2012).

Goodwin, D. & D. Young (2011) *Protective Packaging for Distribution*. Pennsilvania, USA. DEStech Publications, Inc.

Hanlon, J. F., R. J. Kelsey & H. E. Forcinio (1998) *Handbook of Package Engineering*. Technomic Publishing Company, Inc.

Harrison, M. (2004) *Vehicle Refinement: Controlling Noise and Vibration in Road Vehicles*. Oxford, UK: Butterworth-Heinemann.

Hartley, L. R., P. K. Arnold (1994) Indicators of Fatigue in Truck Drivers. *Applied Ergonomics,* 25(3), 143 - 156.

Hellstrom, D. & M. Saghir (2007) Packaging and Logistics Interactions in Retail and Supply Chains. *Packaging, Technology and Science,* 20, 197 - 216.

IEA (2003) *IEA Triennial Report, 2001-2003*. Santa Monica, CA, USA.

INCEPN (2008) Packaging in Perspective, Advisory Committee on Packaging. INCEPN.

ISO (2008) ISO BS EN 60068-2-6: Environmental Testing. In *Part 2-6: Tests – Test Fc: Vibration (Sinusoidal)*.

ISO (2009) ISO 11228 Ergonomics. Manual Handling. In *Part 3: Handling of low loads at high*. ISO.

ISO (2009b) ISO 11228. Ergonomics. Manual Handling. In *Part 2: Pushing and pulling*. ISO.

ISO (2009c) ISO 11228. Ergonomics. Manual Handling. In *Part 1: Lifting and carrying*. ISO.

ISTA (2012) Guidlines for Selecting and Using ISTA Test Procedures and Projects. East Lansing, Michigan, USA.

ISTA (2010) Resource Book 2010. East Lansing, MI, USA.

Jalili, N. (2002) *The Mechanical Systems Design Handbook Modelling, Measurement and Control; Chapter 12: Semi-Active Suspension Systems*. USA. CRC Press LLC.

Jarimopas, B., S. P. Singh & W. Saengnil (2005) Measurement and Analysis of Truck Transport Vibration Levels and Damage to Packaged Tangerines during Transit. *Packaging Technology and Science,* 18, 179 - 188.

Jing, L. & Q. Liangsheng (2000) Feature Extraction Based on Morlet Wavelet and its Application for Mechanical Fault Diagnosis. *Journal of Sound and Vibration,* 234, 135 - 148.

Joint Industry Unsaleables Steering Committee (JIUSC) (2006) 2006 Unsaleables Benchmark Report. http://www.gmaonline.org.

Kenco (2012) Terracycle - Out Smart Waste [Online]. Available: http://www-.terracycle.co.uk/en-UK/brigades/the-kenco-eco-refill-brigade-r.html. [Accessed: 10th July 2012].

Kipp, W. I. (2000) (updated 2008). Vibration Testing Equivalence - How Many Hours of Testing Equals How Many Miles of Transport. In *ISTA Conference 2000*. ISTA.

Kipp, W. (2001) Accelerated Random Vibraiton With Time history Shock for improved Laboratory Simulation. In *IoPP Annual Members Meeting*. San Jose, California.

Kipp, W. (2008a) Environmental Data Recording, Analysis and Simulation of Transport Vibrations. *Packaging, Technology and Science,* 21, 437 - 438.

Kipp, W. (2008b) Random Vibration Testing Of Packaged-Products: Considerations For Methodology Improvement. In *IAPRI World Conference on Packaging*. Bangkok, Thailand. ISTA.

Koojiman, J. (2000) Environmental impact of packaging – performance in the household.

Law. S. S. & X.Q. Zhu (2005) Bridge dynamic responses due to road surface roughness and braking of vehicle. *Journal of Sound and Vibration*. 282. 805 – 830.

Leemans, V., H. Magin, M. F. Destain, (2002) On-line fruit grading according to their external quality using machine vision. *Biosystems Engineering*. 83, 397 – 404.

Levy, G. M. (1999) *Packaging, Policy and Environment*. Aspen Publishers Inc.

Liew, K. M. & Q. Wang (1998) Application of Wavelet Theory for Crack Identification in Structures. 124, 152 - 157.

Lin, J. (2001) Feature Extraction of Machine Sound Using Wavelet and its Application in Fault Diagnosis. *NDT & E International,* 34.

Lu, F., Y. Ishikawa, H. Kitazawa & T. Satake (2010) Effect of Vehicle Speed on Shock and Vibration Levels in Truck Transport. *Packaging, Technology and Science,* 23, 101 - 109.

Lu, F., Y. Ishikawa, T. Shiina & T. Satake (2008) Analysis of Shock and Vibration in Truck Transport in Japan. *Packaging Technology and Science,* 21, 479 - 489.

Lutes, L. D. & S. Sarkani. (2004) *Random Vibrations: Analysis of Structural and Mechanical Systems*. Oxford, UK: Butterworth-Heinemann.

Macdonald, J. (1994) Quality in Retail and Distribution. *The TQM Magazine,* 6, 11 - 14.

Mallat, S. (1999) *A Wavelet Tour of Signal Processing*. Elsevier Academic Press.

Marsh, K. & B. Bugusu (2007) Food Packaging - Roles, Materials and Environmental Issues. *Journal of Food Science* 72, 39 - 55.

Marsh, K. S. (1997) *The Wiley Encyclopaedia of Packaging Technology*. 2nd Edition. Wiley. New York, USA.

Meyers, H. M. & M. J. Lubliner. (1998) *The Marketer's Guide to Sucessful Packaging Design*. Chicago, usa. NTC Business Books.

Miege, A. J. P. & D. Cebon (2005) Optimal Roll Control of an Articulated Vehciel: Theory and Model Validation. *Vehicle System Dynamics,* 43, 867 - 893.

Mintel (2012) Food and Drink Packaging Trends - UK, January 2012. London, UK.

MoD (1999) Defence Standard 00-35, Part 5: Induced Mechanical Environments; Ministry of Defence

Nei, D., N. Nakamura, P. Roy, T. Orikasa, Y. Ishikawa, H. Kitazawa & T. Shiina (2008) Wavelet Analysis of Vibration and Shock on the Truck Bed. *Packaging, Tehcnology and Science,* 21, 491 - 499.

Newland, D. E. (1994) *An Introduction to Random Vibrations, Spectral and Wavelet Analysis*. England: Longman Scientific and Technical.

OECD. (2002) *Transport Logistics: Shared Solutions to Common Challenges*. OECD.

Office of National Statistics (ONS) (2011a). Percentage of Unclassified Roads Where Maintenance Should be Considered by Region, England: 2006/06 to 2010/11. Department for Transport. London, UK.

Office of National Statistics (ONS) (2011b). Road Condition Indicator (RCI) Scores by Percentage of Classified Roads, by Local Authority, England: 2006/07 to 2010/11. Department for Transport. London, UK.

Olorunda, A. O. & M. A. Tung (1985) Simulated Transit Studies on Tmatoes; Effects of Compressive Load, Container, Vibration and maturity on Mechanical Damage. *International Journal of Food Science and Technology,* 20**,** 669 - 678.

Otari, S., S. Odof, J. B. Nolot, P. Vasseur, J. Pellot, N. Krajka & D. Erre (2011) Statistical Characterization of Acceleration Levels of Random Vibrations during Transport. *Packaging, Technology and Science,* 24, 177 - 188.

Pacejka, H. B. (2006) *Tyre and Vehicle Dynamics*. 2nd Edition. Oxford, UK. Butterworth-Heinemann.

Paine, F. A. & Paine, H. Y. (1992) *A Handbook of Food Packaging*. Blackie Academic and Professional.

Paull, R. E. (1999) Effect of Temperature and Relative Humidity on Fresh Commodity Quality. *Postharvest Biology and Technology*, 15(3), 263 - 277.

Peleg, K. (1985) Produce-handling, Packaging and Distribution. Haifa, Israel: Department of Argicultural Engineering Technology.

Philip, P., J. Taillard, M. A. Quera-Salva, B. Bioulac & T. Akerstedt (1999) Simple Reation Time, Duration of Driving and Sleep Deprivation in Young Versus Old Automobile Drivers. *Journal of Sleep Research,* 8, 9 - 14.

Pilditch, J. (1972) *The Silent Salesman*. London: Business Books Ltd. Packaging Systems. Environmental Resources Management.

Piringer, O. G., Baner, A. L. (2008) *Plastic Packaging: Interactions with Food and Pharmaceuticals*. 2nd Edition. Wiley.

Pollock, D. S. G. (1999) *Handbook of Time Series Analysis, Sisgnal Processing and Dynamics*. Elsevier.

Rajamani, R. (2012) *Vehicle Dynamics and Control*. 2nd Edition. New York, USA: Springer.

Ramji, K., A. Gupta, V. H. Saran, V. K. Goel & V. Kumar (2004) Road Roughness Measurements Using PSD Approach. *Journal of the Institution of Engineers (India),* 85, 193 - 201.

Rao, T., G. Rao, K. Rao & A. Purushottam (2010) Analysis of Passive and Semi Active Controller Suspension Systems for Ride Comfort in an Omnibus Passing Over a Speed Bump. *International Journal of Research and Reviews in Applied Sciences,* 5.

Richards, D. P. (1990) A Review of Analysis and Assessment Methodologies for Road Transportation Vibration and Shock Data. *Environmental Engineering,* 3.

Riverford (2012) Packaging [Online]. Available: http://www.riverfordenvironment.co.uk/. [Accessed: 16th June 2012].

Robinson, G. (2006) Globalization of the Packaging Supply Chain. In *Dimensions 06*. San Antonio, Texas: ISTA.

Rouillard, V. (2007a) On the Non-Gaussian Nature of Random Vehicle Vibrations. In *Proceedings of the World Congress on Engineering*. London, UK.

Rouillard, V. (2007b) The synthesis of road vehicle vibrations based on the statistical distribution of segment lengths. In *5th Australasian Congress on Applied Mechanics*. Brisbane, Australia.

Rouillard, V. (2008) Generating Road Vibration Test Schedules from Pavement Profiles for Packagin Optimization. *Packaging Technology and Science,* 21, 501 - 514.

Rouillard, V. & M. Lamb (2008) On the Effects of Sampling Parameters When Surveying Distribution Vibrations. *Packaging Technology and Science,* 21, 467 - 477.

Rouillard, V. & M. Sek (2010) Synthesizing Nonstationary, Non-Gaussian Random Vibrations. *Packaging, Technology and Science,* 23, 423 - 439.

Rouillard, V. & M. A. Sek (2000) Monitoring and Simulating Non-stationary Vibrations for Package Optimization. *Packaging Technology and Science,* 13, 149 - 156.

Rouillard, V. & M. A. Sek (2001) Simulation of Non-Stationary Vehicle Vibrations. *Proceedings of the Institution of Mechancial Engineers - Part D - Journal of Automobile Engineering,* 215(10), 1069 - 1075.

Rouillard, V. & M. A. Sek (2005) The Use of Intrinsic Mode Functions to Characterise Shock and Vibration in the Distribution Environment. *Packaging Technology and Science,* 18(1), 39 - 51.

Rushton, A., P. Croucher & P. Baker. (2010) *The Handbook of Logistics and Distribution Management*. Kogan Page Limited.

Sahambi, J. S. (1997) Using Wavlet Transforms for ECG Characterization, An on-line Digital Signal Processing System. *Engineering in Medicine and Biology Magazine,* 16, 77 - 83.

Sainsburys, First Full Range of Milk Bags to Hit UK Supermarkets [Online]. Available: http://www.j-sainsbury.co.uk/media/latest-stories/2010/20100811-first-full-range-of-milk-bags-to-hit-uk-supermarkets/. [Accessed: 28th August 2012].

Saskatchewan Highways and Transportation (SHT) (2001) Standard Test Procedures Manual [Online]. Available: http://www.highways.gov.sk.ca-/indexstp/.

Sek, M. A. (1996) A modern technique of Transportation Simulation for Package Performance Testing. *Packaging Technology and Science,* 9, 327 - 343.

Shiavi, R. (2007) *Introduction to Applied Statistical Signal Analysis: Guide to Biemedical and Electrical Engineering Applications*. Third Edition. Elsevier, 201 - 228

Shires, D. (2011) On the time compression (test acceleration) of broadband random vibration tests. *Packaging Technology and Science,* 4, 75 - 82.

Shires, D. & W. White. 2011. The Comparison of Different Vibration Test Methodologies. In *Transport Packaging Forum,* ed. ISTA. Florida, USA: ISTA.

Singh, B. N. & A. K. Tiwari (2006) Optimal Selection of Wavelet Basis Function Applied to ECG Signal Denoising. *Digital Signal Processing,* 16, 257 - 287.

Singh, J., S. P. Singh & E. Joneson (2006) Measurement and Analysis of US Truck Vibration for Leaf Spring and Air Ride Suspension and Development of Tests to Simulate These Conditions. *Packaging, Technology and Science,* 19, 309 - 323.

Singh, S. P., J. R. Antle & G. G. Burgess (1992) Comparison Between Lateral, Longitudinal and Vertical Vibration Levels in Commercial Truck Shipments. *Packaging, Technology and Science,* 5, 71 - 75.

Singh, S. P., E. Joneson, J. Singh & G. Grewal (2008) Dynamic Analysis of Less-than-truckload Shipments and Test Method to Simulate This Environment. *Packaging Technology and Science,* 21, 453 - 466.

Singh, S. P., A. P. S. Sandhu, J. Singh & E. Joneson (2007) Measurement and Analysis of Truck and Rail Shipping Environment in India. *Packaging Technology and Science,* 20, 381 - 392.

Singh, S. P. & M. Xu (1993) Bruising in Apples as a Function of Truck Vibration and Packaging. *Applied Engineering in Agriculture,* 9, 455 - 460.

Skills (2008) UK Trade performance: Patterns in UK and Global Trade Growth. In *BIS Economics Paper No. 8*.

Smith, A., P. Watkiss, G. Tweddle, A. McKinnon, M. Browne, A. Hunt, C. Treleven, C. Nash & S. Cross. (2005) The Validity of Food Miles as an Indicator of Sustainable Development. DEFRA. http://archive.defra.gov.uk/evidence/economics/foodfarm-/reports/documents/foodmile.pdf

Smith, J. D. (1989) *Vibration, Measurement and Analysis*. UK: Butterworth & Co Ltd.

Smithers Pira (2012) *Distribution and Environmental Testing Facilities and Equipement*. Smithers Pira. Leatherhead, UK

Steedman, P. & T. Falk. (2009) From A to B: A Snapshot of the UK Distribution System. Food Ethics Council.

Suciu, C. V., T. Tobiishi & R. Mouri (2012) Modelling and Simulation of a Vehicle Suspension with Variable Damping Versus the Excitation Frequency. *Journal of Telecommunications and Information Technology,* 1, 83 - 89.

Sun, L., Z. Zhang & J. Ruth (2001) Modelling Indirect Statistics of Surface Roughness. *Journal of Transportation Engineering*, March/April, 105 - 111.

Tang, B., Liu, W., Song, T. (2010) Wind Turbine Fault Diagnosis Based on Morlet Wavelet Transformation and Wigner-Ville Distribution. *Renewable Energy.* 35, 2862-2866.

Tesco. Eco-Friendly Packaging [Online]. Available: http://www.tesco.com/-greenerliving/greener_tesco/what_tesco_is_doing/

Thomson, W. T. (1983) Theory of Vibration with Applications. 2nd Edition. London. *Allen & Unwin*

Timm, E. J., G. K. Brown & P. R. Armstrong (1996) Apple Damage in Bulk Bins During Semi-Trailer Transport. *Applied Engineering in Agriculture,* 12, 369 - 377.

Twede, D. & R. Goddard (1998) *Packaging Materials*. Surrey, UK: Pira International.

Twede, D. & B. Harte (2011) *Food and Beverage Packaging Technology*. Wiley.

Van Baren, P. (2005) The Missing Knob on your Random Vibration Controller. *Sound and Vibration*. October.

Van Zeebroek, M., V. Van Linden, H. Ramon, J. De Baerdemaeker, B. M. Nicolai & E. Tijskens (2007) Impact Damage of Apples During Transport and Handling. *Postharvest Biology and Technology,* 45, 157 - 167.

Voorbij, A. I. M. & L. P. A. Steenbekkers (2002) The Twisting Force of Aged Consumers When Opening a Jar. *Applied Ergonomics,* 33, 105 - 109.

Voortman, C. (2004) *Global Logistics Management*. Cape Town, South Africa: Juta and Co Ltd.

Vursavus, K. F. Ozguven (2004) Determining the Effects of Vibration Parameters and Packaging Method on Mechanical Damage in Golden Delicious Apples. 311 - 320. Cukurova University, Faculty of Agriculture, Department of Agricultural Machinery.

Wallin, B. (2007) Developing a Random Vibration Profile Standard. In *IAPRI Symposium*. Windsor, UK: ISTA.

Wang, Y. S. (2009) Sound Quality Estimation for Nonstationary Vehicle Noise Based on Discrete Wavelet Transform. *Journal of Sound and Vibration,* 324, 1124 - 1140.

Ward, J. (2012) Road Maintenance Review International Comparison. The Chartered Institution of Highways and Transportation.

Wells, L. E., H. Farley & G. A. Armstrong (2007) The Importance of Packaging Design for Own-Label Food Brands. *International Journal of Retail and Distribution Management,* 35, 677 - 690.

Winder, B., K. Ridgway, A. Nelson & J. Baldwin (2002) Food and Drink Packaging: Who is Complaining and Who Should Be Complaining. *Applied Ergonomics,* 33, 433 - 438.

Wong, M. W. (2011) *Discrete Fourier Analysis*. Springer Basel

World Packaging Organisation (WPO) (2008) Market Statistics and Future Trends in Global Packaging [Online]. Available: http://www.worldpackaging.org-/publications/documents/market-statistics.pdf. [Accessed: 12th September 2012].

WRAP (2005) Courtauld Commitment [Online]. WRAP. http://www.wrap.org.uk-/content/courtauld-commitment-1. [Accessed: 10th June 2012]

WRAP (2010) Courtauld Commitment 2 Targets, Progress and Benefits [Online]. Available: http://www.wrap.org.uk/content/courtauld-commitment-2-0. [Accessed: 10th June 2012]

WRAP (2011) Fruit and Vegetable Resource Map: Mapping fruit and vegetable waste through the retail and wholesale supply chain [Online]. Available: http://www.wrap.org.uk/content/resource-maps-fruit-and-vegetable-sector.

WRAP. (2010b) Packaging Optimisation for Whole, Fresh Chicken [Online]. Available: http://www.wrap.org.uk/content/packaging-optimisation-whole-fres-h-chicken London, UK.

Xiang, M., R. Eschke (2004) Modelling of the Effects of Continual Shock Loads in the Transport Process. *Packaging, Technology and Science*, 17, 31 - 35.

Yokohoma. (2003) *Technical Service Bulletin – Tyre Balance, Vehicle Ride and Vibrations* [Online]. Available: http://www.yokohamatire.com/assets/docs/tsb_-TireBalance_12803.pdf

Young, D., R. Gordon & B. Cook. (1998) Quantifying the Vibration Environment for a Small Parcel System. In *TransPack 97*, 157 - 171. Herndon, VA: IoPP.

Yoxall, A., R. Janson, S. R. Bradbury, J. Langley, J. Wearn & S. Hayes (2006) Openability: Producing Design Limits for Consumer Packaging. *Packaging, Technology and Science,* 19, 219 - 225.

Zhou, R., S. Su, L. Yan & Y. Li (2007) Effect of transport vibration levels on mechanical damage and physiological responses of Huanghua pears. *Postharvest Biology and Technology,* 46, 20 - 28.

European Parliament and Council (EPC) (1994) Packaging and Packaging Waste Directive 94/62/EC.

APPENDIX III. TESTING STANDARDS

POWER SPECTRAL DENSITY PLOTS

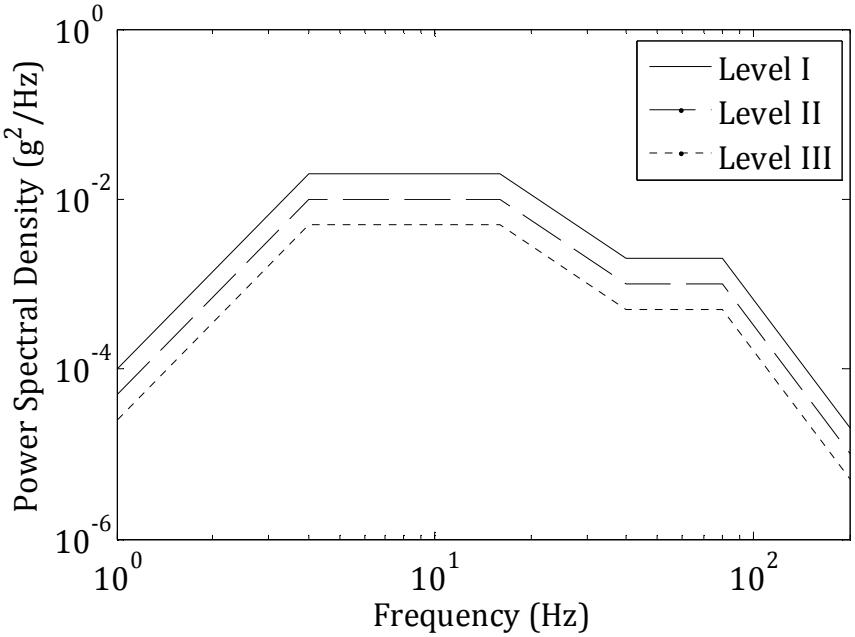

Figure 157: ASTM PSD plots for Truck with leaf spring suspension

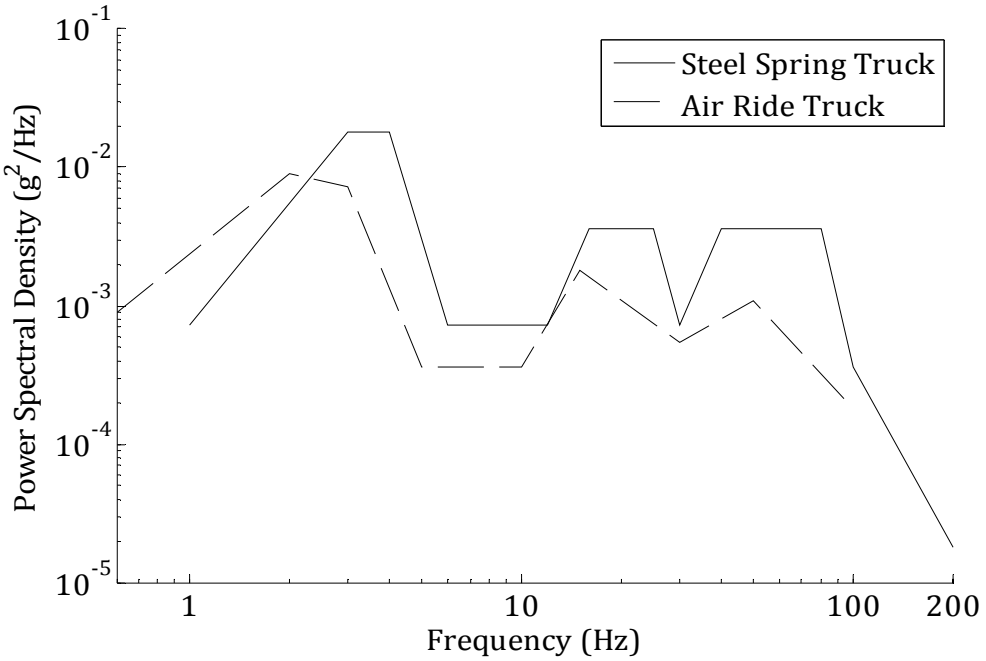

Figure 158: Comparison of ISTA PSD plots for steal spring and air ride suspension trucks

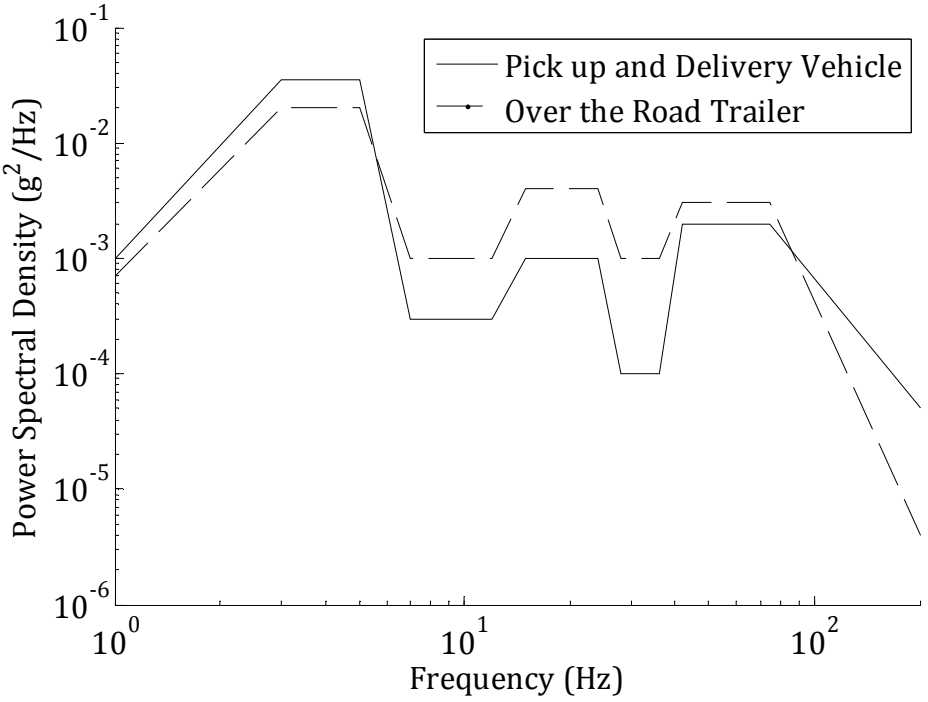

Figure 159: Comparison of ISTA PSD plots for delivery vehicles & over the road trailers

APPENDIX IV. ADDITIONAL INFORMATION

Table 40: Vertical stiffness of tyres (Cebon, 1999)

TYRE	INFLATION PRESSURE (kPa(psi))	LOAD (kN)	STIFFNESS (kN/m)		DAMPING COEFFICIENT (kNs/m)
			STATIC	DYNAMIC*	
Tractor tyre 11-36 (4-ply)	82.7 (12)	6.67	357.5	379.4	2.4
		8.0	357.5	394.0	2.6
		9.34	-	423.2	3.4
	110.3 (20)	6.67	379.4	394.0	2.1
		8.0	386.7	437.8	2.5
		9.34	394.0	423.2	2.5
Tractor tyre 7.5-16 (6-ply)	138 (20)	3.56	175.1	218.9	0.58
		4.45	175.1	233.5	0.66
		4.89	182.4	248.1	0.80
	193 (28)	3.56	218.9	233.5	0.36
		4.45	226.2	262.7	0.66
		4.89	255.4	277.3	0.73
Terra tyre 26X12-12 (2-ply)	15.5 (2.25)	1.78	51.1	-	0.47
	27.6 (4)	1.78	68.6	-	0.49

* Average Non-rolling dynamic stiffness

Table 41: Damping coefficients for car tyres at different pressures (Cebon, 1999)

TYRE	INFLATION PRESSURE (kPa(psi))	DAMPING COEFFICIENT (kNs/m)
Bias-ply 5.60 X 13	103.4 (15)	4.59
	137.9 (20)	4.89
	172.4 (25)	4.52
	206.9 (30)	4.09
	241.3 (35)	4.09
Radial-ply 165 X 13	103.4 (15)	4.45
	137.9 (20)	3.68
	172.4 (25)	3.44
	206.9 (30)	3.43
	241.3 (35)	2.86

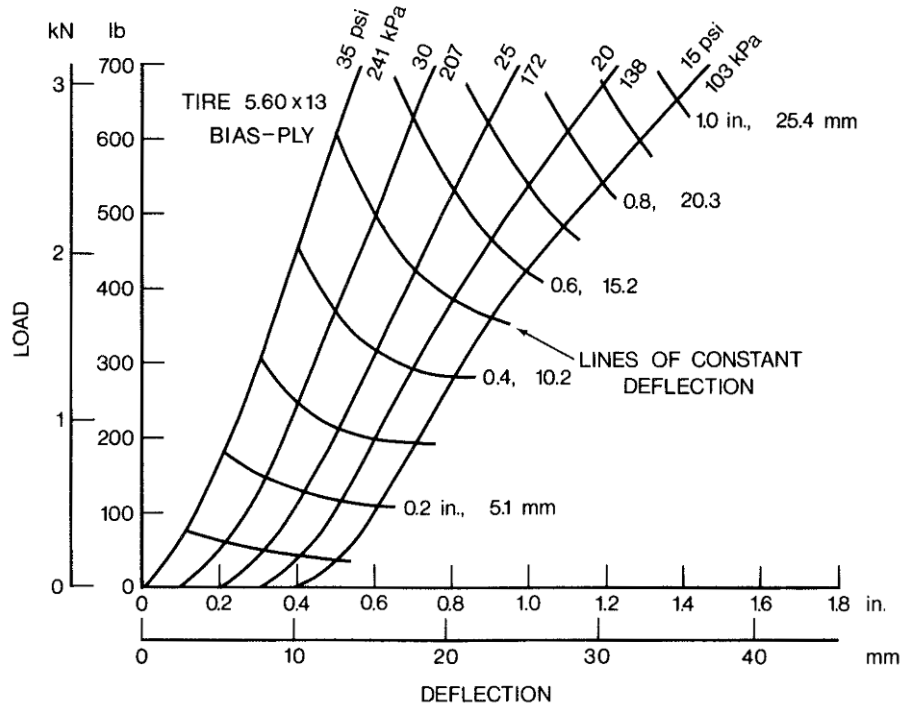

Figure 160: Static load-deflection relationship of a bias-ply car tyre (Cebon, 1999)

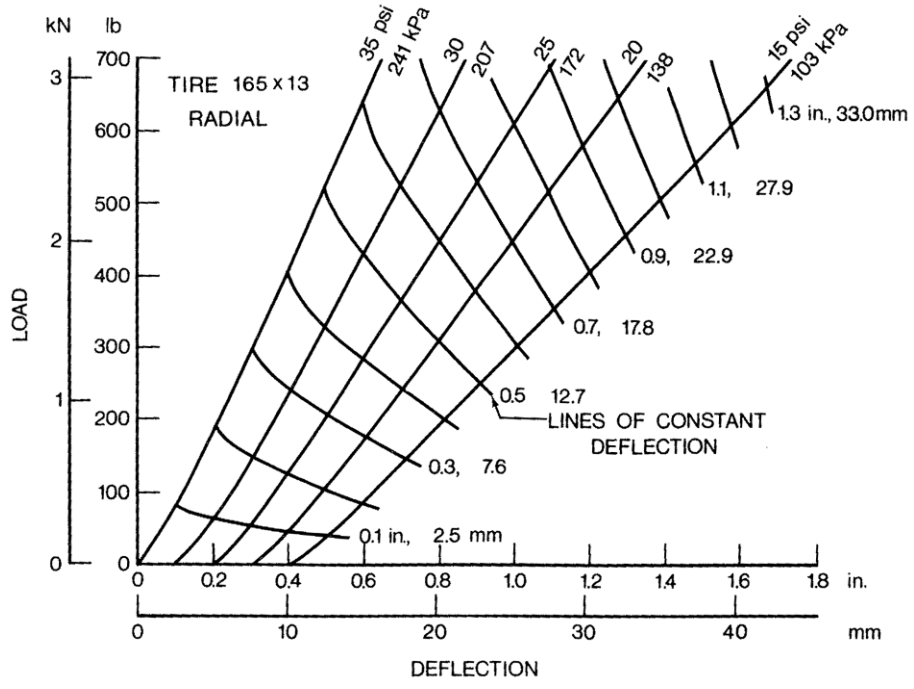

Figure 161: Static load-deflection relationship of a radial-ply car tyre (Cebon,1999)

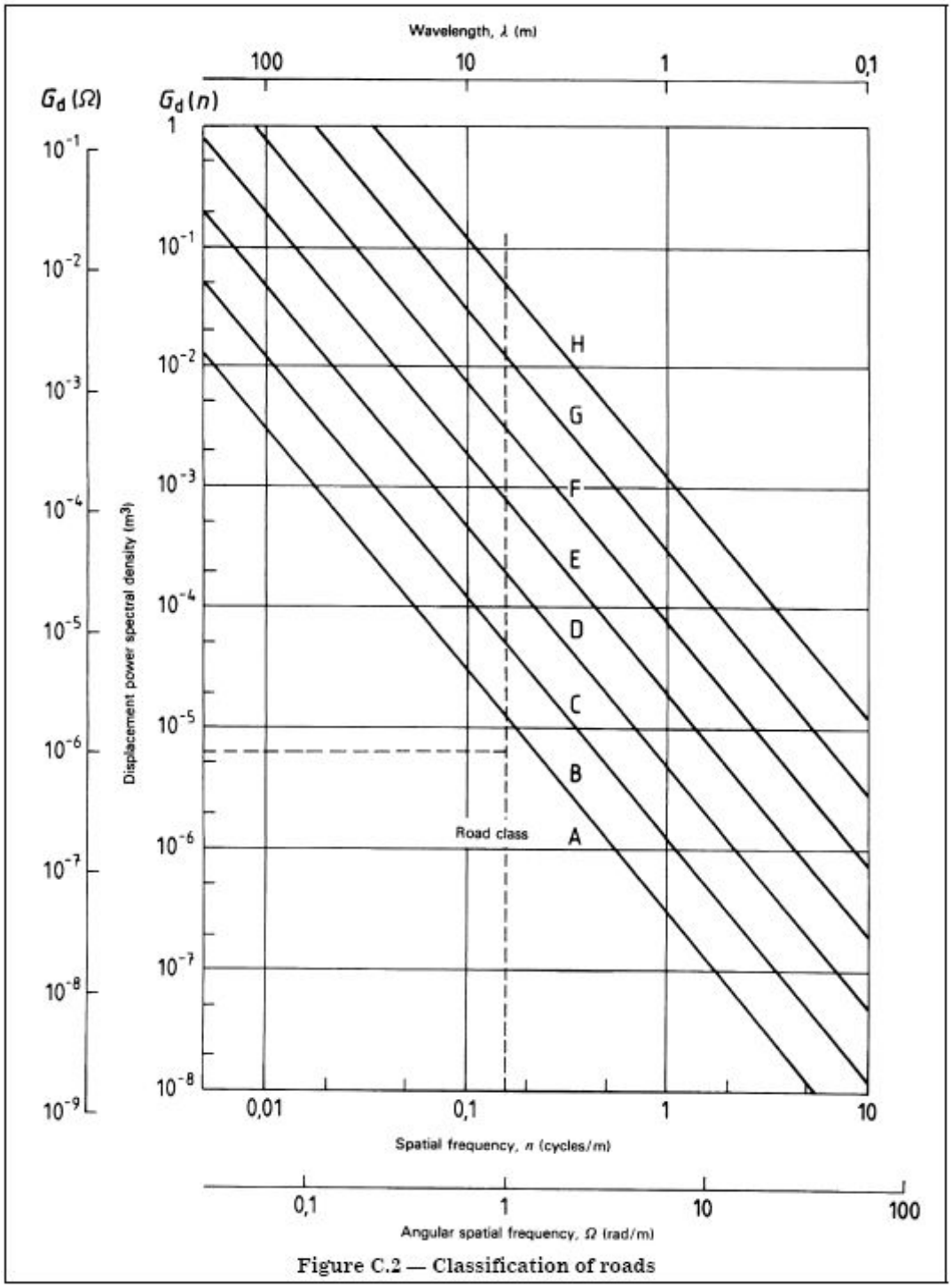

Figure C.2 — Classification of roads

Figure 162: British Standard classification of roads (BS7853, 1996)

Table 42: Information on road segment duration and road class (part 1)

	DRIVER - MD 1			DRIVER - MD 2			DRIVER - BJH 1			DRIVER - BJH 2		
ROAD CLASS	No	ROAD	DURATION (seconds)	No	ROAD	DURATION (seconds)	No	ROAD	DURATION (seconds)	No	ROAD	DURATION (seconds)
5	1	University	75	1	University	53	1	University	65	1	University	180
5												
3	2	Bathwick Hill	189	2	Bathwick Hill 1	80	2	Bathwick Hill	90	2	Bathwick Hill	135
3				3	Bathwick Hill 2	100						
3	3	City	43	4	City	70				3	City	30
3	4	Wells Way	102	5	Wells Way	136	3	Wells Way	70	4	Wells Way	90
4	5	Oldfield Park 1	52	6	Oldfield Park 1	114	4	Oldfield Park 1	185	5	Oldfield Park 1	115
4	6	Oldfield Park 2	50	7	Oldfield Park 2	119				6	Oldfield Park 2	59
4												
4	7	Oldfield Student 1	84	8	Oldfield Student 1	108	5	Oldfield Student 1	55	7	Oldfield Student 1	150
4	8	Oldfield Student 2	160	9	Oldfield Student 2	120						
4				10	Oldfield Student 3	49						
3	9	Lower Bristol Road	154	11	Lower Bristol Road	177	6	Lower Bristol Road	45	8	Lower Bristol Road	147
2	10	NSL (A4)	54	12	NSL (A4)	75	7	NSL	34	9	NSL	153
2							8	A4	44	10	A4	114
2												
3	11	Penn Hill Road	111				9	Penn Hill Road	67	11	Penn Hill Road 1	90
3										12	Penn Hill Road 2	54
3	12	Weston 1	208	13	Weston 1	67	10	Weston 1	80	13	Weston 1	140
3	13	Weston 2	149	14	Weston 2	150				14	Weston 2	110
3	14	Weston 3	85									
5	15	Royal Cresent	30	15	Royal Cresent	107	11	Royal Cresent	45	15	Royal Cresent	100
5												
3	16	Lansdown	115	16	Lansdown	119				16	Lansdown	129
5	17	Camden 1	30	17	Camden 1	125	12	Camden 1	190	17	Camden 1	69
5	18	Camden 2	77	18	Camden 2	82				18	Camden 2	70
5	19	Snow Hill	107	19	Snow Hill	119	13	Snow Hill	85			
3	20	Into City	60	20	Into City	125	14	Into City	145	19	Into City	154
3												

Table 43: Information on road segment duration and road class (part 2)

	DRIVER - HSM 1			DRIVER - HSM 2			DRIVER - JM 1			DRIVER - JM 2		
ROAD CLASS	No	ROAD	DURATION (seconds)	No	ROAD	DURATION (seconds)	No	ROAD	DURATION (seconds)	No	ROAD	DURATION (seconds)
5	1	University	154	1	University 1	110	1	University	115	1	University	130
5				2	University 2	108						
3	2	Bathwick Hill	186	3	Bathwick Hill 1	89	2	Bathwick Hill 1	120	2	Bathwick Hill 1	119
3				4	Bathwick Hill 2	101	3	Bathwick Hill 2	167	3	Bathwick Hill 2	90
3	3	City	57	5	City	110	4	City & Wells Way	195	4	City	142
3	4	Wells Way	104	6	Wells Way	136				5	Wells Way	52
4	5	Oldfield Park 1	104	7	Oldfield Park 1	146	5	Oldfield Park 1	148	6	Oldfield Park	50
4	6	Oldfield Park 2	181	8	Oldfield Park 2	148	6	Oldfield Park 2	127			
4							7	Oldfield Park 3	75			
4	7	Oldfield Student 1	192	9	Oldfield Student 1	130	8	Oldfield Student	115	7	Oldfield Student	84
4				10	Oldfield Student 2	107						
4												
3	8	Lower Bristol Road	65	11	Lower Bristol Road	64	9	Lower Bristol Road	70	8	Lower Bristol Road	160
2	9	NSL	80	12	NSL (A4)	86	10	NSL (A4)	140	9	NSL (A4)	154
2	10	A4 1	102				11	A4	139	10	A4	54
2	11	A4 2	111									
3	12	Penn Hill Road 1	100	13	Penn Hill Road	70	12	Penn Hill Road	124	11	Penn Hill Road	111
3	13	Penn Hill Road 2	103									
3	14	Weston 1	103	14	Weston 1	185	13	Weston 1	154	12	Weston 1	208
3	15	Weston 2	100	15	Weston 2	107	14	Weston 2	75	13	Weston 2	149
3	16	Weston 3	76									
5	17	Royal Cresent	60	16	Royal Cresent	101	15	Royal Cresent	175	14	Royal Cresent 1	85
5										15	Royal Cresent 2	30
3	18	Lansdown	71	17	Lansdown	106	16	Lansdown	147	16	Lansdown	115
5	19	Camden 1	78	18	Camden 1	82	17	Camden 1	100	17	Camden 1	30
5	20	Camden 2	125	19	Camden 2	151				18	Camden 2	77
5	21	Snow Hill	53				18	Snow Hill	52			
3	22	Into City	181	20	Into City	131	19	Into City 1	170	19	Into City	107
3							20	Into City 2	75			

APPENDIX V. WAVELET DECOMPOSTION METHOD - MATLAB CODE

Contents

1. Original Vibration File Information

```
% data = Vehicle vibration signal labelled;
```

```
dt = input('Enter the sample rate [s]:');
file = input('Enter filename to save data to:', 's');
% File already filtered?
filt = input('Does the data need filtering?: [y/n]', 's');
if filt == 'y' || filt == 'Y';
     Fs = 1/dt;
     % % Create band pass filter between Fc2 - Fc1:
     N   = 4;    % Order
     Fc1 = 1;    % 1st cut-off frequency
     Fc2 = 200;  % 2nd cut-off frequency
     % % Construct an FDESIGN object call its BUTTER method
     h = fdesign.bandpass('N,F3dB1,F3dB2' , N, Fc1, Fc2, Fs);
     Hd = design(h, 'butter');
     % % Filter the data file:
     data = filter(Hd, data(:,1), 1);
     clear('Hd', 'h', 'Fc1', 'Fc2', 'N', 'Fs');
end;
```

2. Create Journey Segments To Reduce Processing Time

```
l = length(data)*dt/(10*60);
 if l > 1;
     l = ceil(l);
     for x = 1:l;
         if x == l;
             if x*ceil(10*60/dt) <= length(data);
                 eval(['data', num2str(x), ' = data((x-
1)*ceil(10*60/dt)+1:x*ceil(10*60/dt),:);']);
             else eval(['data', num2str(x), ' = data((x-
1)*ceil(10*60/dt)+1:end,:);']);
             end;
         else eval(['data', num2str(x), ' = data((x-
1)*ceil(10*60/dt)+1:x*ceil(10*60/dt),:);']);
         end;
     end;
 else data1 = data;
 end;

 eval(['save(''', (file), '.mat'');']);
 clearvars -except -regexp dt file l data;
```

3. Level 1 Iteration

```
for seg = 1:l;
    eval(['load(''', (file), '.mat'', ''data', num2str(seg),
''');']);
    eval(['data = data', num2str(seg), ';']);
    for X = 1:3;
        if X > 1;
            data = OUT_DATA;
        end;
```

3.a. CWT of Vibration Signal

```
% Vibration signal = (data);
        [ccfs] = cwt(data(:,1),1:32, 'morl');
```

3.b. Create Gaussian Stationary Signal From PSD

```
% PSD of signal;
        lnfft = 2^11;
        [p,f] = cpsd(data(:,1),data(:,1),[],(lnfft-1),lnfft,(1/dt));
        n = round(length(data)*dt);     % Find how many seconds
needed
        signal = [];                    % Vector to store signal
        for ni = 1:n;
            a = p(1:end-1,:) .* ((lnfft)/(2*dt));
            a = sqrt(a);
            phase = 2*pi*rand(size(a));     % Random phases in [0
2*pi]
            Y = a.*exp(j*phase);            % Complex vector for ifft
% Replicate complex conj
            Y = [conj(Y(2:end,:));0;flipud((Y(2:end,:)))];
            Y = [0;Y];                      % Give it zero mean
            s = (ifft(Y));                  % Inverted transform
            signal = [signal;s];            % Put together = signal
        end;
```

3.c. CWT of Simulated Signal

```
% CWT of simulated signal (signal);
        [ccfs_G] = cwt(signal,1:32, 'morl');
```

3.d. Create Gaussian Envelope

```
% Find the max and min coefficient values in each scale:
        gmax = max(ccfs_G,[],2);
        gmin = min(ccfs_G,[],2);
        clear('-regexp', 'ccfs_G');
```

3.e. Apply Gaussian Envelope to Vibration Signal

```
        PKLOCS = [];
% Find outliers:
        for i = 1:32;
            [colm, row] = find(ccfs(i,:) > gmax(i,:) | ccfs(i,:) <
gmin(i,:));
            PKLOCS = [PKLOCS,row];
        end;
% Create vector to store all locations exceeding limits of envelope
        PTS = sort(unique(PKLOCS))';
        clear('-regexp', 'PKLOCS');
        data = [(1:1:length(data))', (1:1:length(data))', data];
```

3.f. Remove Outlying Segments from Vibration Signal;

```
        hsize = (2^11)/2;
        OUT_DATA = [];          % Store outlying portions of data
        i = 1;                    % For first point set i = 1
        while i <= length(PTS)-1;
            if i > 1;
                ptx = pt1;
```

```
            end;
            pt1 = PTS(i,:);
            pt2 = PTS(i+1,:);
% When considering the 1st outlier:
            if i == 1;
% If PTS i : PTS i+1 < hsize points between considered;
                if pt2-pt1 <= 2*hsize;
% if pt1 < hsize, data segment is taken from the start of the signal
                    if pt1 <= hsize;
% if pt1 < length(data) - hsize, pt1-hsize : pt1+hsize points removed
% If pt1 > length(data) - hsize, pt1-hsize : end are removed;
                        if pt1 <= length(data)-hsize;
                            OUT_DATA = [OUT_DATA;
data(1:pt1+hsize,:)];
% All the points greater than pt1 are found;
                            p = find(PTS > pt1);
% the new i is calculated as the next point in the series;
                            i = p(1,:);
% the old pt1 is stored as ptx for the next iteration;
                            ptx = pt1;
                        else OUT_DATA = [OUT_DATA;
data(1:PTS(end,:),:)];
                            break;  % End if length data reached;
                        end;
% Where i = 1, pt2-pt1 < hsize and pt1 > hsize;
                    else if pt1 <= length(data)-hsize;
                            OUT_DATA = [OUT_DATA; data((pt1-
hsize):pt1+hsize,:)];
                            p = find(PTS > pt1);
                            if isempty(p) == 0;
                                i = p(1,:);
                                ptx = pt1;
                            else break;
                            end;
                        else OUT_DATA = [OUT_DATA; data(pt1-
hsize:PTS(end,:),:)];
                            break;
                        end;
                    end;
% If pt2-pt1 > hsize, skip to next point
                else i = i+1;
                end;
% When i > 1;
            else if pt2-pt1 <= 2*hsize;
% if pt1 is close to the beginning of the signal (i.e.less than
hsize);
                    if pt1 < hsize;
% and if pt1 is close to the end;
                        if pt1 <= length(data)- hsize;
                            if pt1 < ptx + 2*hsize;
                                n = (ptx + hsize);
                            else n = pt1 - hsize;
                            end;
                            OUT_DATA = [OUT_DATA;
data(n+1:pt1+hsize,:)];
                            p = find(PTS > pt1);
                            i = p(1,:);
                            ptx = pt1;
% When pt1 is less than hsizee from the end signal;
```

```
                        else OUT_DATA = [OUT_DATA;
data(pt1:PTS(end,:),:)];
                            i = length(data);
                            break;
                        end;
% when pt1 is not close to beginning of signal or close to the end;
                    else if pt1 <= length(data)-hsize;
                            if pt1 < ptx + 2*hsize;
                                n = (ptx + hsize);
                            else n = pt1-hsize;
                            end;
                            OUT_DATA = [OUT_DATA;
data((n+1):pt1+hsize,:)];
                            p = find(PTS > pt1);
                            if isempty(p) == 0;
                                i = p(1,:);
                                ptx = pt1;
                            else break;
                            end;
% If close to end take end of signal and break;
                        else if pt1 < ptx + 2*hsize;
                                n = (ptx + hsize);
                            else n = pt1-hsize;
                            end;
                            OUT_DATA = [OUT_DATA;
data(n+1:PTS(end,:),:)];
                            i = length(data);
                            break;
                        end;
                    end;
                else i = i+1;
                end;
            end;
        end;


% Put gen_vib segments that are less than half a second back into the
% out_data (sample size deemed too small);
        dif = diff(OUT_DATA(:,1));
        ptz = find(dif > 1 & dif < 2*hsize);
        if isempty(ptz) ~= 1;
        ptz = [ptz; data(end,1)];
        for z = 1:length(ptz);
            if z < length(ptz);
                p1 = OUT_DATA(ptz(z,:),1)+1;
                p2 = OUT_DATA((ptz(z,:)+1),1)-1;
                OUT_DATA = [OUT_DATA; data(p1:p2,:)];
            else p1 = OUT_DATA(ptz(z-1,:)+1,1)+1;
                p2 = data((ptz(z,:)),1);
                if p2-p1 < 2*hsize;
                    OUT_DATA = [OUT_DATA; data(p1:p2,:)];

                end;
            end;
        end;
        end;

        OUT_DATA = sortrows(OUT_DATA,1);

% Find low level vibration = Gaussian Approximation:
```

```
        eval([(file), '_L1_', num2str(X), ' = data;']);
        eval([(file), '_L1_', num2str(X), ' (OUT_DATA(:,1),:) =
[];']);
                if data < ceil(1/dt);
                    OUT_DATA = [OUT_DATA; data];
                    OUT_DATA = sortrows(OUT_DATA,1);
                    eval([(file), '_L1_', num2str(X), ' = [];']);

                end;
        data = OUT_DATA;

        OUT_DATA = OUT_DATA(:,3);
        eval(['',(file), '_L1_', num2str(X), ' = ', (file), '_L1_',
num2str(X), '(:,3);']);
        eval(['save(''', (file), '.mat'', ''-regexp'', ''', (file),
'_L'', ''-append'');']);
        clear('-regexp', 'ccfs_', '_L1');
    end;
% Save data files and save last non-Gaussian (OUT_DATA) as the l+1
Gaussian approximation and renumber data parts so that non are
repeated:
    eval(['', (file), ' L1 ', num2str(X+1), ' = OUT DATA;']);
    eval(['save(''', (file), '.mat'', ''-regexp'', ''', (file),
'_L'', ''-append'');']);
    no = X+1;
    eval(['load(''', (file), '.mat'', ''-regexp'', ''', (file),
'_L1_'');']);
    for X = 1:4;
        eval(['', (file), '_L1s_', num2str(((no)*(seg-1))+X), ' = ',
(file), '_L1_', num2str(X), ';']);
    end;
    eval(['save(''', (file), '.mat'', ''-append'', ''-regexp'', ''',
(file), '_L1_'');']);
    clear -regexp _L1_ data OUT_DATA signal;
end;

% TOTAL Number of segments:
seg = seg*(X);
```

4. Level 2 Iteration

```
% I is the number of iterations of each of the data samples carried
out.
% Maximum number of segments per data sample = I+1;
iter = 0;
for X = 1:seg;
    iter = iter+1
    for I = 1:4;
        if I == 1;
            eval(['load(''', (file), '.mat'', ''', (file), '_L1s_',
num2str(X), ''');']);
            eval(['data = ', (file), '_L1s_', num2str(X), '(:,1);']);
            if isempty(data) == 1;
                break;
            else data = data;
            end;
            eval(['clear(''', (file), '_L1s_', num2str(X), ''');']);
        else
```

```
            eval(['load(''', (file), '.mat'', ''', (file), '_L2_',
num2str(X), '_', num2str(I-1), ''');']);
            eval(['length_predata = length(', (file), '_L2_',
num2str(X), '_', num2str(I-1), ');']);
            eval(['clear(''', (file), '_L2_', num2str(X), '_',
num2str(I-1), ''');']);
            eval(['data = OUT_DATA(:,3);']);
            if length(data) == length_predata;
                break;
            end;
        end;
```

4.a. CWT of Vibration Signal

```
% Vibration signal = Gaussian approximation from 1st iteration =
(data);
        [ccfs] = cwt(data(:,1),1:32, 'morl');
        eval(['save(''', (file), '.mat'', ''-append'', ''ccfs'');']);
        clear -regexp ccfs;
```

4.b. Create Gaussian Stationary Signal From PSD

```
% PSD of signal;
        lnfft = 2^11;
        [p,f] = cpsd(data(:,1),data(:,1),[],(lnfft-1),lnfft,(1/dt));
        n = round(length(data)/lnfft);  % Find how many seconds
needed
        signal = [];
        for ni = 1:n;
            a = p .* ((lnfft)/(2*dt));
            a = sqrt(a);
            phase = 2*pi*rand(size(a));     % Random phases in [0
2*pi]
            Y = a.*exp(j*phase);            % Complex vector for ifft
            Y = [Y;flipud(conj(Y))];        % Replicate complex conj
            Y = [0;Y];                      % Give it zero mean
            s = ifft(Y);                    % Invertedtransform
            signal = [signal;s];     % Put together to create signal
        end;
```

4.c. CWT of Simulated Signal

```
% CWT of simulated signal (signal);
        [ccfs_G] = cwt(signal,1:32, 'morl');
% Find the max and min coefficient values in each scale:
        eval(['gmax = max(ccfs_G,[],2);']);
        eval(['gmin = min(ccfs_G,[],2);']);
```

4.d. Create Gaussian Envelope

```
% Find the max and min coefficient values in each scale:
        clear -regexp ccfs
        eval(['load(''', (file), '.mat'', ''ccfs'');']);
```

4.e. Apply Gaussian Envelope to Vibration Signal

```
        PKLOCS = [];
% Find outliers:
        for i = 1:32;
            [colm, row] = find(ccfs(i,:) > gmax(i,:) | ccfs(i,:) <
gmin(i,:));
            PKLOCS = [PKLOCS,row];
        end;
        PTS = sort(unique(PKLOCS))';
        ccfs = [];
        eval(['save(''', (file), '.mat'', ''-append'', ''ccfs'');']);
        clear -regexp ccfs signal;

        data = [(1:1:length(data))', (1:1:length(data))', data];
```

4.f. Remove Outlying Segments from Vibration Signal;

```
        hsize = (2^11)/2;
        OUT_DATA = [];      % Store outlying portions of data
% For first point set i = 1:
        i = 1;
        while i <= length(PTS)-1;
            if i > 1;
                ptx = pt1;
            end;
            pt1 = PTS(i,:);
            pt2 = PTS(i+1,:);
% When considering the 1st outlier;
            if i == 1;
% If PTS i : PTS i+1 < hsize all points between considered;
                if pt2-pt1 <= 2*hsize;
% if the pt1 < hsize, data segment from start of the signal;
                    if pt1 <= hsize;
% if pt1 < length(data) - hsize, pt1-hsize : pt1+hsize removed;
If pt1 > length(data) - hsize, pt1-hsize : end are removed;
                        if pt1 <= length(data)-hsize;
                            OUT_DATA = [OUT_DATA;
data(1:pt1+hsize,:)];
% All the points greater than pt1 are found;
                            p = find(PTS > pt1);
% the new i is calculated as the next point in the series;
                            i = p(1,:);
% the old pt1 is stored as ptx for the next iteration;
                            ptx = pt1;
                        else OUT_DATA = [OUT_DATA;
data(1:PTS(end,:),:)];
                            break;  % length(data) reached end;
                        end;
% Where i = 1, pt2-pt1 < hsize and pt1 > hsize;
                    else if pt1 <= length(data)-hsize;
                            OUT_DATA = [OUT_DATA; data((pt1-
hsize):pt1+hsize,:)];
                            p = find(PTS > pt1);
                            if isempty(p) == 0;
                                i = p(1,:);
                                ptx = pt1;
                            else break;
                            end;
                        else OUT_DATA = [OUT_DATA; data(pt1-
hsize:PTS(end,:),:)];
```

```
                            break;
                        end;
                    end;
% If pt2-pt1 > hsize, skip to next point;
                else i = i+1;
                end;
% If i > 1
            else if pt2-pt1 <= 2*hsize; % if pt1 and pt2 are close;
% if pt1 is close to the beginning of the signal;
                    if pt1 < hsize;
% and if pt1 is close to the end;
                        if pt1 <= length(data)- hsize;
                            if pt1 < ptx + 2*hsize;
                                n = (ptx + hsize);
                            else n = pt1 - hsize;
                            end;
                            OUT_DATA = [OUT_DATA;
data(n+1:pt1+hsize,:)];
                            p = find(PTS > pt1);
                            i = p(1,:);
                            ptx = pt1;
% When pt1 <  length(signal) -hsize, take the data to the end;
                        else OUT_DATA = [OUT_DATA;
data(pt1:PTS(end,:),:)];
                            i = length(data);
                            break;
                        end;
% when pt1 is not close to beginning of signal or close to end;
                    else if pt1 <= length(data)-hsize;
                            if pt1 < ptx + 2*hsize;
                                n = (ptx + hsize);
                            else n = pt1-hsize;
                            end;
                            OUT_DATA = [OUT_DATA;
data((n+1):pt1+hsize,:)];
                            p = find(PTS > pt1);
                            if isempty(p) == 0;
                                i = p(1,:);
                                ptx = pt1;
                            else break;
                            end;
% If close to end take to the end of signal and break;
                        else if pt1 < ptx + 2*hsize;
                                n = (ptx + hsize);
                            else n = pt1-hsize;
                            end;
                            OUT_DATA = [OUT_DATA;
data(n+1:PTS(end,:),:)];
                            i = length(data);
                            break;
                        end;
                    end;
                else i = i+1;
                end;
            end;
        end;

% Put segments from Gaussian approximation (low level vibration) less
than half a second back in out_data;
        if isempty(OUT_DATA) == 0;
```

```
            dif = diff(OUT_DATA(:,1));
            ptz = find(dif > 1 & dif < 2*hsize+1);
            if isempty(ptz) == 0;
                ptz = [ptz; data(end,1)];
                for z = 1:length(ptz);
                    if z < length(ptz);
                        p1 = OUT_DATA(ptz(z,:),1)+1;
                        p2 = OUT_DATA((ptz(z,:)+1),1)-1;
                        OUT_DATA = [OUT_DATA; data(p1:p2,:)];
                    else p1 = OUT_DATA(ptz(z-1,:)+1,1)+1;
                        p2 = data((ptz(z,:)),1);
                        if p2-p1 < 2*hsize+1;
                            OUT_DATA = [OUT_DATA; data(p1:p2,:)];
                        end;
                    end;
                end;
            else ptz = [];
            end;

        OUT_DATA = sortrows(OUT_DATA,1);
        OUT_DATA = unique(OUT_DATA, 'rows');
        end;
% Find and plot the Gaussian Approximation vibration;
        eval([(file), '_L2_', num2str(X), '_', num2str(I), ' =
data;']);
        if isempty(OUT_DATA) == 0;
            OUT_DATA = unique(OUT_DATA, 'rows');
            eval([(file), '_L2_', num2str(X), '_', num2str(I), '
(OUT_DATA(:,1),:) = [];']);
            eval(['len = length(', (file), '_L2_', num2str(X), '_',
num2str(I), ');']);
        end;
        if len < lnfft;             % < ceil(1/dt);
            OUT_DATA = [OUT_DATA; data];
            OUT_DATA = sortrows(OUT_DATA,1);
            OUT_DATA = unique(OUT_DATA,'rows');
            eval([(file), '_L2_', num2str(X), '_', num2str(I), ' =
[];']);
        end;

        data = OUT_DATA;
        % Save data as Gaussian approximations, if length > 0;
        eval(['l = length(', (file), '_L2_', num2str(X), '_',
num2str(I), ');']);
        if l > 0;
            eval(['', (file), '_L2_', num2str(X), '_', num2str(I), '=
', (file), '_L2_', num2str(X), '_', num2str(I), '(:,3);']);
        end;
        eval(['save(''', (file), '.mat'', ''-regexp'', ''', (file),
'_L2_'', ''-append'');']);
    end;
% Save all segments and save final OUT_DATA as the X + 1 data file;
    eval(['', (file), '_L2_', num2str(X), '_', num2str(I+1), ' =
OUT_DATA;']);
    eval(['save(''', (file), '.mat'', ''-regexp'', ''', (file),
'_L2_'', ''-append'');']);
    clear -regexp OUT_DATA;
    eval(['clear(''-regexp'', ''ccfs_'', ''', (file), '_L2'');']);
    clear -regexp PKLOCS;
    eval(['', (file), '_L1s_', num2str(X), ' = [];']);
```

```
    eval(['save(''', (file), '.mat'', ''-append'', ''', (file), '_',
num2str(X), ''');']);
end;
```

6. Create the Simulation

```
x = 1;
PSD = [];
RMS = [];
KURTOSIS = [];
DURATION = [];
for X = 1:seg;
    for I = 1:5;
        eval(['load(''', (file), '.mat'', ''', (file), '_L2_',
num2str(X), '_', num2str(I), ''');']);
        eval(['data = ', (file), '_L2_', num2str(X), '_', num2str(I),
';']);
        if isempty(data) == 0;
            if size(data,2) > 1;
                data = data(:,3);
            end;

            eval(['clear(''-regexp'', ''', (file), '_L2_'');']);
```

6.a. For Each Part Calculate PSD

```
            lnfft = 2^11;
            if length(data) > 2050;
                olap = 2^11-1;
            else olap = 0;
            end;
            [p,f] = cpsd(data,data,[],olap,lnfft,(1/dt));

            PSD = [PSD, [x;p]];
```

6.b. Evaluate Segment Statistics

```
            rms = norm(data) / sqrt(length(data));
            RMS = [RMS; x, rms];
            k = kurtosis(data);
            KURTOSIS = [KURTOSIS; x, k];
            duration = length(data) * dt;
            DURATION = [DURATION; x, duration];
```

6.c. For Each Part Calculate a Gaussian Stationary Signal From PSD

```
% Inverted PSD to create signal;
            n = round(length(data)*dt);  % Find how many seconds
needed
            n = round(n*(1/dt)/lnfft);
            eval(['signal_', num2str(x), ' = [];']);
            for ni = 1:n;
                a = p(1:end-1,:) .* ((lnfft)/(2*dt));
                a = sqrt(a);
                phase = 2*pi*rand(size(a));  % Random phases in [0
2*pi]
```

```
                Y = a.*exp(j*phase);         % Complex vector for
ifft
                % Replicate complex conj
                Y = [conj(Y(2:end,:));0;flipud((Y(2:end,:)))];
                Y = [0;Y];                   % Give it zero mean
                s = (ifft(Y));               % Inverted transform
% Put together to create signal for each Gaussian approximation part;
                eval(['signal_', num2str(x), ' = [signal_',
num2str(x), ';s];']);
            end;
              eval(['save(''', (file), '.mat'', ''-append'',
''signal_', num2str(x), ''');']);

            x = x+1;
        end;
    end;
end;
x = x-1;

% Save files;
eval(['save(''', (file), '.mat'', ''-append'', ''x'', ''RMS'',
''KURTOSIS'', ''DURATION'', ''f'', ''PSD'');']);
clearvars -except -regexp PSD x f dt lnfft signal file;

% Create spline for simplified PSD for each segment;
xx = [1:1:5, 7, 10, 12, 15, 17, 20:5:50, 60, 80, 100, 150, 200, 250];
figure(100);
hold on;
col = lines(x);
for i = 1:x;
    eval(['yy', num2str(i), ' = spline(f, PSD(2:end, i), xx);']);
    eval(['loglog(xx, yy', num2str(i), ', ''color'', col(i,:));']);
end;

eval(['save(''', (file), '.mat'', ''-append'', ''-regexp'', ''yy'',
''xx'');']);
```

6.d. Randomise Order of Parts to Create Simulation Signal

```
% signal = simulation signal;
% dt = simulation signal dt;
Nofiles = x;
nf = randperm(Nofiles);
signal = [];
for i = 1:Nofiles;
    eval(['load(''', (file), '.mat'', ''signal_', num2str(nf(:,i)),
''');']);
    eval(['signal = [signal; signal_', num2str(nf(:,i)), '];']);
end;

% Plot simulation signal;
figure(65);
plot((0:(1/dt):(length(signal)-1)*(1/dt))', signal);
eval(['save(''', (file), '.mat'', ''signal'', ''-append'');']);
```

Published with MATLAB® 7.11